The Role of TGFβ1 and Macrophage Differentiation in MSU Crystal-Induced Inflammation

By

Stefanie Steiger

Malaghan Institute of Medical Research

Wellington, New Zealand

A thesis

submitted to the Victoria University of Wellington

in fulfilment of the requirements for the degree of

Doctor of Philosophy in Biomedical Science

Victoria University of Wellington

2014

Abstract

Gout is a painful form of inflammatory arthritis that is caused by the deposition of monosodium urate (MSU) crystals in the joints. MSU crystals trigger a local inflammatory response initiated by resident macrophages followed by a large infiltration of leukocytes. The spontaneous resolution of acute gout is associated with the production of transforming growth factor β1 (TGFβ1). The overall objectives of this thesis were to investigate mechanisms that lead to TGFβ1 production and contribute to the resolution of acute gout, the effect of TGFβ1 on the functional phenotype of differentiated macrophages, and possible changes in surface marker expression by macrophages in response to MSU crystals.

To determine macrophage-independent sources of TGFβ1 during the resolution of acute gout and how TGFβ1 production altered MSU crystal-recruited neutrophil functions, neutrophils were purified from MSU crystal-treated mice when levels of TGFβ1 were high. MSU crystal-recruited neutrophils and circulating blood neutrophils were identified as TGF$\beta1^+$ cells. The mechanism for TGFβ1 production by neutrophils was associated with their ability to phagocytose apoptotic neutrophils. TGFβ1 produced by canibalising neutrophils inhibited both respiratory burst and interleukin-1β (IL-1β) production by MSU crystal-activated neutrophils *ex vivo*. Importantly, neutrophils from MSU crystal-challenged mice treated with TGFβ1 neutralising antibody *in vivo* produced elevated levels of superoxide but neutrophil IL-1β production was unaffected. These results show that TGFβ1 produced by canibalising neutrophils can actively suppress neutrophil inflammatory functions and therefore make a significant contribution towards the resolution of gouty inflammation.

To investigate the effect of TGFβ1 on macrophage differentiation *in vitro*, granulocyte macrophage colony-stimulating factor (GM-CSF) bone marrow macrophages (GM-BMMs) and macrophage colony-stimulating factor (M-CSF) bone marrow

macrophages (M-BMMs) were generated in the presence of TGFβ1. TGFβ1 was found to drive a hyper-inflammatory GM-BMM phenotype, while contributing to the differentiation of a hypo-inflammatory M-BMM phenotype specifically in response to MSU crystals. Increased IL-1β production by TGFβ1-differentiated GM-BMMs was associated with enhanced NOD like receptor family, pyrin domain-containing 3 (NLRP3) inflammasome activation and caspase 1/caspase 8 interaction, and a down-regulation of receptor-interacting serine/threonine-protein kinase 3 (RIP3) triggered by MSU crystals. At the same, TGFβ1 inhibited antigen-specific T cell proliferation by GM-BMMs. In contrast, TGFβ1-treated M-BMMs down-regulated the expression of active IL-1β that correlated with decreased IL-1β production, and upregulated RIP3 expression in response to MSU crystals. These data indicate that TGFβ1-treated GM-BMMs exhibited a hyper-inflammatory response to MSU crystal stimulation, whereas M-BMMs were found to be hypo-responsive.

Macrophages were found to upregulate the surface marker NK1.1, which is primarily expressed on natural killer (NK) cells, and occured as a consequence of phagocytosis. Following phagocytosis of MSU crystals, activated macrophages produced IL-1β and tumour necrosis factor α (TNFα), which triggered the upregulation of NK1.1 expression. Macrophage NK1.1 expression is an activation-driven event specific to MSU crystals. However, phagocytosis of apoptotic neutrophils also triggered the upregulation of NK1.1 by macrophages, a non-inflammatory event that is characteristic for the resolution of acute inflammation. These findings suggest that macrophages may develop NK cell-like properties initiated by an activation-driven or apoptotic cell clearance mechanism.

Taken together, the results of this thesis indicate that canibalising neutrophils self-regulate their inflammatory functions via TGFβ1 and that TGFβ1 drives a hyper-inflammatory GM-BMM phenotype, while shutting down inflammatory functions of M-BMMs. These data highlight a regulatory role for TGFβ1 during acute gouty inflammation.

Acknowledgements

First, I would like to express my sincere gratitude to my supervisor Dr Jacquie Harper for giving me the opportunity to do my PhD and for her endless support, faith, patience and guidance. I am extremely appreciative of the effort, time and feedback that she has given me. She has been a great mentor to me.

In the lab, I especially want to thank Odette Shaw, Lisa Shaw, Stephanie Chee and Rene McLaughlin who made lab-life run smoothly and enjoyably. Singing, dancing and a lot of humour has got us through many long working days and overnight experiments, better known as 'timecourse' experiments. And thank you for being patient with me when it came to ordering lab material: Do I have to write down the Cat. number or Lot. number? Lisa would say: "Steffi, I've told you so many times that you need to give me the Cat. number otherwise I won't order those things for you."

Thank you to all my proofreaders: Elizabeth Forbes-Blom, Mali Camberis, Odette Shaw, Rene McLaughlin, Dr Bridget Stocker and Elena Kim. Thanks also to my fellow PhD students for their support, scientific discussions and friendship in the 'Siberia' office and to everyone else at the Malaghan Institute, who have helped me and made my time enjoyable.

My special thanks goes to my friends Pauline Harris, So Nai Lim, Pete Kerr, William-John Martin, Clare Slaney, Pip Brown, Yael Seroussi and Taryn Osmond for always believing in me, for your endless support and words of wisdom during happy and exciting as well as stressful and challenging times. Thank you to my dear friends in Germany Anja Kamper, Juliane Finger and Kathrin Knelange, who have encouraged and looked after me despite the many many kilometers that lie between us. I also wish to thank Elizabeth Forbes-Blom, Sabine Kuhn, Lisa Shaw and Elena Kim for supporting me, cheering me up during coffee breaks and for your friend-

ship. My heartfelt gratitude goes to Davaki Martin for her words of encouragement, support, and bringing happiness and joy into my life. You have all enlightened my life and touched my heart!

Most importantly, I wish to thank my family in particular my parents, Christine and Gert Steiger for their unconditional love, sacrifice, encouragement and endless support throughout my years of study in New Zealand. You have been my pillar of strength and motivation. And for the many parcels that were filled with delicious chocolate and biscuits that have lightened up my days. I am also extremely grateful to my sister Franziska Steiger, who made me an auntie twice in the last few years, for her encouragement, love and for cheering me up. Without your faith, trust and encouragement, I would have not become the person I am now.

Finally, I am very grateful to the organising force of life, whatever it is, for opening up this path in life to me and for expanding my personal development, strength and growth.

Contents

List of Figures

List of Abbreviations

ADP	Adenosine disphosphate
APC	Allophycocyanin (fluorophore)
APCs	Antigen-presenting cells
ASC	Apoptotic speck-like adaptor protein
ATP	Adenosine triphosphate
BMMs	Bone marrow-derived macrophages
BSA	Bovine serum albumin
cIAP1	Cellular inhibitor of apoptosis protein-1
CNS	Central nerve system
CPPD	Calcium pyrophosphate dihydrate
CXCL1	Chemokine (C-X-C motif) ligand 1
DAPI	4',6-diamidino-2-phenylindole
DAMPs	Danger-associated molecular pattern
DC	Dendritic cell
D-PBS	Dulbecco's phosphate buffered saline
DHR-123	Dihydrorhodamine-123
ECL	Enhanced chemiluminescence substrate
ELISA	Enzyme linked immunosorbent assay
FACS	Fluorescence-activated cell sorting
FADD	Fas-associated protein with death domain
FBS	Foetal bovine serum
FITC	Fluorescein isothiocyantae
GLUT9	Glucose transporter 9
GM-CSF	Granulocyte macrophage colony-stimulating factor
GM-BMMs	GM-CSF bone marrow-derived macrophages
Gr-1	Granulocyte antigen-1
HRP	Horse radish peroxidase
IAPs	Inhibitor of apoptosis proteins

IgG	Immunoglobulin G
IL-1β	Interleukin-1 beta
IL-6	Interleukin-6
IL-8	Interleukine-8
INFγ	Interferon gamma
ICAM-1	Intracellular adhesion molecule-1
i.p.	Intraperitoneal
KAR	Killer activation receptor
KIR	Killer-cell immunoglobulin-like receptor
LAL	*Limulus* amebocyte lysate
LPS	Lipopolysccharide
Ly6G	Lymphocyte antigen 6G
MCP-1	Monocyte chemoattractant protein-1
M-CSF	Macrophage colony-stimulating factor
M-BMMs	M-CSF bone marrow-derived macrophages
MFI	Mean fluorescence index
MHCII	Major histocompatibility complex class II molecules
MSU	Monosodium urate monohydrate
NADPH	Nicotinamide adenine dinucleotide phosphate
NLRP3	NOD like receptor family, pyrin domain-containing 3
NET	Neutrophil extracellular traps
NK cells	Natural killer cells
OVA	Ovalbumin
Pam3Cys	Pam3Cys-SKKKK x3 HCl
PE	Phycoerythrin
PECs	Peritoneal exudate cells
PerCP	Peridinin chlorophyll protein
PI	Propidium Iodide
PMA	Phorbol myristate acetate
PMNs	Polymorphonuclear leukocytes

RBC	Red blood cells
RIP3/RIPK3	Receptor-interacting serine/threonine-protein kinase 3
RIPK1	Receptor-interacting serine/threonine-protein kinase 1
ROS	Reactive oxygen species
rpm	Revolutions per minute
SA	Streptavidin
SEM	Standard error of the mean
SOCS	Suppressor of cytokine signaling
STAT	Signal transducers and activators of transcription
TNFα	Tumour necrosis factor alpha
TGFβ1	Transforming growth factor beta1
TG2	Transglutamine 2
TLR	Toll-like receptor
UA	Uric acid
URAT-1	Urate transporter-1
VCAM-1	Vascular cell adhesion molecule-1
WST-1	2-1[4-Iodophenyl)-3-(4-nitrophenyl)-5-(2,4-Disulfophenyl)-2H-tetrazolium, monosodium salt]

Chapter 1

Published in part in **Stefanie Steiger**, Jacquie L. Harper. Mechanisms of Spontaneous Resolution of Acute Gouty Inflammation. *Curr Rheumatol Rep*, 16:392, 2014. (see appendix).

1 Acute Gouty Arthritis, an Autoinflammatory Disease

1.1 History of gout

Gout is a painful arthritic disease that manifests as episodic and debilitating joint inflammation. The ancient Egyptian Imhoteb observed and investigated gout as a distinct disorder in as early as 2640BC [1]. Several centuries later (400BC) Hippocrates, the father of Western medicine, described gout as podagra or the disease of kings, for it was associated with changes in lifestyle and social wealth [1]. In the present day, the prevalence of gout is dramatically increasing across all socio-economic groups in western societies [2; 1; 3]. The incidence of gout in the US increased from 2.9/1000 in 1990 to 5.2/1000 in 1999 [2; 4] and in 2007 approximately 8.3 million US adults have had at least one gout attack [5]. In a study based in England, the prevalence of gout was estimated at 9.5/1000 in 1995 [6]. Previous sub-national studieshave demonstrated high prevalence of gout in the entire New Zealand population [7; 8; 9; 10; 11], particularly among Maori and Pacific people (>7% in all adult males and >30% in older Maori and Pacific men, December 2009) [12]. These statistics emphasize the rising incidence of gout worldwide. Gout sufferers experience debilitating high morbidity and poor quality of life [13]. This impacts significantly on their ability to work and the increasing incidence of gout presents a significant collective burden of disease. A more clear understanding of the inflammatory mechanisms in gout is required to treat and manage the disease effectively. This thesis will provide a significant advance in the understanding of the cellular events that characterise acute gouty inflammation.

1.2 Monosodium urate crystals

Monosodium urate (MSU) crystals have been described and observed in affected joints from gout patients throughout history [11], however it was not until 1962 that Faires and McCarty confirmed MSU crystals as the causative agent in gout attacks. Using synthetically prepared MSU crystals, they injected crystals into the synovial space of their own knees resulting in a gout attack [14].

MSU crystals are the biological form of crystalline uric acid. They range in size from 10 - 25 μm in length, appear needle-like in shape and have the ability to polarise light, a quality known as birefringence (Figure 1.1). MSU crystals can be identified in the synovial fluid of gout patients even after the gout attack has resolved and there is no evidence for clinical inflammation [15; 16]. Once uric acid has crystallised in the joints, it takes a long time for MSU crystals to be redissolved by the body.

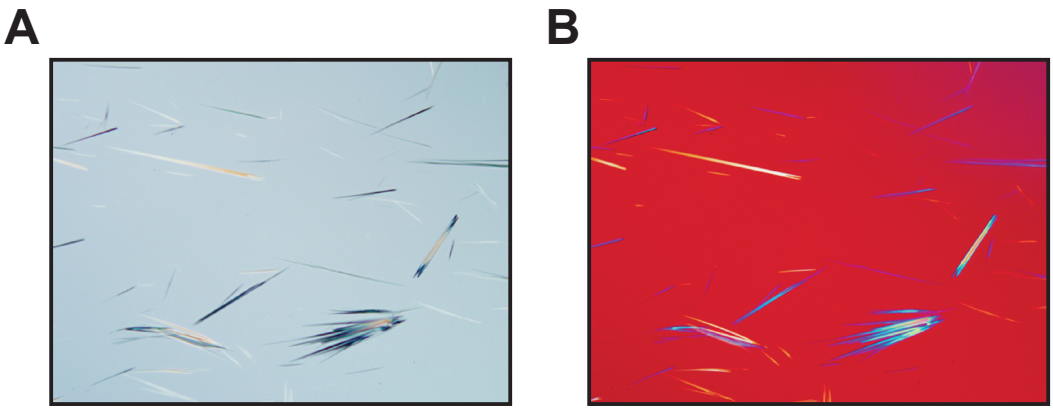

Figure 1.1: Monosodium urate crystals. Monosodium urate (MSU) crystals as visualised under a microscope in normal (**A**) and polarised (**B**) light fields. Pictures provided by Dr William-John Martin.

1.3 Acute and chronic gout

Acute gout is characterised by sudden and periodic attacks of inflammation occurring in one or more joints, which cause severe pain. The deposition of MSU crystals in the joints triggers an acute inflammatory response characterised by swelling, tenderness and redness of the affected joints and tissues (Figure 1.2A). Patients often suffer from fever and chills, which usually takes 6 - 12 hours to develop. These symptoms are associated with the intense influx of leukocytes into the local area. An untreated gout attack will spontaneously resolve within 7 - 10 days [17], however some individuals will never experience complete freedom from the ongoing chronic pain associated with periodic gout attacks, which are known as gout flares [18].

Over several years, the poor management of acute gout may lead to chronic tophaceous gout. This stage is characterised by the accumulation of MSU crystals and immune cells, collectively called tophi, in the joints or soft tissue (Figure 1.2B). The formation of tophi leads to polyarticular bone erosions and deformations resulting in severe tissue and bone damage [19].

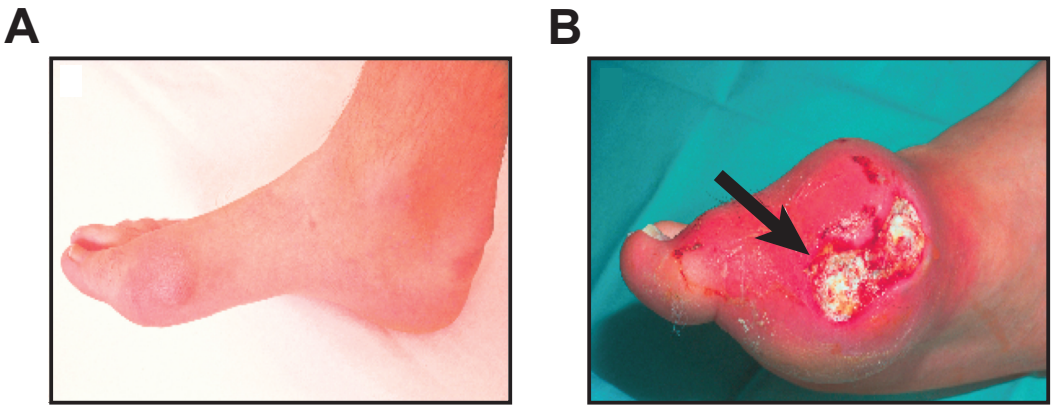

Figure 1.2: Acute and chronic gout. Joint/big toe from patients with acute (**A**) and chronic tophaceous gout (**B**). The black arrow indicates the deposition of MSU crystals (tophus), which ruptured through the skin and caused ulceration. Pictures used with permission from PHARMAC, NZ.

1.4 Uric acid

One of the main predictors of gout risk and development is the concentration of urate in the serum. Uric acid (UA) is the final product of the purine metabolic pathway in the human body. Purines are an important building block required for deoxyribonucleic acid (DNA) and energy carrying molecules, nicotinamide adenine dinucleotide phosphate (NADPH) and adenosine triphosphate (ATP). In humans, one-third of urate, which is deprotonated uric acid, is excreted via the gastrointestinal tract and two-thirds via the kidneys [20]. About 90% of the uric acid filtered by the kidneys is reabsorbed and this process is mediated by specific transporters including urate transporter-1 (URAT-1) [21].

Most mammals, except humans, have uricase or uric acid oxidase, an enzyme responsible for the regulation and breakdown of uric acid into a more soluble molecule allantoin [22]. This explains why urate levels are much higher in humans and why gout is mainly a human disease.

Normal serum urate levels are between 0.14 - 0.36 mM in women and 0.20 - 0.42 mM in men [23]. Clinical hyperuricemia is diagnosed when serum urate levels exceed 0.42 mM, which is approximately the saturation point for uric acid solubility [24]. Such high serum uric acid levels means that individuals have a greater risk of experiencing a gout attack.

1.5 Gout risk factors

1.5.1 Hyperuricemia

Although hyperuricemia is a risk factor for the development of gout, only 25% of individuals with elevated circulating urate levels develop gout [24; 25; 26; 27]. Some individuals can be in the state of asymptomatic hyperuricemia for several years

before suffering a gout attack. These observations suggest that the process from hyperuricemia to MSU crystal formation to inflammation has additional regulatory mechanisms, which are still not fully understood.

1.5.2 Gender and age

Gout is the most common cause of inflammatory arthritis among men over 40 years [28]. In fact, the incidence of gout in men is four times higher than that observed in women [29]. This is possibly due to the uricosuric effect of estrogen, which may help the kidneys to excrete uric acid, and is consistent with the observation that it is rare for women to suffer from gout during menopause [30]. Testosterone has been shown to increase the expression of the genes URAT-1 and glucose transporter 9 (GLUT9) [31; 32], which indicates that gender differences in serum urate levels are associated with the renal urate reabsorption transport system and that this is a possible causative factor for hyperuricemia and gout in males. However, the risk of gout increases with age due to a decrease in renal functions by the elderly and is further complicated by some medications commonly used by the elderly to treat other co-morbid conditions, which have diuretic side effect or can raise serum urate levels [2; 33].

1.5.3 Diet

Throughout history, gout epidemics have been observed in periods of social wealth. The consumption of purine-rich food including shellfish, seafood (trout, sardines), red meat, offal foods (liver, heart, kidney), mushrooms, alcohol and fructose-rich beverages are associated with the development of gout attacks [34; 35; 36; 37]. For example, fructose contributes to increased uric acid levels by interfering with ATP recycling, degrading it to uric acid rather than to ADP then ATP [38; 39]. On the other hand, the intake of dairy food seems to be protective [40; 41].

1.5.4 Genetics

Gout is often a familial disease. Studies using a genome-wide search have identified two genes: URAT-1 and GLUT9, which are linked with urate reabsorption and have a strong influence on the regulation of renal urate excretion [42; 43; 44; 45]. A particular allele of GLUT9 has been associated with reduced serum urate levels in Italian, UK, German and Croatian populations suggesting that genetic polymorphism or mutations of urate transporters contribute to the development of hyperuricemia and gout [46; 47; 48]. Koettgen and colleagues have now identified 18 new loci (such as VEGFA, NFAT5 or TRIM46) using data from <140.000 individuals of European ancestry, that are associated with serum urate concentrations, which may have implications for the treatment and prevention of gout [49].

1.6 Treatment and management of gout

Due to the intensity of the inflammatory response characterising a gout attack, treatments are needed to control acute gouty inflammation and to control hyperuricemia, the precursor to the formation of MSU crystals. Currently, there are two approaches for managing gout: anti-inflammatory drugs and urate lowering therapy.

1.6.1 Anti-inflammatory drugs

Due to the intensity of inflammatory reactions characterising a gout attack, anti-inflammatory agents are primarily used for treating acute gout. This includes the use of glucocorticoids, although non-steroidal anti-inflammatory drugs (NSAIDs) such as indomethacin, etoricoxib, naproxen and ibuprofen are the preferred treatment option [26; 50; 51]. NSAIDs provide marked symptomatic relief within the first 24 hours of administration and are the first drug of choice in gout patients who do not have contraindications against their use [52; 53; 54].

Alternative treatment options to NSAIDs are prednisolone or colchicine, which are used to treat acute gout episodes. The use of oral prednisolone for the treatment of acute gout flares has been shown to be as effective in pain reduction as NSAIDs [55; 56; 57]. Colchicine has a number of therapeutic activities including reducing neutrophil activity and migration by blocking microtubule assembly, phagocytosis and transport of MSU crystals, and reducing adhesion molecules on endothelial cells in response to interleukin-1β (IL-1β) and tumor necrosis factor α (TNFα) [58; 59; 60]. Recently, it has also been demonstrated that colchicine can suppress MSU crystal-induced NLRP3 inflammasome activation and IL-1β processing [61; 62]. Colchicine, however has a narrow therapeutic window (24 hours) as a number of complications can occur during treatment, such as diarrhea, fever, gastrointestinal toxicity and vomiting [63; 64; 65; 54].

Among new therapies for gout, anti-cytokine agents have been explored by targeting the first step in the inflammatory cascade. Due to the central role of IL-1β and the inflammasome in gout, drugs such as canakinumab and triamcinolone acetonide have been developed and studied in acute gout patients with successful results showing pain and inflammation relief as well as reduced risk of new gout flares in these patients [66]. These drugs have been found to inhibit IL-1β and inflammasome functions [67; 68], yet although, anti-IL-1 treatment seems to be highly effective, the main limitation of these drugs is that they are extremely expensive.

1.6.2 Urate lowering therapy

The aim of urate lowering therapy (ULT) is to reduce and maintain serum urate levels below 0.36 mmol/L, the saturation point at which crystal formation occurs. ULT drugs accomplish their effect by either lowering the production of uric acid (uricostatic drugs) or by increasing the renal excretion of uric acid (uricosuric drugs). The uricostatic drug allopurinol has been widely used as an effective ULT treatment, however about 20% of patients with gout are intolerant or refractory to this drug

[69; 70]. For such patients, an appropriate alternative is febuxostat - a drug that selectively inhibits the xanthine-oxidase breakdown to uric acid [70]. Uricosuric drugs, such as probenecid, sulfinpyrazone, benzbromarone and lesinurad, prevent the reabsorption of uric acid by the kidneys and thus increase the excretion of uric acid [71; 44; 45]. Uricosuric drugs have shown good responses with good tolerability in patients suffering from gout [72].

1.7 Cellular inflammation in acute gout

Inflammation often results from exposure to external stimuli, however, auto-inflammatory conditions also occur when inflammation is initiated by self danger signals [73]. Such sterile inflammation is triggered by diseases including acute gouty arthritis, whereby the deposition of MSU crystals in the joints induces a rapid infiltration of cells. This can lead to chronic inflammation resulting in severe tissue and bone damage. While some of the important cells and cellular mediators in acute gout have been identified, much remains unknown. This section will highlight what is currently known about cellular responses in acute gouty inflammation.

1.7.1 Cell activation in acute inflammation

During the initiation of a gout attack, resident cells recognise and respond to MSU crystals. The activation of resident cells including macrophages, mast cells and epithelial cells have been shown to produce pro-inflammatory cytokines (such as IL-1β, TNFα and IL-6) that amplify the local inflammatory reaction [62; 74; 75; 76]. Complement proteins and various chemoattractants (such as MCP-1, IL-8) are also thought to be involved in the activation and recruitment of circulating leukocytes into the joint synovial space [77; 78; 79; 80]. These mediators upregulate adhesion molecules on both the epithelial cells and responding leukocytes, driving further infiltration of neutrophils and monocytes to the site of inflammation. Neutrophils, once recruited may also be directly activated by MSU crystals to recruit more neu-

trophils through the production of IL-8 and S100 proteins [81; 82].

In addition, natural killer (NK) cells can also interact with cells of the innate immune system and modulate gouty inflammation [83]. Recently, it has been demonstrated that the $CD56^{bright}$ subset of NK cells is greatly expanded in the synovial fluid of patients with inflammatory arthritis [84] and can produce large amounts of both pro- and anti-inflammatory cytokines. In a reciprocal contact-dependent activation interface, $CD56^{bright}$ NK cells were capable of engaging with monocytes [85], thus indicating the existence of a positive feedback loop that could contribute to the amplification of the inflammatory response in acute gout [84]. It is not known whether macrophages develop NK cell-like functions, such as lytic properties or expression of specific NK cell markers in response to MSU crystals or whether these functions play a role in augmenting or shutting down acute gouty inflammation.

1.7.2 Recognition of MSU crystals as a danger signal

I: Immune cell recognition of MSU crystals

To promote the generation of an immune response, microbial and yeast cell wall components or viral RNA typically provide the required signals that alert the immune system to danger [86]. In the absence of such signals, there is often no immune defence response or tolerance may develop [87]. Therefore, a danger signal or adjuvant must be present with the foreign antigen in order to prime the production of cytokines via signalling through, for example toll like receptors (TLRs) on resident cells, and to augment an inflammatory response [87; 86]. As a non-infectious agent, MSU crystals were recently described as an endogenous danger signal or adjuvant capable of inducing an inflammatory response. Reports have shown that uric acid released from locally damaged or dead cells acts as a danger signal to antigen-presenting cells such as dendritic cells (DCs) to drive T cell proliferation [88; 89; 90]. This adjuvant effect only occured when uric acid was present at a high concentration consistent with the saturation point for crystallisation. Further studies have shown

that subcutaneous administration of MSU crystals exhibited adjuvant activities by enhancing the tumor rejection process *in vivo* [91; 92]. These data indicate that uric acid and/or MSU crystals have the potential to function as an antigen carrier, adjuvant and danger signal to initiate and augment inflammatory immune responses.

II: Recognition of MSU crystals by innate cells

In order for inflammation to occur, innate cells need to recognise MSU crystals. There is evidence that complement found in the synovial fluid plays a role in the inflammatory response to MSU crystals [93]. In the joints of complement-deficient rabbits, resident macrophages fail to recognise MSU crystals, which results in decreased production of the neutrophil chemoattractant CXCL1 and diminished infiltration of neutrophils after MSU crystal administration [78]. *In vitro* experiments with human serum have shown that MSU crystals are able to activate a variety of complement proteins (such as C1, C3, C5); therefore may play a role in the production of chemokines by cells in the synovial membrane [79; 77; 94; 95]. In addition, pre-coating MSU crystals with immunoglobulin G (IgG) can cause an increase in the production of reactive oxygen species (ROS) in human polymorphonuclear leukocytes *in vitro* [82]. These data indicate that complement binding to MSU crystals can activate both resident macrophages and infiltrating neutrophils. However, even in the absence of serum, MSU crystals are still able to activate immune cells to produce pro-inflammatory mediators indicating a direct recognition mechanism of MSU crystals by innate cells [80].

Currently, the receptors responsible for MSU crystal recognition are not definitively defined. There is evidence to suggest that the pattern recognition receptors TLR2/TLR4 as well as the adaptor molecule CD14 are involved in crystal recognition. Bone marrow-derived macrophages from CD14 knockout mice exhibit impaired recognition and phagocytosis of MSU crystals *in vitro* [96]. In a murine air pouch model, Scott and colleagues demonstrated that TLR2/TLR4 deficiency resulted in decreased IL-1β production and neutrophil infiltration in response to MSU

crystals [58]. These data show that MSU crystals can directly bind to CD14 and TLR2/TLR4 to induce an inflammatory response [58].

In contrast, a recent study has shown that MSU crystal-induced inflammation is mediated by the IL-1 receptor (IL-1R) and MyD88 signalling pathways rather than the TLRs on non-hemopoietic cells [97]. This study suggests that even though CD14 plays a role in MSU crystal recognition by macrophages, CD14-dependent signalling via MyD88 is essential for the production of pro-inflammatory cytokines upon MSU crystal stimulation. The expression of IL-1R on non-hemopoietic cells indicates that the surrounding tissue is important for the amplification of the MSU crystal inflammatory response.

1.7.3 Cytokines and chemokines in MSU crystal-induced inflammation

During acute gout attacks, innate cells stimulated with MSU crystals produce inflammatory mediators. MSU crystal-activated human neutrophils and monocytes produce large amounts of the chemokine IL-8, responsible for recruitment and priming of neutrophils via the IL-8 receptor (CXCR-2) [98; 99]. Previous animal studies have shown that CXCL1 and IL-1β are required for neutrophil recruitment [97; 61] while other pleiotropic mediators, such as granulocyte macrophage colony-stimulating factor (GM-CSF) [100], S100 proteins [81] and complement proteins [80], may also contribute to immune cell recruitment. MSU crystal-stimulated monocytes have been shown to produce TNFα and IL-1β, which prime neutrophils to produce reactive oxygen species (ROS) and augment their recruitment by upregulating the expression of adhesion molecules on endothelial cells [101; 102]. In addition, monocyte recruitment from the bone marrow to the site of inflammation is partially driven by MCP-1, a chemoattractant produced by resident cells [103; 104; 105]. Hence, there are a number of cytokines contributing to the onset and initiation of the inflammatory response in gout.

IL-1β and the inflammasome

MSU crystals stimulate macrophages to secrete the pro-inflamamtory cytokine IL-1β [61] that has been shown to play a pivotal role in gouty inflammation whereby the blockade of IL-1β abrogates inflammation [97]. The cleavage of preformed stores of pro-IL-1β into active IL-1β requires the assembly of a multi-protein complex referred to as the inflammasome [106]. In macrophages, the inflammasome is comprised of the intracellular pattern recognition receptor NACHT-LRR-PYD containing protein-3 (NLRP3), the accessory protein ASC and pro-caspase 1 [107]. Following activation by MSU crystals, the NLRP3 oligomerises and recruits ASC, then binds to pro-caspase 1 resulting in autocatalytic processing and activation [108]. Caspase 1 activation leads to pro-IL-1β cleavage and the secretion of active IL-1β from the cell, as illustrated in Figure 1.3. The pro-inflammatory cascade is further amplified after binding of IL-1β to IL-1R expressed on macrophages, endothelial cells, and neutrophils [97; 109; 110].

Recent studies demonstrated that mice deficient in components of the inflammasome or in IL-1R showed impaired neutrophil recruitment *in vivo* [97; 61]. Furthermore, using a combination of mouse knockouts and bone marrow chimeras, MyD88 signalling induced by IL-1R engagement on non-hematopoietic cells has been shown to be essential for the activity of IL-1β in neutrophil recruitment [97; 102]. These observations suggest that it is the non-hematopoietic cells in the peritoneum including endothelial cells and fibroblasts that respond to IL-1β, while bone marrow-derived monocytes and macrophages are the primary source of IL-1β. In addition, the blockade of IL-1β leads to dramatic improvement of symptoms in patients with gout [67; 68]. Collectively, these *in vitro* and *in vivo* animal studies have identified gout as an IL-1β-dependent auto-inflammatory disease. This has also been confirmed by clinical studies, which address the therapeutic effect of IL-1β blockade [111; 112].

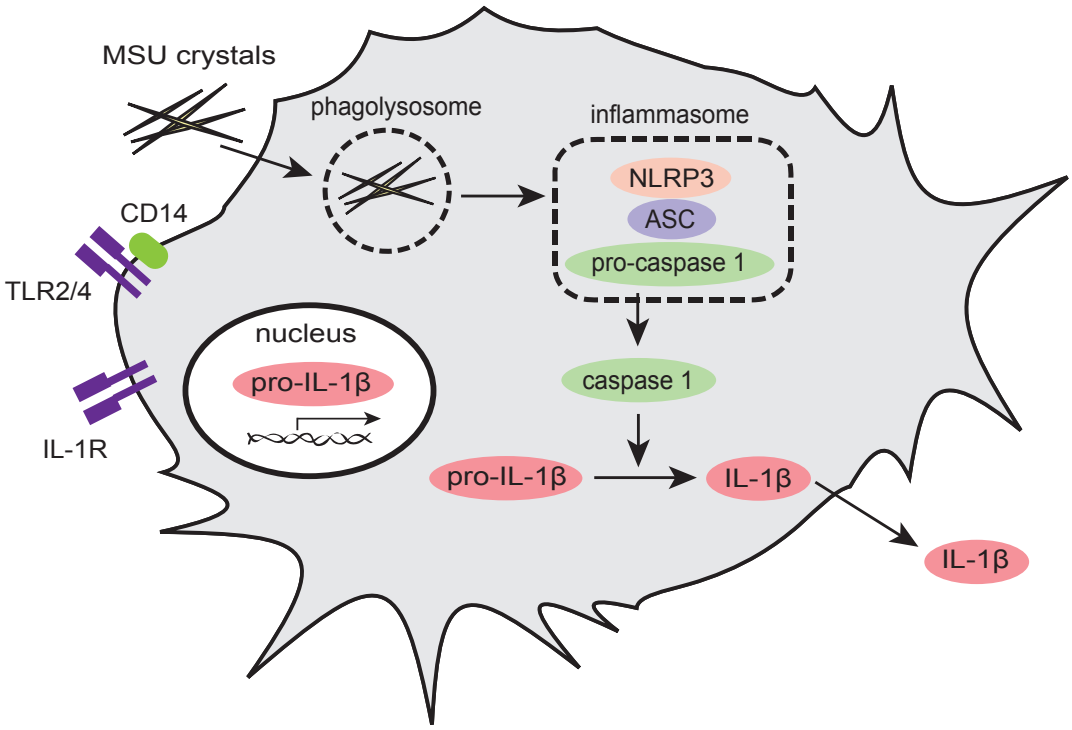

Figure 1.3: Schematic representation of the inflammasome - IL-1β signalling cascade. The uptake of MSU crystals by macrophages leads to the activation of the inflammasome assembly, which triggers active caspase 1 to cleave pro-IL-1β into its active form followed by IL-1β secretion.

1.8 Key innate cells in gout

The key cells involved in acute gouty inflammation are proposed to be neutrophils, monocytes and macrophages. Macrophages and monocytes are the main source of cytokine and chemokine production in gout, while activated neutrophils produce inflammatory mediators such as ROS that augment the inflammatory response and cause tissue damage. Due to their important functional activities, these three cell types will be the focus of this section.

1.8.1 Neutrophils in acute gout

Neutrophils, which are also referred to as polymorphonuclear leukocytes (PMNs), comprise 50 - 70% of circulating white blood cells in humans. When released from the bone marrow under homeostatic conditions, neutrophils have a very short life span and undergo apoptosis within 6 - 10 hours [113; 114] and are subsequently cleared from the circulation by liver and splenic macrophages [115].

I. Neutrophil recruitment

Neutrophils are usually the first cells recruited to the site of tissue damage or infection, and accumulate in high numbers, an important event in immune responses against invading pathogens [116; 117]. Once recruited, their role involves the uptake of pathogens and debris, and they produce hazardous molecules to kill and digest foreign organisms [118]. Recently, the formation of extracellular neutrophil traps (NETs) by neutrophils has been reported as an effective mechanism to trap and kill microbes to avoid the spreading of potential pathogens, thereby promoting the defence against infections [119; 120].

The identification of neutrophils in the synovial fluid is a hallmark for the diagnosis of acute gout. Here, cytokines and chemokines have been shown to strongly participate in neutrophil recruitment. Animal models of gout have demonstrated that IL-8

receptor (CXCR-2) [98] and IL-1β [97; 61; 121] are required for neutrophil recruitment, while other molecules such as TNFα, GM-CSF [100], S100A8 and S100A9 [81] and complement proteins [78; 80] are thought to augment neutrophil mobilisation. IL-1β and TNFα, mainly produced by MSU crystal-activated resident macrophages and monocytes, have been shown to upregulate the adhesion molecules E-selectin, intracellular adhesion molecule-1 (ICAM-1) and vascular cell adhesion molecule-1 (VCAM-1) by human endothelial cells allowing tethering of neutrophils to endothelial cells *in vitro* [102]. Additionally, a role for E-selectin expressed on endothelial cells in supporting neutrophil recruitment has also been shown in *in vivo* animal models of MSU crystal-induced inflammation [122; 123]. These data indicate that neutrophil recruitment is dependent on a number of cell types contributing to the acute inflammatory response.

II. Neutrophil activation

Neutrophil infiltrating the inflamed joints encounter and recognise MSU crystals, which results in their activation and subsequent amplification of inflammation, as illustrated in Figure 1.4. Neutrophil activation by MSU crystals has been proposed to be mediated by FcgRIIIB and the β2-integrin CD11b receptor [124]. On the other hand, the recognition of MSU crystals via TLR2 or TLR4, as previously shown for monocytes/macrophages, has not been assessed for neutrophils [96]. *In vitro* studies have shown that the tyrosine phosphatidylation pathways are important in the activation of human neutrophils by MSU crystals [125; 126; 127; 128].

III. Neutrophil function

Neutrophils exert their detrimental role in acute gouty inflammation through the release of inflammatory mediators including ROS, IL-1β, IL-6, IL-8 and S100A8/A9, and granule constitutes such as proteolytic enzymes and antimicrobial peptides [117; 129], as illustrated in Figure 1.4. Recently, a novel function of neutrophils has been described in gout: the release of NETs [130]. The formation of NETs by MSU crystal-activated neutrophils *in vitro* is linked with IL-1β and ROS production

as well as autophagy [130; 131]. Analysis of synovial fluid and tissue sections from gout patients revealed that NETs can be formed *in vivo*, thereby promoting the inflammatory response [131; 130]. Within the inflamed tissue, exposure to cytokines (such as IL-1β, TNFα and IFNγ), growth factors (such as G-CSF and GM-CSF) and MSU crystals have been shown to activate and subsequently prolong the half-life of recruited neutrophils from hours to days *in vitro* [132]. This may result in the accumulation of neutrophils within the inflamed environment in order to induce a prolonged pro-inflammatory response. Despite the prolonged lifespan of neutrophils treated with MSU crystals, a study has reported that phagocytosis of crystals by neutrophils results in the destabilisation of the phagosome and the leakage of lysosomal enzymes into the cytosol, which results in necrotic cell death and subsequent tissue damage [133] (Figure 1.4). Therefore, a major area of investigation is how neutrophils fit into the network of an inflammatory response and how their pro-inflammatory functions can be controlled to shut down acute inflammation.

1.8.2 Monocytes in gout

I. Monocyte populations and functions

Monocytes are phagocytic mononuclear cells and are thought to play a central role in gout. Two circulating monocyte populations have been identified expressing either low or high levels of Gr-1 in mice ($CD14^{low}$ or $CD14^{high}$ in humans) [134]. The Gr-1^{low} monocytes referred to as resident monocytes have the ability to remain within the bloodstream during homeostasis [134; 135]. Under steady-state conditions, this population migrates between bloodstream and tissue to sample the environment for danger signals [135]. The Gr-1^{high} inflammatory monocytes are recruited in large numbers to the site of inflammation via MCP-1 [134; 135]. *In vitro* studies have shown that murine monocyte-macrophage cell lines, which were exposed to MSU crystals produce TNFα and IL-1β [136; 137]. Freshly isolated human $CD14^{+}$ blood monocytes produced TNFα and IL-1β when stimulated with MSU crystals, indicating that monocytes contribute to gouty inflammation [137; 138]. In contrast,

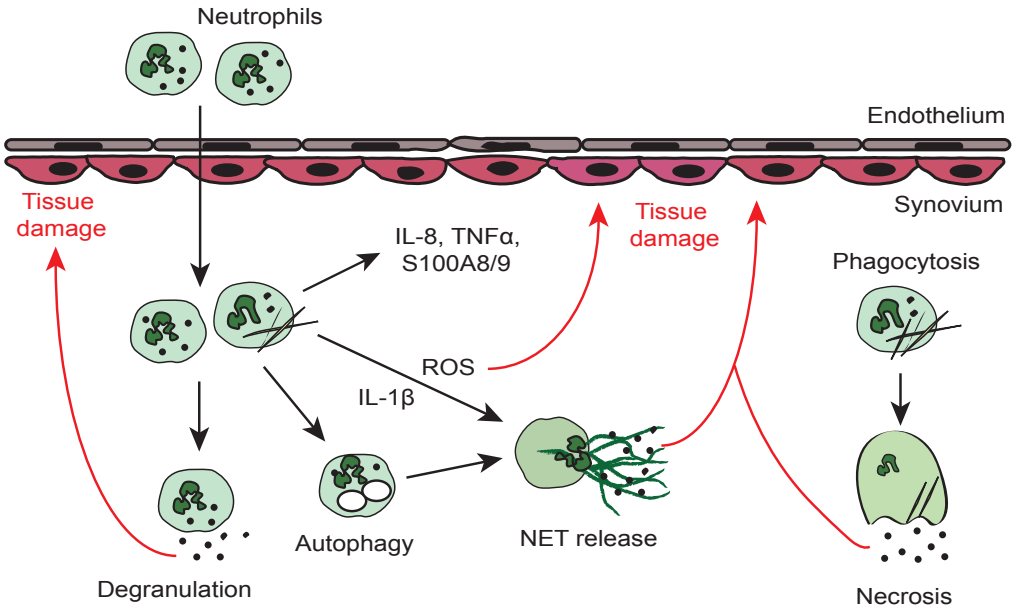

Figure 1.4: Schematic representation of activated neutrophils by MSU crystals. Once recruited, activation of neutrophils by MSU crystals induces degranulation and release of proteolytic enzymes, as well as the secretion of cytokines and inflammatory mediators. Autophagy, IL-1β and ROS are required for the formation of extracellular traps and delivery of neutrophil granular enzymes. Phagocytosis of MSU crystals results in necrotic cell death, which fuel inflammation. ROS production and neutrophils enzymes inflict tissue damage and promote inflammation.

Martin and colleagues have shown that early MSU crystal-recruited monocytes did not respond to MSU crystal stimulation suggesting that they may not be involved in the amplification of gouty inflammation *in vivo* [103].

II. Monocyte differentiation

Once monocytes are recruited from the circulation into the peripheral tissues they have the capacity to differentiate into a number of cell types depending on the local environment and tissue type (e.g. joint, skin, bone). Two important growth factors, GM-CSF and M-CSF have been identified as influencing the differentiation and functions of monocytes. Monocytes that are cultured *in vitro* in the presence of M-CSF will predominantly differentiate into macrophages representing an anti-inflammatory or tissue-like macrophage phenotype (M2-like cells) [139; 140;

141; 142]. Monocytes cultured in GM-CSF and IL-4 will become dendritic cells (DCs) [143], while monocytes cultured with RANKL and M-CSF become osteoclasts [144]. In the presence of high concentrations of GM-CSF, Verreck and colleagues have shown that human monocytes treated with GM-CSF can differentiate into pro-inflammatory macrophages *in vitro*, better known as M1-like macrophages [140; 141]. Furthermore, in a tumor environment M-CSF and IL-10 drive the differentiation of monocytes into alternative activated macrophages, also known as tumor associated macrophages (TAMs) [145; 146; 147; 148].

$CD14^+$ monocyte-differentiated macrophages stimulated with MSU crystals *in vitro* have been shown to lose their ability to produce pro-inflammatory cytokines and instead produce transforming growth factor $\beta 1$ (TGF$\beta 1$), a cytokine linked with the resolution of inflammation. This finding indicated a switch from a pro-inflammatory into an anti-inflammatory phenotype [137; 138]. In contrast, data from an *in vivo* model of gout demonstrated that MSU crystal-recruited monocytes differentiate into a pro-inflammatory (M1-like) macrophage phenotype [149]. Together, these findings highlight the complexity and importance of the inflammatory environment in determining the fate and function of monocytes.

1.8.3 Macrophages in gout

Macrophages are known for their heterogeneity and can be found in most tissues throughout the body, including alveolar macrophages of the lung, serosal macrophages of the peritoneum, type A cells in the joint synovium and microglia of the CNS [147]. Although these macrophages are phenotypically and functionally different depending on their environment, they share common characteristic features including phagocytosis, cytokine and chemokine production (IL-1β, TNFα, IL-6, IL-10, interferon γ (IFNγ), etc.) [150]. Macrophages can be identified by the expression of the M-CSF receptor (CD115, in mice) [151] and F4/80, a surface marker used to identify murine macrophages [152].

Primary and bone marrow-derived marophages have been reported to produce IL-1β, TNFα, MCP-1, IL-18, IFNγ and inducible nitric oxide synthase (iNOS) upon MSU crystal stimulation *in vitro* [61; 97; 153; 154; 155]. During MSU crystal-induced inflammation *in vivo*, depletion of resident macrophages resulted in the abrogation of IL-1β production and neutrophil recruitment [149], thus emphasising a key role for macrophages in the initiation of gouty inflammation. However, macrophages are also thought to be involved in the resolution of gout through the phagocytosis of apoptotic cells, which triggers the production of the anti-inflammatory cytokine TGFβ1 as well as allowing for the safe disposal of MSU crystals [138; 137]. These reports highlight the complexity of macrophage responses depending on the inflammatory environment and supports the need for further investigation into this area.

1.9 Mechanisms of spontaneous resolution of acute gouty inflammation

A characteristic feature of acute gout is its self-resolving nature. In the absence of clinical intervention, a gouty episode will spontaneously resolve after 7 - 10 days [17]. Surprisingly, the pathways behind the spontaneous resolution of gout are not fully understood. There are several regulatory mechanisms that can be linked with shutting down acute inflammation in gout. These are summarised in this section.

1.9.1 Protein coating of MSU crystals

The primary event driving a gout attack is the formation of MSU crystals in the joint. Early studies have described the coating of the MSU crystal surface as an important factor in regulating the inflammatory response [156]. Immunoglobulin G (IgG) coating of the crystals has been linked with driving the inflammatory phase [157], however, MSU crystals isolated during the resolution of inflammation shows

that this IgG coating is lost. There is evidence that activated neutrophils produce an, as yet unidentified, soluble mediator(s) that may interfere with the IgG coating of MSU crystals [158] thereby providing a potential negative feedback loop designed to limit the crystal-induced inflammation. Instead of IgG, MSU crystals isolated during the resolution phase of a gout attack are reported to bind the lipoproteins ApoB and ApoE [156]. ApoB and ApoE coating of MSU crystals has been shown to suppress MSU crystal-induced neutrophil activation [159; 160]. As such, apolipoproteins may play a role in masking MSU crystals from detection by local inflammatory cells and facilitate non-inflammatory crystal uptake and removal (Figure 1.5).

1.9.2 Danger signalling

MSU crystals trigger the release of active IL-1β via the cleavage of pro-IL-1β by the NLRP3 inflammasome. Classically, the signal for pro-IL-1β production is via pattern recognition receptors (PRRs), such as TLR2/4 (Figure 1.5), which are involved in driving inflammation by mediating crystal uptake as well as pro-IL-1β priming [161]. Inflammatory cells appear to shed these molecules during the latter stages of the inflammatory response to MSU crystals. This shedding would potentially abrogate crystal uptake and decrease the ability of cells to replenish stores of pro-IL-1β, thereby blocking the release of active IL-1β.

1.9.3 Pro-resolution mediators

There is a growing body of evidence linking lipid mediators, such as resolvins, protectins, lipoxins and maresins to the resolution of inflammation [162]. These bioactive molecules are generated from essential fatty acids such as omega-3 polyunsaturated acids and have been shown to limit neutrophil trafficking and survival, and enhance apoptotic cell clearance by macrophages [163; 164]. Currently there is little information on the role of these pro-resolution mediators in shutting down acute gout attacks, however, omega-3 fatty acids are able to inhibit NLRP3 inflammasome-

mediated IL-1β secretion and prevent NLRP3-dependent insulin resistance [165]. It is therefore likely that the local generation of omega-3-derived pro-resolution mediators in the joint contribute to the spontaneous resolution of gout (Figure 1.5).

1.9.4 Pro-inflammatory cytokine regulation

IL-1β production is widely accepted as central to the initiation of the inflammatory cascade that culminates in an attack of gout [61]. Studies have shown that MSU crystal-induced inflammation is impaired in mice deficient in IL-1β or IL-1R indicating that IL-1β production and IL-1R signalling play an essential role in driving the inflammatory response [61]. *In vitro* studies show that TGFβ1 can down-regulate IL-1R expression on hemopoietic cells [166; 167] suggesting that TGFβ1 production may contribute towards gout resolution by limiting IL-1β signalling. It is also possible that TGFβ1 can down-regulate the expression of IL-1R on the surrounding synovial tissues (Figure 1.5). This would be particularly important in gout resolution where amplification of IL-1β signalling is strongly linked to IL-1R expression on non-hemopoietic cells [97].

IL-1R antagonism is another mechanism used by the immune system to control IL-1β signalling. IL-1R antagonist (IL-1Ra) is an endogenous mediator that inhibits the pro-inflammatory effect of IL-1β by functioning as a competitive inhibitor of IL-1R [168; 169]. Both *in vitro* and *in vivo* studies have shown that IL-1Ra has the ability to block pro-inflammatory activities of the IL-1 cytokine family, thereby indicating a regulatory role for IL-1Ra in acute inflammation [170; 171; 172]. Elevated levels of IL-1Ra have been found in the synovial fluid from acute gout patients with resolving inflammation, which indicates a link between IL-1Ra production and the shutdown of IL-1β-driven inflammation [173]. Previous reports have also demonstrated that TGFβ1 can induce the secretion of IL-1Ra by human peripheral blood monocytes [174; 175] and the secretion of IL-1Ra by neutrophils has also been reported [176]. Consistent with IL-1Ra playing a role in gout resolution, a number

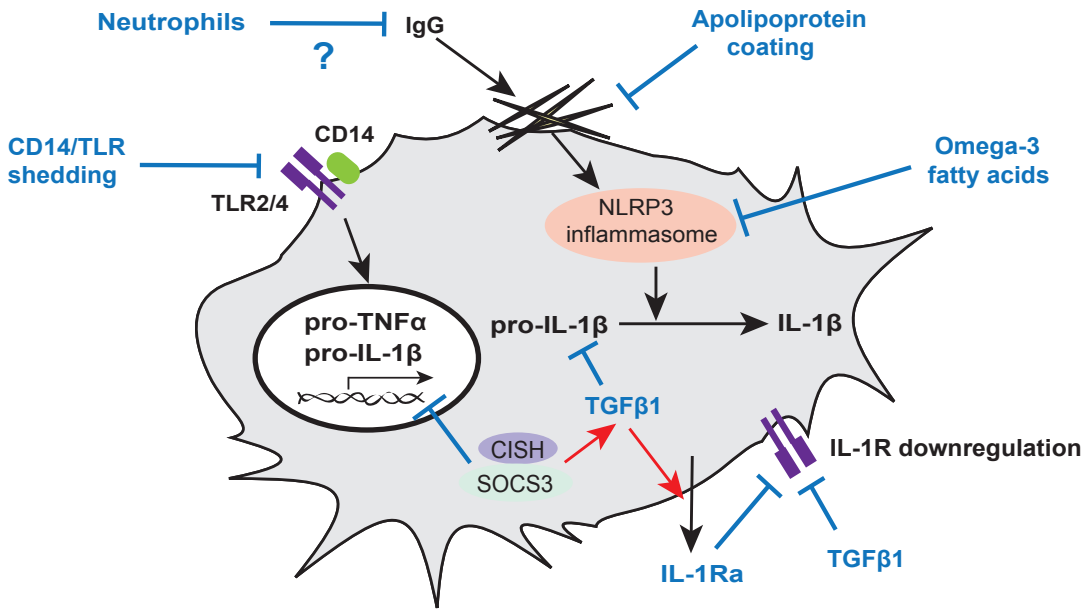

Figure 1.5: Macrophage-specific modulation of inflammatory signalling pathways in response to MSU crystals. Red arrows indicate increased activity, and blue lines represent an inhibitory or negative regulatory effect.

of clinical trials show that the recombinant IL-1Ra anakinra is highly effective at relieving acute gout attacks [67; 177; 178].

Synovial fluids from patients with gouty arthritis have been found to contain higher levels of soluble TNF receptors I and II (sTNFR-I/II) and IL-10 [47]. *In vitro* and *in vivo* studies show that extracellular release of soluble sTNFR-I/II acts to inhibit TNFα signalling by sequestering TNFα, whereas IL-10 has been shown to block MSU crystal-induced inflammation, including suppression of TNFα production *in vivo* [54]. This indicates a role for soluble cytokine receptors in the regulation of acute gout.

There is also evidence that intracellular, negative cytokine regulators could contribute to the resolution of an acute gout attack. Pro-inflammatory cytokine signalling is tightly controlled by a number of mechanisms including the signal transducers and activators of transcription (STATs), and suppressors of cytokine sig-

nalling (SOCS) [173; 179]. Chen and colleagues have shown that mononuclear cells and synovial tissue isolated from the synovium of gout patients significantly upregulate the expression of the SOCS family proteins cytokine-inducible SH2 protein (CISH) and SOCS3 compared to osteoarthritis patients [173]. Increased expression of CISH and SOCS3 is observed in MSU crystal-stimulated human monocyte-derived macrophages indicating that macrophage activation switches on these regulatory pathways. Overexpression of CIS is shown to decrease MSU crystal-induced IL-1β and TNFα production and, at the same time, enhance STAT3-mediated TGFβ1 transcription [173]. These data show a role for increased intracellular CISH and SOCS3 expression in the resolution of acute gout through the ability to negatively regulate pro-inflammatory cytokines, while simultaneously switching on anti-inflammatory cytokine production (Figure 1.5).

1.9.5 Non-inflammatory crystal clearance by macrophages

Previous work has shown that *in vitro*-generated macrophages can phagocytose MSU crystals in a non-inflammatory manner [137]. This implicates the differentiation of infiltrating monocytes into macrophages as a mechanism, which supports the safe removal of MSU crystals during gout as illustrated in Figure 1.6. However, *in vivo* data show that resident macrophages are essential for the induction of inflammation, and *in situ* differentiation of infiltrating monocytes in fact generates a highly pro-inflammatory macrophage phenotype [149]. Further research will be needed to unravel the exact role of this cell population in the progression and resolution of a gout attack.

1.9.6 Apoptosis, cell clearance and TGFβ1 production

Neutrophils are short-lived cells that undergo spontaneous apoptosis, a form of programmed cell death, which can be triggered by ROS production, calcium flux, the activation of caspases, cathepsins and pro-apoptotic proteins, as well as autophagy

[180; 181]. Neutrophil apoptosis then induces non-inflammatory cell clearance, a classical mechanism involved in shutting down inflammation. In MSU crystal-induced inflammation this has been associated with the clearance of apoptotic neutrophils by macrophages [182; 183], as illustrated in Figure 1.6. The importance of apoptotic cell clearance in the resolution of inflammation has been recently illustrated where deficiency of TG2 expression, a receptor shown to facilitate phagocytosis of apoptotic neutrophils by macrophages, leads to increased neutrophil accumulation and enhanced MSU crystal inflammation *in vivo* [184].

Clearance of apoptotic cells by macrophages is a process strongly linked with the production of TGFβ1 [182]. In patients with acute gout, TGFβ1 has been demonstrated to be present at a high level in the synovial fluid during the resolution phase of the inflammatory response [185; 186]. Gout patients carrying the TT genotype for the TGFβ1 polymorphism 869T/C have lower levels of TGFβ1 indicating a link between longer acute gout attacks and impaired TGFβ1 production [187]. Exogenous administration of TGFβ1 in rodent models of MSU crystal-induced inflammation has also led to significantly attenuated cellular recruitment [161]. Accordingly, the induction of TGFβ1 production via apoptotic cell clearance plays an important part in controlling gouty inflammation.

In vitro studies have shown that in the presence of IL-1β, TNFα and TGFβ1 monocyte-derived macrophages increase their ability to phagocytose apoptotic neutrophils [188]. MSU crystal-recruited monocytes display increased phagocytic activity as they differentiate *in vivo*, which indicates that these monocyte-derived macrophages may play a key role in inflammatory cell clearance in gout resolution [149]. It is therefore possible that the early inflammatory environment induced by MSU crystals actively supports clearance of apoptotic inflammatory cells thereby indirectly programming the shutdown of a gout attack (Figure 1.6).

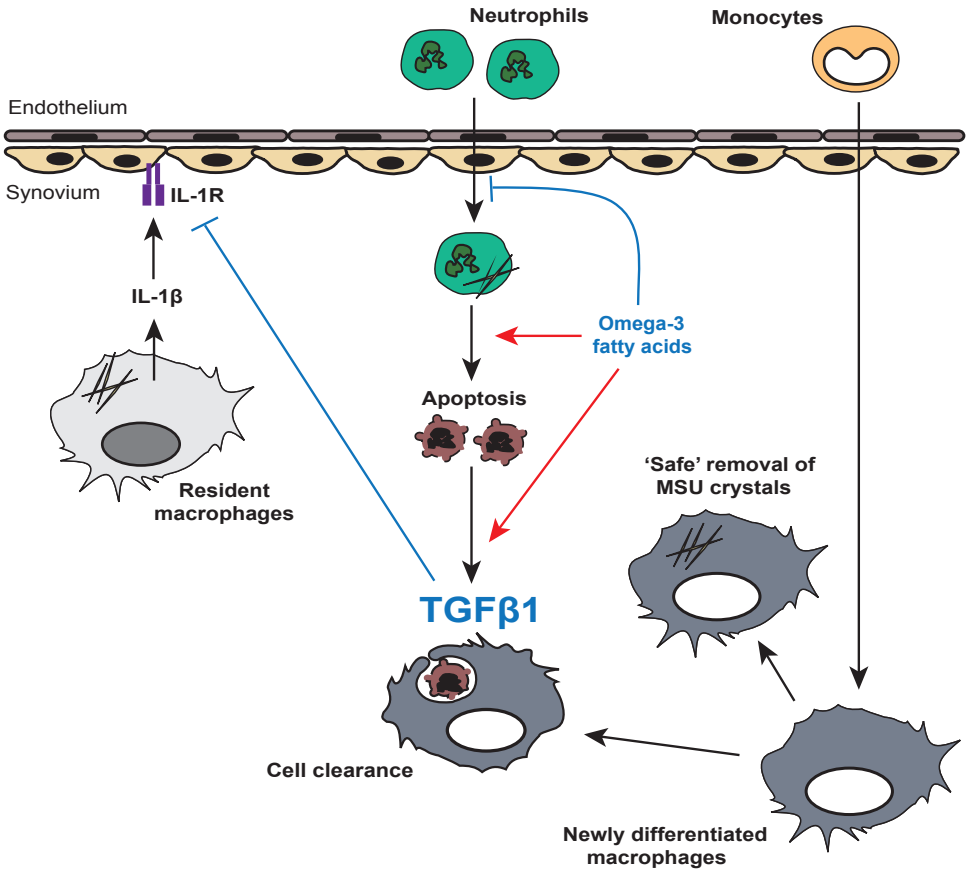

Figure 1.6: Cellular profile of mechanisms implicated in the self-resolving MSU crystal-induced inflammatory response. Red arrows indicate increased activity, and blue lines represent an inhibitory or negative regulatory effect.

1.10 Using research models to investigate gout

In order to study acute gouty inflammation it is necessary to develop research models. The first animal model for gout was introduced by Faires and McCarty, whereby they injected synthetic MSU crystals into dog knees [14]. Faires and colleagues were able to reproduce the same symptoms that they had observed in dogs, after they self-administered MSU crystals into their own knees, which included pain, swelling and redness.

1.10.1 Murine joint model of gout

Over the last decades, mouse and rat models have been developed for studying gouty inflammation in more detail. Even though using a murine model of joint inflammation better mimics the human joint synovial space, the small size of murine joints limits the range of investigations that can be performed. Because of this, alternative murine models have been established using either the peritoneum or the subepidermis to follow inflammatory responses to MSU crystals.

1.10.2 Murine peritoneal model of gout

The peritoneal model of gout was first used by Getting and colleagues [75]. The peritoneal cavity contains cell types similar to those in the joint synovium including macrophages, epithelial cells, mast cells, fibroblasts and lymphocytes. Injection of MSU crystals into the peritoneum triggers the recruitment of leukocytes including neutrophils and monocytes, as well as the production of cytokines and chemokines, which are known to be associated with acute gouty inflammation. However, limitations of this model include the absence of certain cell types such as osteoclasts and chondrocytes that are specific to bone niches, as well as the absence of tissue such as cartilage and bone. Moreover, due to the relatively large space within the peritoneum, the cavity is lacking the mechanically induced algesia caused by oedema, an event that normally occurs within the joint during a gout attack. Despite these disadvantages, this model has provided relevant immunological data, which has been verified by numerous clinical studies.

1.10.3 Murine air pouch model

In the air pouch model, a subcutaneous injection of sterile air on the back of rats (or mice) is performed in order to form an air sac, which mimics the joint synovium. Injection of MSU crystals into this space triggers the recruitment of leukocytes.

This particular model has been previously described by Schlitz and colleagues [189]. The limitations of this model are similar to the peritoneal model, whereby there is an absence of cell subtypes normally found within the bone niche. The formation of the air pouch may also initiate inflammation, which could cause a background inflammatory environment altering cell numbers or cell phenotype.

Within this thesis, the peritoneal model was chosen as inflammatory model for gout, as it induces an unmanipulated inflammatory background with cellular infiltration. The model also mimics clinical gout and is widely used in the literature.

1.11 Aims of this study

The research summarised in this chapter implicates neutrophils, monocytes and macrophages as the key cells in acute gout. To date, several mechanisms have been shown to be involved in the spontaneous resolution of gouty inflammation including cell clearance, TGFβ1 and monocyte differentiation. This thesis will address and clarify the role of TGFβ1 in acute gout, especially during the resolution phase and during monocyte differentiation.

Accordingly, the aims of this study are:

Aim 1: To identifiy macrophage-independent sources of TGFβ1 during the resolution phase of MSU crystal-induced inflammation and to determine the regulatory effect of TGFβ1 on neutrophil inflammatory functions.

Aim 2: To investigate the effect of TGFβ1 on the functional phenotype of *in vitro* differentiated GM-CSF and M-CSF bone marrow-derived macrophages.

Aim 3: To investigate changes in surface marker expression by macrophages in response to MSU crystals.

Chapter 2

2 Materials and Methods

2.1 Reagents

Buffer/Media	
Dulbecco's phosphate-buffered saline (D-PBS)	Life Technologies, NZ
Dulbecco's modified eagle's media & F12 nutrient mixture (DMEM/F12)	Life Technologies, NZ
Hanks' balanced salt solution (HBSS)	Life Technologies, NZ
Macrophage-serum free & specialty media (SFM)	Life Technologies, NZ
Roswell park memorial institute -1640 media (RPMI-1640) media	Life Technologies, NZ

Chemicals/Miscellaneous materials	
10% neutral buffered formalin	Sigma-Aldrich, NZ
β-Mercaptoethanol (β-ME)	Life Technologies, NZ
Acetone	Life Technologies, NZ
Ac-YVAD-CMK (caspase 1 inhibitor)	Cayman Chemicals, USA
β-glycerophosphate	Sigma-Aldrich, NZ
Biotinylated conjugated annexinV	BD Pharmingen, NZ
Blue-fluorescent reactive dye	Life Technologies, USA
Bovine serum albumin (Fraction V, IgG free)	Life Technologies, NZ
CytochalasinD	Life Technologies, NZ
Calcium pyrophosphate dihydrate	Sigma-Aldrich, NZ
Dihydrorhodamine (DHR)-123	Life Technologies, NZ
Ethanol	BDH Chemicals NZ Ltd.
Fetal bovine serum	Sigma-Aldrich, NZ
FITC annexinV	BD Bioscience, NZ
Fluospheres fluorescent microspheres (0.5 μm, 505.515 nm, 2% solids)	Life Technologies, NZ

Glutamax	Life Technologies, NZ
Glycine	BDH Prolabo, Belgium
GolgiStop	BD Bioscience, NZ
4-(2-Hydroxyethyl)piperazine-1 -ethanesulfonic acid (HEPES)	Sigma-Aldrich, NZ
Heparin	Hameln Pharmaceuticals GmbH, Germany
Igepal CA-630	Sigma-Aldrich, NZ
IL-6 neutralising antibody (clone: MP5-20F3)	eBioscience, USA
Lipopolysaccharide, *E. coli* 0111:B4 (LPS)	Sigma-Aldrich, NZ
Lympholyte-M cell separation solution	Cedarlane, Canada
Lymphoprep	Axis-Shield PoC AS, Norway
Recombinant murine GM-CSF	PeproTech, USA
Recombinant murine M-CSF	PeproTech, USA
Magnesium chloride	BDH Laboratory, UK
MES SDS running buffer (20x)	Novex, Life Technologies, USA
Methanol	BDH Chemicals NZ Ltd.
NuPAGE antioxidant	Life Technologies, USA
NuPAGE sample reducing agent (10x)	Life Technologies, USA
NuPAGE LDS sample buffer (4x)	Life Technologies, USA
NuPAGE 4-12% Bis-Tris gels	Life Technologies, USA
Novex sharp pre-stained protein standard	Novex, Life Technologies, USA
Penicillin-streptomycin	Life Technologies, NZ
Phenylmethylsulfonyl fluoride (PMSF)	Sigma-Aldrich, NZ
Phorbol myristate acetate (PMA)	Sigma-Aldrich, NZ
Prolong gold anti-fade with DAPI	Life Technologies, NZ
Propidium iodide	BD Bioscience, NZ
Protease inhibitor	Roche, Germany
Protein A - sepharose beads	BioVision Inc., USA
Puregene RBC lysis buffer	QIAGEN Science, Germany

Potassium chloride	Riedel-DE HAEN AG, Germany
PVDF membrane (protein blotting)	Bio-Rad, USA
Q-VD-OPh (general caspase inhibitor)	R&D Systems, USA
Saponin	Sigma-Aldrich, NZ
Sodium Azide	Sigma-Aldrich, NZ
Sodium chloride	BDH Laboratory, UK
Sodium dodecyl sulfate	BDH Chemicals NZ Ltd.
Sodium hydroxide (NaOH)	BDH Chemicals NZ Ltd.
TGFβ1 neutralising antibody	R&D Systems, USA
TNFα neutralising antibody	eBioscience, USA
Trypan blue stain	Life Technologies, NZ
Tween20	Sigma-Aldrich, NZ
UltraPure Tris	Life Technologies, NZ
Uric acid (UA)	Sigma-Aldrich, NZ
WST-1	Dojindo, Kumamoto, Japan
Z-IETD-FMK (caspase 8 inhibitor)	R&D Systems, USA

2.1.1 Antibodies for flow cytometry and immunofluorescent labelling

All antibodies used for flow cytometry or immunofluorescent labelling were titrated before use to determine the ideal concentration. For cell surface marker expression of fluorescently labelled antibodies, the corresponding isotype antibodies were used as experimental controls.

Antibodies	
AlexaFluor 555-streptavidin (SA)	Life Technologies, NZ
AlexaFluor 488 anti-mouse 7/4	AbD Serotec, USA
AlexaFluor 647 anti-mouse Ly49D	eBioscience, USA
APC rat anti-mouse CD11c	BD Bioscience, NZ
APC rat anti-mouse Gr-1	BD Bioscience, NZ

APC rat anti-mouse Ly6G	BD Bioscience, NZ
Biotinylated anti-mouse CD115	eBioscience, USA
Biotinylated anti-mouse Ly6G	BD Bioscience, NZ
Biotinylated anti-mouse NK1.1	eBioscience, NZ
FITC rat anti-mouse CD11b	BD Bioscience, NZ
FITC rat anti-mouse MHCII	BD Pharmingen, NZ
FITC rat anti-mouse 7/4	AbD Serotec, USA
FITC rat anti-mouse Ly49A	BD Pharmingen, NZ
FITC conjugated-streptavidin (SA)	eBioscience, NZ
FITC rat anti-mouse NK1.1	eBioscience, NZ
Mouse anti-TGFβ1 antibody (clone 2Ar2)	Abcam, UK
PE rabbit anti-active caspase-3	BD Bioscience, NZ
PE rat anti-mouse F4/80	Biolegend, USA
PE rat anti-mouse CD86	BD Bioscience, NZ
PE rat anti-mouse NK1.1	eBioscience, USA
PerCP rat anti-mouse F4/80	Biolegend, USA
PerCP rat anti-mouse Ly6G	BD Bioscience, NZ
PerCP Cy5.5 rat anti-mouse CD14	Biolegend, USA

Isotype controls

AlexaFluor 488 goat anti-mouse IgG1 (γ1 chain)	BD Bioscience, NZ
APC rat anti-mouse IgG1	eBioscience, NZ
Biotinylated rat anti-mouse IgG2a,κ	eBioscience, NZ
FITC rat anti-mouse IgG2b,κ	BD Pharmingen, NZ
FITC rat anti-mouse IgG2a,κ	eBioscience, NZ
PE rat anti-mouse IgG2a,κ	eBioscience, NZ
PerCP Cy5.5 rat anti-mouse IgG2a,κ	eBioscience, NZ

Others

Anti-mouse FcγRII antibody (2.4G2) was kindly provided by Thomas Backstrom from the Malaghan Institute of Medical Research.

2.1.2 Antibodies for western blotting and immunoprecipitation

All antibodies used for western blotting and immunoprecipitation were polyclonal antibodies with a mouse and human species reactivity and used at concentrations recommended by manufacturer's instructions.

Antibody	*Molecular weight*	*Source*
Anti-ASC/TMS1	22kDa	Novus Biologicals, USA
Anti-cIAP1	69 kDa	Abcam, UK
Anti-caspase 1/ICE	pro form: 45 kDa active form: 20 kDa	Invitrogen, USA
Anti-CIAS1/NALP3	116 kDa	Abcam, UK
Anti-caspase 8	pro form: 54/56 kDa p41/43 subunit active form: 18/10 kDa	R&D Systems, USA
Anti-hIL-1	pro form: 35 kDa active form: 17 kDa	BioVision Inc, USA
Anti-β-actin	42 kDa	Sigma-Aldrich, USA
RIPK1	74 kDa	Novus Biologicals, USA
RIP3	57 kDa	ProSci Inc., USA
Goat anti-rabbit IgG-HRP		SantaCruz Biotech, USA
Goat anti-mouse IgG-HRP		SantaCruz Biotech, USA

2.1.3 Kits

Biotin/Avidin blocking kit	Invitrogen, NZ
Bioplex bead array kits	Bio-Rad, CA, USA
Diff-Quik kit	Dade Behring, Newark, USA
IL-1β ELISA kit	R&D Systems, Minneapolis, USA
Limulus amebocyte lysate kit	Associates of Cape Cod, Inc., Falmouth, MA, USA
TGFβ1 ELISA kit	R&D Systems, Minneapolis, USA

2.2 Buffers and Media

AnnexinV binding buffer

The efficient binding of annexinV to phosphatidylserine on the surface of apoptotic cells requires a high calcium-containing buffer. This buffer was composed of PBS, 10 mM HEPES, 140 mM NaCl and 2.5 mM $CaCl_2$ at pH 7.4 and filtered sterile. Storage at 4°C, used within one month of preparation.

FACS buffer

FACS buffer was used as staining media to label cell surface markers with fluorescent antibodies. This solution contained 0.1% bovine serum albumin (BSA) and 0.01% sodium azide in PBS (pH 7.4). Storage at 4°C.

Red Blood Cell (RBC) lysis buffer

Endotoxin-free puregene RBC lysis buffer was used to remove contaminating red blood cells from blood and bone marrow samples as well as peritoneal lavage fluids as required. Cells were suspended in 5 ml RBC lysis buffer and incubated for 10 minutes at 37°C, washed twice in D-PBS and resuspended in the appropriate media. If RBC lysis was incomplete, the process was repeated.

Complete media

Endotoxin-free RPMI-1640 and DMEM/F12 media were purchased from Invitrogen. In all cases in which the term 'complete media' appears, refers to media supplemented with 10% FBS, 100 units/ml penicillin-streptomycin and 2 mM glutamax. Stored at 4°C, but used for cell preparation at room temperature.

PBS buffers

There were two sources of PBS used:

1. **PBS**: PBS powder was purchased from Life Technologies, made up to the appropriate volume in distilled water and the pH adjusted to 7.4 according to manufacturer's instruction. This PBS buffer was used for procedures, which did not require endotoxin-free PBS, such as FACS buffer, annexinV buffer and saponin buffer.
2. **D-PBS**: Endotoxin-free PBS in liquid form as D-PBS, and used to harvest and wash cells, which were used in culture.

Saponin buffer

Saponin buffer was used to permeabilise the cell membrane, to allow intracellular staining with fluorescent antibodies. This buffer was composed of 0.1% saponin, 0.1% BSA and 0.01% sodium azide in PBS buffer and stored at 4°C.

Blocking buffer for immunofluorescent labelling

Blocking buffer was used to block non-specific binding sites for fluorescent labelling of cells with antibodies. The blocking buffer was composed of 0.1% saponin, 0.1% BSA, 0.01% sodium azide and 10% FBS in D-PBS. Stored at 4°C.

Protein lysis buffer

Isolation buffer was used for isolating cytoplasmic protein from *ex vivo* cultured murine cells. The buffer was composed of 10 mM HEPES, 1.5 mM $MgCl_2$, 10 mM KCl, 10 mM Na_2MoO_4 in distilled water and stored at 4°C. A mix of proteinase inhibitors, 20 mM β-glycerophosphate, 2 mM Na_3VO_4 and 1 mM phenylmethylsul-

fonyl fluoride (PMSF) were added into the isolation buffer and kept on ice before use.

Transfer buffer

Transfer buffer was used to transfer proteins from the gel onto a PVDF membrane. The transfer buffer was composed of 100 ml of TG stock buffer (containing 3% Tris, 14.4% Glycine in distilled water), 200 ml methanol, 700 ml distilled water and 1 ml of 10% sodium dodecyl sulfate (SDS). Stored at 4°C.

Stripping buffer

Stripping buffer was used to disrupt primary and secondary antibody binding on the western blot membrane. The buffer was composed of 0.1 M Glycine dissolved in 200 ml PBS buffer (pH 2). Before use, 2% Tween20 was added into buffer.

2.3 Preparation of crystals

Monosodium urate crystals (MSU)

MSU crystals were prepared as follow: 250 mg uric acid was boiled in 45 ml of 30 mM NaOH/MilliQ water until completely dissolved. The uric acid solution was filtered sterile using a 0.2 μm vacuum driven disposable bottle top filter, and stored at 26°C for 7 days to encourage the formation of crystals. The resulting MSU crystals were washed with ethanol and acetone and then air-dried under sterile conditions. The MSU crystals were needle shaped (5 - 25 μm in length) and showed optical birefringence under the microscope [103]. MSU crystals used were endotoxin free as determined by *Limulus* amebocyte lysate (LAL) assay kit ($<$ 0.01 EU / 10 mg).

Other crystal types used for in vitro assays

Magnesium urate (MgU) crystals, calcium urate (CaU) crystals, potassium urate (KU) crystals and ammonium urate (NH4U) crystals were made and kindly provided by Henry Hudson, Malaghan Institute of Medical Research. Calcium pyrophosphate dihydrate (CPPD) was purchased from Sigma-Aldrich, NZ.

2.4 Endotoxin levels

As bacterial endotoxin can activate innate immune cells, all glassware and reagents used for cell culture were both sterile and endotoxin free. All plasticware such as microplates, flasks, culture tubes and pipettes were endotoxin free. All reagents used were either certified as low endotoxin or tested for endotoxin levels by LAL assay.

2.4.1 *Limulus* amebocyte lysate (LAL) assay

The LAL assay kit contains *E. coli* control endotoxin standard, chromogenic substrate and endotoxin-free water. The chromogenic LAL assay measures the endotoxin levels in the samples such as MSU crystals by reading the absorbance at 405 nm. The following were tested for endotoxin levels by LAL assay kit.

MSU crystals	< 0.01 EU / 10 mg
MilliQ water	< 0.01 EU / ml
Cleaned and autoclaved glassware	< 0.01 EU / ml

2.4.2 Purchased reagents

5 M NaCl	Sigma-Aldrich, NZ	< 0.3 EU / ml
D-PBS	Invitrogen, NZ	< 0.03 EU / ml
RPMI-1640	Invitrogen, NZ	< 0.03 EU / ml
HBSS	Invitrogen, NZ	< 0.03 EU / ml
Puregene RBC lysis buffer	QIAGEN, CA, USA	< 0.03 EU / ml
Fetal bovine serum	Sigma-Aldrich, NZ	< 0.13 EU / ml

2.5 Animal studies

2.5.1 Maintenance and ethical approvals

All mice were bred and housed in a conventional animal facility at the Malaghan Institute of Medical Research, Wellington, New Zealand. All animals used for the experiments were aged between 8 - 10 weeks. The experiments were approved by the Victoria University Animal Ethics Committee and carried out in accordance with the Commitee's guidlines for the care of animals (Ethics approval numbers 2011R19M and 2012R17M).

2.5.2 Mouse strain sources

C57Bl/6J male mice were originally purchased from the Jackson Laboratory (Bar Harbour, ME, USA).

OTII male mice expressing the transgenic T cell receptor specific for $OVA_{323-339}$ presented on I-A^b respectively were originally obtained from Professor Frank Carbone, Melbourne University (Melbourne, Victoria, Australia).

2.5.3 Murine peritoneal model of MSU crystal-induced inflammation

C57Bl/6J male mice were injected intraperitoneally (i.p.) with 3 mg MSU crystals suspended in 0.5 ml D-PBS and at different time points mice were sacrificed by carbon dioxide asphyxiation followed by cervical dislocation.

Blood was then collected by cardiac puncture into 1.5 ml eppendorf tubes containing 50 μl of 125 units/ml heparin in D-PBS and stored on ice.

The peritoneal exudate cells (PECs) were harvested by peritoneal lavage from naive and MSU crystal-treated mice. 3 ml of D-PBS containing 25 units/ml heparin

was injected into the peritoneum near the inguinal fat pads. The peritoneum was then massaged for 10 seconds before the lavage fluid was withdrawn using the same syringe needle and placed on ice.

2.5.4 *In vivo* TGFβ1 neutralisation

For TGFβ1 neutralising experiments *in vivo*, C57Bl/6J mice were injected with 1 mg of the anti-TGFβ1 antibody 30 minutes prior to MSU crystal administration. After 8 and 18 hours, the mice were euthanised by carbon dioxide asphyxiation followed by cervical dislocation.

2.6 Processing and isolation of cell types

2.6.1 Preparation of peritoneal lavage cells

PECs from naive and MSU crystal-treated mice were harvested by peritoneal lavage as described in section 2.5.3. Cells were retrieved from the lavage fluid by centrifugation (1500 rpm, 5 minutes) and washed twice with D-PBS. The lavage supernatants were stored for cytokine/chemokine analysis at -20^{o}C (section 2.8) and the pelleted cells resuspended in complete RPMI-1640 for further analysis.

2.6.2 Preparation of mouse blood

Blood was collected by cardiac puncture from MSU crystal-treated mice. Under sterile conditions, the red blood cells were lysed by resuspending the blood in 5 ml RBC lysis buffer and incubated at 37°C for 15 minutes. Cells were subsequently washed twice with D-PBS by centrifuging at 1500 rpm for 5 minutes before further separation steps were performed.

2.6.3 Preparation of cells from lymph nodes

OTII mice were euthanased by carbon dioxide asphyxiation followed by cervical dislocation. The inguinal and mesenteric lymph nodes were removed and disrupted with the back of the plunger of a 1 ml syringe and flushed with complete RPMI-1640 through a 40 μm nylon cell strainer into a 50 ml Falcon tube. The suspension was then centrifuged at 1500 rpm for 5 minutes and any red blood cells were lysed as described in section 2.2, if required. Cells were washed twice and resuspended in complete RPMI-1640, and placed on ice until further use.

2.6.4 Extraction and preparation of bone marrow cells

C57Bl/6J mice were euthanased by carbon dioxide asphyxiation followed by cervical dislocation. The hind leg bones were detached from the hip, and muscle and connective tissue removed from the femur and tibia. These were placed in RPMI-1640 on ice. Under sterile conditions, the ends of the bones were snipped and the bone marrow cells flushed into a 50 ml Falcon tube using a 25-gauge needle and a 10 ml syringe containing DMEM/F12. The cell suspension was strained through a 40 μm cell strainer and washed once with DMEM/F12. Red blood cells were lysed for blood (section 2.2) and immediately washed twice and resuspended in 5 ml DMEM/F12. 5 ml of Lymphoprep cell separation media was added below the cell suspension using a sterile disposable glass pasteur pipette (Poulten + Graf Ltd., Germany) and centrifuged at 1600 rpm for 20 minutes (with brake off). The cells were gently removed from the interface using a sterile transfer pipette, washed twice with complete DMEM/F12 and then resuspended at the appropriate concentration.

2.6.5 Enrichment of MSU crystal-recruited peritoneal and blood neutrophils

Peritoneal exudate cells were harvested by lavage from C57Bl/6J mice treated with MSU crystals for 8 and 18 hours (section 2.5.3) and prepared as described in section 2.6.1. Individual samples were pooled in sterile 15 ml tubes, washed twice in D-PBS and resuspended in 5 ml D-PBS. 4 ml of Lympholyte-M cell separation media was added below the cell suspension using a sterile disposable glass pasteur pipette and the cells were centrifuged for 20 minutes at 2400 rpm at 10°C. The supernatant was carefully removed by decanting, and the pelleted neutrophil fraction washed twice in D-PBS, then resuspended in complete RPMI-1640 and placed on ice until further use.

The blood cells were processed as described in section 2.6.2. After red blood cell lysis, cells were resuspended in 5 ml D-PBS and 4 ml of Lympholyte-M cell separation media was added below the cell suspension following centrifugation for 20 minutes at 2400 rpm at 10°C. The enriched blood neutrophils were collected from the bottom of the 15 ml tube, washed twice in D-PBS and resuspended in complete RPMI-1640. Cells were kept on ice until further use.

2.6.6 Cell counting

Cells were counted by using 10 μl of the cell suspension mixed with 90 μl of 0.4% Trypan Blue Stain. This mixture was placed on a haemocytometer and the viable cells that did not contain the dye were counted under 10x magnification with an Olympus BX40 (Olympus, Central Valley, PA, USA) microscope.

2.7 *Ex vivo* and *in vitro* assays

2.7.1 *Ex vivo* neutrophil assays

Blood and peritoneal neutrophils from 8 and 18 hour MSU crystal-treated mice were purfied by density gradient (section 2.6.5) and cultured *ex vivo* at 2x10^5 cells/ml, 200 μl per well in 96-well flat-bottom plates (Falcon BD Labware, USA). Cells were incubated in the presence or absence of MSU crystals (200 μg/ml) for up to 24 hours at 37°C. At various times, supernatants were collected and stored at -20°C until analysis. Neutrophils were then harvested and analysed for the expression of the surface marker annexinV, CD11b, Ly6G and Gr-1 as well as for intracellular caspase 3 and TGFβ1 by flow cytometry (section 2.9).

In assays investigating intracellular expression of TGFβ1, neutrophils were cultured in the presence of GolgiStop (1:1000) to block cytokine secretion.

To investigate the effect of apoptosis, phagocytosis and TGFβ1 on neutrophil function, purified neutrophils were incubated in the absence or presence of a general caspase inhibitor Q-VD-OPh (20 μM), the phagocytosis inhibitor CytochalasinD (20 μg/ml) or with the anti-TGFβ1 antibody (35 μg/ml) over time.

2.7.2 Neutrophil phagocytosis assay

MSU crystal-recruited peritoneal neutrophils were isolated and purified as described in section 2.6.5. Neutrophils were labelled with PerCP-Ly6G and then incubated *ex vivo* for 18 hours in serum free RPMI-1640 to induce apoptosis. Apoptotic neutrophils (PerCP-Ly6G$^+$) were then co-incubated in RPMI-1640 with freshly isolated MSU crystal-recruited live neutrophils that had been labelled with APC-Ly6G (apoptotic cell:live cell ratio 5:1) in the presence of GolgiStop (1:1000). After 8 hours, the cells were harvested and analysed by flow cytometry for the expression of APC-Ly6G, PerCP-Ly6G, and intracellular TGFβ1. Live neutrophils that had

phagocytosed apoptotic neutrophils were identified as APC-Ly6G$^+$/PerCP-Ly6G$^+$ cells (double positive cells).

2.7.3 Measurement of neutrophil superoxide production

Neutrophil superoxide production was measured using the colorimetric dye water-soluble tetrazolium 1 (WST-1) as previously described by Tan and colleagues [190].

Purified MSU crystal-recruited neutrophils were suspended in phenol red-free RPMI-1640 and added to a 96-well flat-bottom plate at 2x10^5 cells per well with 250 μg/ml WST-1 and incubated with anti-TGFβ1 antibody (35 μg/ml) or MSU crystals (200 μg/ml) or with a combination of both reagents at 37°C for 1 hour. After 1 hour, MSU crystals were removed from the supernatant by centrifugation and 100 μl of the crystal-free supernatants was transferred into another 96-well flat-bottom plate. The plate was loaded into a Versamax spectrophotometer (Molecular Devices) and the absorbance (450 nm) measured.

2.7.4 Differentiation of bone marrow-derived macrophages

Bone marrow cells were obtained as described in section 2.6.4. The viable cells were adjusted to a concentration of 4x10^6 cells/ml in complete DMEM/F12 media containing 50 μM β-ME supplemented with either 1000 units/ml GM-CSF or 5000 units/ml M-CSF, and cultured in T25 culture flasks (5 ml of 4x10^6 cell suspension per flask) overnight. On day one, the non-adherent cells were collected and resuspended at 1x10^6 cells/ml in complete DMEM/F12 media containing either GM-CSF or M-CSF. The GM-CSF and M-CSF cell suspensions were then plated at 1x10^6 cells/3 ml in six-well plates and treated either with 1 ng/ml or 10 ng/ml recombinant human TGFβ1, or left untreated. The cells were fed on day three and five, each time by replacing 1 ml media with 1 ml fresh complete DMEM/F12 containing either 1000 units/ml GM-CSF or 5000 units/ml M-CSF and/or 1 ng/ml or 10 ng/ml

rhTGFβ1. On day seven, supernatants from the cell cultures were collected and the cells washed twice with D-PBS before fresh complete DMEM/F12 media was added. The GM-CSF and M-CSF macrophages were then primed with 50 pg/ml LPS overnight. Following LPS priming, supernatants were collected and BMMs washed with D-PBS, and complete macrophage-SFM media added to the cell culture.

In assays investigating the effect of TGFβ1 on bone marrow-derived macrophages (BMMs) after they have been differentiated with either GM-CSF (1000 units/ml) or M-CSF (5000 units/ml) for seven days, BMMs were treated with 1 ng/ml or 10 ng/ml rhTGFβ1, or left untreated for one day or for an additional five days. After treatment with TGFβ1 for one or five days, cells were washed twice with D-PBS and fresh complete DMEM/F12 media containing 50 pg/ml LPS was added overnight. Following LPS priming, TGFβ1-differentiated BMMs were washed with D-PBS and complete M-SFM media added to the cell culture before stimulation assay was carried out (section 2.7.5).

2.7.5 TGFβ1-differentiated BMM stimulation assay

TGFβ1-differentiated GM-CSF and M-CSF BMMs were obtained as described in section 2.7.4. After LPS priming, 2 ml of complete M-SFM media was added to the BMM cell culture (1x10^6 cells per well in six-well plates) and the cells were either left unstimulated or treated with 200 μg/ml MSU crystals, 100 ng/ml LPS and/or in the prescence of the caspase 1 inhibitor YVAD (10 μg/ml) or the caspase 8 inhibitor IETD (10 μM) or a combination of both inhibitors, and incubated for 18 hours at 37°C. After incubation, supernatants were collected and stored at -20°C for cytokine analysis (section 2.8), and BMMs were harvested and analysed for the expression of surface markers by flow cytometry (section 2.9). In other experiments, BMMs were washed with D-PBS and prepared for the isolation of cytoplasmic protein for western blot analysis (section 2.11).

Next to stimulation with MSU crystals and LPS, TGFβ1-differentiated BMMs were also stimulated *in vitro* with Pam3Cys (100 ng/ml) or left untreated for 18 hours. Supernatants from the cell culture were collected and analysed for IL-1β by ELISA (section 2.8).

2.7.6 *In vitro* T cell proliferation assay

In vitro T cell proliferation assays were performed for $CD4^+$ T cells from OTII mice. GM-CSF and M-CSF BMMs (section 2.7.4) were incubated with 100 ng/ml LPS in complete RPMI-1640 for 18 hours. After incubation, LPS-primed BMMs were washed and harvested using cold D-PBS to detach the cells from the bottom of the 6-well plates. GM-CSF and M-CSF BMMs were then resuspended in complete RPMI-1640 and loaded with 1 μM ISQ peptide ($OVA_{323-339}$ protein) specific for CD4 T cell cross-presentation. During the 2 hour incubation with peptide, lymph nodes were harvested from OTII mice and made into cell suspension as described in section 2.6.3. Following peptide loading, BMMs were washed and resuspended at $1x10^5$ cells/ml in complete RPMI-1640, and serially titrated at 2 fold dilution with a starting concentration of $1x10^4$ cells per well into 96-well culture plates. BMMs were either stimulated with 200 μg/ml MSU crystals or left untreated prior to the addition of T cells, at $1x10^5$ cells/well and the cells were then incubated for 3 days at 37°C. After incubation, 1 μCi $[^3H]$-thymidine (GE Healthcare, UK) was added to each well and incubated for an additional 18 hours. Cells were harvested onto filtermats (PerkinElmer Life Science, Finland) using an automated cell harvester (Tomtec Inc., USA). Thymidine incorporation was used to measure T cell proliferation using a Wallac 1450 MicrobetaPlus Liquid Scintillation Counter (Wallac, USA).

2.7.7 Measurement of intracellular ROS production by BMMs

To measure intracellular ROS production by TGFβ1 differentiated BMMs (section 2.7.7), cells were suspended in HBSS and transfered into a 96-well flat-bottom plate

at 1x10^5 cells per well with 10 μM DHR-123 solution and incubated at 37°C for 5 minutes to allow DHR-123 uptake. After incubation, cells were washed and then stimulated with MSU crystals (200 μg/ml) or PMA (0.2 μg/ml) at 37°C for 45 minutes. The reaction was then stopped by placing the cell culture plate on ice. As controls, BMMs were also incubated with DHR-123 solution following stimulation with MSU crystals and PMA at 4°C for 45 minutes. The cells were stained for the surface marker F4/80, CD11b and CD14 using cold FACS buffer and analysed for their expression by flow cytometry (section 2.9).

2.7.8 *In vitro* peritoneal macrophage assays

Peritoneal exudate cells (PECs) from naive mice were obtained as described in section 2.6.1. The peritoneal macrophages were resuspended in complete macrophage-SFM media and cultured at 2x10^5 cells/ml, 200 μl per well in 96-well flat-bottom plates.

Stimulation of macrophages

Macrophages were plated as above and stimulated with different crystals MSU, CPPD, CaU, MgU, NH4U and KU (200 μg/ml) and non-crystalline 100 ng/ml LPS for up to 24 hours at 37°C. At different time points, supernatants were collected and stored at -20°C for further analysis (section 2.8). Cells were harvested and analysed for the expression of the surface markers NK1.1, CD11b, F4/80, Ly49A and Ly49D as well as the apoptotic markers annexinV and caspase 3 by flow cytometry (section 2.9).

Blockade of cytokines and apoptosis

In assays investigating the effect of cytokines on NK1.1 expression, macrophages were cultured in the absence or presence of anti-IL-1β (5 μg/ml), the caspase 1 inhibitor YVAD (10 μg/ml), anti-IL-6 (5 μg/ml), anti-TNFα (5 μg/ml) and caspase 8 inhibitor IETD (10 μM). After 1 hour, macrophages were stimulated with 200

μg/ml MSU crystals or left untreated, and at different time points supernatants were collected and cells harvested and prepared for flow cytometry as above.

Phagocytosis assay

In assays investigating the effect of phagocytosis on the expression of NK1.1, macrophages were stimulated with 200 μg/ml MSU crystals or co-cultured with apoptotic neutrophils (apoptotic neutrophils:macrophages, cell ratio 5:1) or fluorescent beads for up to 24 hours. Phagocytosis was inhibited using CytochalasinD (10 μg/ml). At different time points, supernatants were collected for cytokine analysis (section 2.8), and cells harvested and analysed for surface marker expression of NK1.1, F4/80, CD11b and Ly6G by flow cytometry (section 2.9).

2.8 Cytokine analysis

Cytokine levels from the peritoneal lavage fluid and culture supernatants were assayed either by multiplex bead array (section 2.1.3) and analysed on a Bioplex flow cytometer, or with ELISA kits (section 2.1.3) and analysed on a Versamax spectrophotometer. Each measurement system was used according to manufacturer's instructions.

Cytokines	Measurement system
IL-1β, TGFβ1	ELISA
IL-1α, TNFα, IL-6, CXCL1, MCP-1	Multiplex bead array

2.9 Flow cytometry

For cell surface labelling, 200 μl of the cell suspension was transfered into a 96-well round-bottom plate. The cells were centrifuged for 5 minutes at 1500 rpm, the supernatants decanted and the cells were then incubated with anti-mouse FcγRII

antibody (2.4G2) (section 2.1.1) in 50 μl FACS buffer for 10 minutes at 4°C. After incubation, cells were washed in FACS buffer and incubated with the appropriate 25 μl master mix of fluorophore-labelled antibodies (section 2.1.1) or blue-fluorescent reactive dye (Life Technologies, USA) for 15 minutes at 4°C. Isotype-matched antibodies were used as experimental controls. Cells were then washed in 200 μl FACS buffer, filtered through gauze (20 μm) and transferred into Titertube micro tubes (Bio-Rad, USA). Flow cytometry analysis was performed on a BD FACSCalibur (BD, USA) and the data then analysed using the software FlowJo 9.7.4 (Tree Star Inc., Ashland, OR, USA).

2.9.1 AnnexinV / propidium iodide (PI) staining

Apoptotic and necrotic cell death of cells was determined by using fluorescently labelled annexinV protein and PI. PI binds to the DNA when the cell membrane becomes permeable. The viable cells were identified as double negative cells (annexinV^- /PI^-), while annexinV single positives indicated early apoptotic cells and PI single positive as necrotic cells. Late apoptotic were annexinV^+/PI^+.

At different time points, cells (200 μl) were transferred into a 96-well plate and centrifuged (1500 rpm, 5 minutes), the supernatants decanted and the cells resuspended in annexinV binding buffer. Non-specific binding was blocked using anti-mouse FcγRII antibody (2.4G2) for 10 minutes at 4°C. After incubation, cells were washed in 200 μl annexinV binding buffer and stained with FITC-annexinV for 15 minutes at 4°C. Cells were washed and resuspended in annexinV binding buffer. 5 minutes before analysis, 10 μg/ml PI was added to the samples and annexinV/PI staining determined using a FACSCalibur flow cytometer.

2.9.2 Intracellular staining of cells

Cells were labelled with the cell surface markers (such as F4/80, CD11b or Ly6G) as described above in section 2.9 and then fixed with 10% neutral buffered formalin for 10 minutes at room temperature. Cells were then washed and incubated in saponin buffer for 20 minutes at 4°C. Following incubation, cells were stained with the antibodies TGFβ1 - IgG1-AlexaFluor 488, NK1.1-FITC and the apoptosis marker caspase 3 (section 2.1.1) for 30 minutes at 4°C. After intracellular antibody staining, cells were washed and resuspended in FACS buffer, and flow cytometry analysis was performed on FACSCalibur.

2.10 Histology

2.10.1 Morphological staining of cells

Diff-Quik staining was used to visualise the morphology of cells harvested from the peritoneal lavage samples. 100 μl of cells (1x10^6 cells/ml) were centrifuged for 5 minutes at 800 rpm onto glass slides (LabServ, NZ) using a Shandon Cytospin 4 cytocentrifuge (Thermo Scientific, UK) and were air-dried. The cells were then fixed for 5 seconds in Diff-Quik fixative (1.8 mg/ml Triarylmethane dye methyl alcohol), stained 10 seconds in Diff-Quik Solution 1 (1 g/l Xanthine dye) following a 7 second staining in Diff-Quik Solution 2 (0.625 g/l Azure A, 0.625 g/l Methylene blue). Excess dye was washed off with water. Slides were examined using an Olympus BX51 microscope (bright field).

2.10.2 Immunofluorescent staining of cells

Purified neutrophils from blood and peritoneum of MSU crystal-treated mice (section 2.6.5) and apoptotic neutrophils, which had been cultured *ex vivo* for 24 hours in the presence of GolgiStop (1:1000) were spun onto glass slides at 500 rpm

for 6 minutes. Cells were washed with PBS and then fixed with 200 μl ice-cold methanol:acetone (50:50). After 10 minutes, cells were washed with PBS and non-specific binding was blocked by incubation with blocking buffer (section 2.2) for 30 minutes at 37°C. Slides were washed with PBS and cells stained with the surface marker anti-mouse Ly6G-biotin (section 2.1.1) at 37°C for 2 hours. After 3 wash steps, the AlexaFluor 555-SA was added, and the cells incubated for 1 hour at 4°C. Saponin buffer (section 2.2) was used to permeabilise the cells, which were then stained for intracellular TGFβ1 using a mouse anti-TGFβ1 monoclonal antibody (section 2.1.1) for 2 hours at 37°C. Cells were washed with saponin buffer and treated for 1 hour with the secondary antibody AlexaFluor 488-goat anti-mouse IgG1 (section 2.1.1). Excess antibody was removed by washing with PBS, and cells were fixed with 10% neutral buffered formalin (section 2.1) for 10 minutes at room temperature. One drop of ProLong Gold anti-fade with DAPI was applied. DAPI was used to stain the cell nuclei. The slides were then mounted with a cover slip (Paul Marienfeld GmbH & Co., Germany) and imaged using an Olympus BX51 fluorescence microscope.

2.11 Western blot analysis

2.11.1 Cytoplasmic protein extraction

After differentiation of GM-CSF and M-CSF BMMs (section 2.7.4) and stimulation (section 2.7.5) *in vitro*, cells were washed twice with cold D-PBS to remove serum and non-adherent cells. Cells were lysed directly on the plate by adding 50 μl of the protein lysis buffer (section 2.2). A cell scraper was used to detach the adherent cells and the cell lysate was transfered into a 1.5 ml Eppendorf tube. Cells were immediately mixed by pipetting up and down and put on ice for 20 minutes. After incubation, cell lysate was collected to the bottom of the tube by centrifugation (9000 rpm, 10 seconds) and 3 μl of 10% Igepal CA-630 added, followed by vortexing for 10 seconds and incubation on ice for 2 minutes. The

insoluble material was pelleted by centrifugation for 30 seconds at 13000 rpm and the supernatant, containing the extracted protein, was transferred to a new Eppendorf tube and stored at -80°C until further analysis.

2.11.2 Protein quantification

Cytoplasmic protein was obtained as described in section 2.13.1. The protein concentrations were quantified by Bradford assay using a Bio-Rad protein assay protocol as per manufacturer's instructions. Briefly, each sample was quantified in duplicates with 5 μl of protein sample, 25 μl of Reagent A + S, and 200 μl of Reagent B, and incubated for 15 minutes at room temperature. The colour generated was proportional to the amount of protein and the absorbance was measured at 750 nm wavelength. BSA standards were used to generate a standard curve and the colorimetric quantification was carried out using a Versamax microplate reader and SOFTmax PRO 4.0 software.

2.11.3 Protein sample preparation

The protein concentrations were determined as described in section 2.13.2 and the required volume of protein samples was added into eppendorf tubes containing the required amount of MilliQ water, 4x NuPAGE LDS sample buffer and 10x NuPAGE sample reducing buffer. The protein was denatured by incubation at 95°C for 6 minutes and then put on ice.

2.11.4 Western blot procedure

NuPAGE 4-12% Bis-Tris gels (Life Technologies, USA) were placed in a NuPAGE tank and the outer chamber was filled with MES SDS running buffer and the inner chamber filled with 200 ml MES SDS running buffer and 500 μl NuPAGE Antioxidant. 15 μg of the samples were loaded and in one lane, 6 μl of a sharp pre-stained

protein standard used as a molecular weight marker/loading control. To allow better protein separation, the gels were first run at 120 V for 15 minutes before the voltage was increased to 150 V for further 60 minutes using a Bio-Rad Powerpac 300.

The gels were placed into a transfer cassette with PVDF membranes (hydrated in 100% methanol, Bio-Rad, US) and sandwiched, with bubbles removed, between blotting paper and sponges soaked in transfer buffer. The sandwich transfer cassette was placed in a Bio-Rad criterion blotter gel box and run for 2 hours at 300 mA. After the transfer was completed, the membranes were rinsed twice with T-PBS (PBS buffer with 0.1% Tween20) and non-specific protein binding blocked using 2% milk powder in T-PBS for 1 hour at room temperature on a shaker.

The primary antibodies (section 2.1.2) were diluted in the appropriate concentration in blocking buffer and incubated at 4°C overnight on a rocker. After incubation, the membranes were washed in T-PBS for 5 minutes on a shaker and incubated with the appropriate secondary antibody (goat anti-rabbit IgG or goat anti-mouse IgG - conjugated to the horse radish peroxidase (HRP) enzyme) at 1:2000 at room temperature for 1 hour on a shaker. The membranes were washed with PBS and Western Lightning ECL Pro (PerkinElmer Inc., USA) added to detect HRP activity. Membranes were imaged using a GelLogic 4000 PRO Carestream and pictures were taken using Carestream Molecular Imaging Software to identify the specific proteins in the cell lysate samples.

After imaging, the membranes were incubated in stripping buffer (section 2.2) at 70°C for 45 minutes to remove the primary and secondary antibody from the western blot membranes. After stripping, membranes were incubated in blocking buffer for 1 hour at room temperature and reprobed with a second primary antibody and then incubated at 4°C overnight on a rocker and so forth. Each membrane was stripped and reprobed at the most four times.

2.11.5 Immunoprecipitation

Cytoplasmic protein was collected from *in vitro* TGFβ1-differentiated GM-BMMs as described in section 2.11.1. Immunoprecipitation was used to isolate the caspase 1 protein from the cytoplasmic protein fractions of cultured GM-BMMs. 20 μl of protein A - sepharose beads were incubated with 1 μg/ml of the caspase 1 antibody (section 2.1.2) at 4°C for 1 hour. The bead/antibody mix was washed three times with wash buffer (PBS + 0.02% Tween20) by centrifugating at 13000 rpm for 1 minute and the supernatants discarded. Cytoplasmic protein samples (150 μl) were then incubated with the bead/antibody mix on a rotating wheel at 4°C overnight. After incubation, the samples were washed three times with wash buffer and resuspended in PBS buffer. To separate the caspase 1 protein/antibody mix from the beads, 25 μl of 4x NuPAGE LDS sample buffer was added to the sample and then incubated at 70°C for 10 minutes in a shaking heat block (300 rpm). The samples were spun at 13000 rpm at 4°C for 1 minute and 20 μl of the supernatants loaded onto a NuPAGE 4-12% Bis-Tris gel. Western blot procedure was carried out as described in section 2.11.4. Caspase 8 was used as primary antibody to investigate whether the caspase 1 protein from the GM-BMM samples was immunoprecipitated with caspase 8, specifically whether caspase 1 and caspase 8 are associated and interact.

2.12 Statistical analysis

Statistic analysis was performed using GraphPad Prism (GraphPad software, version 5.0., USA). Student's paired, two-tailed t-test was used to calculate significance between two groups. Between three or more samples, one-way analysis of variance (ANOVA) with Tukey's post test was used. When using two parameters with multiple groups, two-way ANOVA with Bonferroni's post test was carried out. Statistical significance was determined when $P < 0.05$.

Chapter 3

Published in part in **Stefanie Steiger** and Jacquie L. Harper. Neutrophil Canibalism Triggers Transforming Growth Factor β1 Production and Self Regulation of Neutrophil Inflammatory Function in Monosodium Urate Monohydrate Crystal-Induced Inflammation in Mice. *Arthritis&Rheumatism*, 65(3):815-823, 2013. (see appendix)

3 The Contribution of Neutrophils in the Resolution of MSU Crystal-Induced Inflammation

3.1 Introduction

Inflammation is a defensive mechanism against pathogen invasion but it can also occur in response to the release of danger-associated molecular patterns (DAMPs) by the body. Included amongst the DAMPs is UA. In high concentrations, UA forms MSU crystals, the widely recognised inflammatory trigger for gouty arthritis [73]. This acute inflammatory response is characterised by localised swelling in the affected joints and periarticular tissues, reddening of the skin, and debilitating pain in patients having a gout attack. Interestingly, in the absence of clinical intervention, this acute gouty inflammation will spontaneously resolve after 7 - 10 days [17].

A characteristic feature of many auto-inflammatory innate responses including gout is the infiltration of neutrophils to the site of inflammation. During these responses, stimulation of neutrophils triggers the production of toxic ROS via the activation of the NADPH oxidase otherwise known as the respiratory burst [191; 192]. Although the release of free radicals by activated neutrophils is generally beneficial to host defences, these processes must be tightly regulated, as inappropriate ROS production such as that associated with MSU crystal-induced auto-inflammation in gout can be cytotoxic, which results in cell and tissue damage [193; 194].

The deposition of MSU crystals triggers a rapid inflammatory infiltration of neutrophils and monocytes, the release of pro-inflammatory mediators such as TNFα and chemokines following phagocytosis and activation of MSU crystals [195; 74; 103; 196]. IL-1β is a pivotal cytokine involved in the auto-inflammatory cascade in response to MSU crystals. This cytokine is mainly produced by resident macrophages, but there is evidence that the infiltrating neutrophils also have the capacity to pro-

duce IL-1β [197; 198; 198] and could therefore augment local IL-1β levels to drive inflammation.

In patients suffering a gout attack, the spontaneous resolution of inflammation is associated with elevated levels of TGFβ1 in the synovial fluid of affected joints [185]. The exogenous administration of TGFβ1 has also been shown to significantly attenuate MSU crystal-induced cellular recruitment *in vivo* [161]. Furthermore, human TGFβ1 gene polymorphisms have been linked with longer inflammatory attacks and increased tophus formation in the joints [187]. These findings identify TGFβ1, a key mediator commonly involved in the resolution and tissue repair [182; 138], as an important cytokine in MSU crystal-induced inflammation.

A key process in shutting down an inflammatory response is the efficient clearance of apoptotic cells [183]. At the site of inflammation, neutrophils undergo spontaneous apoptosis and are phagocytosed by macrophages, a mechanism involved in the resolution of acute gouty inflammation and the production of TGFβ1 [182; 184]. To date, little is known about alternative sources of TGFβ1 other than macrophages, and the importance of TGFβ1 during the resolution phase of MSU crystal-induced inflammation and its regulatory effect on respiratory burst and IL-1β production by MSU crystal-recruited neutrophils.

3.2 Aims

The aims of this chapter were to identify macrophage-independent sources of TGFβ1 during the resolution phase of MSU crystal-induced inflammation. In addition, to determine the regulatory effect of TGFβ1 on ROS and IL-1β production by MSU crystal-recruited neutrophils.

3.3 Results

3.3.1 TGFβ1 profile in MSU crystal-induced inflammation

The resolution of acute gouty inflammation has been associated with the production of the anti-inflammatory cytokine TGFβ1 [173]. Elevated levels of TGFβ1 have been found in the synovial fluid of patients suffering from gout [185; 186]. To determine how the levels of TGFβ1 changed during the inflammatory response in a murine peritoneal model of acute gout *in vivo*, peritoneal lavage fluids from MSU crystal-treated mice were collected over time (section 2.6.1) and analysed for secreted TGFβ1 by enzyme-linked immunosorbent assay (ELISA) (section 2.8). As shown in Figure 3.1A, TGFβ1 levels increased in the peritoneum of MSU crystal-treated mice within 4 hours, peaking at 8 hours and remained elevated for up to 72 hours after MSU crystal administration, before returning to background level after 7 days.

Previous time course experiments have shown that following *in vivo* MSU crystal administration, pro-inflammatory cytokine levels peak in the peritoneum between 4 - 8 hours [103]. To confirm that this was also the case in this study, IL-1β levels were measured in the peritoneal fluid from mice at 8 and 18 hours post MSU crystal administration (section 2.8). As expected, the pro-inflammatory cytokine levels of IL-1β peaked at 8 hours and were significantly decreased by 18 hours (Figure 3.1B). Together, these findings showed that the levels of TGFβ1 induced by MSU crystals mirrored the classical pro-inflammatory cytokine profile and that TGFβ1 was produced early during the inflammatory response.

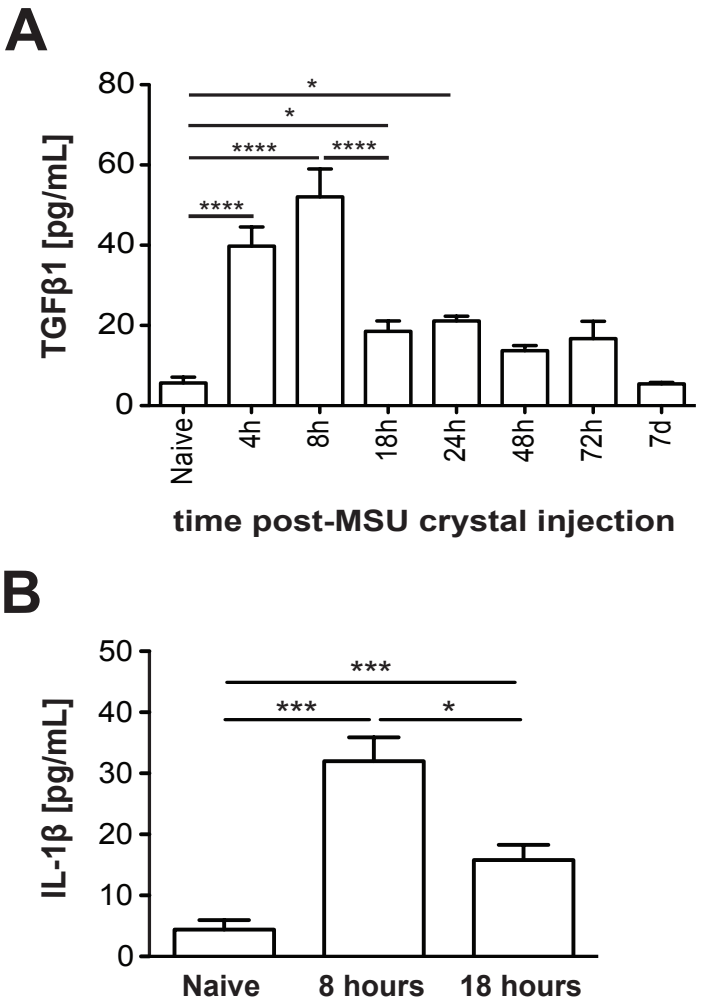

Figure 3.1: Profile of TGFβ1 and IL-1β in response to MSU crystals *in vivo*. Mice were injected with MSU crystals (3 mg, i.p.) and at different time points, peritoneal lavage fluid was collected in 3 ml PBS, and TGFβ1 (**A**) and IL-1β (**B**) levels analysed by ELISA. Values are the mean -/+ SEM (n = 5 mice per group) and representative of up to three experiments. * = $P < 0.05$, *** = $P < 0.001$, **** = $P < 0.0001$ by one-way ANOVA with Tukey's post test.

3.3.2 Neutrophils are a source of TGFβ1

A hallmark feature of gout is the early infiltration of neutrophils and monocytes to the site of inflammation. To determine which cells could be producing TGFβ1 in response to MSU crystal administration, MSU crystal-recruited peritoneal cells were isolated (section 2.6.1) and analysed by flow cytometry (section 2.9) to identify TGF$\beta1^{+}$ cells. Based on the TGFβ1 profile (Figure 3.1A) and the high number of neutrophils [103] at the site of inflammation, 18 hours after MSU crystal administration was chosen as the time point of interest.

To identify the infiltrating cells during the period of high TGFβ1 levels, peritoneal cells were harvested by lavage from mice 18 hours after MSU crystal administration (section 2.6.1). The peritoneal exudate cells were stained with fluorescent antibodies for cell surface markers (Clone 7/4, Gr-1, Ly6G, CD11b, F4/80). MSU crystal-recruited neutrophils were identified as Gr-1^{high} $7/4^{+}$ Ly6G^{high} CD11b^{+} (Figure 3.2A, G1) and monocytes as Gr-$1^{intermediate}$ $7/4^{+}$ Ly6G^{-} CD11b^{+} (Figure 3.2A, G2). In naive mice, the resident cell population of macrophages were $7/4^{intermediate}$ Gr-1^{-} F4/80^{+} CD11b^{+} (Figure 3.2B, G3).

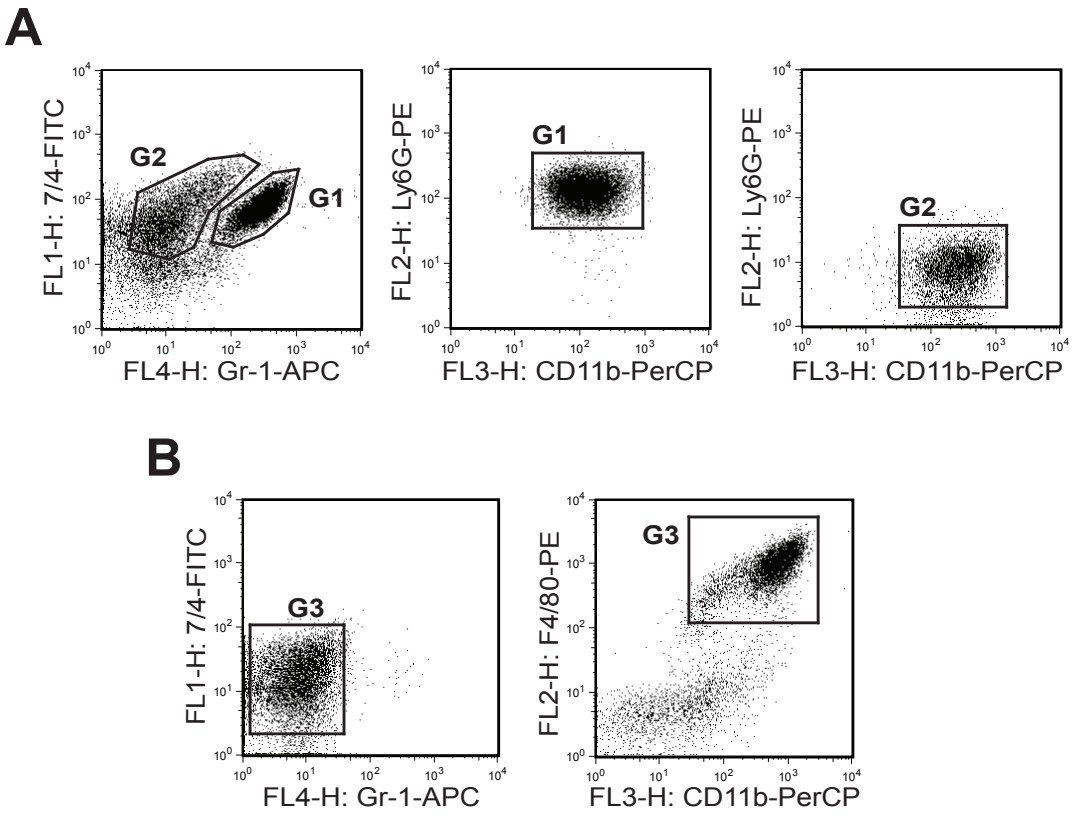

Figure 3.2: Identification of infiltrating cells in response to MSU crystals *in vivo*. Mice were injected intraperitoneally with MSU crystals (3 mg). 18 hours post MSU crystal administration, the peritoneal exudate cells were harvested by lavage with 3 ml PBS and the cells were identified by flow cytometry. **A** Neutrophils were identified as Gr-1^{high} $7/4^{+}$ $Ly6G^{high}$ $CD11b^{+}$ (G1), and monocytes identified as Gr-$1^{intermediate}$ $7/4^{+}$ $Ly6G^{-}$ $CD11b^{+}$ (G2). **B** Macrophages harvested from naive mice were identified as $7/4^{intermediate}$ Gr-1^{-} $F4/80^{+}$ $CD11b^{+}$ (G3). Results are representative of three independent experiments.

As shown in Figure 3.3A, there was a significant monocyte and neutrophil infiltration within the first 18 hours after challenge with MSU crystals. Analysis of the different infiltrating cell populations for intracellular TGFβ1 expression showed that both infiltrating monocytes and neutrophils expressed TGFβ1 (Figure 3.3B). The production of TGFβ1 by monocytes/macrophages during an inflammatory response is well documented [199]. However, the ability of neutrophils to produce TGFβ1 has not been previously reported. To confirm the results obtained by flow cytometry (Figure 3.3B), MSU crystal-recruited neutrophils were isolated and stained for intracelluar TGFβ1 using fluorescence microscopy. In order to carry out this experiment, an efficient purification method was required to get a pure neutrophil population.

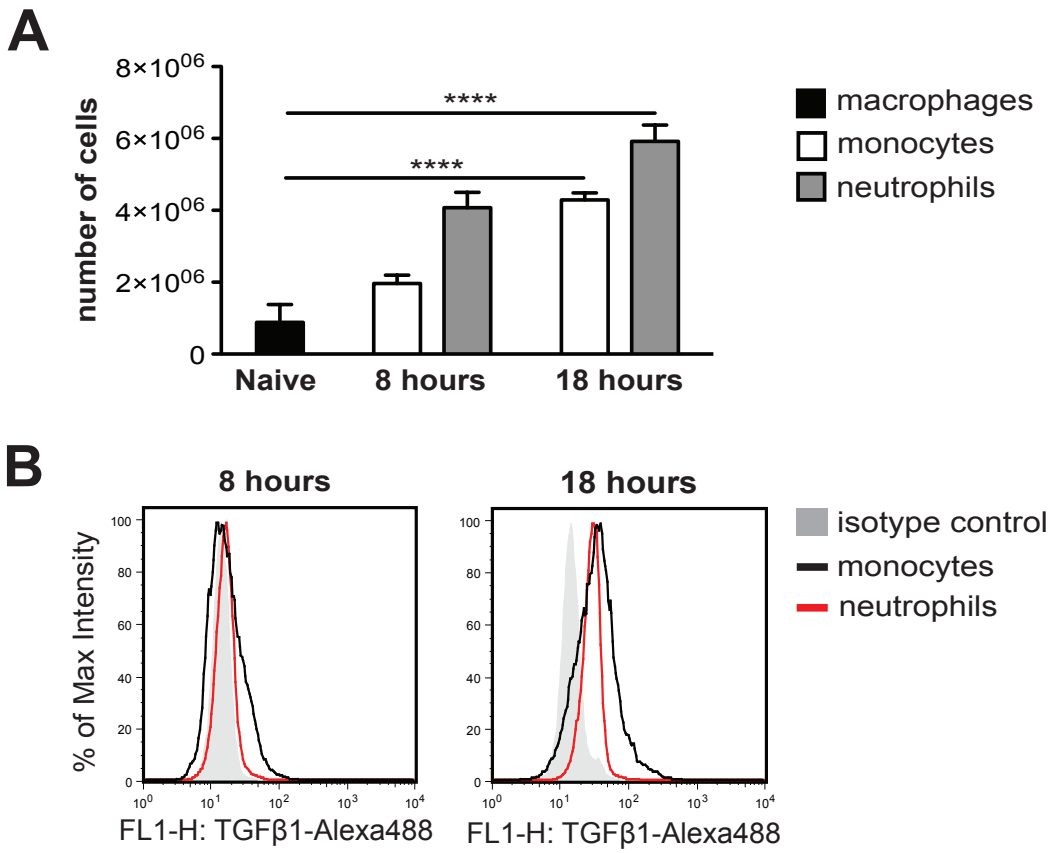

Figure 3.3: Expression of TGFβ1 by monocytes and neutrophils Mice were injected with MSU crystals (3 mg, i.p.), and after 8 and 18 hours peritoneal exudate cells were harvested by lavage (3 ml PBS). **A** Number of infiltrating monocytes and neutrophils from 8 and 18 hours MSU crystal-treated mice. **B** Peritoneal monocytes and neutrophils were stained for intracellular TGFβ1 and analysed by flow cytometry. Values are the mean -/+ SEM (n = 4 mice per group) and the results are representative of two separate experiments. **** = $P < 0.0001$ (two-way ANOVA with Bonferroni's post test).

Firstly, it was necessary to obtain a pure neutrophil population. Peritoneal exudate cells were harvested from mice that had been treated with MSU crystals for 18 hours and the neutrophils were purified using a Lympholyte-M density gradient (section 2.6.5). The neutrophil population was then analysed for the expression of the surface marker CD11b and the specific neutrophil marker Ly6G by flow cytometry. As shown in Figure 3.4A, neutrophils were identified as $CD11b^+$ $Ly6G^+$ cells with a purity of greater than 90%. These cells also exhibited classical neutrophil morphology with multi-lobed nuclei (hypersegmented), as shown in Figure 3.4B. These findings confirmed that this purification method efficiently purified the $CD11b^+$ $Ly6G^+$ cells from the peritoneum of MSU crystal-treated mice.

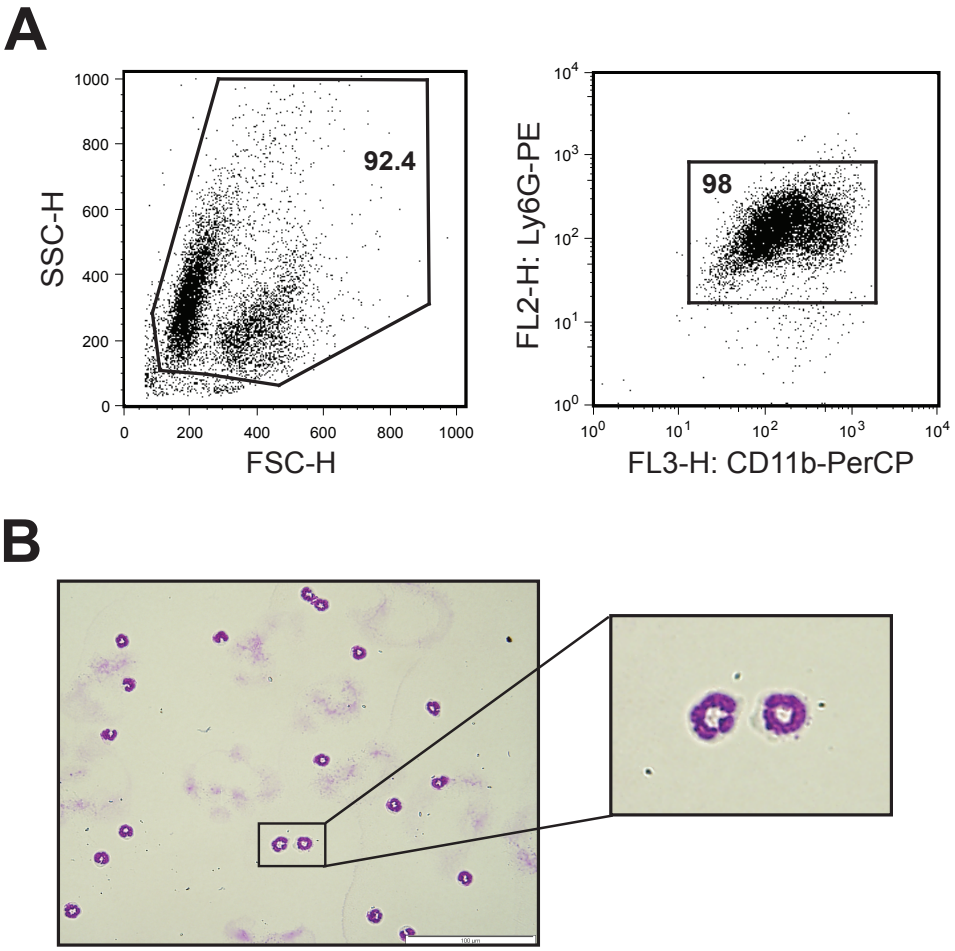

Figure 3.4: Purification of neutrophils from MSU crystal-treated mice *in vivo*. Mice were injected with MSU crystals (3 mg, i.p.). After 18 hours, peritoneal cells were harvested by lavage (3 ml PBS) and neutrophils purified using a Lympholyte-M density gradient. **A** The purified neutrophil population was identified as $CD11b^+$ $Ly6G^+$ by flow cytometry. **B** Purified neutrophils were stained using a hematoxylin and eosin (H&E) staining method and examined microscopically. Original magnification 40x. Scale bar represents 100 μm. Results are representative of three separate experiments.

After the initiation of acute inflammation, the pro-inflammatory cytokine levels of IL-1β returned to background within 18 hours after MSU crystal administration indicating a switch towards resolution (Figure 3.1B). To confirm that TGFβ1 levels were elevated at that time, peritoneal lavage fluid from 18 hour MSU crystal-challenged mice was collected and analysed for TGFβ1 by ELISA. Consistent with the clinical inflammatory profile, TGFβ1 levels in the lavage fluid from MSU crystal-treated mice were significantly higher than those in the lavage fluid from naive mice (Figure 3.5A). Neutrophils are present in high numbers 18 hours after MSU crystal administration; therefore neutrophils from 18 hours MSU crystal-treated mice were purified and stained for the surface marker Ly6G and intracellular TGFβ1. Immunofluorescent histology (section 2.10.2) showed that Ly6G$^+$ neutrophils (red) expressed intracellular TGFβ1 (green) (Figure 3.5B). This finding identified MSU crystal-recruited neutrophils as a potential source of TGFβ1 production *in vivo*.

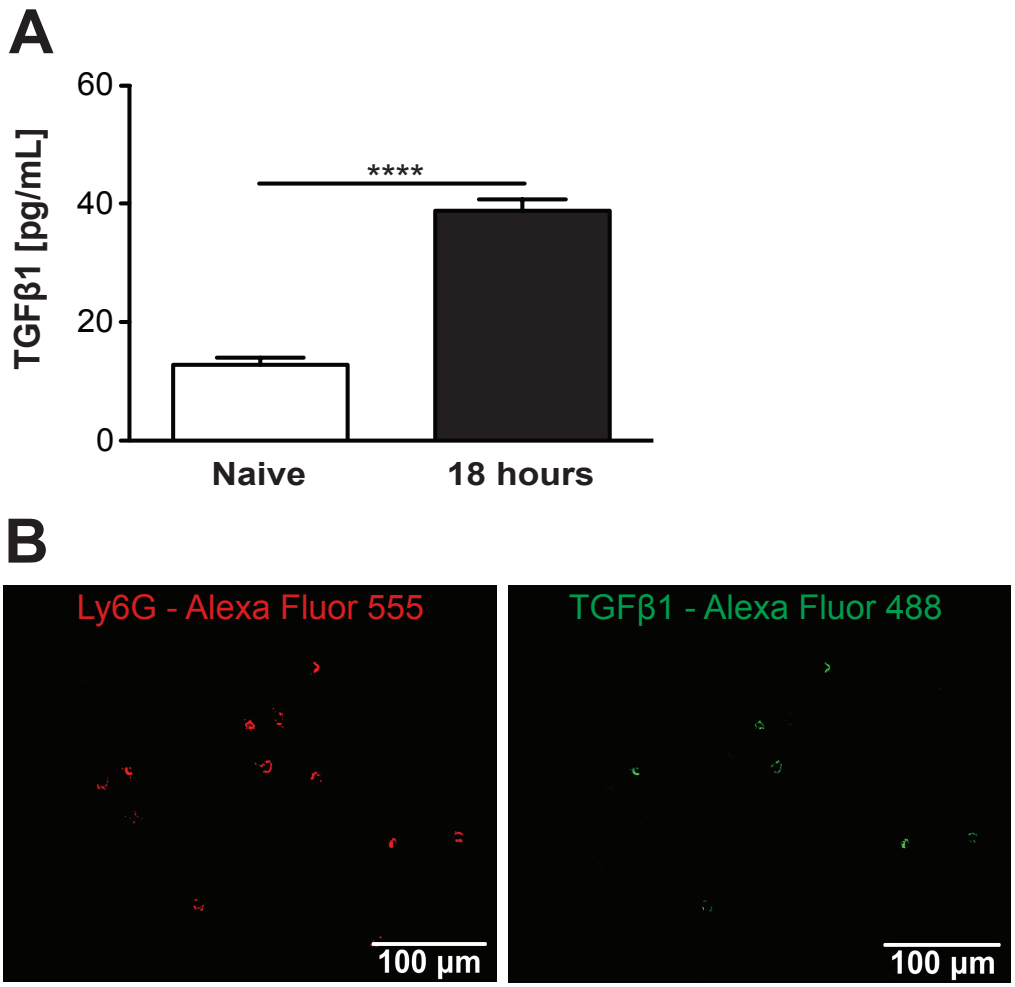

Figure 3.5: Neutrophils are a source of TGFβ1 *in vivo*. Mice were injected with MSU crystals (3 mg, i.p.). After 18 hours, the peritoneal cells were harvested by lavage (3 ml PBS). **A** TGFβ1 levels in peritoneal lavage fluid were analysed by ELISA. **B** Fluorescence microscopy of purified neutrophils from the peritoneum (Ly6G$^+$, red) expressing intracellular TGFβ1 (green). Scale bars represent 100 μm. Values are the mean -/+ SEM of three independent experiments. **** = $P < 0.0001$ by Student's t-test.

3.3.3 TGFβ1 production in *ex vivo* cultured peritoneal neutrophils

To determine whether freshly isolated TGFβ1$^+$ neutrophils were also secreting TGFβ1 during *ex vivo* culture, MSU crystal-recruited neutrophils from 18 hour treated mice were purified, as previously shown and cultured *ex vivo* under serum free conditions for 24 hours. The culture supernatants were collected and analysed for TGFβ1 (section 2.8). Interestingly, cultured neutrophils secreted significantly higher levels of TGFβ1 compared to freshly isolated neutrophils from the peritoneum (Figure 3.6A). *Ex vivo* cultured neutrophils were also stained for the surface marker Ly6G (red) and intracellular TGFβ1, and analysed by immunofluorescent histology (section 2.10.2). As shown in Figure 3.6B, *ex vivo* cultured Ly6G$^+$ neutrophils were positive for TGFβ1 (green). These results showed that *ex vivo* cultured neutrophils secreted more TGFβ1 compared to freshly isolated MSU crystal-recruited neutrophils.

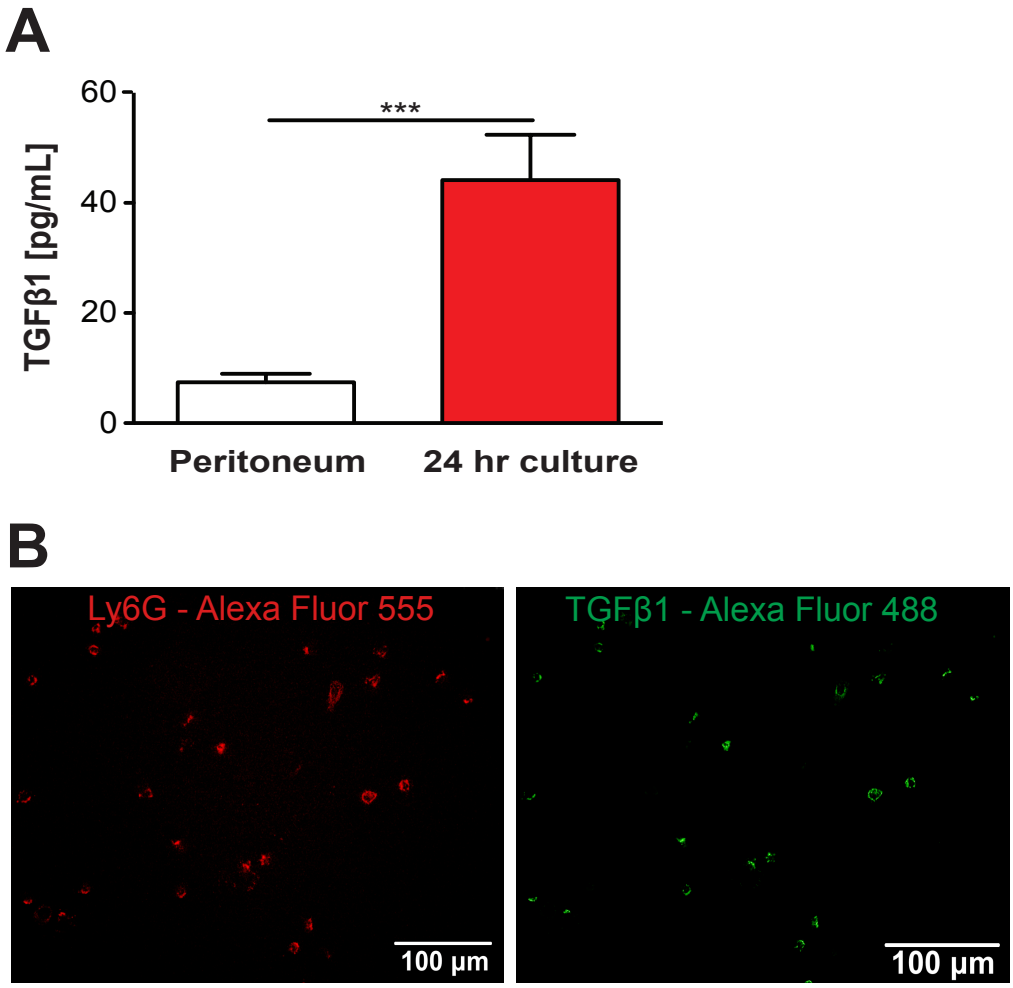

Figure 3.6: TGFβ1 production by *ex vivo* cultured peritoneal neutrophils. Mice were treated with MSU crystals (3 mg, i.p.). After 18 hours, peritoneal neutrophils were purified and cultured in serum free media *ex vivo* for 24 hours. **A** Culture supernatants were analysed for secreted levels of TGFβ1 by ELISA. **B** Fluorescence microscopy of purified cultured neutrophils from the peritoneum (Ly6G$^+$, red) expressing TGFβ1 (green). Scale bars represent 100μm. Values are the mean -/+ SEM and are representative of two independent experiments. *** = $P < 0.001$ by Student's t-test.

3.3.4 TGFβ1 production by apoptotic peritoneal neutrophils

Having confirmed that neutrophils were a source of TGFβ1 in MSU crystal-induced inflammation, the mechanism which triggers neutrophil TGFβ1 production was investigated. Neutrophils are known to have a very short life span and undergo spontaneous apoptotic cell death [200; 201]. To identify a possible link between TGFβ1 and apoptosis, neutrophils were purified 18 hours following MSU crystal administration (section 2.6.5) and cultured *ex vivo* for 24 hours. The neutrophils ($CD11b^+$ $Ly6G^+$) were then stained with the apoptosis marker annexinV and analysed by flow cytometry (section 2.9). As shown in Figure 3.7A, the percentage of $annexinV^+$ neutrophils following *ex vivo* culture significantly increased compared to freshly isolated MSU crystal-recruited neutrophils indicating that neutrophils underwent apoptotic cell death.

Neutrophils were also cultured *ex vivo* in the presence of GolgiStop to prevent the release of TGFβ1 for 24 hours. *Ex vivo* cultured neutrophils, as well as freshly isolated neutrophils, were then stained for the intracellular apoptosis marker caspase 3 in combination with intracelluar TGFβ1, and their expression determined by flow cytometry (section 2.9). As shown in Figure 3.7B, the percentage of apoptotic neutrophils (caspase 3^+) increased when neutrophils were cultured *ex vivo* for 24 hours (red box) compared to the freshly isolated neutrophils (black box). Importantly, only apoptotic neutrophils upregulated TGFβ1 (Figure 3.7C, red line).

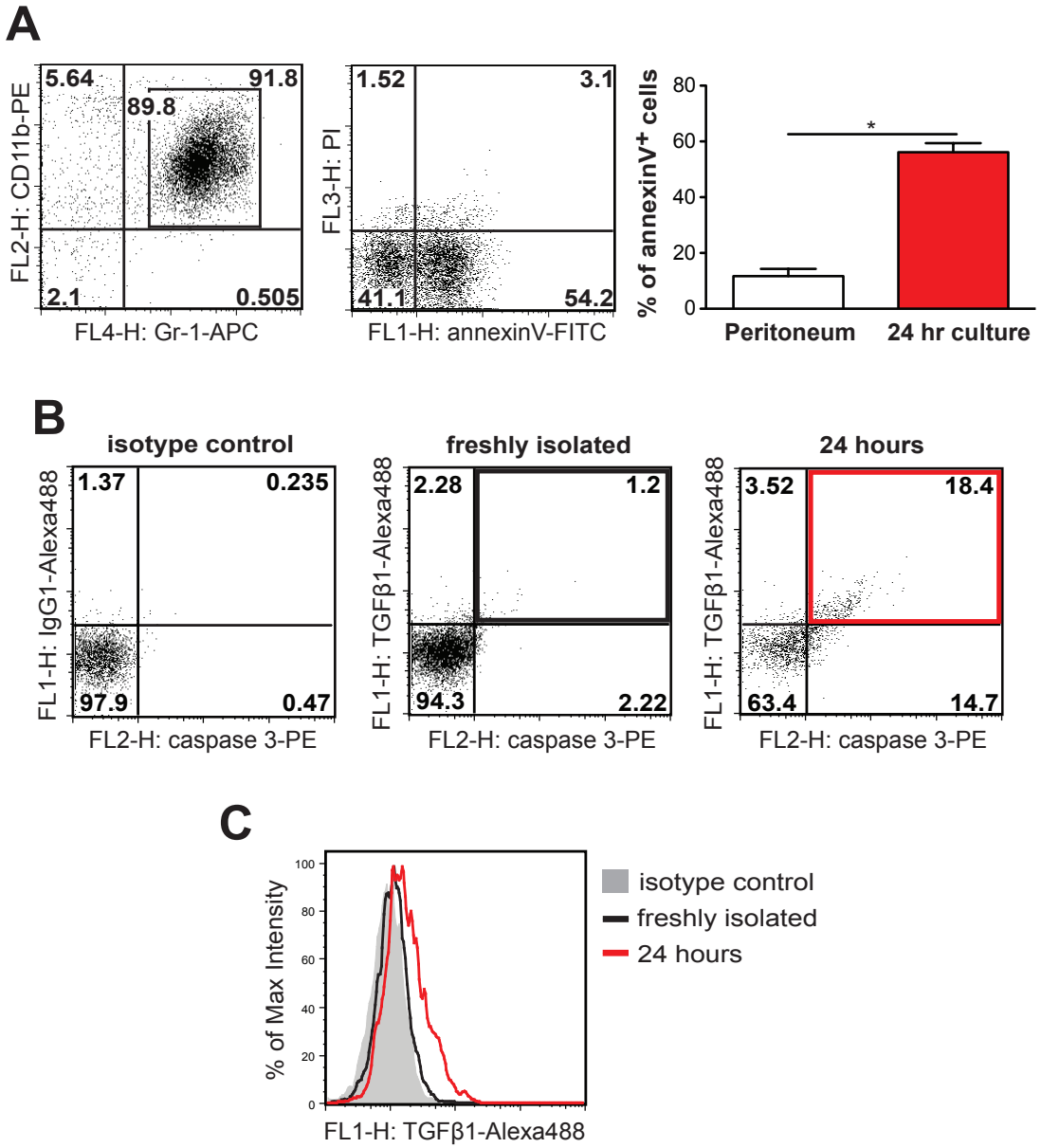

Figure 3.7: TGFβ1 production by apoptotic peritoneal neutrophils. Mice were treated with MSU crystals (3 mg, i.p.). After 18 hours, peritoneal neutrophils were purified and cultured *ex vivo* for 24 hours. **A** Percentage of freshly isolated neutrophils from the peritoneum and 24 hour cultured neutrophils ($CD11b^+$ $Gr\text{-}1^+$) expressing the apoptotic marker annexinV, as determined by flow cytometry. **B, C** Purified peritoneal neutrophils were cultured *ex vivo* in the presence of GolgiStop (1:1000) for 24 hours. Freshly isolated and cultured neutrophils co-expressing the apoptotic marker caspase 3 and TGFβ1 (**B**), and the TGF$\beta1^+$ expression by caspase 3^+ neutrophils (**C**) as determined by flow cytometry. Values are the mean -/+ SEM and are representative of two independent experiments. * = $P < 0.05$ by Student's t-test.

The previous results in Figure 3.7 were conducted for a single time point only. To determine the association between TGFβ1 and apoptosis over a period of 24 hours, MSU crystal-recruited neutrophils were purified and cultured *ex vivo*. The levels of secreted or intracellular TGFβ1 were analysed in the absence or presence of GolgiStop by flow cytometry respectively (section 2.9). As shown in Figure 3.8A and 3.8B, the *ex vivo* cultured neutrophils exhibited an increase in both the percentage of TGF$\beta1^+$ neutrophils and the levels of secreted TGFβ1 over time. Neutrophil TGFβ1 generation was also associated with an upregulation of the apoptotic markers annexinV and caspase 3 (Figure 3.8C and 3.8D). In summary, these findings showed that an increase in neutrophil TGFβ1 production was associated with increased neutrophil apoptosis indicating a possible link between neutrophil TGFβ1 production and apoptotic cell death.

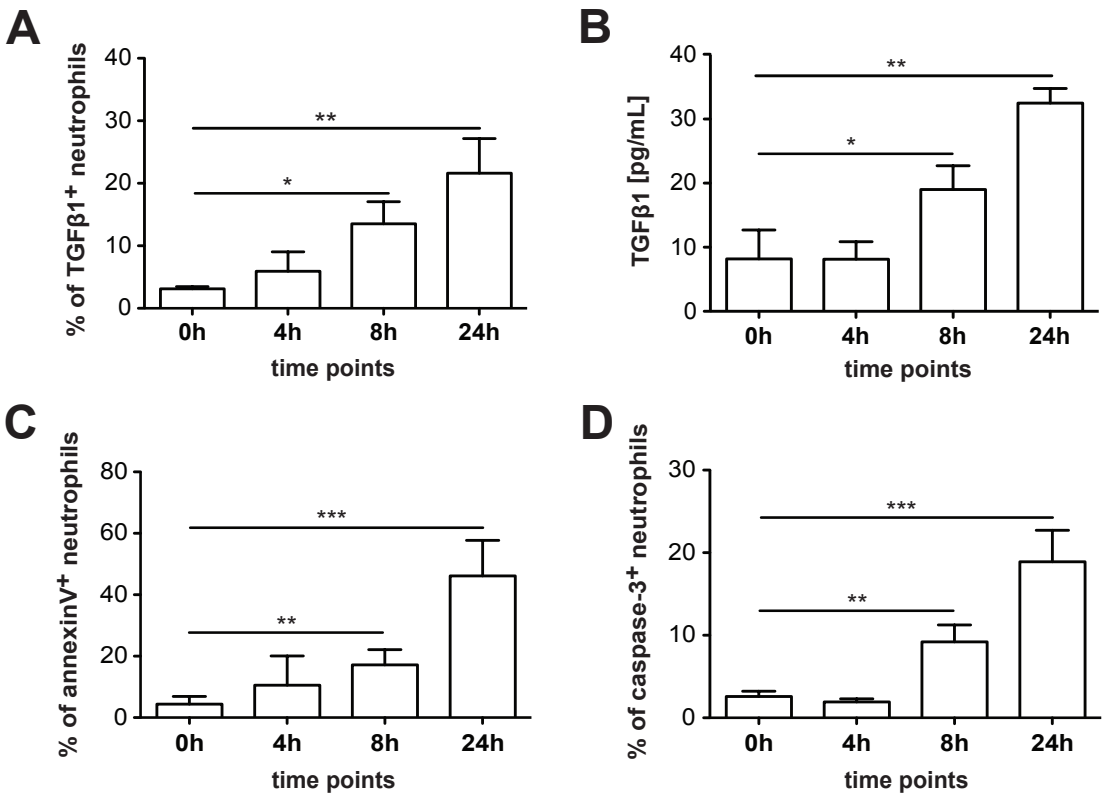

Figure 3.8: Increased TGFβ1 production in *ex vivo* cultured peritoneal neutrophils. Mice were treated with MSU crystals (3 mg, i.p.). After 18 hours, peritoneal neutrophils were purified and cultured *ex vivo* for up to 24 hours. **A** Neutrophils were cultured in the presence of GolgiStop (1:1000) and at respective time points, the percentage of Ly6G$^+$ TGFβ1$^+$ neutrophils was determined by flow cytometry. **B** The levels of TGFβ1 in the culture supernatants (in the absence of GolgiStop) were measured by ELISA. **C, D** Percentage of Ly6G$^+$ neutrophils expressing the apoptotic markers annexinV (**C**) and caspase 3 (**D**), as determined by flow cytometry. Values represent the mean -/+ SEM of three independent experiments. * = $P < 0.05$, ** = $P < 0.01$, *** = $P < 0.001$ by one-way ANOVA with Tukey's post analysis.

3.3.5 Neutrophil TGFβ1 production is linked to neutrophil apoptosis

Neutrophils are the shortest lived cells among circulating leukocytes and have been shown to rapidly undergo apoptotic cell death [182; 200]. This process of neutrophil apoptosis can be regulated via a number of different caspases, including caspase 1, 3, 4 and 8 [202; 203; 204]. To confirm the relationship between neutrophil apoptosis and TGFβ1 production, neutrophil apoptosis was inhibited using a general caspase inhibitor Q-VD-OPh (20μM), and the production of TGFβ1 was monitored for up to 24 hours (section 2.7.1). At different time points, the supernatants from *ex vivo* cultured neutrophils were collected and the levels of secreted TGFβ1 measured by ELISA (section 2.8). Neutrophils were stained for the apoptotic markers annexinV and caspase 3, and analysed by flow cytometry (section 2.9). To determine intracellular TGFβ1 by flow cytometry, neutrophils were treated with GolgiStop during the *ex vivo* culture. As shown in Figure 3.9A and 3.9B, the number of annexinV$^+$ and caspase 3$^+$ neutrophils were significantly decreased when the cells were treated with the caspase inhibitor Q-VD-OPh indicating that neutrophil apoptosis was successfully inhibited. The blockade of neutrophil apoptosis resulted in fewer TGFβ1$^+$ neutrophils (Figure 3.9C) and correlated with a decrease in the levels of secreted TGFβ1 (Figure 3.9D). These findings indicated that neutrophil apoptosis was required for the production of TGFβ1 by neutrophils.

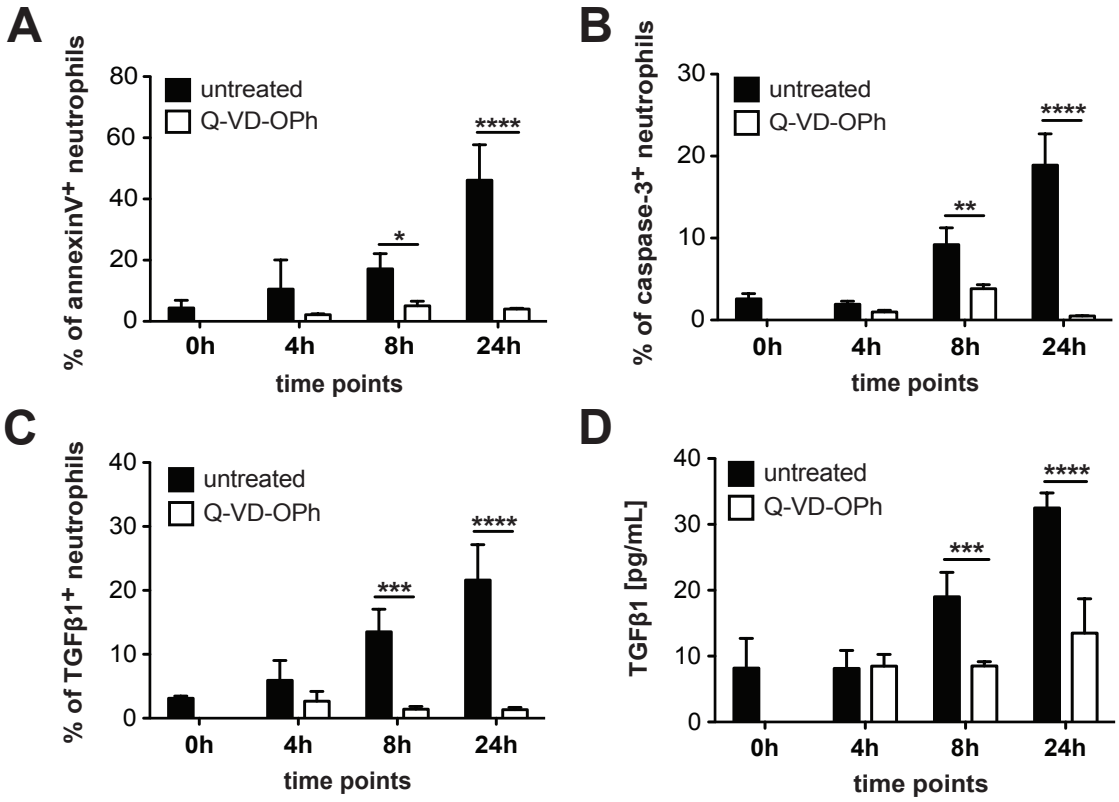

Figure 3.9: Neutrophil TGFβ1 production is linked to neutrophil apoptosis. Mice were injected with MSU crystals (3 mg, i.p.). After 18 hours, MSU crystal-recruited neutrophils were purified from the peritoneal lavage and cultured in the presence of the general caspase inhibitor Q-VD-OPh (20μM) *ex vivo* for 24 hours. To measure intracellular TGFβ1, cells were also treated with GolgiStop (1:1000). **A, B** The percentage of Ly6G$^+$ neutrophils expressing the apoptotic marker annexinV (**A**) and caspase 3 (**B**) was measured by flow cytometry. **C** The percentage of TGFβ1$^+$ neutrophils was determined by flow cytometry. **D** The levels of TGFβ1 in the culture supernatants were measured by ELISA. Values represent the mean -/+ SEM. Results are representative of two independent experiments. * = $P < 0.05$, ** = $P < 0.01$, *** = $P < 0.001$, **** = $P < 0.0001$ (two-way ANOVA with Bonferroni's post test).

3.3.6 TGFβ1 production by apoptotic blood neutrophils

In MSU crystal-induced inflammation, neutrophils infiltrate into a highly pro-inflammatory microenvironment where they become activated by MSU crystals, and produce cytokines and chemokines. In order to examine whether the phenomenon of neutrophil TGFβ1 production was a general function of neutrophils rather than an effect of their activation status, circulating blood neutrophils were collected by cardiac puncture from MSU crystal-treated mice after 18 hours (section 2.6.2) and purified using a Lympholyte-M density gradient (2.6.5). Between 60 - 70% of the white blood cells were identified as Gr-1$^+$ neutrophils by flow cytometry (Figure 3.10A). Purified circulating blood neutrophils were stained for the surface marker Ly6G and intracellular TGFβ1, and examined under a fluorescence microscope (section 2.10.2). As shown in Figure 3.10B, a small number of Ly6G$^+$ blood neutrophils were identified as TGFβ1$^+$. These findings demonstrated that like MSU crystal-recruited peritoneal neutrophils, circulating neutrophils were also able to produce TGFβ1. This raised the question of whether the process of apoptosis by circulating neutrophils is also required for the production of TGFβ1.

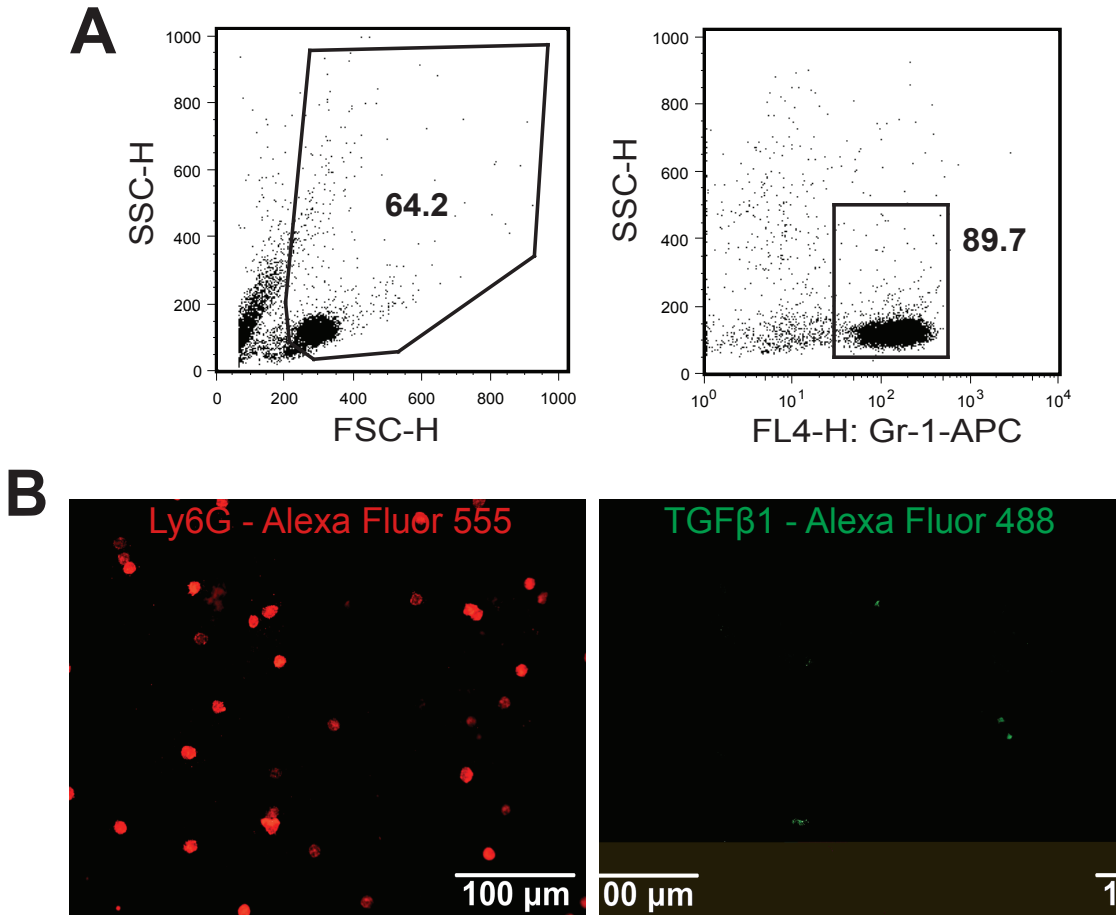

Figure 3.10: TGFβ1$^+$ blood neutrophils. Mice were treated with MSU crystals (3 mg, i.p.). After 18 hours, blood neutrophils were collected by cardiac puncture and purified using a Lympholyte-M density gradient. **A** Blood neutrophils were analysed by flow cytometry to determine their purity (Gr-1$^+$ cells). **B** Fluorescence microscopy staining of purified blood neutrophils (Ly6G$^+$, red) expressing intracellular TGFβ1 (green). Scale bars represent 100μm.

In order to investigate whether TGFβ1 production by blood neutrophils was also the result of apoptotic cell death, blood neutrophils were purified 18 hours following MSU crystal administration and cultured *ex vivo* in the presence of GolgiStop for up to 24 hours. The blood neutrophils were analysed for the expression of caspase 3 and intracellular TGFβ1 as well as secreted levels of TGFβ1 in the culture supernatants. As shown in Figure 3.11A, the percentage of caspase 3^+ cells increased when the blood neutrophils (Gr-1^+) were cultured *ex vivo* for 24 hours (red box) compared to the freshly isolated neutrophils (blue box). Approximately 48% of these caspase 3^+ blood neutrophils were identified as TGF$\beta1^+$ illustrated by an increase in the expression of TGFβ1 by *ex vivo* cultured neutrophils compared to uncultured neutrophils (Figure 3.11B). This was consistent with an increase in the levels of secreted TGFβ1 in *ex vivo* cultured blood neutrophils over time (Figure 3.11C). In summary, these data indicated that apoptosis of circulating naive neutrophils was required for TGFβ1 production and that apoptosis-driven TGFβ1 production was not dependent on MSU crystal activation of neutrophils *in vivo*.

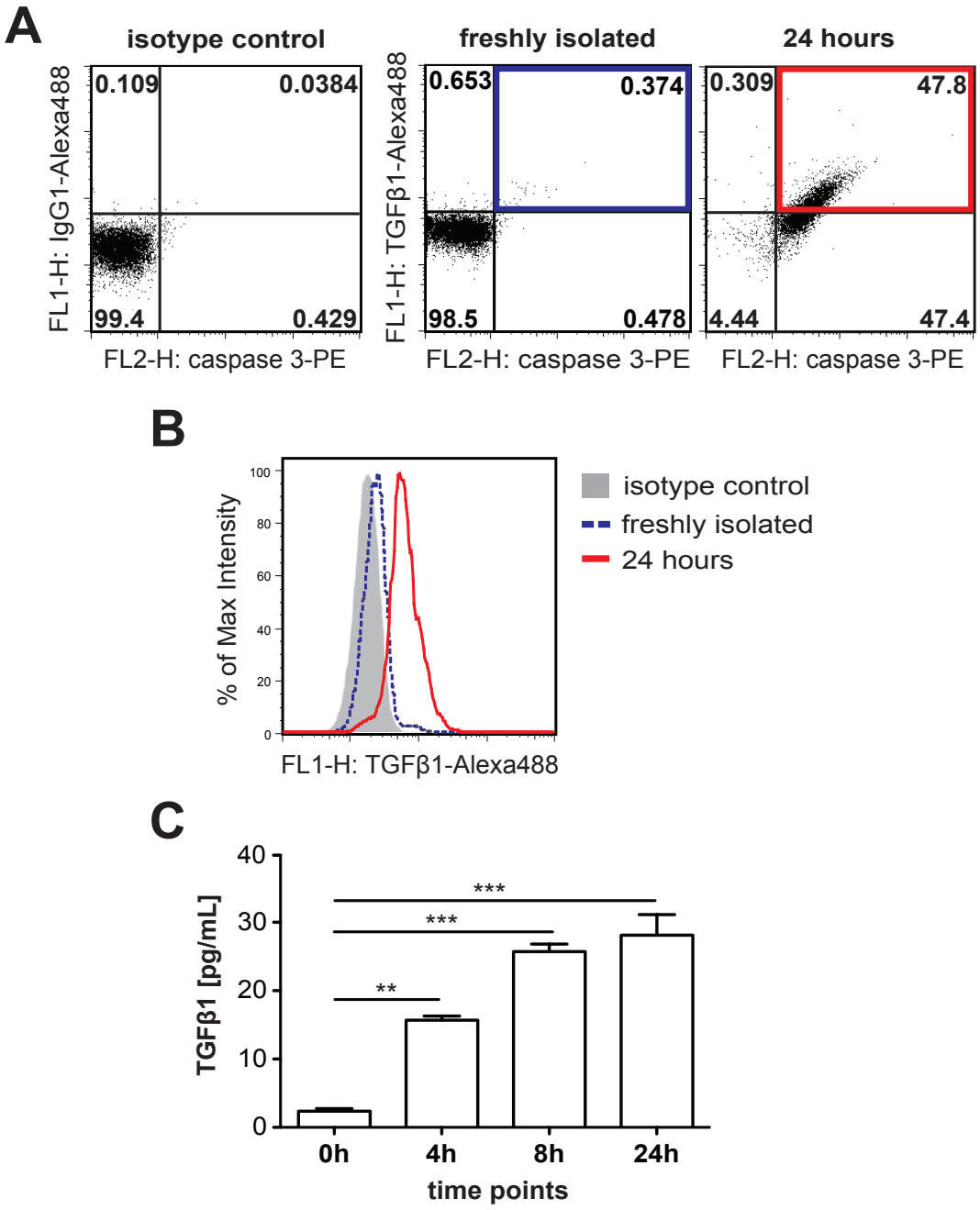

Figure 3.11: TGFβ1 production by apoptotic blood neutrophils. Mice were injected with MSU crystals (3 mg, i.p.). After 18 hours, blood neutrophils were purified and cultured *ex vivo* for 24 hours. **A, B** Percentage of Gr-1$^+$ blood neutrophils co-expressing the apoptotic marker caspase 3 and TGFβ1 (**A**), and the TGFβ1$^+$ expression by caspase 3$^+$ neutrophils (**B**) as determined by flow cytometry. **C** TGFβ1 levels from supernatants of cultured blood neutrophils were measured by ELISA. Values represent the mean -/+ SEM of two independent experiments. ** = $P < 0.01$, *** = $P < 0.001$ by one-way ANOVA with Tukey's post analysis.

3.3.7 TGFβ1 production by neutrophils is linked to neutrophil self-clearance

Studies have shown that the process of recognition and clearance of apoptotic neutrophils by macrophages is an important mechanism involved in the generation of macrophage TGFβ1 and the resolution of acute inflammation [182; 183; 199]. However, neutrophils are also professional phagocytes [191] and they are present in high numbers at sites of acute inflammation whereas the macrophages are rare.

This led to the hypothesis that neutrophil phagocytosis of apoptotic cells triggers the generation of TGFβ1.

To test this hypothesis, MSU crystal-recruited peritoneal neutrophils were purified and cultured *ex vivo* in the presence of CytochalasinD (section 2.7.1), a phagocytosis inhibitor which has been widely used to block the uptake of apoptotic cells by macrophages [205; 206; 207]. At different time points, intracellular TGFβ1 production by neutrophils was analysed by flow cytometry and the TGFβ1 levels in culture supernatants measured by ELISA. As shown in Figure 3.12A, the blockade of neutrophil phagocytosis resulted in a decrease in the percentage of TGF$\beta1^+$ neutrophils.

In contrast, *ex vivo* culture of neutrophils in the presence of CytochalasinD caused an increase in the secreted levels of TGFβ1 (Figure 3.12B) over time. CytochalasinD has been shown to have effects on neutrophil morphology, exocytosis and disruption of the actin cytoskeleton [208; 209; 210]; therefore the viability of neutrophils was investigated. As shown in Figure 3.12C, the percentage of necrotic neutrophils (PI^+) in the presence of CytochalasinD had increased over time. These data indicated that CytochalasinD was inducing membrane disruption in neutrophils thus causing non-specific release of TGFβ1 as a result of necrotic cell death. Based on the evidence that CytochalasinD caused necrotic cell death of neutrophils, an alternative approach was employed to investigate the association between phagocytosis of apoptotic cells and TGFβ1 production by neutrophils.

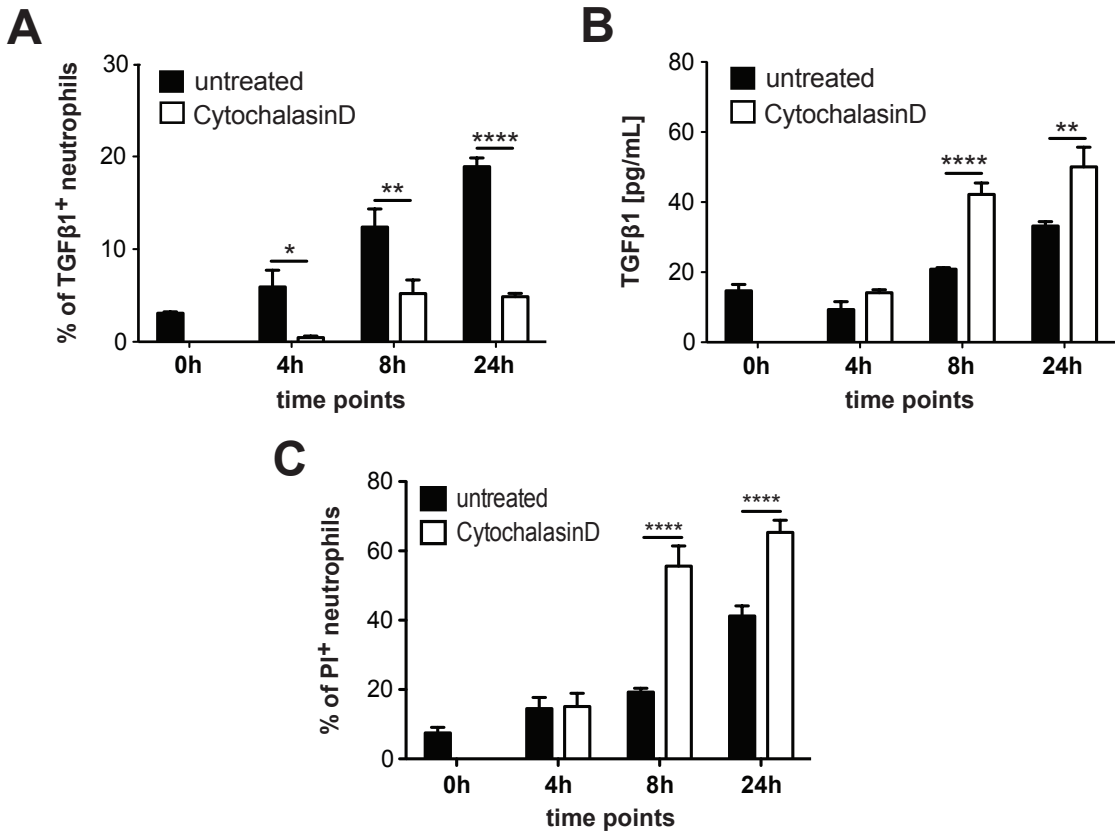

Figure 3.12: TGFβ1 production by neutrophils is linked to neutrophil self-clearance. Mice were injected with MSU crystals (3 mg, i.p.). After 18 hours, MSU crystal-recruited neutrophils were purified from the peritoneal cavity and cultured in the presence of the phagocytosis inhibitor CytochalasinD (20 μg/ml) *ex vivo* for 24 hours. **A** The percentage of TGF$\beta1^+$ neutrophils was analysed by flow cytometry. **B** The levels of TGFβ1 in culture supernatants were measured by ELISA. **C** The percentage of PI^+ neutrophils was analysed by flow cytometry respectively. Values represent the mean -/+ SEM of two independent experiments. * = $P < 0.05$, ** = $P < 0.01$, **** = $P < 0.0001$ (two-way ANOVA with Bonferroni's post test).

3.3.8 Phagocytosis of apoptotic neutrophils induces neutrophil TGFβ1 production

As CytochalasinD caused necrosis, an alternative approach was used to determine if phagocytosis of apoptotic neutrophils was inducing neutrophil TGFβ1 production. First, MSU crystal-recruited neutrophils were purified and cultured *ex vivo* overnight to induce apoptosis. These apoptotic neutrophils were then incubated *ex vivo* with freshly isolated MSU crystal-recruited neutrophils at a cell ratio of 5:1 (apoptotic cell:live cell) for 8 hours. The TGFβ1 levels in supernatants from the single cell culture of live or apoptotic neutrophils, and the co-culture consisting of both live and apoptotic cells were measured by ELISA. As shown in Figure 3.13A, the levels of secreted TGFβ1 from co-incubation of live and apoptotic neutrophils were significantly higher than in the supernatants from the single cell cultures of live or apoptotic neutrophils. This indicated that phagocytosis of apoptotic neutrophils by live neutrophils could be the primary trigger for neutrophil TGFβ1 production.

To confirm that phagocytosis was triggering TGFβ1 production, freshly isolated MSU crystal-recruited neutrophils labelled with the surface marker APC-Ly6G were incubated with apoptotic neutrophils labelled with PerCP-Ly6G (apoptotic cell:live cell, ratio 5:1) in the presence of GolgiStop *ex vivo* for 8 hours (section 2.7.2) and then stained for intracellular TGFβ1. Flow cytometry analysis of the cell culture confirmed that live neutrophils (APC-Ly6G$^+$, green box) were able to phagocytose apoptotic neutrophils (PerCP-Ly6G$^+$, black box) as shown in the double positive population (APC-Ly6G$^+$ / PerCP-Ly6G$^+$, red box) in Figure 3.13B. Interestingly, the expression of TGFβ1 was greatest in live cells that had phagocytosed apoptotic cells (red line) compared to the single cell populations, apoptotic neutrophils (black line) or live neutrophils (green), as shown in Figure 3.13C. Taken together, these results confirmed that the clearance of apoptotic cells by neutrophils was a primary trigger for inducing TGFβ1 production.

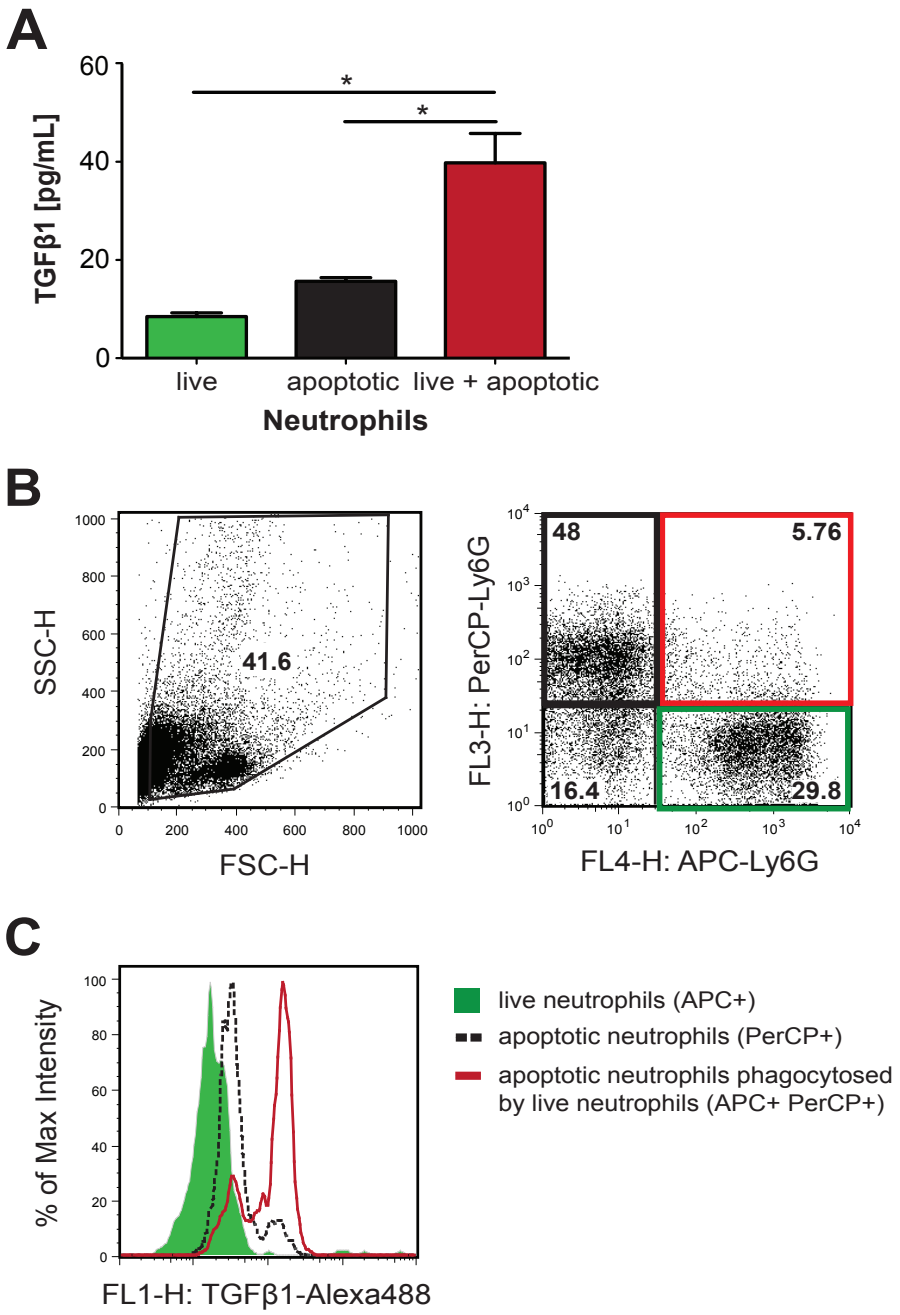

Figure 3.13: Phagocytosis of apoptotic neutrophils induces neutrophil TGFβ1 production. Mice were injected with MSU crystals (3 mg, i.p.). After 18 hours, neutrophils were purified and cultured for 8 hours *ex vivo*. **A** Supernatants from apoptotic neutrophils, live neutrophils or the co-culture were analysed for TGFβ1 by ELISA. **B, C** Apoptotic neutrophils (PerCP-Ly6G$^+$) and live neutrophils (APC-Ly6G$^+$) were co-cultured for 8 hours *ex vivo*. The cell culture was analysed by flow cytometry to compare the levels of TGFβ1 expression in the single positive neutrophil populations versus the live cell population that had phagocytosed apoptotic neutrophils (APC-Ly6G$^+$ / PerCP-Ly6G$^+$). Values represent the mean -/+ SEM of two independent experiments. * = $P < 0.05$ (one-way ANOVA with Tukey's post test).

3.3.9 TGFβ1 production suppresses neutrophil respiratory burst and IL-1β production *ex vivo*

Previous studies have shown that phagocytosis of apoptotic neutrophils can suppress pro-inflammatory responses to external stimuli, including the production of cytokines and reactive oxygen species (ROS) [199; 211]. IL-1β is a primary signal for the inflammatory cascade, and ROS production by neutrophils is an important effector function that can directly contribute to cell and tissue damage [193; 212]. To investigate whether neutrophil TGFβ1 production could be modulating superoxide and IL-1β production, MSU crystal-recruited neutrophils were purified and incubated *ex vivo* with either an anti-TGFβ1 antibody (35 μg/ml), or stimulated with MSU crystals (200 μg/ml) or a combination of both (section 2.8.1). Superoxide production was measured immediately using the colorimetric dye WST-1 (section 2.7.3). To measure IL-1β levels, supernatants were collected from the neutrophil culture after 4 hours and analysed by ELISA (section 2.8).

Restimulation of the neutrophils *ex vivo* resulted in an increase in the production of both neutrophil superoxide (Figure 3.14A) and IL-1β (Figure 3.14B) compared to untreated neutrophils. Interestingly, in the presence of the neutralising TGFβ1 antibody, the neutrophils exhibited a significant increase in both the production of superoxide (Figure 3.14A) and IL-1β (Figure 3.14B), with or without MSU crystals.

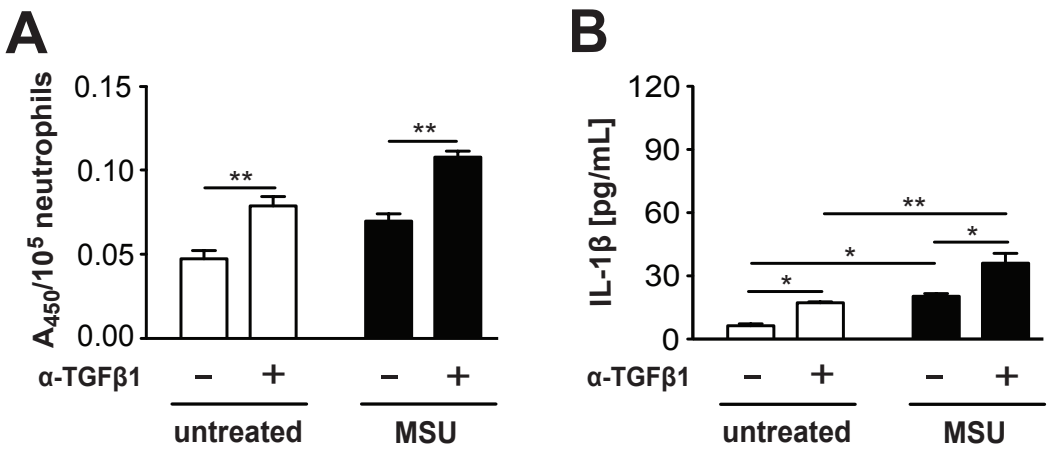

Figure 3.14: TGFβ1 production suppresses neutrophil respiratory burst and IL-1β production *ex vivo*. Mice were injected with MSU crystals (3 mg, i.p.). After 18 hours, neutrophils were purified from the peritoneal cavity. Freshly isolated MSU crystal-recruited neutrophils were cultured *ex vivo* -/+ MSU crystal stimulation (200 μg/ml) and -/+ anti-TGFβ1 antibody (35 μg/ml) and **A** superoxide production and **B** IL-1β production measured by ELISA after 4 hours in culture. Values represent the mean -/+ SEM of two independent experiments. * = $P < 0.05$, ** = $P < 0.01$ (two-way ANOVA with Bonferroni's post test).

Neutrophils were also tested for their ability to regulate other pro-inflammatory cytokines such as TNFα, IL-6 and the neutrophil chemokine (C-X-C motif) ligand 1 (CXCL1). As shown in Figure 3.15A - C, *ex vivo* restimulation of neutrophils with MSU crystals, the anti-TGFβ1 antibody or the combination of both had no effect on the production of TNFα, IL-6 or CXCL1. Taken together, these results indicated that neutrophil phagocytosis and TGFβ1 production were important for regulating neutrophil respiratory burst and IL-1β production *ex vivo*.

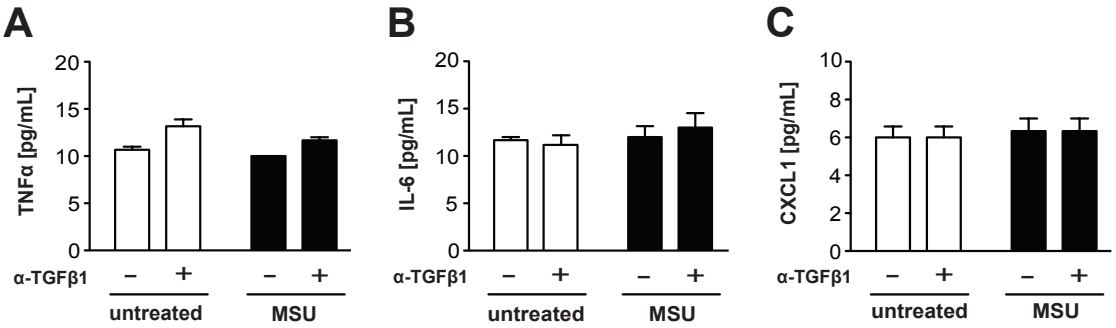

Figure 3.15: Neutrophil TGFβ1 production does not alter the cytokines TNFα, IL-6 or the chemokine CXCL1. Mice were injected with MSU crystals (3 mg, i.p.). After 18 hours, neutrophils were purified from the peritoneal cavity. Freshly isolated MSU crystal-recruited neutrophils were cultured *ex vivo* -/+ MSU crystal stimulation (200 μg/ml) and -/+ anti-TGFβ1 antibody (35 μg/ml) for 4 hours. The levels of the cytokines (**A**) TNFα, (**B**) IL-6 and (**C**) CXCL1 in culture supernatants were measured by multiplex bead array. Values represent the mean -/+ SEM of two independent experiments.

3.3.10 TGFβ1 production suppresses neutrophil respiratory burst *in vivo*

Finally, the effect of TGFβ1 on MSU crystal-induced neutrophil superoxide and IL-1β production was investigated *in vivo*. Mice were injected intraperitoneally with the anti-TGFβ1 antibody (1 mg) 30 minutes prior to MSU crystal treatment (3 mg) (section 2.5.4). After 8 and 18 hours, MSU crystal-recruited neutrophils were harvested and purified, and superoxide production was measured immediately (section 2.7.3). Neutrophils were also cultured *ex vivo* for 4 hours, and the culture supernatants collected and analysed for IL-1β (section 2.8). As shown in Figure 3.16A, neutrophils that were isolated 18 hours after MSU crystal administration produced more superoxide than neutrophils isolated 8 hours after MSU crystal administration. TGFβ1 neutralisation did not alter superoxide production by neutrophils, isolated 8 hours after MSU crystal treatment. However, TGFβ1 neutralisation caused a significant increase in superoxide production by neutrophils 18 hours following MSU crystal administration.

In contrast, MSU crystal-recruited neutrophils from the 18 hour time point produced less IL-1β compared to neutrophils isolated 8 hours after MSU crystal administration (Figure 3.16B). Interestingly, TGFβ1 neutralisation did not affect IL-1β production by neutrophils isolated at 8 and 18 hours. These findings showed that neutralisation of TGFβ1 resulted in an increase in superoxide production by neutrophils without altering IL-1β production *in vivo*.

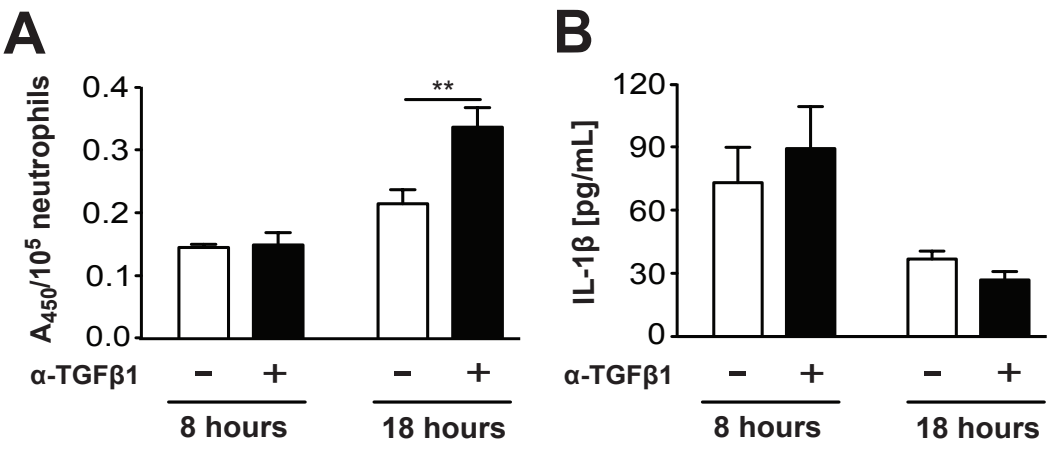

Figure 3.16: TGFβ1 production suppresses neutrophil respiratory burst *in vivo*. Mice were injected with the anti-TGFβ1 antibody (1 mg, i.p.) 30 minutes prior MSU crystal administration (3 mg, i.p.). After 8 and 18 hours, MSU crystal-recruited peritoneal neutrophils were harvested and purified, and **A** superoxide production was measured. **B** Purified peritoneal neutrophils were cultured for 4 hours *ex vivo* and IL-1β production in culture supernatants measured by ELISA. Values represent the mean -/+ SEM of two independent experiments. ** = $P < 0.01$ (two-way ANOVA with Bonferroni's post test).

3.4 Summary

The process of phagocytosis of apoptotic neutrophils and TGFβ1 production is a characteristic feature of the spontaneous resolution of acute inflammation and it is traditionally attributed to macrophage function [199; 183]. Like macrophages, neutrophils are professional phagocytes [191]. Previous research has shown that phagocytosis of apoptotic neutrophils can suppress pro-inflammatory responses via cytokines and ROS [199; 211]. The results presented in this chapter show that the process of phagocytosis of apoptotic neutrophils by neutrophils triggers the production of TGFβ1, which further leads to the suppression of superoxide and IL-1β production by MSU crystal-activated neutrophils *in vitro*. However, although neutralising TGFβ1 *in vivo* resulted in an increase in superoxide production by neutrophils, it did not alter IL-1β production. This indicated that neutrophil-derived TGFβ1 may only be one mechanism involved in regulating active IL-1β during a neutrophil-driven inflammatory response *in vivo*.

The results presented in this chapter show that the process of neutrophil canibalism triggers neutrophil TGFβ1 production, which leads to the suppression of neutrophil respiratory burst and acts as a non-essential moderator of IL-1β production, as shown in Figure 3.17. This indicated that neutrophils also contribute to the spontaneous resolution of acute gouty inflammation via phagocytosis-driven TGFβ1 production.

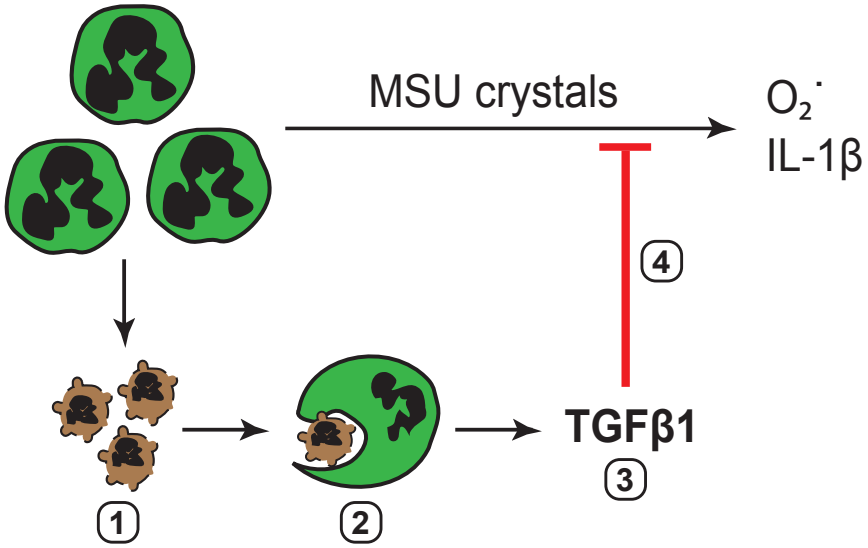

Figure 3.17: Neutrophils and the resolution of inflammation. Neutrophils undergo apoptosis (1) and are phagocytosed by live neutrophils (2) leading to the production of TGFβ1 (3) and the suppression of MSU crystal-induced neutrophil inflammatory responses (4). O2- = superoxide; IL-1β = interleukin-1 beta.

Chapter 4

4 The Effect of TGFβ1 on GM-BMMs and M-BMMs in Response to MSU Crystals

4.1 Introduction

Macrophages are known for their heterogeneity and diversity depending on the inflammatory microenvironment. Two major cytokines that influence the differentiation and function of macrophages are GM-CSF and M-CSF; well documented growth factors. Recent reports have shown that human monocytes treated with GM-CSF differentiate into a pro-inflammatory macrophage subset *in vitro*, better known as M1-like macrophages [140; 141]. In the presence of M-CSF, human monocyte-derived macrophages can be differentiated into an anti-inflammatory or tissue-resident macrophage phenotype (M2-like cells) [140; 141; 142].

One study has now shown that in a peritoneal model of acute inflammation, MSU crystal-recruited monocytes differentiate into hyper-inflammatory macrophages *in vivo* [149]. The polarisation of this pro-inflammatory macrophage phenotype is dependent on the growth factor GM-CSF [unpublished data, manuscript submitted]. Results presented previously in Figure 3.1A show that this phenotype also develops in the presence of high levels of TGFβ1. However, the effect of TGFβ1 on the development of GM-CSF and M-CSF macrophages in acute gouty inflammation *in vivo* remains unknown. To gain more insight into how both CSFs (GM-CSF and M-CSF) and TGFβ1 contribute to macrophage differentiation and inflammatory responses, the current study focused on the effect of TGFβ1 on the function of *in vitro* generated bone-marrow derived macrophages (BMMs).

4.2 Aim

The aim of this chapter was to investigate the effect of TGFβ1 on the functional phenotype of *in vitro* generated GM-CSF and M-CSF BMMs.

4.3 Results

4.3.1 Differentiation of GM-CSF and M-CSF BMMs

To investigate the effect of TGFβ1 on the functional properties of GM-CSF-differentiated macrophages (GM-BMMs) and M-CSF-differentiated macrophages (M-BMMs), murine bone marrow cells were harvested (section 2.6.4) and cultured *in vitro* with either GM-CSF (1000 units/ml) or M-CSF (5000 units/ml) in the absence or presence of recombinant human TGFβ1 (1 ng/ml or 10 ng/ml) for seven days (section 2.7.4). The concentrations of GM-CSF and M-CSF for the differentiation of macrophages were used according to the literature [213; 214]. As illustrated in Figure 4.1, the cells were fed with the appropriate media containing the growth factors GM-CSF and M-CSF, and/or rhTGFβ1 on day one, three and five.

On day seven, the non-adherent cells were removed by extensive washing and the adherent BMMs were primed with 50 pg/ml lipopolysaccharide (LPS) overnight (section 2.7.4). Unlike monocytes and due to the sterile *in vitro* culture environment, macrophages need a co-stimulating or priming signal first, for example LPS, to induce the synthesis of cytokine gene expression, including inactive pro-IL-1β [215; 216; 217; 218]. Following LPS priming, TGFβ1-differentiated GM-BMMs and M-BMMs were then stimulated with MSU crystals (200 μg/ml) or LPS (100 ng/ml) or left untreated (control) for 18 hours (section 2.7.5). After stimulation, culture supernatants were collected and analysed for different cytokines and chemokines by ELISA or multiplex bead array (section 2.8), and/or cells were harvested for flow cytometry analysis (section 2.9) or cytoplasmic protein collected for western blot

analysis (section 2.11).

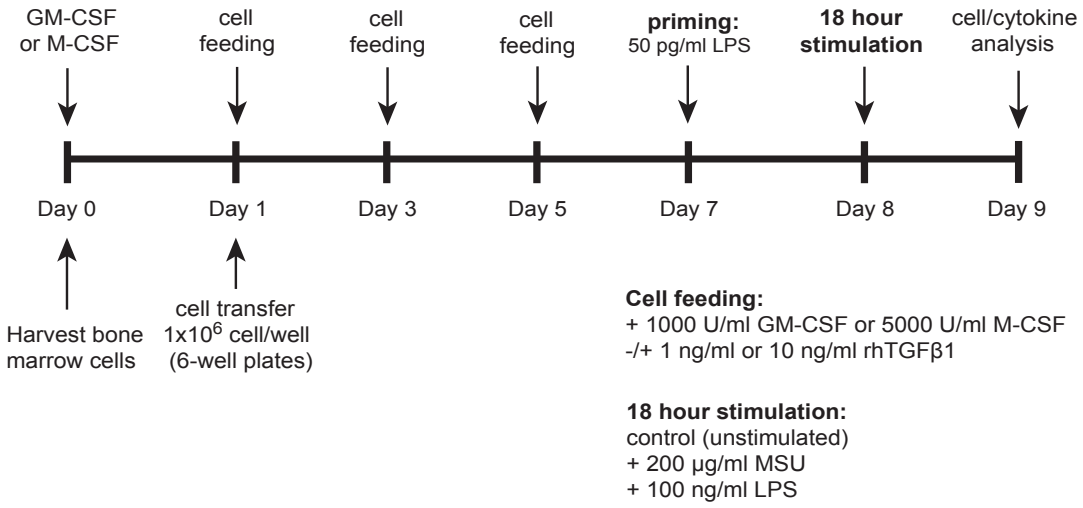

Figure 4.1: Experimental layout of *in vitro* TGFβ1-differentiated GM-CSF and M-CSF bone marrow-derived macrophages.

4.3.2 TGFβ1 drives a pro-inflammatory GM-BMM phenotype

Cytokine analysis showed that after MSU crystal stimulation, GM-BMMs produced the pro-inflammatory cytokines IL-1α and IL-1β (Figure 4.2). Interestingly, in response to TGFβ1 MSU crystal-stimulated GM-BMMs significantly increased the production of IL-1β and IL-1α. TGFβ1 treatment had no effect on the cytokine levels of TNFα and IL-6, or the chemokines MCP-1 and CXCL1 produced by MSU crystal-stimulated GM-BMMs. In response to LPS, GM-BMMs produced low levels of IL-1β but high levels of TNFα, MCP-1 and CXCL1, that were unaffected by TGFβ1.

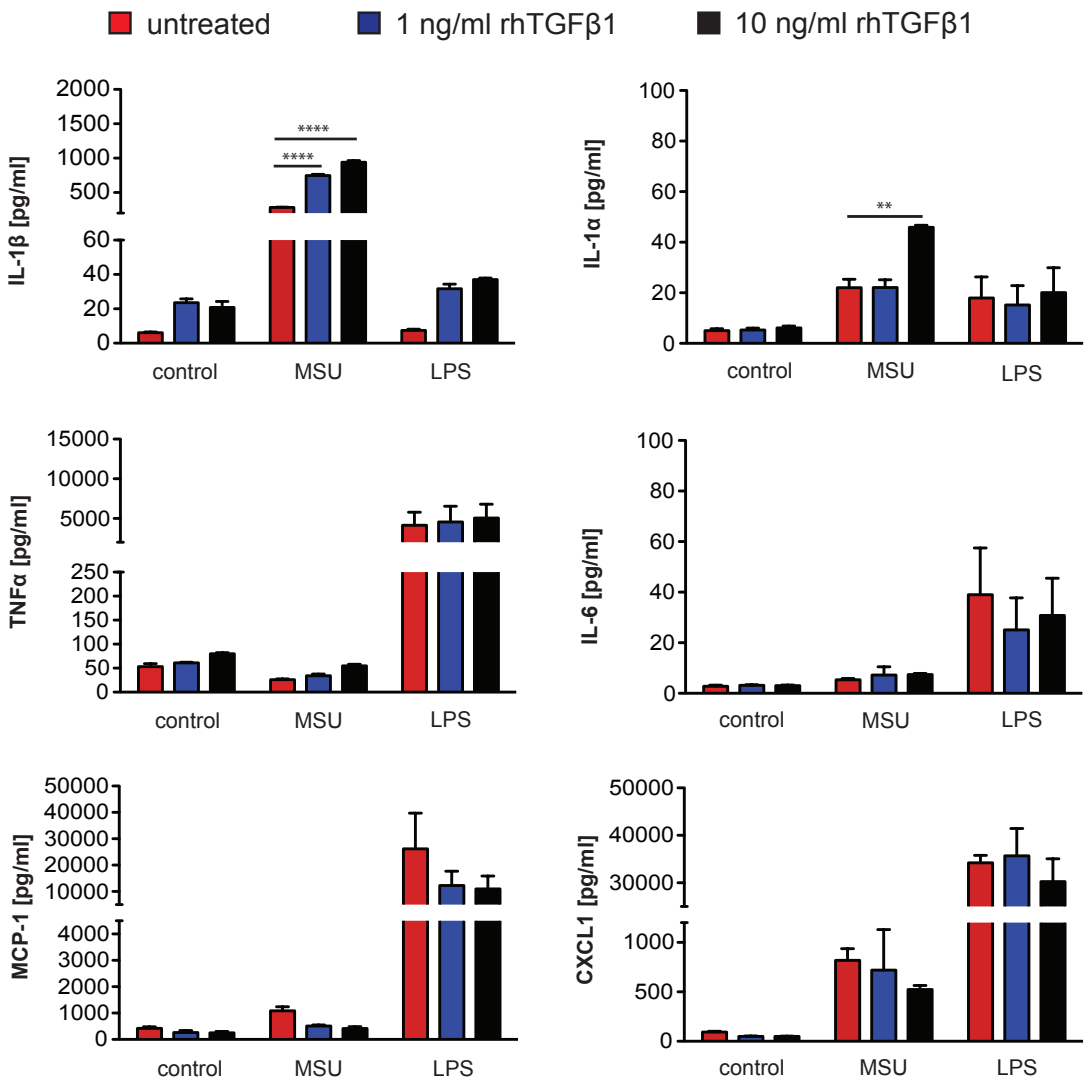

Figure 4.2: Cytokine production by *in vitro* stimulated TGFβ1-differentiated GM-BMMs. Bone marrow cells were harvested and cultured *in vitro* with the growth factor GM-CSF (1000 units/ml) in the presence of recombinant human TGFβ1 (1 ng/ml or 10 ng/ml) for 7 days following priming with 50 pg/ml LPS overnight. GM-BMMs were then stimulated with MSU crystals (200 μg/ml) or LPS (100 ng/ml) or left untreated (control) for 18 hours. Supernatants from cell culture were collected and analysed for IL-1β, IL-1α, TNFα, IL-6, MCP-1 and CXCL1 by ELISA and multiplex bead array. Values are the mean -/+ SEM and representative of three experiments. ** = $P < 0.01$, **** = $P < 0.0001$ (two-way ANOVA with Bonferroni's post test).

The non-adherent GM-BMMs were also tested for their functional properties. After priming with LPS, the cells were stimulated with MSU crystals (200 μg/ml) or LPS (100 ng/ml) for 18 hours and the supernatants collected for cytokine analysis (section 2.8). The MSU crystal-stimulated non-adherent cells produced significantly lower levels of IL-1β than the adherent GM-BMMs that decreased further with TGFβ1 treatment (Figure 4.3). The non-adherent cells failed to produce TNFα, IL-6, MCP-1 and secreted only low levels of CXCL1. TGFβ1 treatment had no effect on LPS-stimulated cells apart from decreased MCP-1 levels. These results confirmed that only the adherent TGFβ1-differentiated GM-BMMs exhibited an enhanced inflammatory phenotype in response to MSU crystals similar to that identified *in vivo* [103]. Therefore, all further experiments carried out within this chapter focused on the adherent macrophage population.

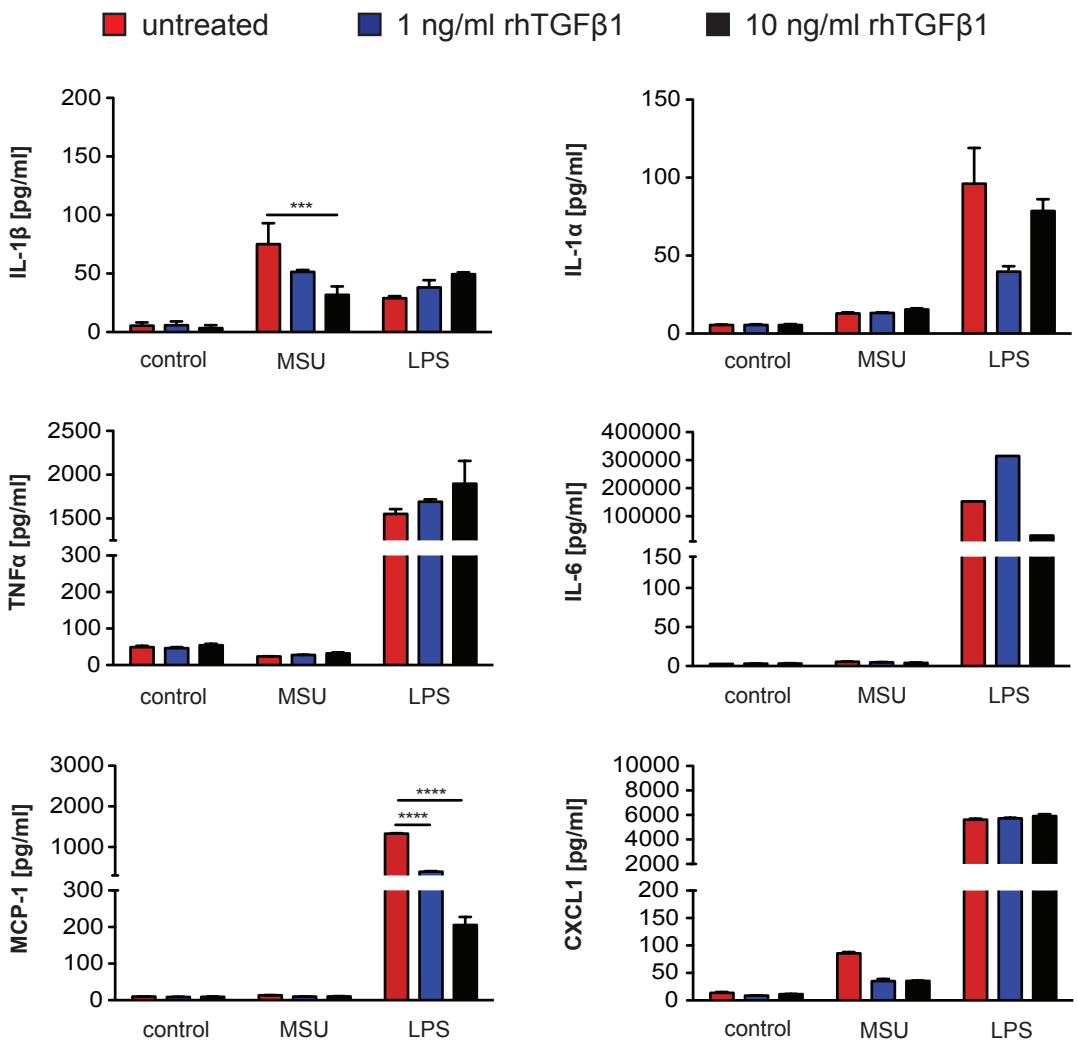

Figure 4.3: Cytokine production by *in vitro* stimulated non-adherent TGFβ1-differentiated GM-BMMs. Bone marrow cells were harvested and cultured *in vitro* with GM-CSF (1000 units/ml) in the presence of rhTGFβ1 (1 ng/ml or 10 ng/ml) for 7 days. Non-adherent cells were removed and transfered into new 6-well plates (1x10^6 cells/ml) following priming with 50 pg/ml LPS overnight. Non-adherent GM-BMMs were then stimulated with MSU crystals (200 μg/ml) or LPS (100 ng/ml) or left untreated (control) for 18 hours. Supernatants from cell culture were collected and analysed for IL-1β, IL-1α, TNFα, IL-6, MCP-1 and CXCL1 by ELISA and multiplex bead array. Values are the mean -/+ SEM and representative of two experiments. *** = $P < 0.001$, **** = $P < 0.0001$ (two-way ANOVA with Bonferroni's post test).

As shown in Figure 4.4, MSU crystal-stimulated M-BMMs produced significantly reduced levels of IL-1β following TGFβ1 treatment, whereas the levels of IL-1α, TNFα, IL-6, MCP-1 and CXCL1 were unaffected. Unlike GM-BMMs, TGFβ1 treatment significantly increased the production of all cytokines and chemokines by LPS stimulated M-BMMs. During the 7 day *in vitro* culture of M-BMMs, non-adherent cells were not observed in the culture plates; therefore, only the adherent M-BMMs were characterised within this chapter. Taken together, these findings showed that, with respect to MSU crystal stimulation, TGFβ1 was driving a hyper-inflammatory GM-BMM phenotype, but a hypo-inflammatory M-BMM phenotype.

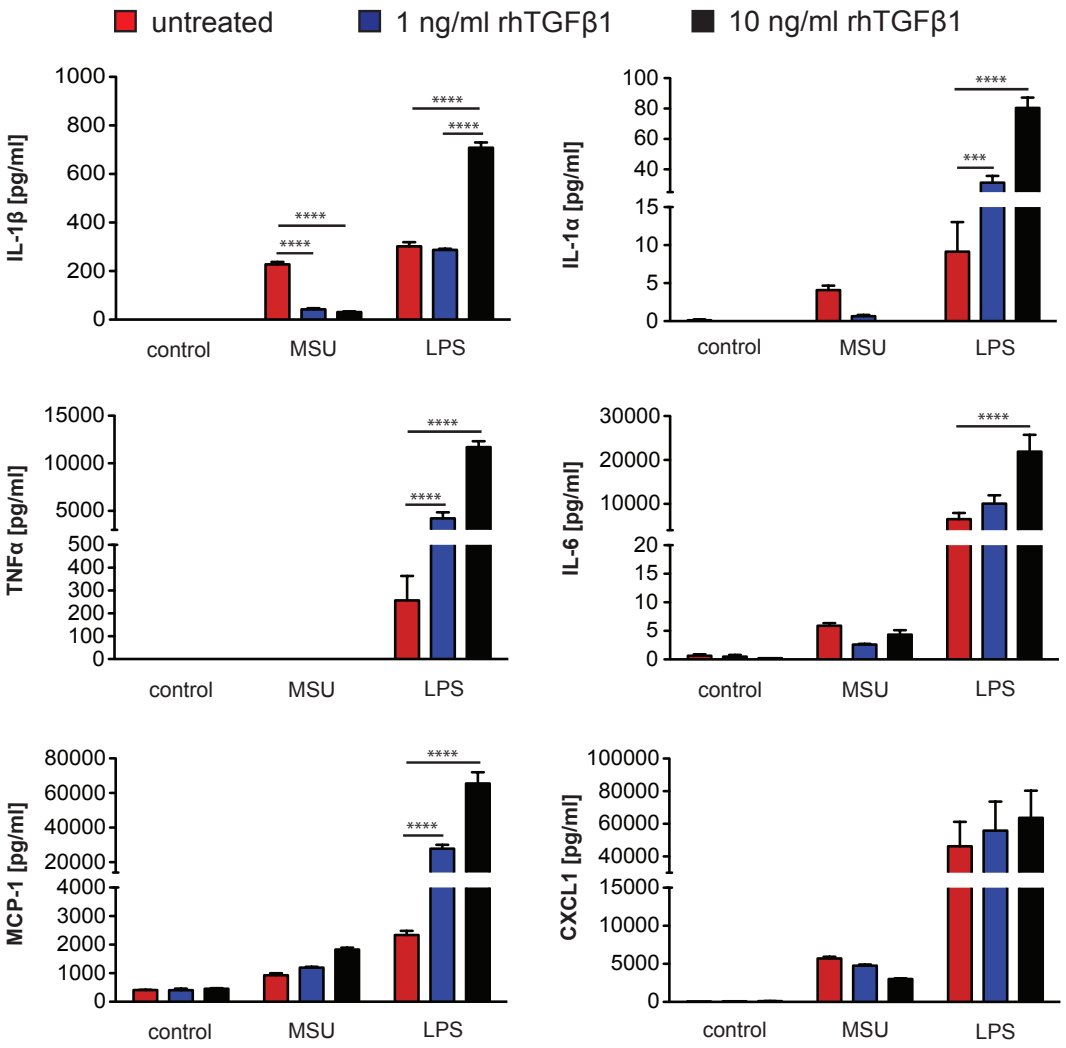

Figure 4.4: Cytokine production by *in vitro* stimulated TGFβ1-differentiated M-BMMs. Bone marrow cells were harvested and cultured *in vitro* with M-CSF (5000 units/ml) in the presence of rhTGFβ1 (1 ng/ml or 10 ng/ml) for 7 days following priming with 50 pg/ml LPS overnight. M-BMMs were then stimulated with MSU crystals (200 μg/ml) or LPS (100 ng/ml) or left untreated (control) for 18 hours. Supernatants from cell culture were collected and analysed for IL-1β, IL-1α, TNFα, IL-6, MCP-1 and CXCL1 by ELISA and multiplex bead array. Values are the mean -/+ SEM and representative of two experiments. *** = $P < 0.001$, **** = $P < 0.0001$ (two-way ANOVA with Bonferroni's post test).

4.3.3 The effect of TGFβ1 on BMM polarisation

In the preceeding experiments, GM-BMMs and M-BMMs were differentiated in the presence of TGFβ1 for seven days following stimulation. To investigate whether TGFβ1 had the same effect on fully differentiated GM-BMMs and M-BMMs, both macrophage populations were differentiated with GM-CSF or M-CSF for seven days prior to the culture in the absence or presence of TGFβ1 (1 ng/ml or 10 ng/ml) for one or five days (section 2.7.4). LPS-primed BMMs were stimulated with either MSU crystals (200 μg/ml) or LPS (100 ng/ml) for 18 hours, and the IL-1β levels in the culture supernatants measured by ELISA (section 2.8). IL-1β production by MSU or LPS-stimulated GM-BMMs was not affected by one or five days TGFβ1 treatment (Figure 4.5A and B).

In comparison to GM-BMMs, one and five day TGFβ1 treatment resulted in a significant decrease in the production of IL-1β by MSU crystal-stimulated M-BMMs (Figure 4.5C and D). Interestingly, TGFβ1 treatment for one day had no significant effect on the IL-1β levels by LPS-stimulated M-BMMs (Figure 4.5A) that was significantly reduced after five days of TGFβ1 treatment (Figure 4.5B). These results were in contrast to the IL-1β production obtained in Figure 4.4 showing that LPS-stimulated M-BMMs produced significantly more IL-1β when differentiated in the presence of TGFβ1.

Together, these findings indicated that TGFβ1 was required during the differentiation process to drive the hyper-inflammatory GM-BMM phenotype in response to MSU crystals. In addition, TGFβ1 induced a hypo-inflammatory M-BMM phenotype after MSU crystal stimulation that was independent of whether M-BMMs were treated with TGFβ1 during or after differentiation.

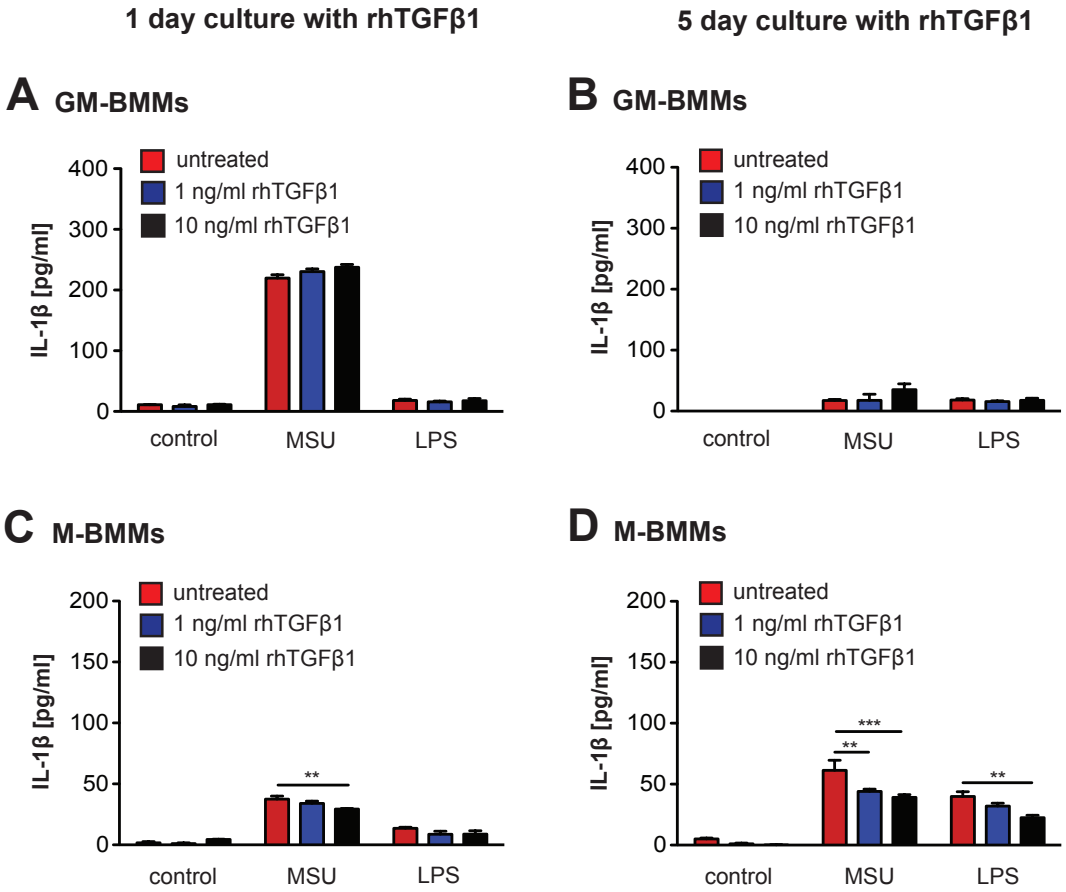

Figure 4.5: TGFβ1 required during differentiation to drive pro-inflammatory GM-BMMs. Bone marrow cells were harvested and cultured *in vitro* with GM-CSF (1000 units/ml) or M-CSF (5000 units/ml) for 7 days. After 7 days, rhTGFβ1 (1 ng/ml or 10 ng/ml) was added into the GM-BMM or M-BMM culture for 1 day or 5 days, respectively. BMMs were then primed with 50 pg/ml LPS overnight following stimulation with MSU crystals (200 μg/ml) or LPS (100 ng/ml), or left untreated (control) for 18 hours. Supernatants from the 1 day (**A, C**) or 5 days (**B, D**) cultures were collected and analysed for IL-1β by ELISA. Results are representative of two experiments. ** = $P < 0.01$, *** = $P < 0.001$ (two-way ANOVA with Bonferroni's post test).

4.3.4 TGFβ1 induces pro-inflammatory GM-BMM phenotype independent of stimuli

In addition to MSU crystals, TLR agonists such as LPS and Pam3Cys have been shown to trigger an inflammatory response in monocytes and macrophages, leading to the activation of the NLRP3 inflammasome and the production of IL-1β [219]. To determine whether the hyper-inflammatory GM-BMM phenotype and the hypo-inflammatory M-BMM phenotype emerging in the presence of TGFβ1 were also triggered in response to different inflammatory stimuli, LPS-primed GM-BMMs and M-BMMs were stimulated with LPS (100 ng/ml), Pam3Cys (100 ng/ml) or MSU cystals (200 μg/ml) for 18 hours (section 2.7.5). After stimulation, supernatants from the cell cultures were collected and analysed for IL-1β by ELISA (section 2.8).

Consistent with the previous results in Figure 4.2, TGFβ1-differentiated GM-BMMs produced significantly more IL-1β upon MSU crystal stimulation compared to untreated GM-BMMs (Figure 4.6A). Similarly, stimulation of GM-BMMs with LPS and Pam3Cys also triggered the production of IL-1β, which significantly increased upon TGFβ1 treatment. TGFβ1 treatment induced a significant decrease in the levels of IL-1β in MSU crystal-stimulated M-BMMs (Figure 4.6B) consistent with previous data obtained in Figure 4.4. Interestingly, TGFβ1 treatment significantly increased the production of IL-1β by LPS or Pam3Cys-stimulated M-BMMs.

These results confirmed that TGFβ1 contributed to the differentiation of a hyper-inflammatory GM-BMM phenotype, whereas M-CSF-differentiated macrophages were pushed towards a less responsive M-BMM phenotype specifically in response to MSU crystals. Based on the differential effect of TGFβ1 on GM-BMMs vs M-BMMs, the remainder of this chapter focused on investigating the effect of TGFβ1 on MSU crystal-stimulated GM-BMMs and M-BMMs.

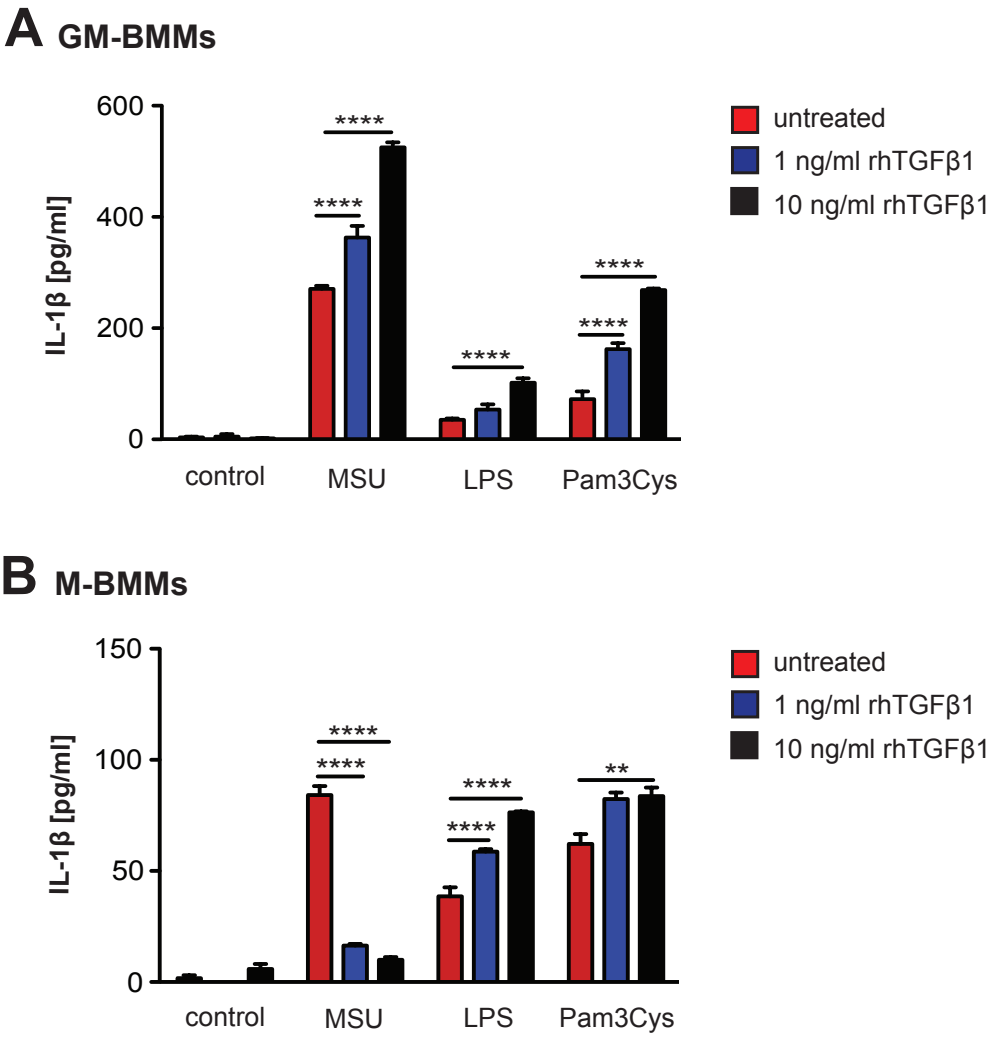

Figure 4.6: TGFβ1 induced pro-inflammatory response by GM-BMMs independent of stimuli. Bone marrow cells were harvested and cultured *in vitro* with GM-CSF (1000 units/ml) and M-CSF (5000 units/ml) in the presence of rhTGFβ1 (1 ng/ml or 10 ng/ml) for 7 days following priming with 50 pg/ml LPS overnight. After priming, GM-BMMs and M-BMMs were stimulated with MSU crystals (200 μg/ml), LPS (100 ng/ml) or Pam3Cys (100 ng/ml) for 18 hours. Supernatants from the GM-BMM (**A**) and M-BMM (**B**) culture were collected and analysed for IL-1β by ELISA. Results are representative of two separate experiments. ** = $P < 0.01$, **** = $P < 0.0001$ (two-way ANOVA with Bonferroni's post test).

4.3.5 TGFβ1 suppresses T cell proliferation by GM-BMMs

Macrophages have been shown to play a role in bridging innate and adaptive immune responses. They have the ability to act as antigen presenting cells (APCs) initiating T cell responses, and to maintain tolerance [220; 221]. APCs express major histocompatibility complex class II (MHCII) molecules on their cell surface, therefore they are able to present antigen to CD4 T cells [222; 223]. For the activation of naive CD4 T cells, two signals are required: the first signal is provided by the recognition of MHCII on APCs and the second signal is a co-stimulatory signal via CD86, which is expressed on activated APCs. Recent studies have shown that GM-BMMs can activate and present antigen to T cells [224], whereas M-BMMs are defective in APC functions [225]. There is also evidence showing that TGFβ1 has immunosuppressive activities by inhibiting T cell proliferation [226]. In order to confirm the functional differences between GM-BMMs and M-BMMs and the effect of TGFβ1 on their APC function, GM-BMMs and M-BMMs were primed with LPS (100 ng/ml) for 18 hours (section 2.7.6) and then analysed for the expression of CD86 and MHCII by flow cytometry (section 2.9).

Mature GM-BMMs expressed high levels of CD86 and MHCII (Figure 4.7A). The expression of both CD86 and MHCII was down-regulated upon TGFβ1 treatment. This was consistent with previous reports showing that TGFβ1 down-regulates CD86 and MHCII expression on GM-CSF-differentiated BMMs [227; 228]. On the other hand, M-BMMs expressed low levels of CD86 and MHCII compared to GM-BMMs (Figure 4.7B, red line). TGFβ1 treatment induced the upregulation of CD86 but decreased the expression of MHCII by M-BMMs.

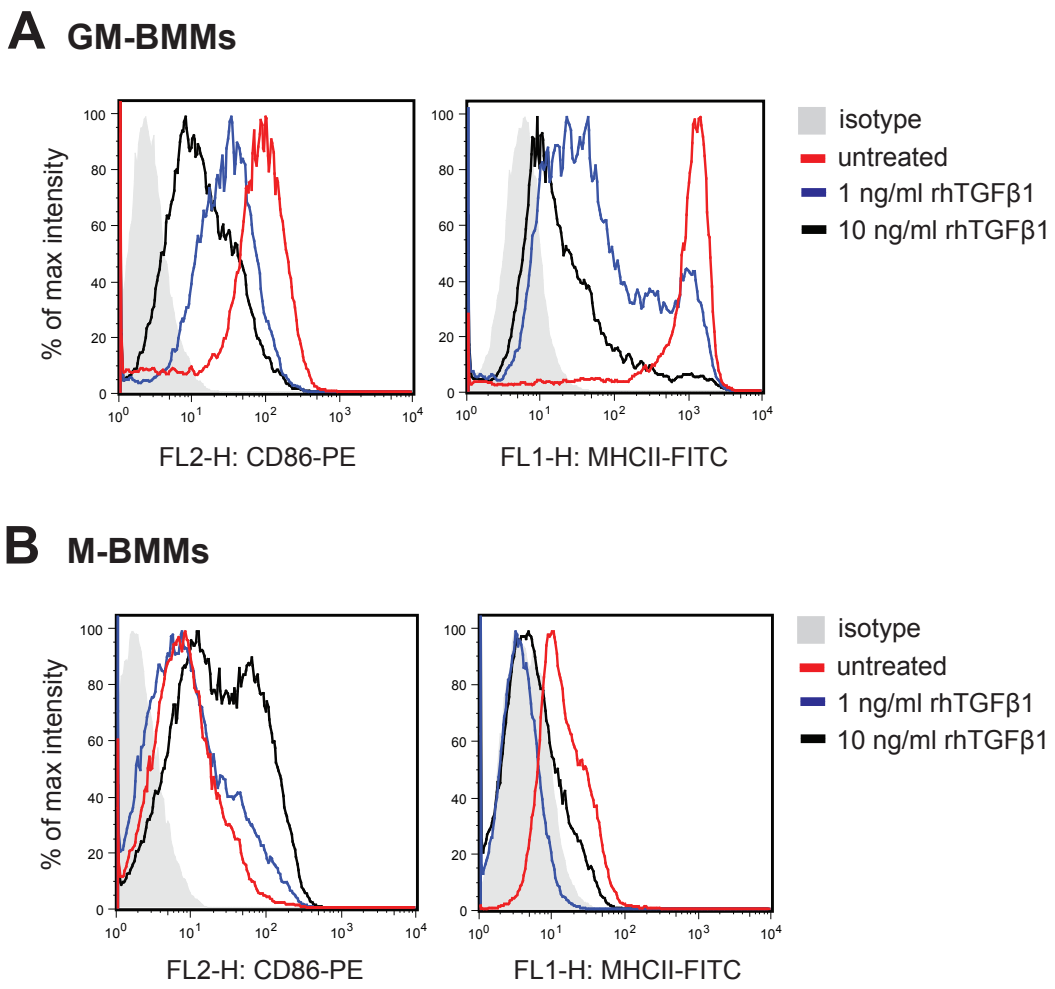

Figure 4.7: TGFβ1 down-regulates antigen-presenting capacity of LPS-primed GM-BMMs and M-BMMs. Bone marrow cells were harvested and cultured *in vitro* with the growth factor GM-CSF (1000 units/ml) and M-CSF (5000 units/ml) in the presence of recombinant human TGFβ1 (1 ng/ml or 10 ng/ml) for 7 days following priming with 100 ng/ml LPS overnight. The TGFβ1-differentiated GM-BMMs (**A**) and M-BMMs (**B**) were analysed for the expression of the surface marker MHCII and CD86 by flow cytometry. Results are representative of two independent experiments.

Next, *in vitro* T cell proliferation assays were performed to assess the effect of TGFβ1 on the ability of GM-BMMs and M-BMMs to induce OVA-specific $CD4^+$ T cell proliferation. Mature GM-BMMs and M-BMMs were pulsed with OVA peptide and at varying cell numbers co-incubated for three days with T cells harvested from lymph nodes of OTII transgenic mice. After incubation, 1 μCi [^{3}H]-thymidine was added to each well and cells were incubated for an additional 18 hours. As a measure of T cell proliferation, the amount of [^{3}H]-thymidine incorporated into the cellular DNA was determined by liquid scintillation counting (section 2.7.6).

As shown in Figure 4.8A, GM-BMMs efficiently induced antigen-dependent CD4 T cell proliferation that was significantly inhibited upon TGFβ1 treatment. This indicated an immunosuppressive effect of TGFβ1 on antigen presenting capacity, consistent with down-regulated expression of MHCII (Figure 4.7A). In contrast, M-BMMs failed to induce CD4 T cell proliferation independent of TGFβ1 treatment (Figure 4.7C) confirming the inability of M-BMMs to act as APCs to induce T cell proliferative responses.

Recent reports have also shown that MSU crystals exhibit adjuvant activities and are able to augment the proliferation of T cells by dendritic cells (DCs) [88; 90; 89]. De-En Hu and colleagues have also shown that in a murine tumour model, administration of MSU crystals enhanced the tumour rejection process [91]. To investigate the adjuvant effect of MSU crystals on TGFβ1-differentiated BMMs, OVA-loaded GM-BMMs and M-BMMs were activated with MSU crystals (200 μg/ml) and proliferation assays were carried out (section 2.7.6).

MSU crystal-activated GM-BMMs were less efficient stimulators of CD4 T cell proliferation (Figure 4.8B, red line) compared to unstimulated GM-BMMs (Figure 4.8A, red line). TGFβ1 treatment further inhibited the low T cell stimulatory activity. This indicated that MSU crystal activation of GM-BMMs did not rescue the inhibitory antigen-presenting effect of TGFβ1. As expected, TGFβ1-differentiated

M-BMMs did not induce CD4 T cell proliferation upon MSU crystal activation (Figure 4.8D). Taken together, these findings demonstrated that TGFβ1 suppressed the antigen presenting and T cell proliferative capability of GM-BMMs indicating that TGFβ1 switched off the adaptive immune response but promoted the innate immune response by driving a hyper-inflammatory GM-BMM phenotype. In contrast, M-BMMs were defective in functioning as APCs. Based on these interesting results, a more detailed phenotypic analysis on TGFβ1-treated GM-BMMs and M-BMMs was carried out.

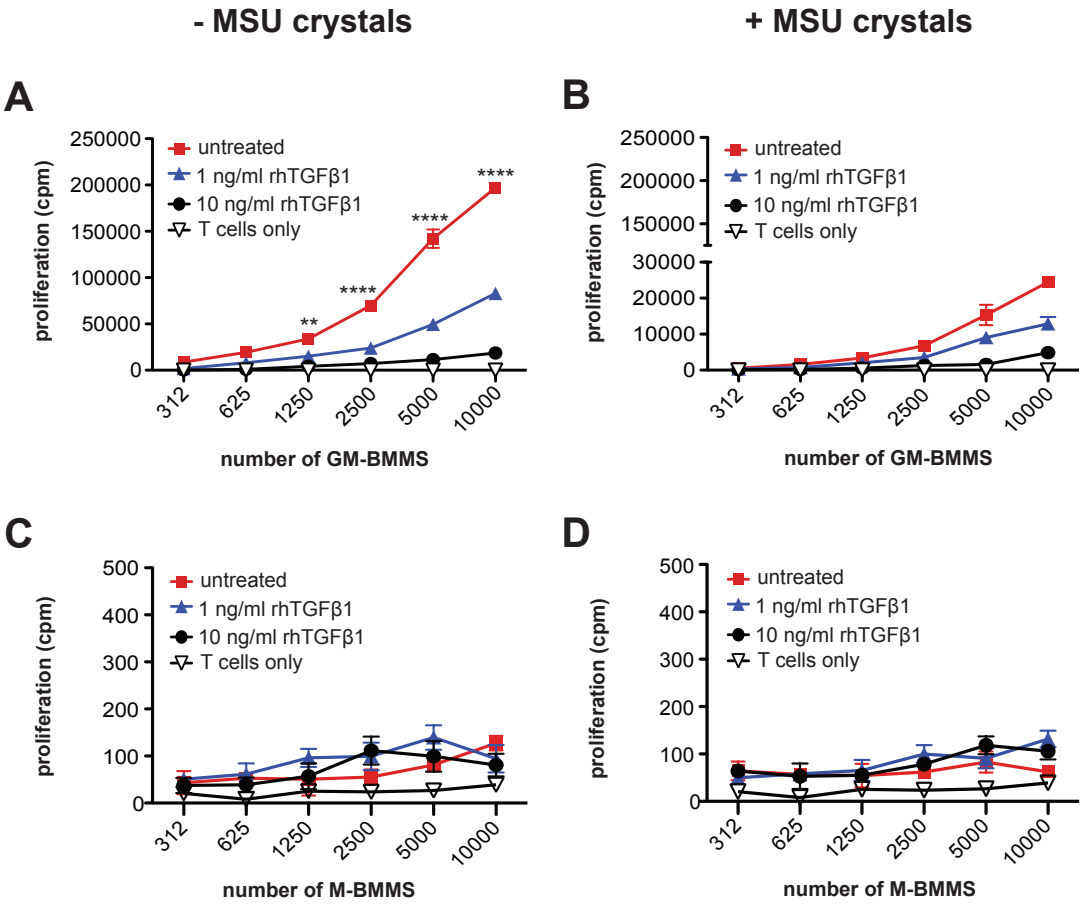

Figure 4.8: TGFβ1 suppresses CD4 T cell proliferation by GM-BMMs. Bone marrow cells were harvested and cultured *in vitro* with the growth factor GM-CSF (1000 units/ml) and M-CSF (5000 units/ml) in the presence of recombinant human TGFβ1 (1 ng/ml or 10 ng/ml) for 7 days following priming with 100 ng/ml LPS overnight. Mature GM-BMMs and M-BMMs were loaded with 1 μM ISQ peptide ($OVA_{323-339}$ protein) for 2 hours. Unstimulated GM-BMMs (**A**) or M-BMMs (**C**) and MSU crystal-stimulated (200 μg/ml) GM-BMMs (**B**) and M-BMMs (**D**) were then co-incubated at various numbers with T cells harvested from lymph nodes of OTII mice for 3 days. After incubation, 1 μCi [^{3}H]-thymidine was added to each well and incubated for an additional 18 hours. T cell proliferation was measured by thymidine incorporation using a liquid scintillation counter. Values are the mean -/+ SEM and representative of three independent experiments. ** = $P < 0.01$, **** = $P < 0.0001$ (two-way ANOVA with Bonferroni's post test).

4.3.6 Morphology of TGFβ1-differentiated BMMs

First, the effect of TGFβ1 on the morphology of differentiated GM-BMMs and M-BMMs was investigated. LPS-primed GM-BMMs showed classical macrophage round shape-like morphology (Figure 4.9A), whereas M-CSF induced a majority of more elongated tissue-resident macrophage morphology (Figure 4.9B). TGFβ1 treatment, however had no effect on the morphology of GM-BMMs, but induced more elongated M-BMMs.

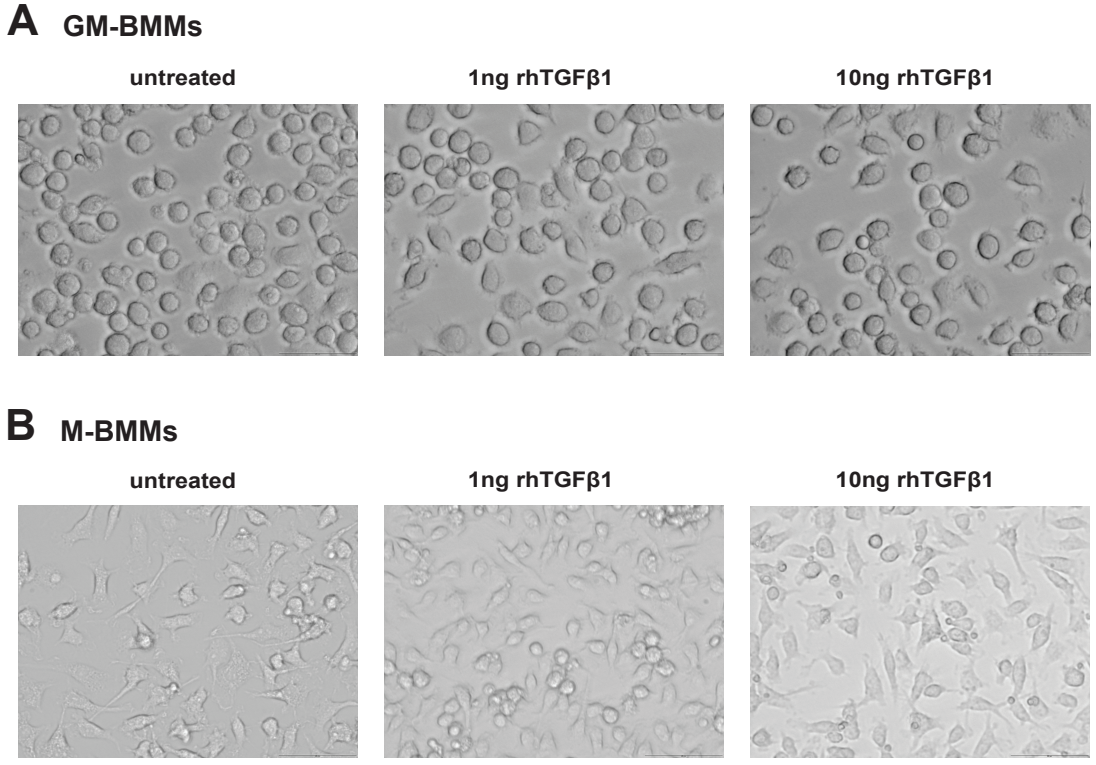

Figure 4.9: Morphology of *in vitro* TGFβ1-differentiated GM-BMMs and M-BMMs. Bone marrow cells were harvested and cultured *in vitro* with the growth factors GM-CSF (1000 units/ml) or M-CSF (5000 units/ml) in the presence of recombinant human TGFβ1 (1 ng/ml or 10 ng/ml) for 7 days. The differentiated GM-BMMs (**A**) and M-BMMs (**B**) were primed with 50 pg/ml LPS overnight and then examined under a microscope. Original magnification 40x. Results are representative of three independent experiments.

4.3.7 Phenotyping of primed TGFβ1-differentiated BMMs

To determine how TGFβ1 affected the surface phenotype during the differentiation of GM-BMMs and M-BMMs, LPS-primed GM-BMMs and M-BMMs were analysed for the expression of a variety of surface markers by flow cytometry (section 2.9). GM-BMMs expressed the common macrophage surface marker F4/80, CD14 and CD11b, and low levels of the M-CSF receptor CD115 and the activation marker CD86 (Figure 4.10A, red line). Since GM-CSF is widely used to generate monocyte-derived dendritic cells (DCs) *in vitro*, the adherent GM-BMMs were also stained with the DC surface markers CD11c and MHCII. As shown in Figure 4.10A, GM-BMMs expressed both CD11c and MHCII (red line). TGFβ1 treatment resulted in the upregulation of the activation marker CD86 and the macrophage maturation marker F4/80 but in the down-regulation of CD11b, CD11c and MHCII (Figure 4.10A, blue and black line) indicating that TGFβ1-differentiated GM-BMMs lost their DC-like phenotype and differentiated towards a mature and activated macrophage phenotype.

LPS-primed M-BMMs also expressed the macrophage surface marker F4/80, CD14 and CD11b (Figure 4.10B, red line). In contrast to GM-BMMs, M-BMMs expressed low levels of CD11c and MHCII (red line). Previous reports have shown that the M-CSF receptor CD115 is expressed on macrophages and that signalling through the CD115 pathway upon activation with M-CSF is involved in regulating growth, survival and differentiation by monocytes and macrophages [229; 230; 231]. As expected, M-CSF-differentiated BMMs expressed high levels of the M-CSF receptor CD115 (Figure 4.10B, red line). TGFβ1 treatment caused the down-regulation of CD115 expression. TGFβ1 had only minor effects on the expression of F4/80, CD14 and CD11b by M-BMMs. These findings showed that TGFβ1 treatment induced a less differentiated M-CSF macrophage phenotype (M-BMMs) as indicated by a down-regulation of CD115.

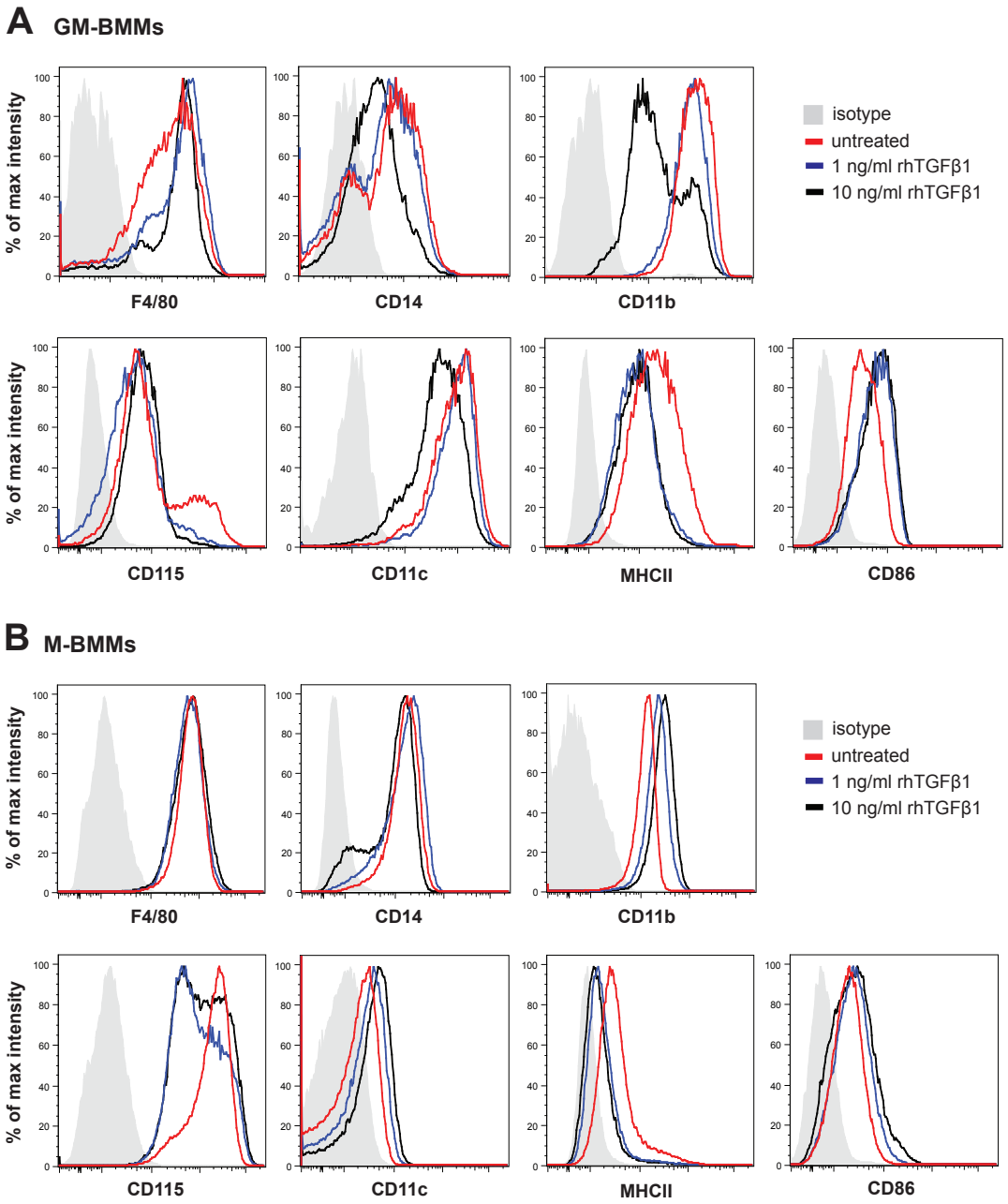

Figure 4.10: Surface marker expression by *in vitro* primed TGFβ1-differentiated GM-BMMs and M-BMMs. Bone marrow cells were harvested and cultured *in vitro* with GM-CSF (1000 units/ml) or M-CSF (5000 units/ml) in the presence of recombinant human TGFβ1 (1 ng/ml or 10 ng/ml) for 7 days following priming with 50 pg/ml LPS overnight. The TGFβ1-differentiated GM-BMMs (**A**) and M-BMMs (**B**) were analysed for the expression of the surface marker F4/80, CD14, CD11b, CD115, CD11c, MHCII and CD86 by flow cytometry. Results are representative of three independent experiments.

4.3.8 The effect of TGFβ1 on MSU crystal-stimulated GM-BMMs and M-BMMs

To investigate the effect of TGFβ1 on phenotypic surface changes by stimulated GM-BMMs and M-BMMs, LPS-primed GM-BMMs and M-BMMs were treated with MSU crystals (200 μg/ml) for 18 hours and then analysed for the expression of a variety of surface markers by flow cytometry (section 2.9). TGFβ1 treatment induced the upregulation of the surface marker F4/80, CD14, CD11c and TGFβRII by unstimulated GM-BMMs (Figure 4.11). MSU crystal-stimulated GM-BMMs significantly down-regulated the expression of F4/80 and CD11b upon TGFβ1 treatment but increased the expression of CD11c compared to unstimulated GM-BMMs (control).

In contrast, TGFβ1 treatment induced a significant down-regulation of the surface marker F4/80, CD11b, CD115 and TGFβRII on M-BMMs, whereas an upregulation in CD14 expression (Figure 4.12). MSU crystal-stimulated M-BMMs significantly down-regulated the expression of F4/80 and CD115 upon TGFβ1 treatment but increased the expression of CD14, CD11c and CD11b compared to unstimulated M-BMMs (control). In particular, the abrogation of CD115 expression by TGFβ1-differentiated M-BMMs indicated the development of a less differentiated M-CSF macrophage phenotype.

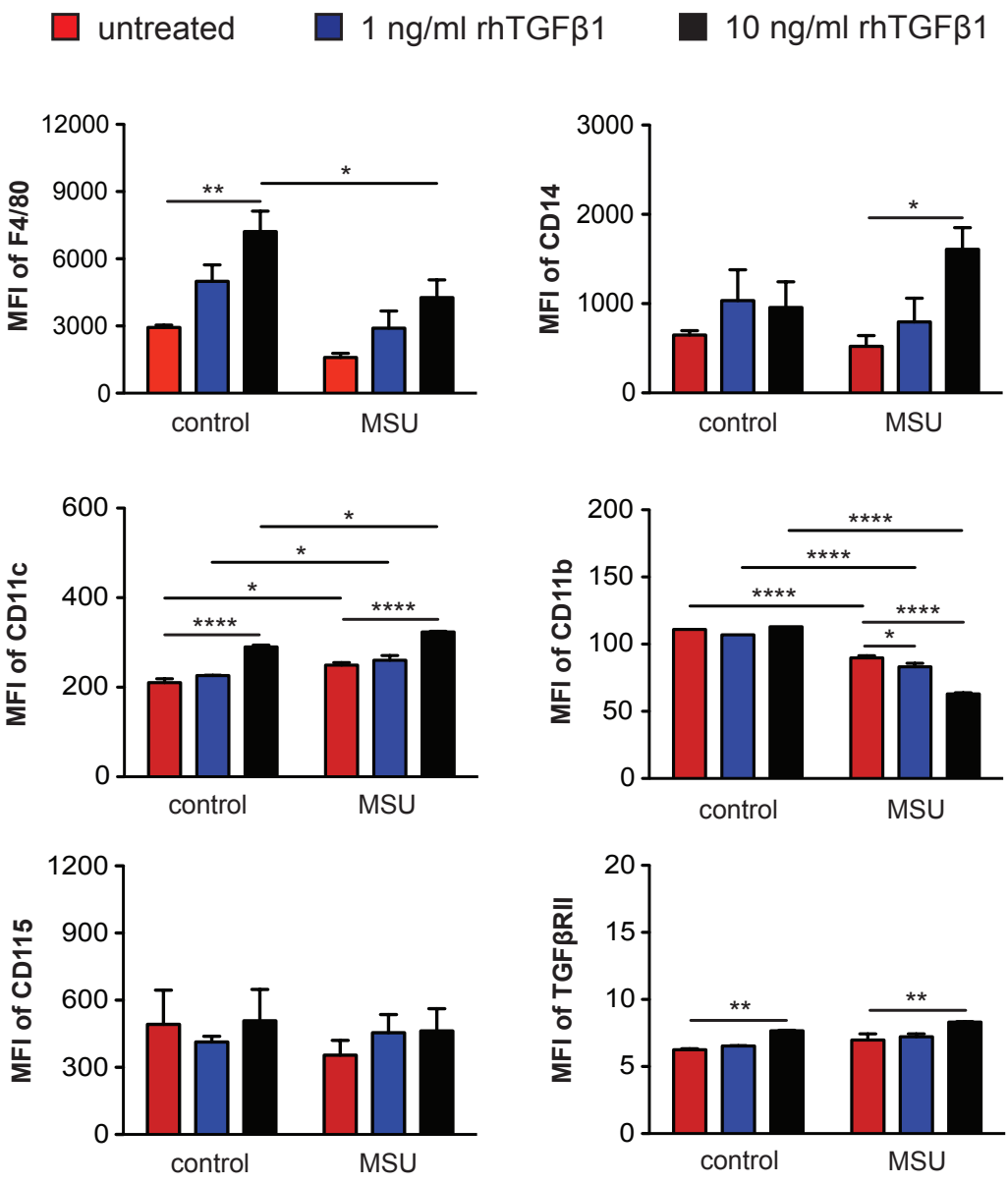

Figure 4.11: Surface marker expression by MSU crystal-stimulated TGFβ1-differentiated GM-BMMs. Bone marrow cells were harvested and cultured *in vitro* with GM-CSF (1000 units/ml) in the presence of rhTGFβ1 (1 ng/ml or 10 ng/ml) for 7 days following priming with 50 pg/ml LPS overnight. After priming, GM-BMMs were stimulated with MSU crystals (200 μg/ml) or left untreated (control) for 18 hours. The TGFβ1-differentiated GM-BMMs were analysed for the expression of the surface marker F4/80, CD14, CD11c, CD11b, CD115 and TGFβRII by flow cytometry. Values are the mean -/+ SEM and representative of up to three experiments. * = $P < 0.05$, ** = $P < 0.01$, **** = $P < 0.0001$ (two-way ANOVA with Bonferroni's post test).

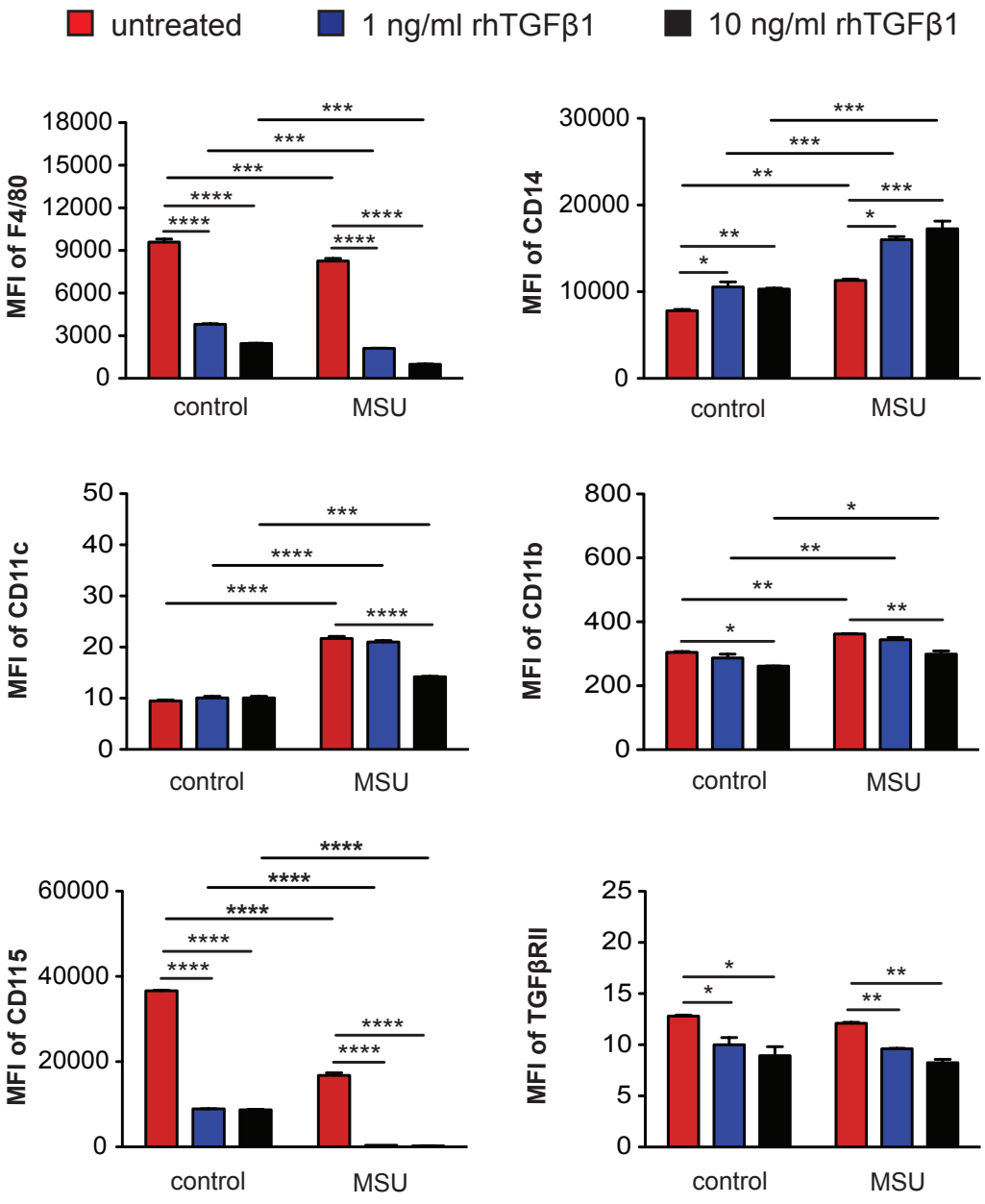

Figure 4.12: Surface marker expression by MSU crystal-stimulated TGFβ1-differentiated M-BMMs. Bone marrow cells were harvested and cultured *in vitro* with M-CSF (5000 units/ml) in the presence of rhTGFβ1 (1 ng/ml or 10 ng/ml) for 7 days following priming with 50 pg/ml LPS overnight. After priming, M-BMMs were stimulated with MSU crystals (200 μg/ml) or left untreated (control) for 18 hours. The TGFβ1-differentiated M-BMMs were then analysed for the expression of the surface marker F4/80, CD14, CD11c, CD11b, CD115 and TGFβRII by flow cytometry. Values are the mean -/+ SEM and representative of up to three separate experiments. * = $P < 0.05$, ** = $P < 0.01$, *** = $P < 0.001$, **** = $P < 0.0001$ (two-way ANOVA with Bonferroni's post test).

4.3.9 Enhanced NLRP3 inflammasome activity in TGFβ1-differentiated GM-BMMs is not induced via ROS

Recent reports have shown that reactive oxygen species (ROS) can also activate the NLRP3 inflammasome leading to the production of IL-1β after exposure to different danger signals such as asbestos, silica or MSU crystals [232; 233; 234]. To test whether TGFβ1 was driving this hyper-inflammatory GM-BMM (M1-like) phenotype via ROS production, LPS primed TGFβ1-differentiated GM-BMMs and M-BMMs were incubated with the fluorescent dye DHR-123 to measure intracellular ROS for 5 minutes (section 2.7.7) and then stimulated with either MSU crystals (200 μg/ml) or phorbol myristate acetate (PMA, control) at 37^{o}C for 45 minutes. After stimulation, BMMs were placed on ice to stop the reaction, and the expression of DHR-123 was determined by flow cytometry (section 2.9).

The data in Figure 4.13A and B showed that TGFβ1 treatment did not trigger an upregulation of the expression of intracellular ROS (DHR-123) by GM-BMMs independent of whether these cells were stimulated with MSU crystals or PMA or left untreated. However, M-BMMs treated with 1 ng/ml TGFβ1 significantly downregulated the expression of intracellular ROS (DHR-123), which was not observed at a concentration of 10 ng/ml TGFβ1 (Figure 4.13C and D). This partial effect of TGFβ1 on intracellular ROS was independent of the stimuli. Collectively, these results demonstrated that TGFβ1 was driving the hyper-inflammatory GM-BMM phenotype independent of ROS.

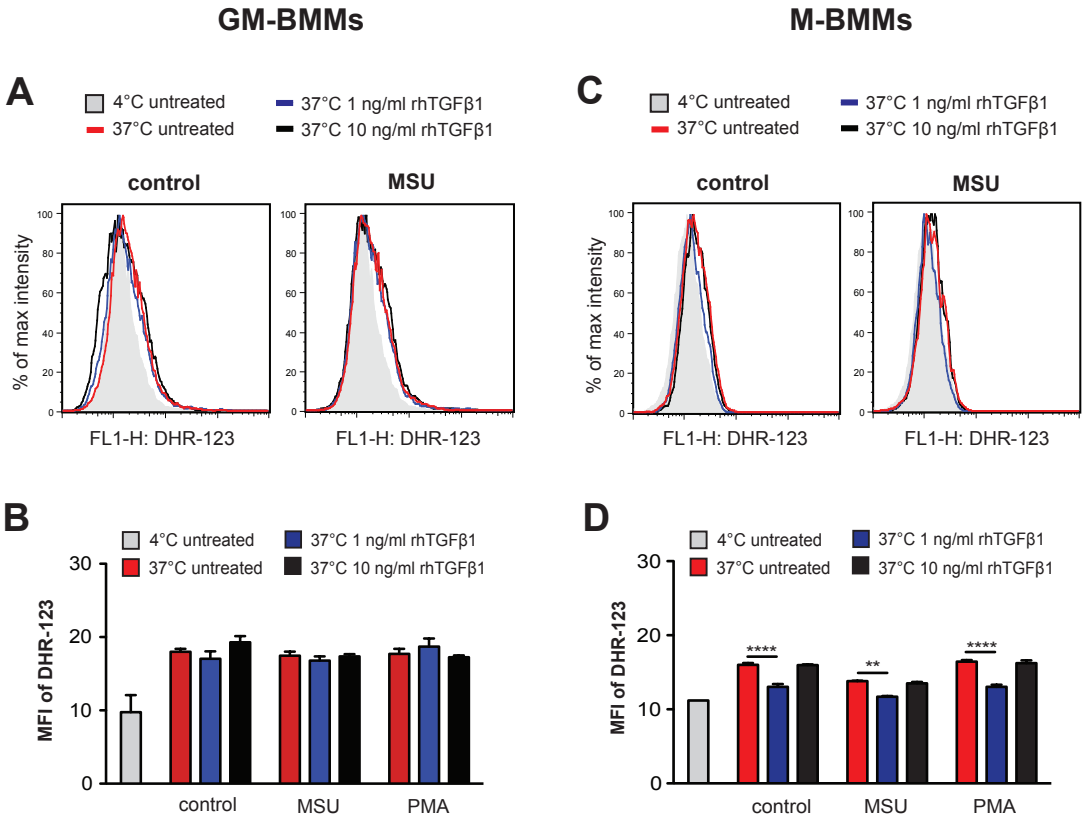

Figure 4.13: Intracellular ROS production by TGFβ1-differentiated GM-BMMs and M-BMMs. Bone marrow cells were harvested and cultured *in vitro* with the growth factor GM-CSF and M-CSF in the presence of rhTGFβ1 (1 ng/ml or 10 ng/ml) for 7 days following priming with 50 pg/ml LPS overnight. GM-BMMs and M-BMMs were then incubated with DHR-123 (10 μM) for 5 minutes at 37^{o}C, washed with D-PBS and stimulated with MSU crystals (200 μg/ml) or PMA (0.2 μg/ml) for 45 minutes at 37^{o}C. As control, untreated BMMs were incubated at 4^{o}C. After stimulation, cells were placed on ice to stop the reaction and analysed for the expression of DHR-123 by flow cytometry. The expression of intracellular ROS (DHR-123) by MSU crystal-activated or control GM-BMMs (**A**) and M-BMMs (**C**) shown as histogram. The expression of intracellular ROS (DHR-123) by MSU crystal and PMA-stimulated GM-BMMs (**B**) and M-BMMs (**D**). Results are representative of two independent experiments. ** = $P < 0.01$, **** = $P < 0.0001$ (two-way ANOVA with Bonferroni's post test).

4.3.10 TGFβ1 does not induce apoptotic cell death by GM-BMMs and M-BMMs

Recent studies have shown that TGFβ1 can induce apoptotic cell death [235; 236; 237] and that apoptosis by stimulated macrophages can also result in the release of IL-1β, a form of cell death termed pyroptosis [238; 239; 240]. To determine whether TGFβ1 was inducing apoptotic cell death in cultured GM-BMMs and M-BMMs leading the pro-inflammatory response by GM-BMM, TGFβ1-differentiated GM-BMMs and M-BMMs were stimulated with MSU crystals (200 μg/ml) for 18 hours. After stimulation, BMMs were harvested and stained with PI to identify live (PI^-) and dead (PI^+) cells by flow cytometry (section 2.9). As shown in Figure 4.14, TGFβ1 treatment did not induce a significant change in the percentage of PI^+ cells upon stimulation indicating that TGFβ1 treatment did not trigger cell death in GM-BMMs (Figure 4.14A) or M-BMMs (Figure 4.14B).

To further confirm the cell survival data, stimulated GM-BMMs and M-BMMs were harvested and stained with trypan blue stain. The number of viable cells that did not contain the dye (trypan $blue^-$) and the dead cells (trypan $blue^+$) were counted under a microscope and the percentage of live and dead BMMs calculated from the total cell numbers (section 2.6.6). TGFβ1 treatment did not induce a significant increase in the percentage of dead GM-BMMs (Figure 4.15A, trypan $blue^+$) or M-BMMs (Figure 4.15B, trypan $blue^+$). These findings confirmed that the effect of TGFβ1 in driving this hyper-inflammatory GM-BMM phenotype was independent of cell death.

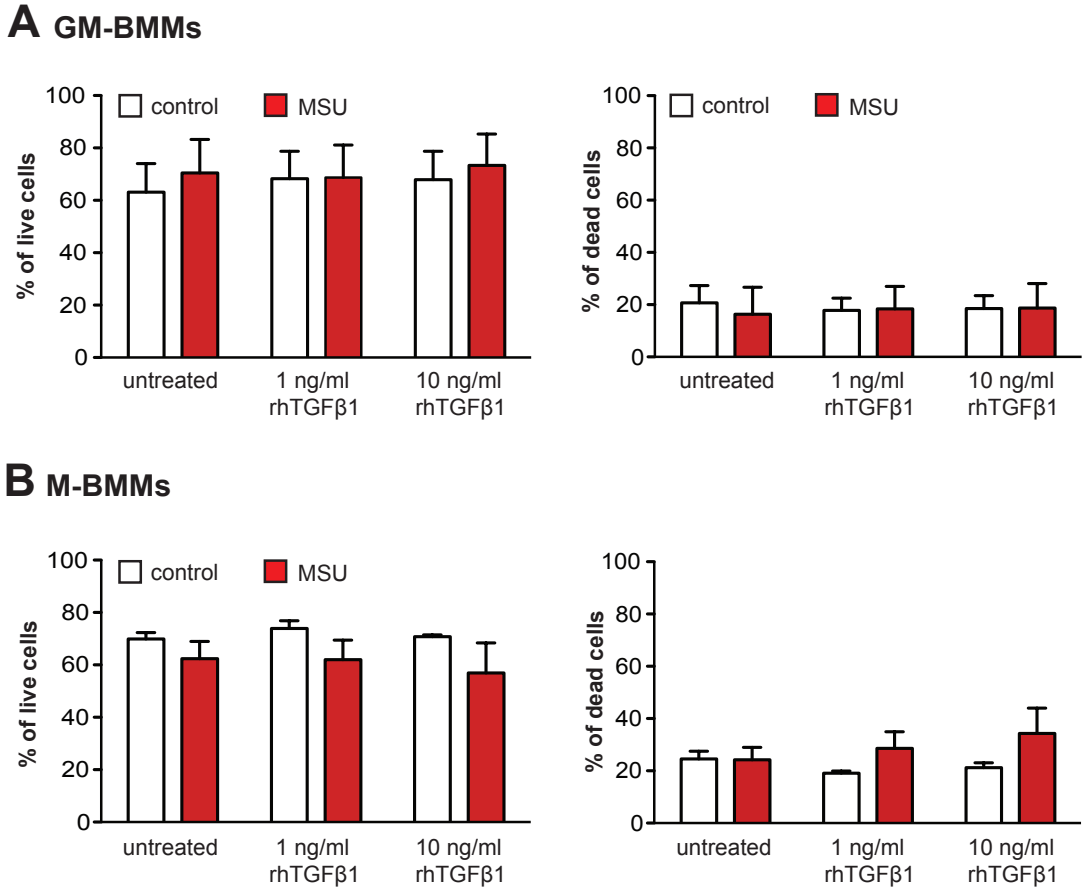

Figure 4.14: Cell viability by TGFβ1-differentiated GM-BMMs and M-BMMs. Bone marrow cells were harvested and cultured *in vitro* with the growth factor GM-CSF (1000 units/ml) and M-CSF (5000 units/ml) in the presence of rhTGFβ1 (1 ng/ml or 10 ng/ml) for 7 days following priming with 50 pg/ml LPS overnight. After priming, BMMs were stimulated with MSU crystals (200 μg/ml) or left untreated (control) for 18 hours. GM-BMMs (**A**) and M-BMMs (**B**) were stained with PI and the percentage of live (PI^-) and dead (PI^+) cells determined by flow cytometry. Results are representative of two separate experiments.

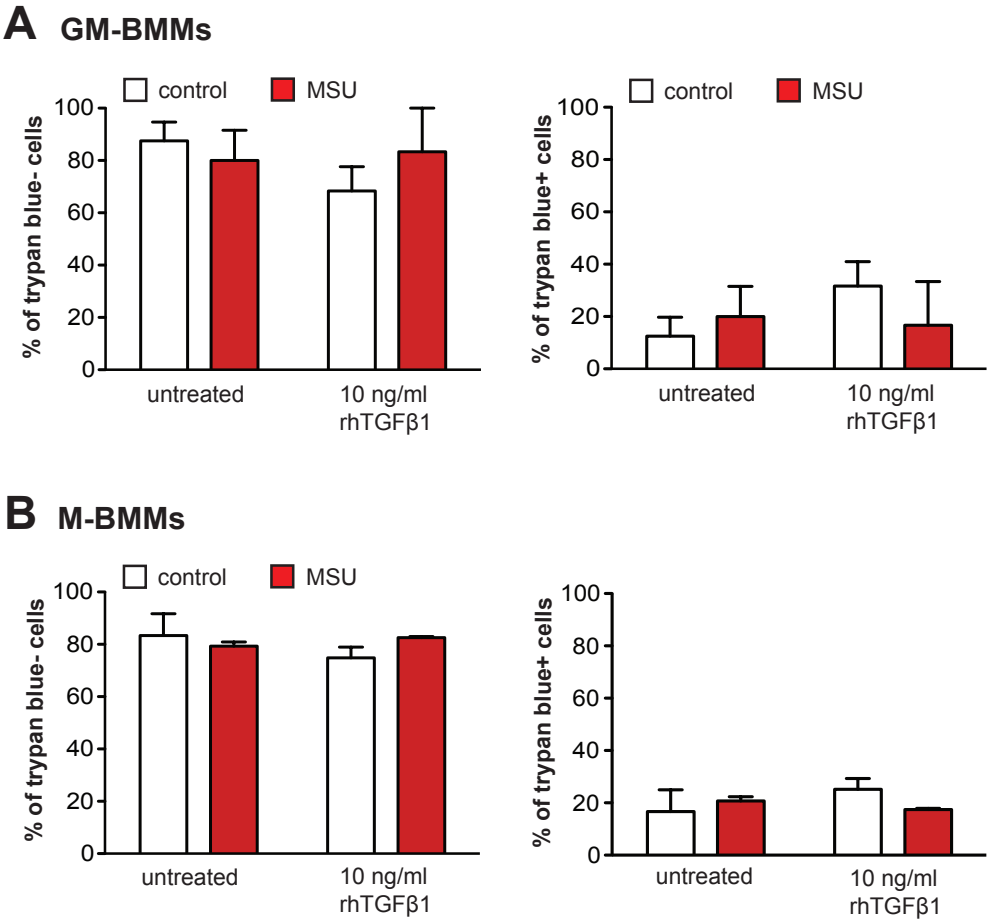

Figure 4.15: Cell viability by TGFβ1-differentiated GM-BMMs and M-BMMs. Bone marrow cells were harvested and cultured *in vitro* with the growth factor GM-CSF (1000 units/ml) and M-CSF (5000 units/ml) in the presence of rhTGFβ1 (10 ng/ml) for 7 days following priming with 50 pg/ml LPS overnight. After priming, BMMs were stimulated with MSU crystals (200 μg/ml) or left untreated (control) for 18 hours. The percentage of live (trypan blue$^-$) and dead (trypan blue$^+$) GM-BMMs (**A**) and M-BMMs (**B**) determined by trypan blue exclusion under a microscope. Results are representative of two separate experiments.

Recent studies have also shown that the process of apoptotic cell death by macrophages can be regulated by a number of different caspases including active caspase 3 [241; 242]. Therefore, another approach was used to prove that the hyper-inflammatory GM-BMM phenotype was not driven via TGFβ1-induced cell death. To do so, LPS-primed GM-BMMs and M-BMMs were treated with GolgiStop following stimulation with MSU crystals (200 μg/ml) for 18 hours. The cells were then stained for intracellular caspase 3 and the percentage of caspase 3^+ cells determined by flow cytometry (section 2.9.2). The percentage of caspase 3^+ GM-BMMs did not significantly change upon TGFβ1 treatment in response to MSU crystals indicating that TGFβ1 was not inducing cell death (Figure 4.16A). This was also the case for TGFβ1-treated M-BMMs upon stimulation (Figure 4.16B).

Using three different cell viability approaches, the findings confirmed that TGFβ1 treatment did not result in apoptotic cell death in MSU crystal-stimulated GM-BMMs and M-BMMs, and therefore suggested that the hyper-inflammatory GM-BMM phenotype occuring was not a consequence of TGFβ1-mediated cell death via pyroptosis.

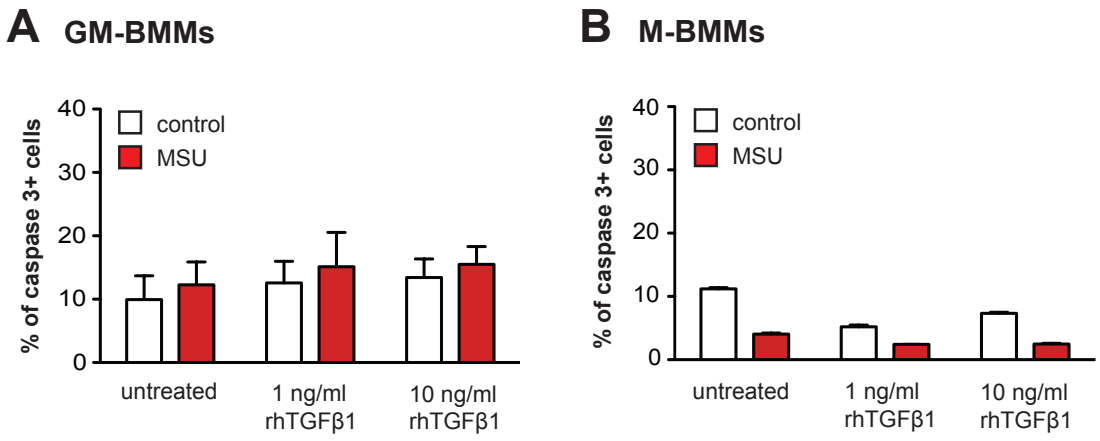

Figure 4.16: Cell viability by TGFβ1-differentiated GM-BMMs and M-BMMs. Bone marrow cells were harvested and cultured *in vitro* with the growth factor GM-CSF (1000 units/ml) and M-CSF (5000 units/ml) in the presence of recombinant human TGFβ1 (1 ng/ml or 10 ng/ml) for 7 days following priming with 50 pg/ml LPS overnight. After priming, BMMs were stimulated with MSU crystals (200 μg/ml) or left untreated (control) for 18 hours. GM-BMMs (**A**) and M-BMMs (**B**) were then stained for intracellular caspase 3 and the percentage of caspase 3^+ BMMs determined by flow cytometry. Results are representative of two independent experiments.

4.3.11 TGFβ1-differentiated GM-BMMs require caspase 1 and caspase 8 for IL-1β production

IL-1β production is a tightly regulated cellular process. The cleavage of IL-1β is triggered by danger signals such as MSU crystals, ROS and LPS [232; 233; 243] leading to the formation and activation of the NLRP3 inflammasome. The NLRP3 inflammasome consisting of NLRP3, ASC and pro-caspase 1 then activates caspase 1, which triggers the cleavage of pro-IL-1β to release active IL-1β. Whilst the inflammasome components contribute to IL-1β processing, it is not clear whether the production of IL-1β could also occur via a NLRP3-independent pathway in response to MSU crystal stimulation. Recent reports have shown that caspase 8 exerts non-apoptotic functions including the suppression of necrotic cell death (necroptosis), inhibition of the transcription factor NF-κB and the production of IL-1β [244; 245]. To determine whether caspase 1 and caspase 8 were regulating MSU crystal-induced IL-1β production by TGFβ1-differentiated BMMs, primed GM-BMMs and M-BMMs were treated with the caspase 1 inhibitor YVAD (10 μg/ml) or the caspase 8 inhibitor IETD (10 μM), or a combination of both for 30 minutes prior to MSU crystal stimulation (200 μg/ml) for 18 hours (section 2.7.5). Supernatants from the cell cultures were collected and analysed for IL-1β by ELISA (section 2.8).

TGFβ1 treatment significantly increased the levels of IL-1β by GM-BMMs stimulated with MSU crystals (Figure 4.17A). This IL-1β production significantly diminished when GM-BMMs were treated with either the caspase 1 inhibitor (YVAD) or the caspase 8 inhibitor (IETD) or a combination of both inhibitors. Consistent with previous results, MSU crystal-stimulated M-BMMs significantly decreased the levels of IL-1β upon TGFβ1 treatment (Figure 4.17B). These results demonstrated that the blockade of both caspases effectively blocked M-BMMs IL-1β production and that both caspase 1 and caspase 8 were required for the production of IL-1β by MSU crystal-stimulated BMMs.

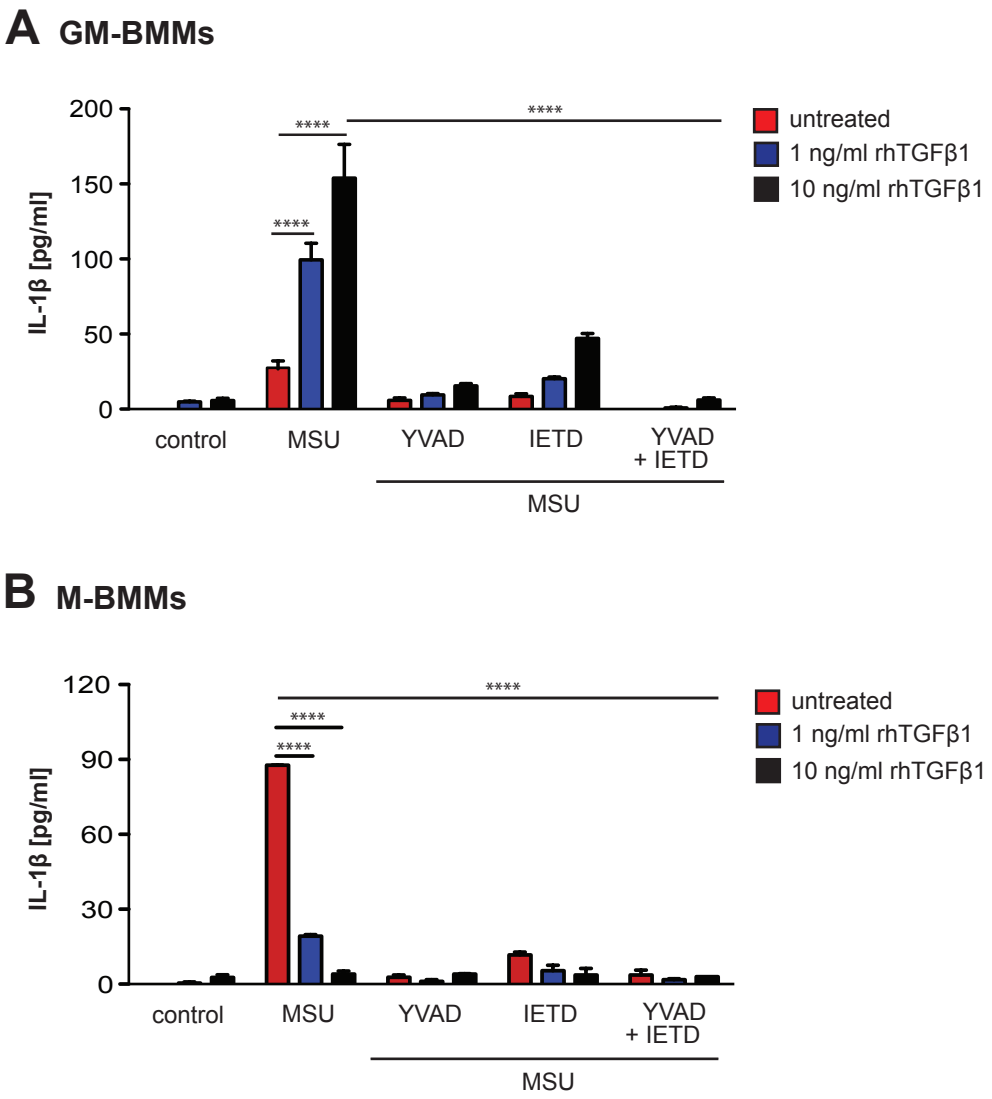

Figure 4.17: Caspase 1/caspase 8 are involved in IL-1β processing by TGFβ1-differentiated GM-BMMs. Bone marrow cells were harvested and cultured *in vitro* with GM-CSF (1000 units/ml) and M-CSF (5000 units/ml) in the presence of recombinant human TGFβ1 (1 ng/ml or 10 ng/ml) for 7 days following priming with 50 pg/ml LPS overnight. After priming, BMMs were treated with the caspase 1 inhibitor YVAD (10 μg/ml) or the caspase 8 inhibitor IETD (10 μM) or a combination of both for 30 minutes prior to MSU crystal stimulation (200 μg/ml) for 18 hours. IL-1β levels were measured from the GM-BMM (**A**) and M-BMM (**B**) culture supernatants by ELISA. Results are representative of two independent experiments. **** = $P < 0.0001$ (two-way ANOVA with Bonferroni's post test).

IL-1β processing via the NLRP3 inflammasome

To investigate the impact of TGFβ1 on the regulation of the NLRP3 inflammasome and the generation of IL-1β by MSU crystal-stimulated BMMs as illustrated in Figure 4.18 (red arrows), cytoplasmic protein from unprimed, LPS-primed and MSU crystal-stimulated GM-BMMs and M-BMMs were collected and western blot analysis on the expression of NLRP3, pro-/active caspase 1, ASC, pro-/active IL-1β and β-actin (used as loading control) performed (section 2.11).

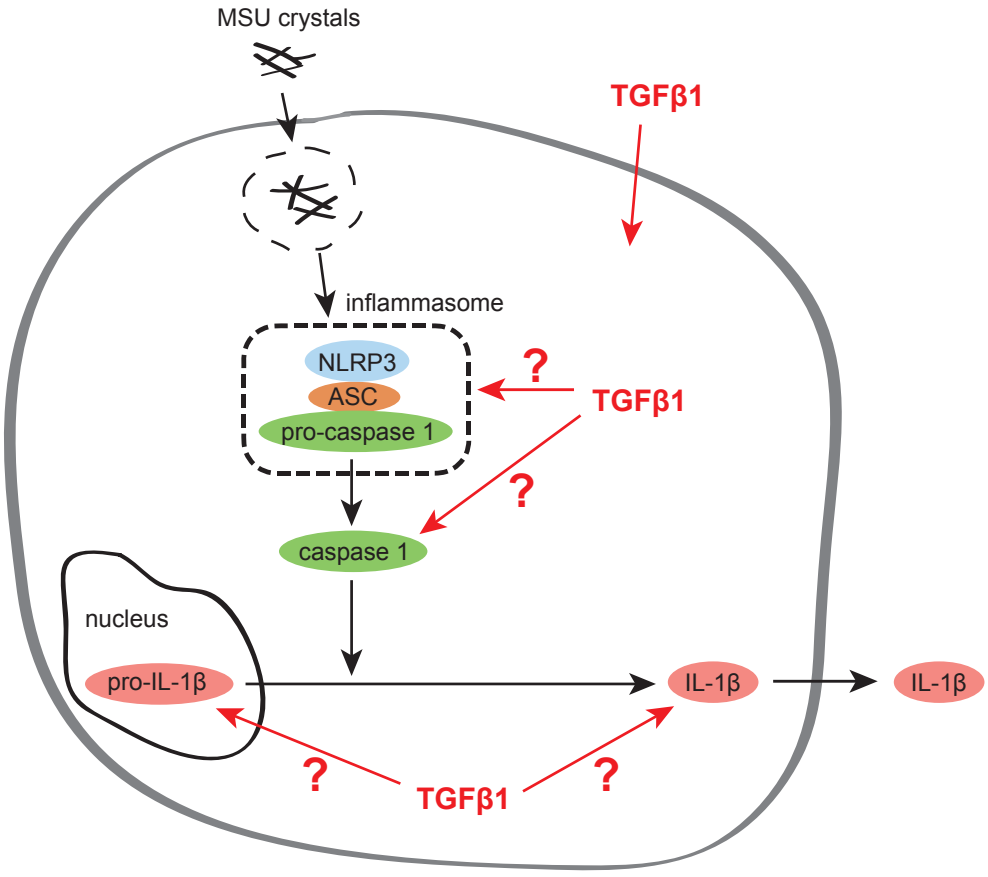

Figure 4.18: IL-1β signalling pathway in response to MSU crystals. MSU crystals induce the formation and activation of the NLRP3 inflammasome (NLRP3, ASC, pro-caspase 1) leading to the activation of caspase 1. Active caspase 1 triggers the cleavage of pro-IL-1β into active IL-1β for secretion.

As expected, LPS priming of GM-BMMs induced the upregulation of NLRP3, ASC, pro-/active caspase 1 and pro-IL-1β compared to unprimed GM-BMMs (Figure 4.19, red box). In primed GM-BMMs, TGFβ1 treatment caused a decrease in NLRP3, ASC and pro-IL-1β expression but an increase in pro-caspase 1. Following MSU crystal stimulation, TGFβ1 treatment increased the expression of pro-caspase 1, pro-/active IL-1β by GM-BMMs (Figure 4.19, green box).

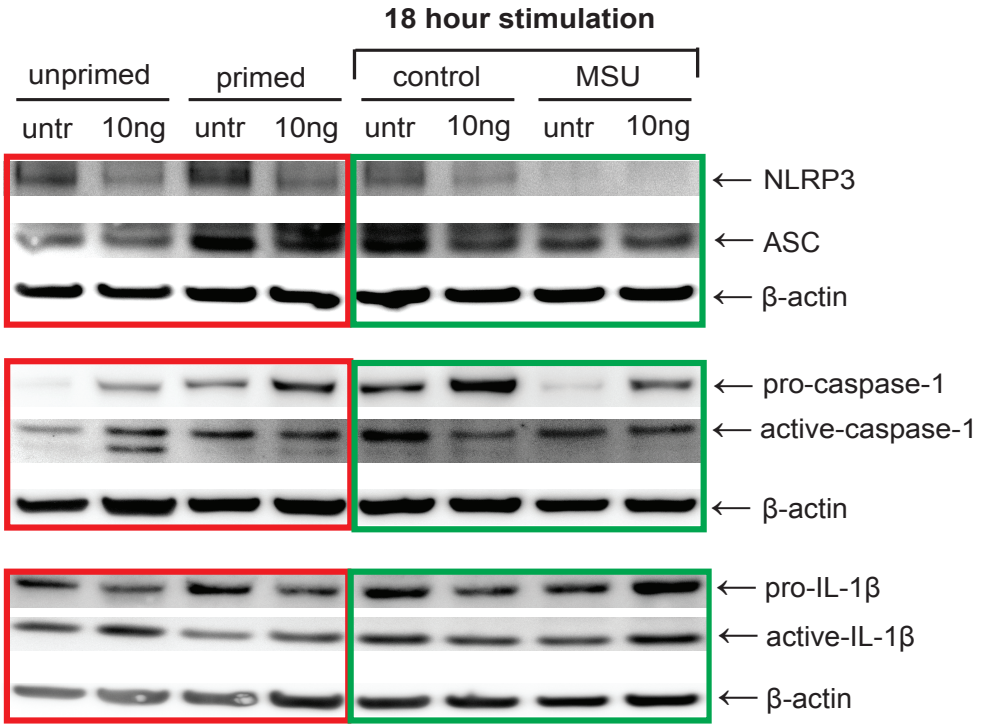

Figure 4.19: IL-1β signalling cascade by TGFβ1-differentiated GM-BMMs. Bone marrow cells were harvested and cultured *in vitro* with GM-CSF (1000 units/ml) in the presence of rhTGFβ1 (10 ng/ml) for 7 days following priming with 50 pg/ml LPS overnight. After priming, GM-BMMs were stimulated with MSU crystals (200 μg/ml) or left untreated (control) for 18 hours. From each culture step, cytoplasmic protein was collected and western blot analysis on NLRP3 (116 kDa), pro-caspase 1 (45 kDa), active caspase 1 (20 kDa), ASC (22 kDa) and pro-IL-1β (35 kDa), active IL-1β (17 kDa) including β-actin (42 kDa) as loading control carried out (section 2.11). Results are representative of two separate experiments.

TGFβ1 treatment increased the expression of NLRP3, ASC, pro-/active caspase 1 by LPS-primed M-BMMs (Figure 4.20, red box). In response to MSU crystals, TGFβ1 treatment triggered an increase in the expression of pro-caspase 1 and pro-IL-1β by M-BMMs but decreased the expression of active IL-1β (Figure 4.20, green box) that was consistent with decreased IL-1β levels in culture supernatants (Figure 4.17B).

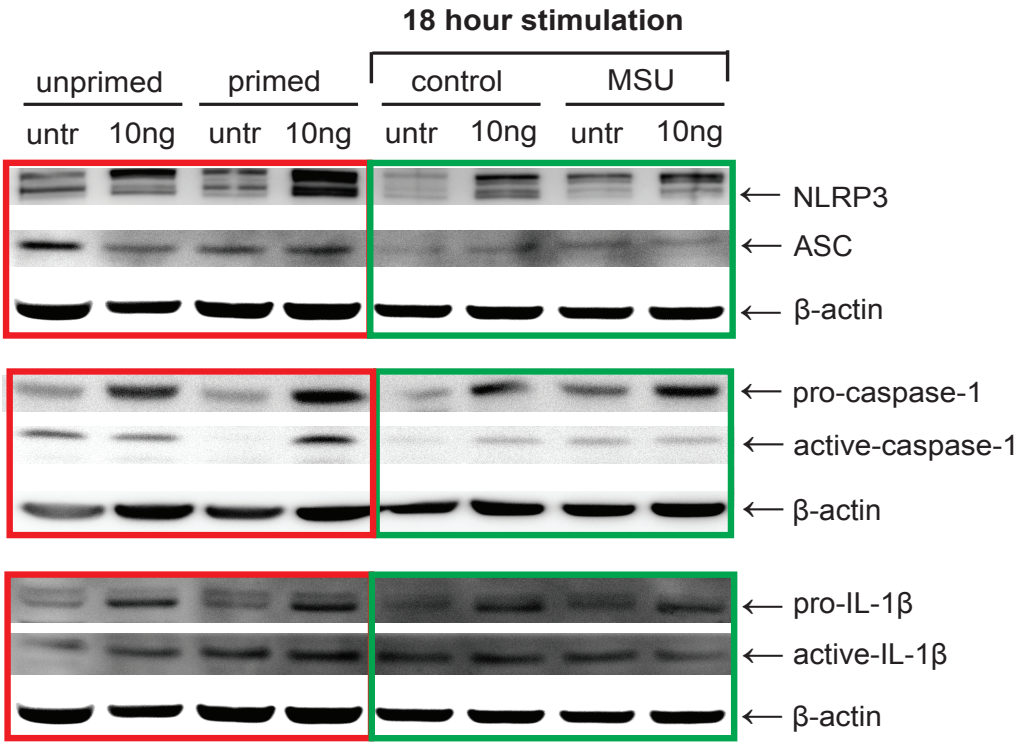

Figure 4.20: IL-1β signalling cascade by TGFβ1-differentiated M-BMMs. Bone marrow cells were harvested and cultured *in vitro* with M-CSF (5000 units/ml) in the presence of rhTGFβ1 (10 ng/ml) for 7 days following priming with 50 pg/ml LPS overnight. After priming, M-BMMs were stimulated with MSU crystals (200 μg/ml) or left untreated (control) for 18 hours. From each culture step, cytoplasmic protein was collected and western blot analysis on NLRP3 (116 kDa), pro-caspase 1 (45 kDa), active caspase 1 (20 kDa), ASC (22 kDa) and pro-IL-1β (35 kDa), active IL-1β (17 kDa) including β-actin (42 kDa) as loading control carried out (section 2.11). Results are representative of two separate experiments.

Taken together, western blot analysis of the NLRP3-dependent signalling pathway confirmed that TGFβ1 was driving a hyper-inflammatory GM-BMM phenotype by augmenting active IL-1β expression (Figure 4.19). In contrast, TGFβ1 was contributing to the differentiation of a hypo-inflammatory M-BMM phenotype demonstrated by down-regulation of active IL-1β (Figure 4.20).

IL-1β processing via caspase 8 and the ripoptosome

The results obtained in Figure 4.17 showed that caspase 8 was also required for IL-1β production by MSU crystal-stimulated BMMs. Recent reports have shown that the generation of IL-1β via caspase 8 is associated with the inhibitor of apoptosis (IAP) proteins [246] and that IAPs can be regulated by TGFβ1 [247]. Caspase 8 is known to be activated by a complex called the ripoptosome containing pro-caspase 8, FADD, RIPK1 [248] leading to the activation of RIP3, which can cleave IL-1β [246; 249; 250; 251]. Therefore, it was of interest to investigate the effect of TGFβ1 on caspase 8 activation and further upstream events by MSU crystal-stimulated BMMs, as illustrated in Figure 4.21. To do so, cytoplasmic protein from unprimed, LPS-primed and MSU crystal-stimulated GM-BMMs and M-BMMs were collected and western blot analysis on the expression of pro-/active caspase 8, cIAP1, RIP3, RIPK1 and β-actin performed (section 2.11).

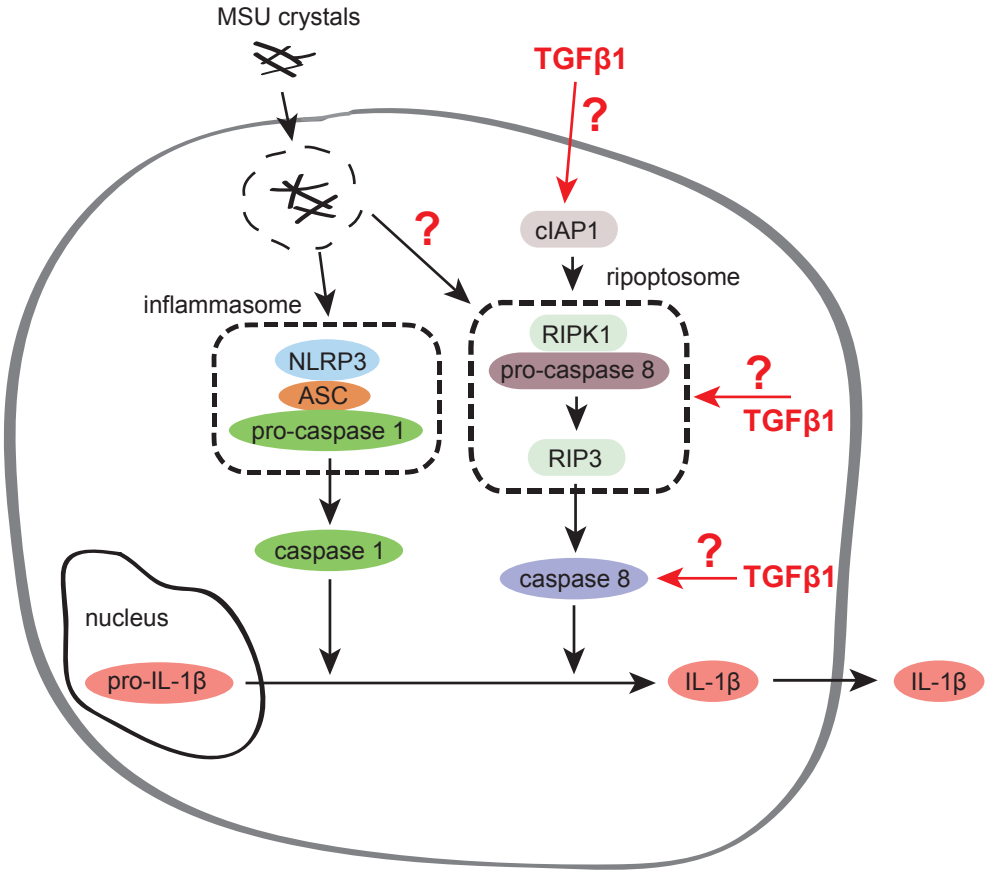

Figure 4.21: Signalling cascade via caspase 8 by TGFβ1-differentiated BMMs. Upon MSU crystal stimulation, BMMs also require caspase 8 for the production of IL-1β. This involves the association of cIAP1 with the ripoptosome containing RIPK1, pro-caspase 8 and RIP3, which leads to the activation of caspase 8. Active caspase 8 triggers the cleavage of pro-IL-1β into the active IL-1β form for secretion.

As shown in Figure 4.22, LPS-primed GM-BMMs expressed pro-caspase 8, cIAP1, RIP3 and RIPK1 that did not differ from the unprimed cells (red box). TGFβ1 treatment decreased the expression of RIP3 but increased cIAP1, whereas no difference was observed in the expression of caspase 8 or RIPK1. Upon MSU crystal stimulation, GM-BMMs down-regulated cIAP1 and active caspase 8 (p18) but the amounts of active RIP3 or RIPK1 did not change (Figure 4.22, green box). Interestingly, MSU crystal stimulation by TGFβ1-treated GM-BMMs triggered the upregulation of RIP3 compared to unstimulated TGFβ1-treated GM-BMMs. However, TGFβ1 treatment did not change the expression of caspase 8, cIAP1 or RIPK1 by MSU crystal-stimulated GM-BMMs (green box).

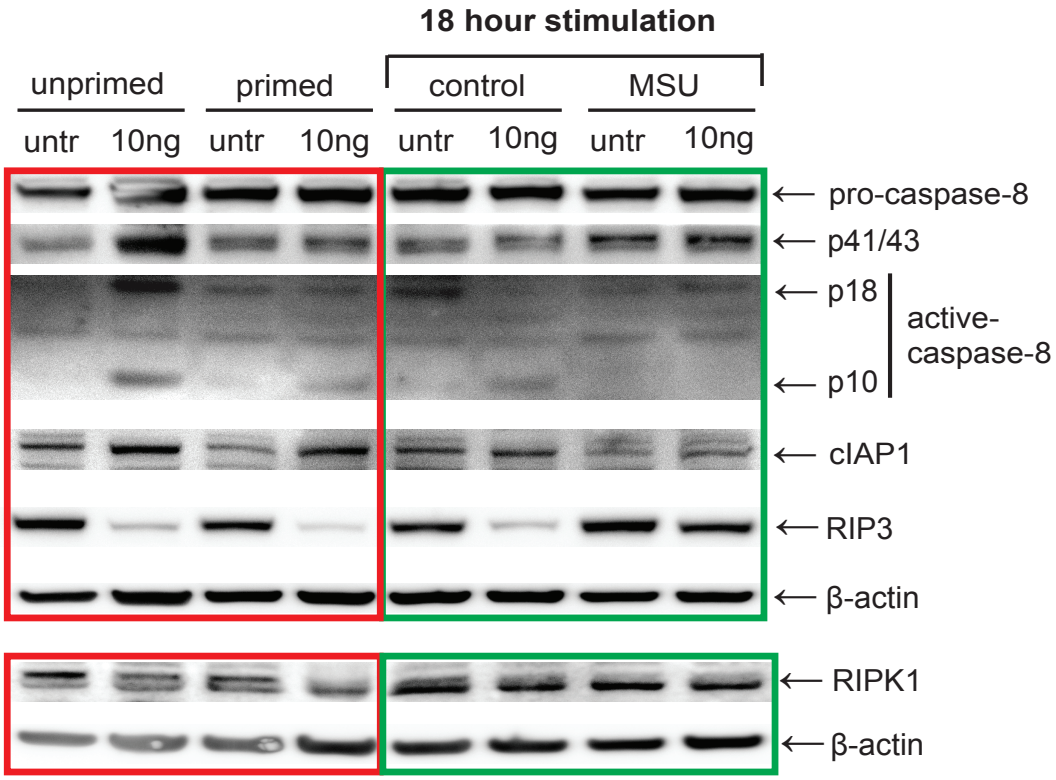

Figure 4.22: Ripoptosome involved in IL-1β signalling by TGFβ1-differentiated GM-BMMs. Bone marrow cells were harvested and cultured *in vitro* with GM-CSF (1000 units/ml) in the presence of rhTGFβ1 (10 ng/ml) for 7 days following priming with 50 pg/ml LPS overnight. After priming, GM-BMMs were stimulated with MSU crystals (200 μg/ml) or left untreated (control) for 18 hours. From each culture step, cytoplasmic protein was collected and western blot analysis on cIAP1 (70 kDa), RIPK1 (75 kDa), RIP3 (57 kDa), pro-caspase 8 (54/56 kDa), caspase 8 subunits (p41/43), active-caspase 8 (p18 and p10) including β-actin (42 kDa) as loading control carried out (section 2.11). Results are representative of three separate experiments.

LPS-primed M-BMMs expressed more pro-/active-caspase 8 and RIPK1 but down-regulated the expression of RIP3 and cIAP1 compared to the unprimed cells (Figure 4.23, red box). TGFβ1 treatment increased the expression of RIPK1, RIP3 and cIAP1 in primed M-BMMs. MSU crystal stimulation resulted in the upregulation of RIP3 and cIAP1, whereas caspase 8 or RIPK1 did not change (Figure 4.23, green box). Interestingly, TGFβ1 treatment triggered the upregulation of RIP3 and RIPK1 by MSU crystal-stimulated M-BMMs but had no effect on the expression of caspase 8 or cIAP1 (green box). These findings showed that TGFβ1 treatment down-regulated the expression of RIP3 in GM-BMMs but upregulated RIP3 expression in M-BMMs.

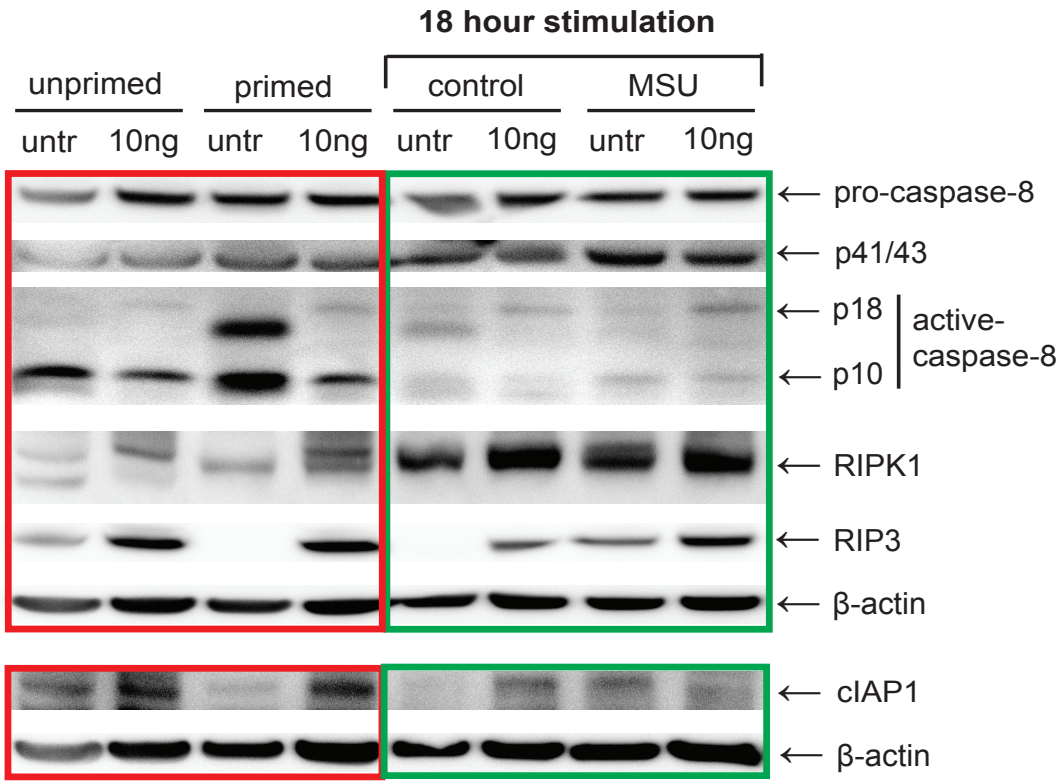

Figure 4.23: Ripoptosome involved in IL-1β signalling by TGFβ1-differentiated M-BMMs. Bone marrow cells were harvested and cultured *in vitro* with M-CSF (5000 units/ml) in the presence of rhTGFβ1 (10 ng/ml) for 7 days following priming with 50 pg/ml LPS overnight. After priming, M-BMMs were stimulated with MSU crystals (200 μg/ml) or left untreated (control) for 18 hours. From each culture step, cytoplasmic protein was collected and western blot analysis on cIAP1 (70 kDa), RIPK1 (75 kDa), RIP3 (57 kDa), pro-caspase 8 (54/56 kDa), caspase 8 subunits (p41/43), active-caspase 8 (p18 and p10) including β-actin (42 kDa) as loading control carried out (section 2.11). Results are representative of two separate experiments.

4.3.12 Caspase 8 and caspase 1 interaction in MSU crystal-stimulated GM-BMMs

The previous results showed that caspase 8 was involved in processing IL-1β by MSU crystal-stimulated BMMs. However, it remained unclear whether caspase 8 was acting on the processing of IL-1β via the NLRP3-independent pathway or whether caspase 8 was directly associated with the NLRP3 inflammasome e.g. caspase 1 leading to the generation of a TGFβ1-driven hyper-inflammatory GM-BMM phenotype. To investigate a possible link between caspase 8 and caspase 1 by TGFβ1-differentiated GM-BMMs, immunoprecipitation experiments were carried out. Therefore, GM-BMMs were stimulated with MSU crystals (200 μg/ml) or left untreated for 18 hours and cytoplasmic protein was collected. Immunoprecipitation (IP) for caspase 1 with protein A - sepharose beads was carried out (section 2.11.5) and the cell lysates as well as the IP samples were co-immunoprecipitated with the caspase 8 and caspase 1 antibodies by western blot analysis (section 2.11.4)

Immunoprecipitation of caspase 1 in GM-BMMs demonstrates that pro-caspase 1 associated with pro-caspase 8, which was shown by the presence of pro-caspase 8 in the IP caspase 1 samples (Figure 4.24, top red box). Pro-caspase 8 was also observed in the cytoplasmic protein samples confirming the expression of caspase 8 by GM-BMMs (top blue box). These findings identified an association between caspase 8 and caspase 1 in GM-BMMs that was enhanced by TGFβ1 treatment. This indicated that caspase 8 might enhance caspase 1 activity to drive the hyper-inflammatory GM-BMM response to MSU crystals.

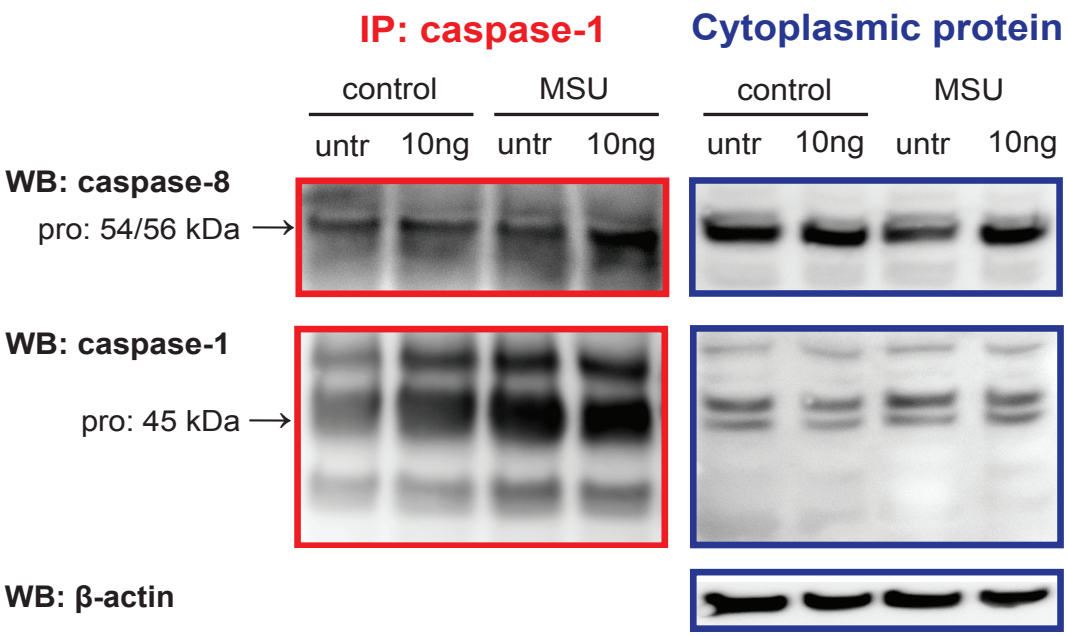

Figure 4.24: The association between caspase 8 and caspase 1 by TGFβ1-differentiated GM-BMMs. Bone marrow cells were harvested and cultured *in vitro* with GM-CSF (1000 units/ml) in the presence of rhTGFβ1 (10 ng/ml) for 7 days following priming with 50 pg/ml LPS overnight. After priming, GM-BMMs were stimulated with MSU crystals (200 μg/ml) or left untreated (control) for 18 hours and cytoplasmic protein was then collected. Caspase 1 was immunoprecipitated (IP) with protein A - sepharose beads (section 2.11.5) and co-immunoprecipitated with the caspase 8 and caspase 1 antibodies detected by western blot analysis (section 2.11.4). Results are representative of one experiment.

4.4 Summary

In vivo studies have shown that the differentiation of monocytes into a hyper-inflammatory macrophage phenotype in response to MSU crystals *in vivo* is driven by GM-CSF [149][unpublished data, manuscript submitted]. The data herein demonstrated that TGFβ1 further enhances the hyper-inflammatory GM-BMM phenotype when present during the differentiation process. Interestingly, TGFβ1 had the opposite effect on M-BMMs resulting in suppression of the MSU crystal response.

Activation of IL-1β by GM-BMMs and M-BMMs required both caspase 8 and caspase 1. Western blot analysis showed that TGFβ1 enhanced the hyper-inflammatory activity of GM-BMMs, which was associated with an upregulation of pro-caspase 1 and pro-/active IL-1β expression. In addition, TGFβ1-treated M-BMMs down-regulated the expression of active IL-1β that was consistent with decreased IL-1β production. MSU crystal-stimulated GM-BMMs down-regulated the expression of RIP3 upon TGFβ1 treatment. The opposite pattern was observed for RIP3 in TGFβ1-treated M-BMMs indicating that TGFβ1 has a differential effect on the ripoptosome in GM-BMMs and M-BMMs. Finally, immunoprecipitation on GM-BMMs showed enhanced caspase 1/caspase 8 interaction in activated cells supporting co-dependency of caspase 1/caspase 8 on increased IL-1β production in GM-CSF-differentiated macrophages.

Together, the findings highlighted the differential effect of TGFβ1 on macrophage differentiation in acute gouty inflammation. It appeared that TGFβ1 suppresses M-CSF differentiated macrophages, which are representative of tissue-resident macrophages (M2-like cells) primarily present during the initiation of MSU crystal-induced inflammation. In contrast, TGFβ1 was driving a pro-inflammatory GM-CSF macrophage phenotype (M1-like cells) towards hyper-responsiveness to ongoing inflammatory insults.

Chapter 5

5 The Expression of NK1.1 by Macrophages

5.1 Introduction

During the course of this thesis, macrophages were found to upregulate NK1.1 expression in response to MSU crystals. NK1.1 is a surface marker, identified by the PK136 monoclonal antibody [252], that is expressed on other innate cells including natural killer T (NKT) cells and natural killer (NK) cells [253; 254; 255]. NK cells have been reported to interact with cells of the innate immune system such as monocytes and macrophages with a potential role in modulating gouty inflammation [83]. A recent study demonstrated that the $CD56^{bright}$ subset of NK cells is greatly expanded in the synovial fluid of patients with inflammatory arthritis [84] and can produce large amounts of both pro-inflammatory and anti-inflammatory cytokines. In a reciprocal contact-dependent activation interface, $CD56^{bright}$ NK cells were capable of engaging with monocytes [85], indicating the existence of a positive feedback loop, which could contribute to the amplification of the inflammatory response in acute gout [84].

Data on the functional role of NK1.1 expression is limited. However, previous studies indicate that signalling through NK1.1 can trigger NK cells to apoptose, and can activate NKT cells to produce IL-4 [256]. In addition, $CD11c^+$ $NK1.1^+$ dendritic (NKDC) cells have been described as capable of cytotoxic killing of target cells [257]. To date, the upregulation of NK1.1 by macrophages ($F4/80^+$ $CD11b^+$) has not been previously reported.

5.2 Aim

The aim of this chapter was to investigate the phenomenon of the upregulation of the NK1.1 surface expression by macrophages in response to MSU crystals.

5.3 Results

5.3.1 MSU crystal-stimulated macrophages express NK1.1

The activation of resident macrophages by MSU crystals plays a pivotal role in the initiation of the inflammatory response driving the production of pro-inflammatory mediators and cell recruitment [103]. However, little is known about changes in surface marker expression on MSU crystal-activated macrophages. To confirm MSU crystal-induced NK1.1 expression, peritoneal macrophages were harvested by lavage from naive mice (section 2.6.1) and cultured *in vitro* in the presence of MSU crystals (200 μg/ml) for 24 hours (section 2.7.8). After incubation, the cells were stained with fluorescent antibodies for the cell surface marker F4/80, CD11b and NK1.1 and analysed by flow cytometry (section 2.9). Resident peritoneal macrophages were identified as F4/80$^+$ CD11b$^+$ (Figure 5.1A). Macrophages that had been stimulated with MSU crystals upregulated the surface marker NK1.1 (red line) compared to freshly isolated macrophages (black line) and unstimulated cultured macrophages (blue line) (Figure 5.1B). These results showed for the first time that MSU crystal-stimulated macrophages upregulate the surface marker NK1.1.

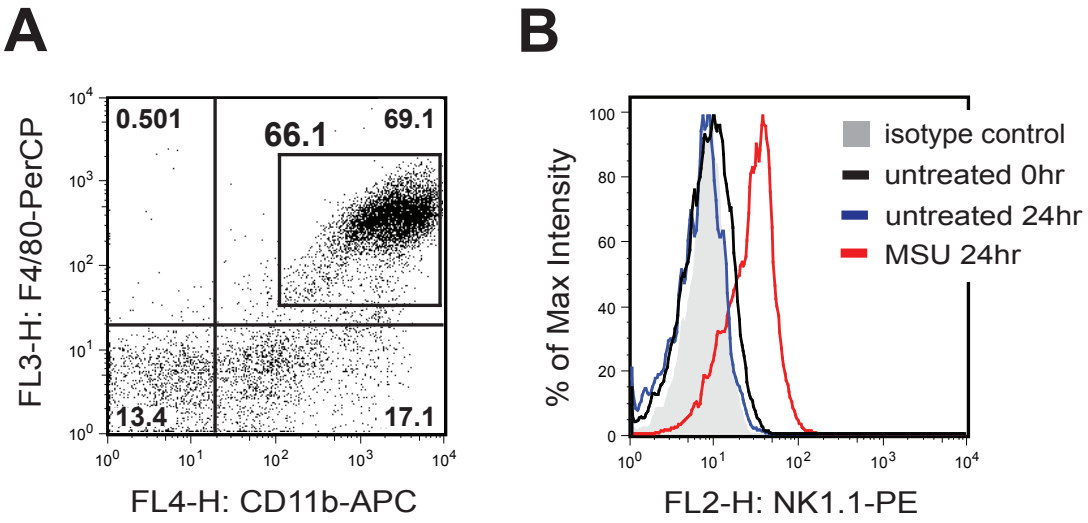

Figure 5.1: NK1.1 expression by MSU crystal-stimulated macrophages. Peritoneal lavage fluid from naive mice was collected by lavage (3 ml PBS). **A** Peritoneal macrophages were identified as F4/80$^+$ CD11b$^+$ by flow cytometry. **B** Peritoneal cells were cultured *in vitro* in the presence of MSU crystals (200 μg/ml) for 24 hours and the expression of NK1.1 by macrophages (F4/80$^+$ CD11b$^+$) determined by flow cytometry. Results are representative of eight separate experiments.

To determine whether NK1.1 upregulation was a general feature of macrophage activation, peritoneal macrophages from naive mice were harvested (section 2.6) and stimulated with 200 μg/ml MSU crystals or 100 ng/ml LPS (section 2.7.8) *in vitro* for up to 24 hours. Only MSU crystal-stimulated macrophages exhibited a significant and rapid increase in both the percentage of NK1.1$^+$ cells and the expression of NK1.1 compared to untreated or LPS-stimulated macrophages over time (Figure 5.2A).

Macrophages produce the pro-inflammatory cytokine IL-1β in response to MSU crystals via the activation of the NLRP3 inflammasome, a pivotal event in MSU crystal-induced inflammation [97; 61]. Accordingly, supernatants from the cell culture of MSU crystal and LPS-stimulated macrophages were also collected and analysed by ELISA for secreted levels of IL-1β (section 2.8). As shown in Figure 5.2B, the activation of macrophages with MSU crystals induced a significantly stronger IL-1β response compared to LPS stimulation. These results indicated that the upregulation of NK1.1 by MSU crystal-activated macrophages might be linked to IL-1β production.

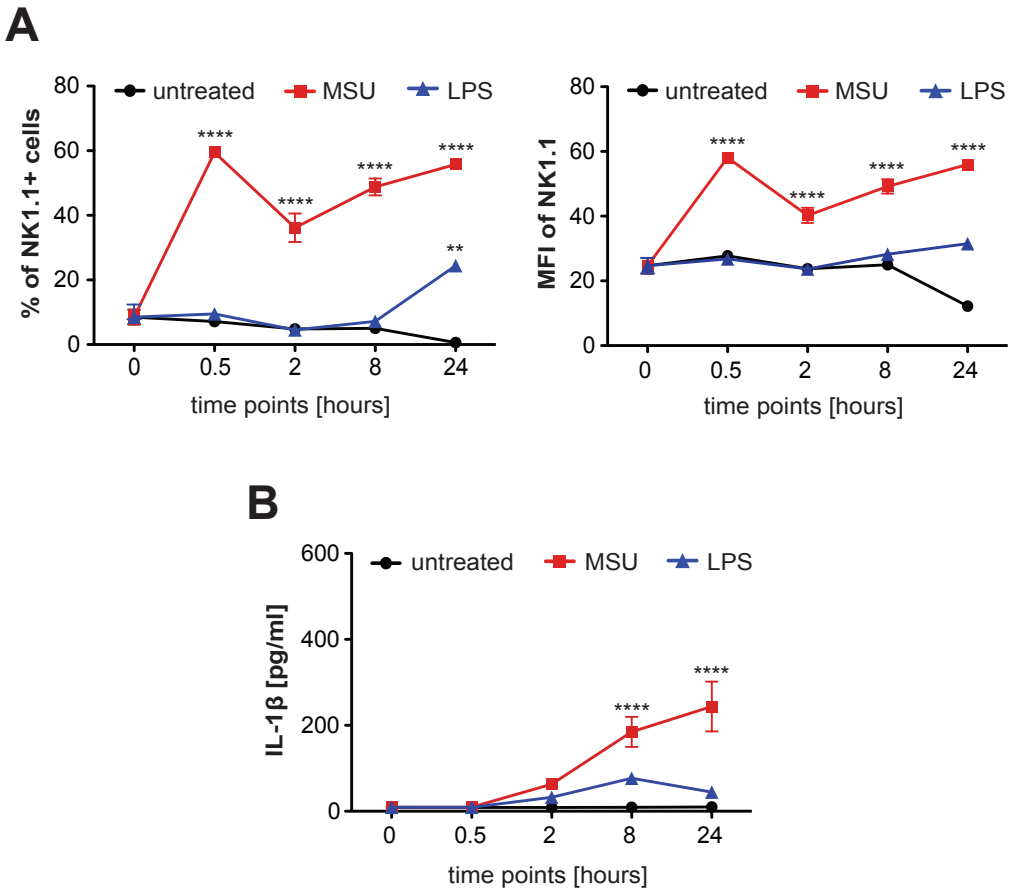

Figure 5.2: Increased NK1.1 expression by macrophages stimulated with MSU crystals. Peritoneal fluid from naive mice was collected by lavage (3 ml PBS) and peritoneal macrophages cultured *in vitro* in the presence of MSU crystals (200 μg/ml) or LPS (100 ng/ml) for up to 24 hours. At different time points, **A** the percentage of NK1.1$^+$ macrophages and the expression of NK1.1 determined by flow cytometry, and **B** culture supernatants were collected and analysed for IL-1β by ELISA. Values are the mean -/+ SEM and representative of three separate experiments. ** = $P < 0.01$, **** = $P < 0.0001$ (two-way ANOVA with Bonferroni's post test).

5.3.2 NK1.1 expression by MSU crystal-stimulated macrophages is partially dependent on IL-1β and TNFα

To investigate whether MSU crystal-induced NK1.1 upregulation was linked to IL-1β production, peritoneal macrophages were harvested (section 2.6) and cultured *in vitro* in the prescence of the anti-IL-1β antibody (5 μg/ml) prior to stimulation with MSU crystals (200 μg/ml) for up to 24 hours (section 2.7.8). At different time points, supernatants from the cell culture were analysed for the levels of IL-1β by ELISA and the percentage of NK1.1$^+$ macrophages was determined by flow cytometry. As shown in Figure 5.3A, IL-1β by MSU crystal-stimulated macrophages was successfully neutralised using an IL-1β neutralising antibody. IL-1β neutralisation resulted in a decrease in the percentage of NK1.1$^+$ macrophages upon MSU crystal stimulation (blue line) compared to MSU crsytal-activated macrophages (red line) (Figure 5.3C).

The activation of macrophages by MSU crystals initiates a signalling cascade via the stimulation of the NLRP3 inflammasome, which triggers the activation of caspase 1, an enzyme responsible for the cleavage of pro-IL-1β into the active IL-1β form [121]. To identify a possible link between NK1.1 upregulation and caspase 1, macrophages were treated with the caspase 1 inhibitor YVAD (5 μg/ml) prior to MSU crystal stimulation. As shown in Figure 5.3B, inhibition of caspase 1 caused a significant decrease in the levels of IL-1β by MSU crystal-activated macrophages that correlated with a decrease in the percentage of NK1.1$^+$ MSU crystal-activated macrophages (Figure 5.3D). These findings indicated that the NK1.1 upregulation by MSU crystal-activated macrophages was partially dependent on IL-1β production via activation of the NLRP3 inflammasome.

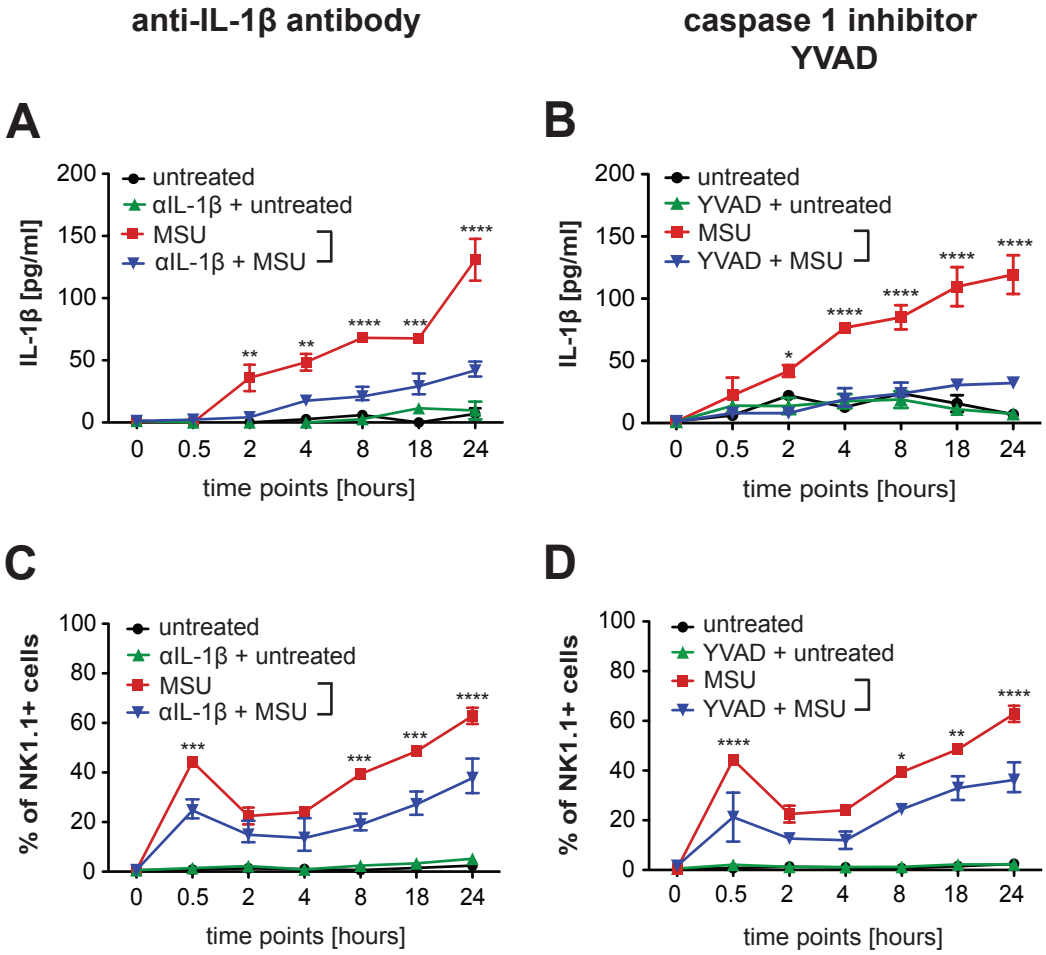

Figure 5.3: NK1.1 expression by MSU crystal-stimulated macrophages partially dependent on IL-1β. Peritoneal lavage fluids were harvested from naive mice and macrophages cultured *in vitro* in the presence of anti-IL-1β antibody (5 μg/ml) or the caspase 1 inhibitor YVAD (5 μg/ml) prior MSU crystal stimulation (200 μg/ml) for up to 24 hours. **A, B** At different time points, culture supernatants from anti-IL-1β (**A**) and YVAD (**B**) treated cells were collected and analysed by ELISA. **C, D** At different time points, macrophages were harvested and the percentage of NK1.1$^+$ macrophages from anti-IL-1β (**C**) and YVAD (**D**) treated cells was determined by flow cytometry. Values are the mean -/+ SEM and representative of two independent experiments. * = $P < 0.05$, ** = $P < 0.01$, *** = $P < 0.001$, **** = $P < 0.0001$ (two-way ANOVA with Bonferroni's post test).

Macrophages also produce the cytokines IL-6 and TNFα during the initiation phase of MSU crystal-induced inflammation [103]. To investigate whether IL-6 and TNFα could modulate MSU crystal-induced NK1.1 expression, macrophages were harvested (section 2.6) and cultured *in vitro* in the presence of anti-IL-6 antibody (5 μg/ml) or anti-TNFα antibody (5 μg/ml), then stimulated with MSU crystals (200 μg/ml) (section 2.7.8). As shown in Figure 5.4A, the percentage of NK1.1$^+$, MSU crystal-activated macrophages was not significantly altered by neutralising IL-6. However, neutralisation of TNFα resulted in fewer NK1.1$^+$ macrophages upon MSU crystal stimulation (Figure 5.4B). These findings indicated that NK1.1 up-regulation by MSU crystal-stimulated macrophages was also partially dependent on TNFα.

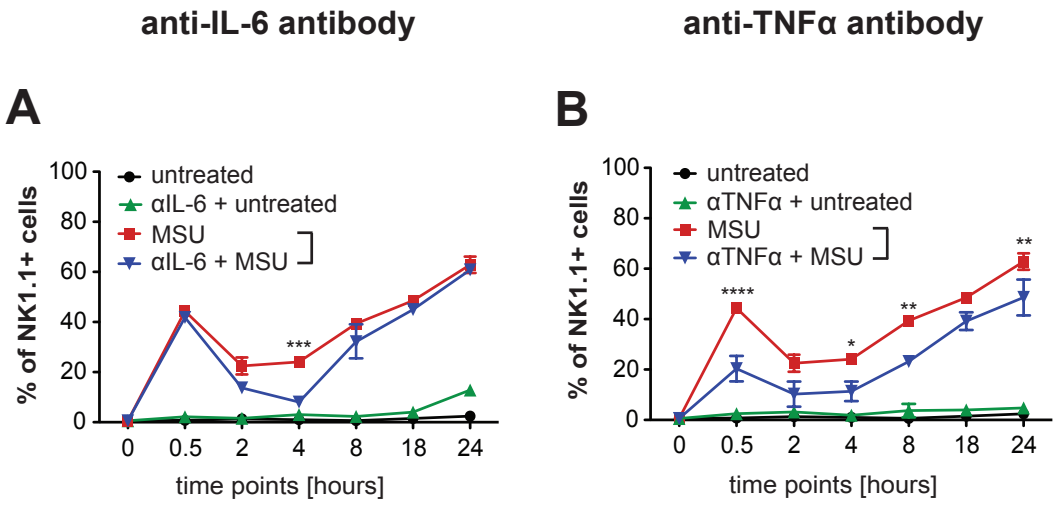

Figure 5.4: NK1.1 expression by MSU crystal-stimulated macrophages partially dependent on TNFα. Peritoneal lavage fluids were harvested from naive mice and macrophages cultured *in vitro* in the presence of anti-IL-6 antibody (5 μg/ml) (**A**) and anti-TNFα antibody (5 μg/ml) (**B**) prior stimulation with MSU crystals (200 μg/ml) for 24 hours. **A, B** At different time points, macrophages were harvested and the percentage of NK1.1$^+$ macrophages from anti-IL-6 (**A**) and anti-TNFα (**B**) treated cells determined by flow cytometry. Values are the mean -/+ SEM and representative of two independent experiments. * = $P < 0.05$, ** = $P < 0.01$, *** = $P < 0.001$, **** = $P < 0.0001$ (two-way ANOVA with Bonferroni's post test).

5.3.3 NK1.1 expression by macrophages is specific to MSU crystals

In order to investigate whether changes in urate crystal composition could affect NK1.1 expression by macrophages, peritoneal macrophages were harvested (section 2.6) and cultured *in vitro* in the presence of urate crystals with different cations for 24 hours. Macrophage were treated with MSU, calcium urate (CaU), ammonium urate (NH4U), potassium urate (KU) or magnesium urate (MgU) crystals (section 2.3). In addition to urate crystals, macrophages were also stimulated with calcium pyrophosphate dehydrate (CPPD) crystals, the causative agent in pseudogout [258; 259]. At different time points, macrophages were harvested, and the percentage of NK1.1$^+$ cells and the expression of NK1.1 determined by flow cytometry. Only MSU crystals induced an increase in both the percentage of NK1.1$^+$ macrophages and the expression of NK1.1 by macrophages (Figure 5.5A).

Macrophages were also tested *in vitro* for their ability to produce IL-1β in response to MSU, CPPD, CaU, MgU, NH4U and KU crystals (200 μg/ml). As shown in Figure 5.5B, only macrophages that had been activated with MSU crystals produced significant levels of IL-1β. These findings indicated that the phenomenon of macrophage NK1.1 upregulation was only induced by MSU crystals and not in response to any other crystal types, and that NK1.1 upregulation was linked with the production of IL-1β by macrophages.

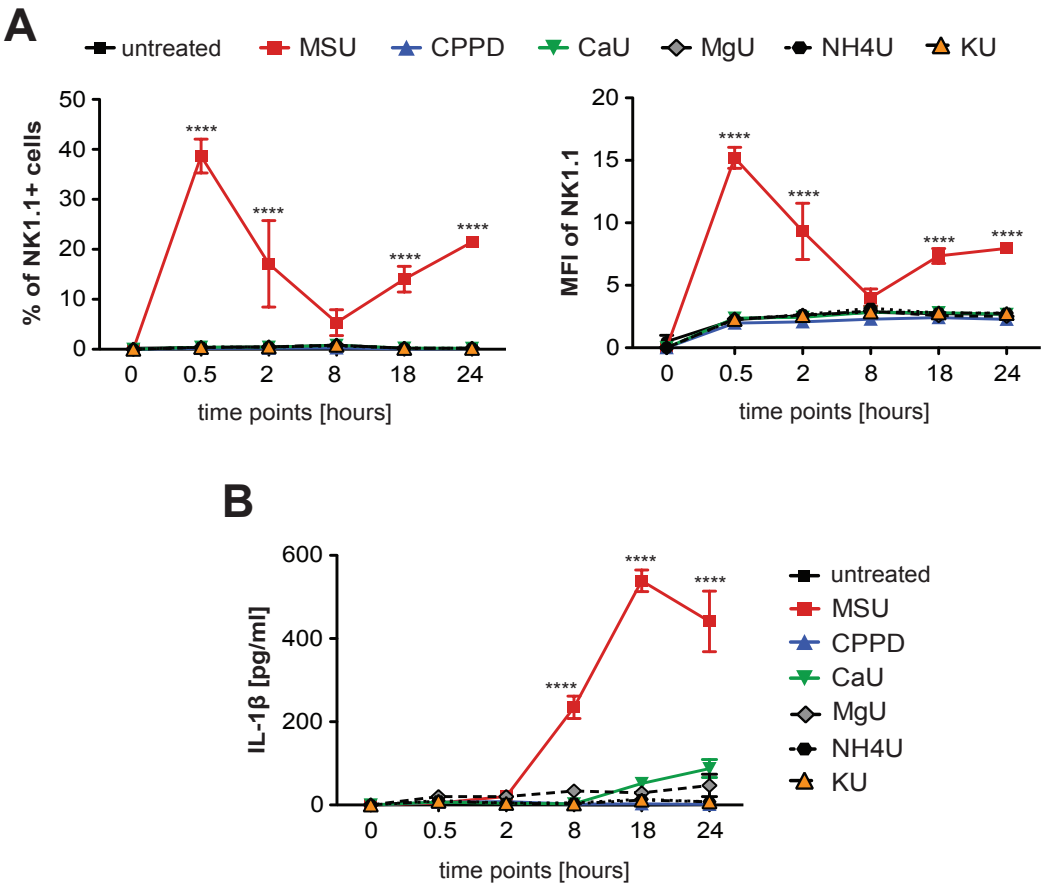

Figure 5.5: Macrophage NK1.1 upregulation induced by MSU crystals requires sodium. Peritoneal lavage fluids were harvested from naive mice and macrophages cultured *in vitro* in the presence of different crystals (MSU, CPPD, CaU, MgU, NH4U and KU) at a concentration of 200 μg/ml for up to 24 hours. **A** At different time points, cells were collected and the percentage of NK1.1$^+$ macrophages and the expression of NK1.1 determined by flow cytometry. **B** Culture supernatants were collected and IL-1β levels analysed by ELISA. Values are the mean -/+ SEM and representative of two separate experiments. **** = $P < 0.0001$ (two-way ANOVA with Bonferroni's post test).

5.3.4 Expression of NK1.1 by MSU crystal-stimulated macrophages is independent of caspase 8

Macrophages produce IL-1β via the activation of NLRP3 inflammasome leading to the cleavage of caspase 1 and the maturation of pro-IL-1β into active IL-1β, also known as the canonical signalling pathway [61; 121; 260]. However, a recent study describes the involvement of a non-canonical IL-1β activation pathway via caspase 8 activation [245; 261].

To determine whether caspase 8 was involved in the IL-1β signalling cascade and the upregulation of NK1.1 expressed by MSU crystal-activated macrophages, peritoneal macrophages were harvested (section 2.6) and cultured *in vitro* in the presence of the caspase 8 inhibitor IETD (20 μM and 30 μM) prior to MSU crystal stimulation (200 μg/ml) for 8 and 24 hours (section 2.7.8). After incubation, supernatants from the cell culture were collected and analysed for IL-1β by ELISA. As shown in Figure 5.6A, macrophages that were stimulated with MSU crystals produced significantly more IL-1β compared to untreated macrophages. Consistent with findings in chapter 4, the inhibition of caspase 8 significantly blocked the production of IL-1β by MSU crystal-activated macrophages. Despite lowering IL-1β production, flow cytometry analysis of macrophages showed that the inhibition of caspase 8 did not significantly alter the percentage of NK1.1$^+$ macrophages after MSU crystal treatment (Figure 5.6B). These findings showed that the upregulation of NK1.1 by MSU crystal-activated macrophages was independent of caspase 8.

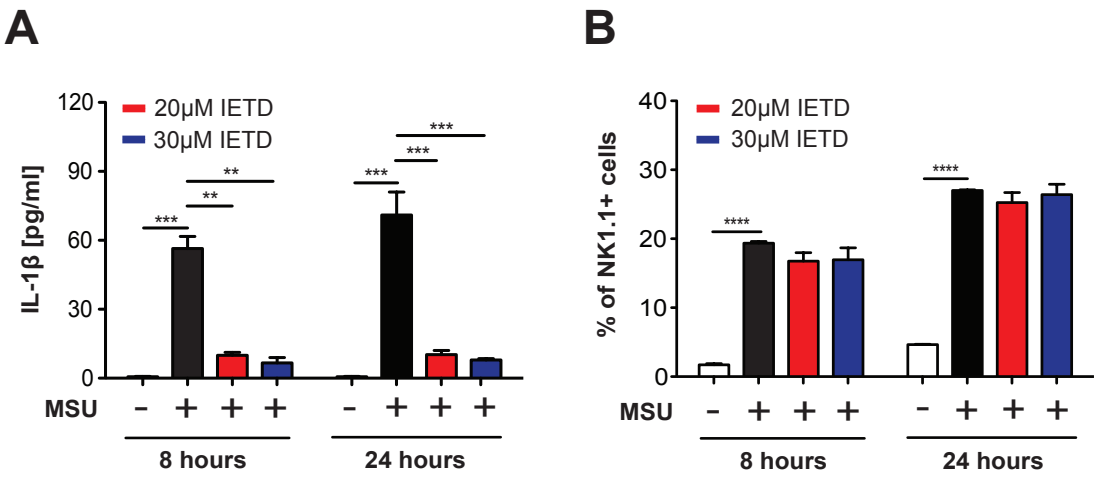

Figure 5.6: NK1.1 expression by MSU crystal-stimulated macrophages is caspase 8-independent. Peritoneal lavage fluids were harvested from naive mice and macrophages cultured *in vitro* in the presence of the caspase 8 inhibitor IETD (20 μM and 30 μM). After 1 hour, macrophages were stimulated with MSU crystals (200 μg/ml) or left untreated. At different time points, supernatants from the cell culture were collected and the levels of IL-1β (**A**) analysed by ELISA, and the cells were harvested and the percentage of NK1.1$^+$ macrophages (**B**) determined by flow cytometry. Values are the mean -/+ SEM and representative of two independent experiments. ** = $P < 0.01$, *** = $P < 0.001$, **** = $P < 0.0001$ (one-way ANOVA with Bonferroni's post test).

5.3.5 Peritoneal macrophages express the NK inhibitory receptor Ly49A

Human natural killer (NK) cells and NKT cells have been shown to express receptors specific for major histocompatibility complex class I molecules (MHC class I) [262; 263] that either activate or inhibit NK cell activities. The ability of NK cells to kill depends on the balance between the activating killer cell-Ig (KAR) and the inhibitory killer cell Ig-like (KIR) receptor. In mice, these receptors are defined as Ly49 NK cell receptors [264; 265]. The Ly49A NK cell receptor has an inhibitory effect on NK cells and has been shown to bind to self MHC class I molecules on other cells to stop NK cell killing [266; 267; 268]. The Ly49D activating receptor on the other hand binds to non-self molecules that are upregulated on stressed or transformed cells resulting in NK cell-mediated lysis [269; 270; 271; 272; 273]. The ability of macrophages to express these specific NK cell receptors has not been previously reported.

To look at Ly49A and Ly49D expression, peritoneal macrophages were harvested (section 2.6) and cultured *in vitro* in the presence of MSU crystals (200 μg/ml) for up to 24 hours (section 2.7.8). At different time points, cells were analysed by flow cytometry and the percentage of macrophages expressing the NK cell inhibitory receptor Ly49A and the NK cell activating receptor Ly49D were determined (section 2.9). As shown in Figure 5.7A, the percentage of Ly49A$^+$ macrophages increased overtime regardless of their activation status. The NK cell activating receptor Ly49D was not expressed on macrophages (Figure 5.7B). These results showed that the NK cell inhibitory receptor Ly49A was expressed by cultured macrophages independent of their activation status, which indicated that macrophages may develop the ability to recognise MHC class I on other cells.

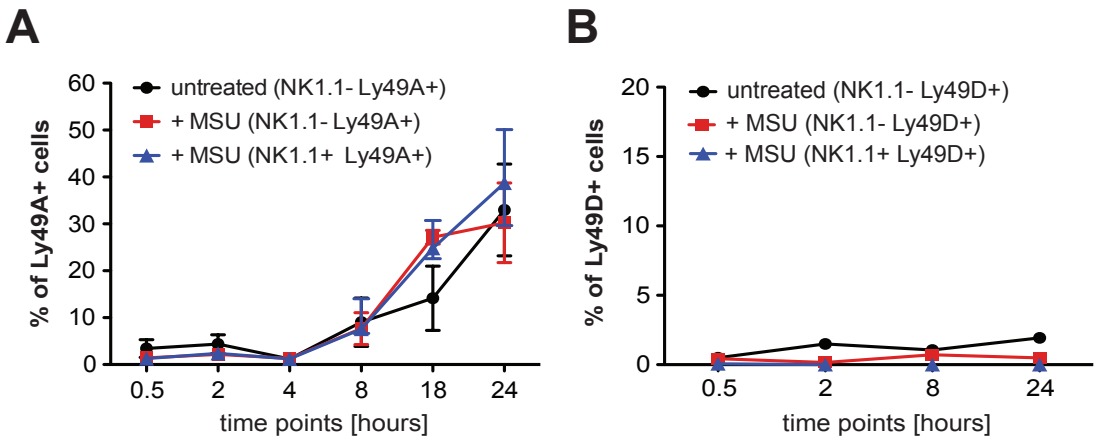

Figure 5.7: NK inhibitory receptor expression by macrophages. Peritoneal lavage fluid was harvested from naive mice and macrophages stimulated *in vitro* with 200 μg/ml MSU crystals for up to 24 hours. At different time points, macrophages (F4/80$^+$ CD11b$^+$) were harvested and the percentage of NK1.1$^-$ and NK1.1$^+$ cells expressing the NK inhibitory receptor Ly49A (**A**) and the NK activating receptor Ly49D (**B**) determined by flow cytometry. Values are the mean -/+ SEM and representative of two independent experiment.

5.3.6 Upregulation of surface NK1.1 by macrophages upon MSU crystal stimulation but not intracellular NK1.1

The upregulation of NK1.1 by MSU crystal-stimulated macrophages occured rapidly within the first hour (Figure 5.2A), possibly due to a translocation of an existing pool of intracellular NK1.1 to the cell surface. To test this, peritoneal macrophages were harvested (section 2.6) and cultured *in vitro* in the presence of MSU crystals (200 μg/ml) for 1 hour. After incubation, macrophages were first stained for surface NK1.1-PE, fixed with formalin and then stained for intracellular NK1.1-FITC (intracellular staining of cells, section 2.9.2), and analysed by flow cytometry. As shown in Figure 5.8A, macrophages expressed intracellular NK1.1 (black line). The intracellular NK1.1 levels did not change upon MSU crystal stimulation (red line) despite upregulation of extracellular NK1.1 expression by activated macrophages (red line, Figure 5.8B). These results showed that MSU crystal-induced upregulation of NK1.1 expression by macrophages did not result from the translocation of NK1.1 from an intracellular store to the extracellular membrane surface.

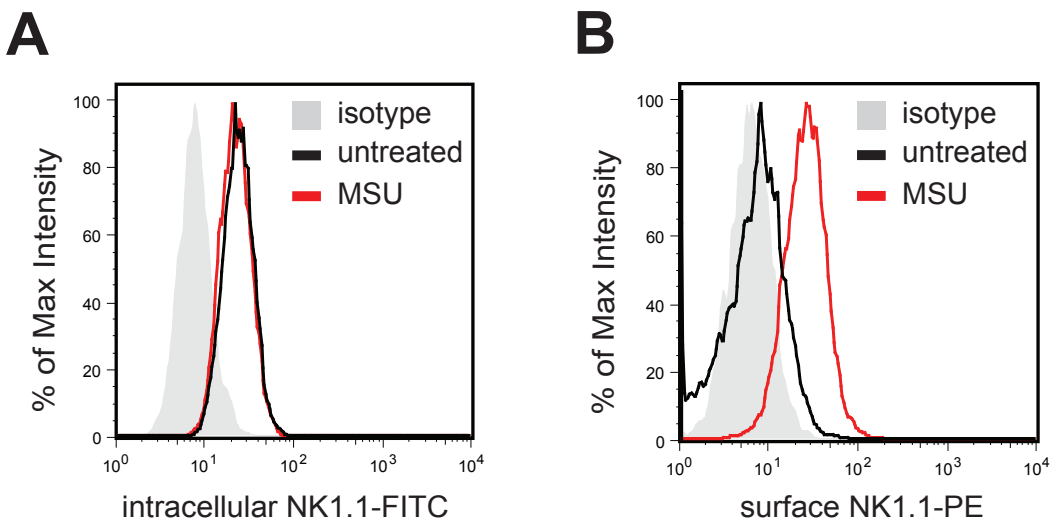

Figure 5.8: MSU crystals upregulate surface NK1.1 expression by macrophages but not intracellular NK1.1. Peritoneal lavage fluid from naive mice was harvested and macrophages cultured *in vitro* in the absence (black line) or in the presence of MSU crystals (200 μg/ml) (red line) for 1 hour. After incubation, macrophages (F4/80$^+$ CD11b$^+$) were harvested and the percentage of intracellular NK1.1-FITC$^+$ (**A**) and surface NK1.1-PE$^+$ (**B**) determined by flow cytometry. Values are the mean -/+ SEM and representative of two independent experiments.

5.3.7 NK1.1 expression by MSU crystal-activated macrophages

Macrophages are professional phagocytes [183]. Previous data have shown that phagocytosis of MSU crystals by macrophages is a primary mechanism involved in the initiation of MSU crystal-induced inflammation [121]. To determine whether phagocytosis of MSU crystals was required for NK1.1 expression by macrophages, peritoneal macrophages were harvested and cultured *in vitro* in the presence of the phagocytosis inhibitor CytochalasinD (section 2.7.8), which has been widely used to block the uptake of apoptotic cells by macrophages [205; 206; 207]. Previous studies and results in chapter 3 (Figure 3.12C) showed that CytochalasinD can cause neutrophil membrane disruption and cell death [208; 209; 210]; therefore the viability of CytochalasinD-treated macrophages was investigated. Treatment of macrophages with 10 μg/ml CytochalasinD had no effect on the percentage of live cells (annexinV^-, Figure 5.9A) or apoptotic cells (annexinV^+, Figure 5.9B) compared to untreated macrophages after 24 hours in culture. Based on these findings, 10 μg/ml CytochalasinD was used to investigate the association between phagocytosis of MSU crystals and NK1.1 upregulation by macrophages.

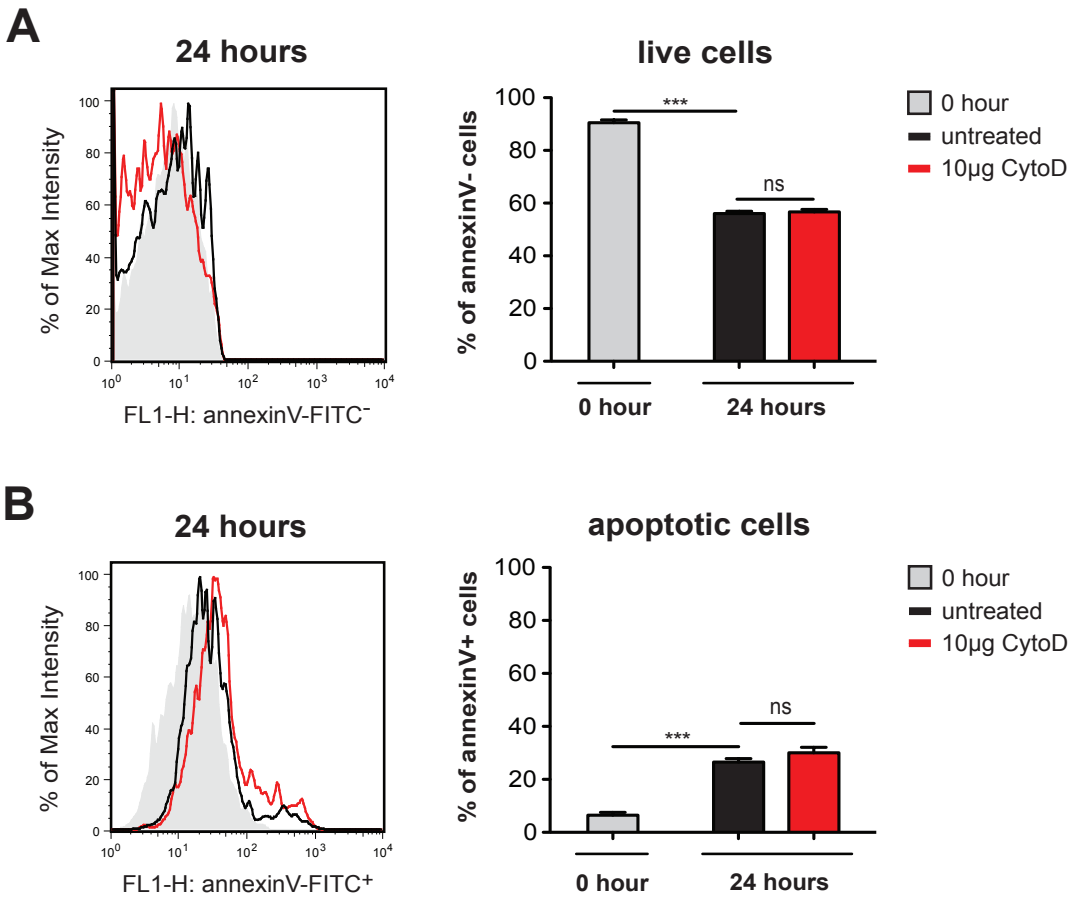

Figure 5.9: CytochalasinD does not induce cell death by macrophages. Peritoneal lavage fluids were harvested from naive mice and macrophages cultured in the presence of the phagocytosis inhibitor CytochalasinD (10 μg/ml) *in vitro* for 24 hours. The percentage of live macrophages (annexinV$^-$) (**A**) and the percentage of apoptotic macrophages (annexinV$^+$) (**B**) was determined by flow cytometry. Values are the mean -/+ SEM and representative of two independent experiments. *** = $P < 0.001$ (two-way ANOVA with Bonferroni's post test).

To investigate a possible link between phagocytosis of MSU crystals and NK1.1 upregulation by macrophages, peritoneal macrophages were harvested and cultured *in vitro* in the presence of the phagocytosis inhibitor CytochalasinD (10 μg/ml) prior to MSU crystal stimulation (200 μg/ml) (section 2.7.8). After incubation, macrophages were stained for NK1.1 and culture supernatants analysed for IL-1β by ELISA. As shown in Figure 5.10A and B, both the percentage of NK1.1$^+$ macrophages and the NK1.1 expression by macrophages increased in response to MSU crystals (black bars) compared to untreated macrophages (white bars). The blockade of phagocytosis of MSU crystals resulted in a significant decrease in both the percentage of NK1.1$^+$ cells as well as NK1.1 expression by macrophages (red bars).

Stimulation with MSU crystals triggered the production of high levels of IL-1β by macrophages. As expected IL-1β production was significantly decreased when phagocytosis of MSU crystals was inhibited confirming that the internalisation of MSU crystals was required for inducing macrophage IL-1β (Figure 5.10C). These findings confirmed that NK1.1 upregulation by macrophages required phagocytosis of MSU crystals.

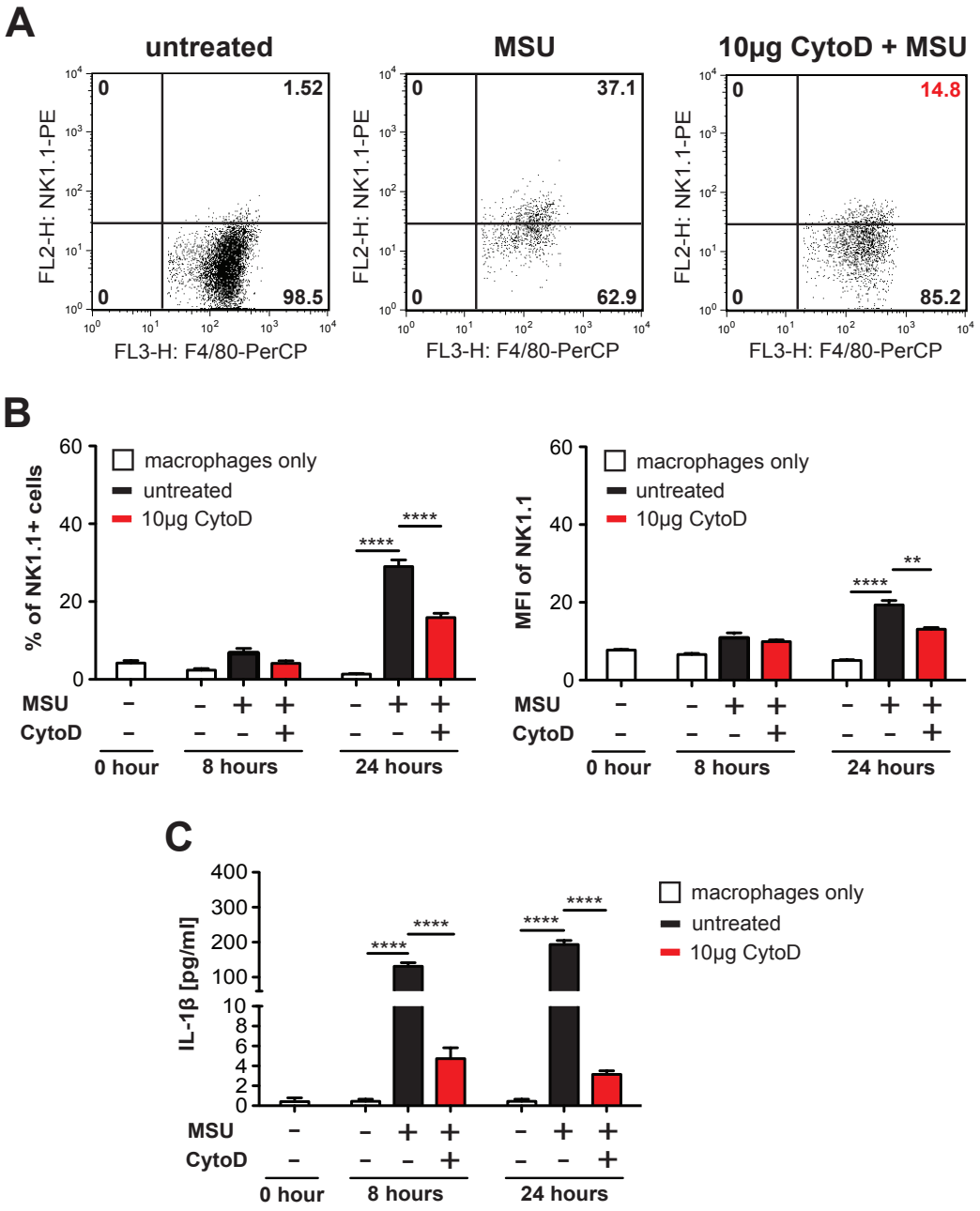

Figure 5.10: Macrophage NK1.1 upregulation is dependent on phagocytosis of MSU crystals. Peritoneal lavage fluids were harvested from naive mice and macrophages cultured *in vitro* in the presence of the phagocytosis inhibitor CytochalasinD (10 μg/ml) prior MSU crystal stimulation (200 μg/ml) or left untreated for 8 and 24 hours. **A** The percentage of NK1.1$^+$ macrophage (F4/80$^+$) from the 24 hour culture was determined by flow cytometry. **B** After 8 and 24 hours, the cell culture was analysed for the percentage of NK1.1$^+$ macrophages and the expression of NK1.1 by flow cytometry. **C** Supernatants from the cell culture were analysed for levels of IL-1β by ELISA. Values are the mean -/+ SEM and representative of two independent experiments. ** = $P < 0.01$, **** = $P < 0.0001$ (two-way ANOVA with Bonferroni's post test).

5.3.8 Phagocytosis of apoptotic neutrophils triggers NK1.1 expression by macrophages

Since the observed upregulation of NK1.1 by MSU crystal-activated macrophages was a phagocytosis-driven event, it was hypothesised that other phagocytosis events might also trigger NK1.1 expression. The clearance of apoptotic neutrophils by macrophages has been reported as a key mechanism involved in the resolution of MSU crystal-induced inflammation [182; 183; 199]. Therefore, the process of phagocytosis of apoptotic neutrophils as a possible mechanism for triggering NK1.1 expression was investigated. MSU crystal-recruited neutrophils were purified (section 2.6.5) and cultured *ex vivo* overnight to induce apoptosis as described in section 3.3.4. These apoptotic neutrophils were then co-cultured *in vitro* with peritoneal macrophages (apoptotic neutrophils:macrophages, cell ratio 5:1) for 24 hours (section 2.7.8). After incubation, macrophages were stained for the surface marker F4/80, Ly6G and NK1.1, and the percentage of F4/80$^+$ Ly6G$^+$ cells determined by flow cytometry.

As shown in Figure 5.11A, macrophages that were co-cultured with apoptotic neutrophils (F4/80$^+$ Ly6G$^+$) exhibited an increase in both the percentage of NK1.1$^+$ cells and the expression of NK1.1 compared to the single cell population of macrophages (F4/80$^+$ NK1.1$^+$, white bars). It was noted that NK1.1 expression and the percentage of NK1.1$^+$ cells by macrophage phagocytosis of apoptotic neutrophils were significantly greater (80 - 90%) than that induced in macrophages stimulated with MSU crystals (20 - 30%) (Figure 5.10B). The co-culture of macrophages with apoptotic neutrophils (black bars) did not induce a significant increase in the levels of IL-1β compared to macrophages only (white bars) (Figure 5.11B). These findings showed that phagocytosis of apoptotic neutrophils by macrophages was triggering NK1.1 upregulation and that IL-1β was not essential for increased macrophage NK1.1 expression.

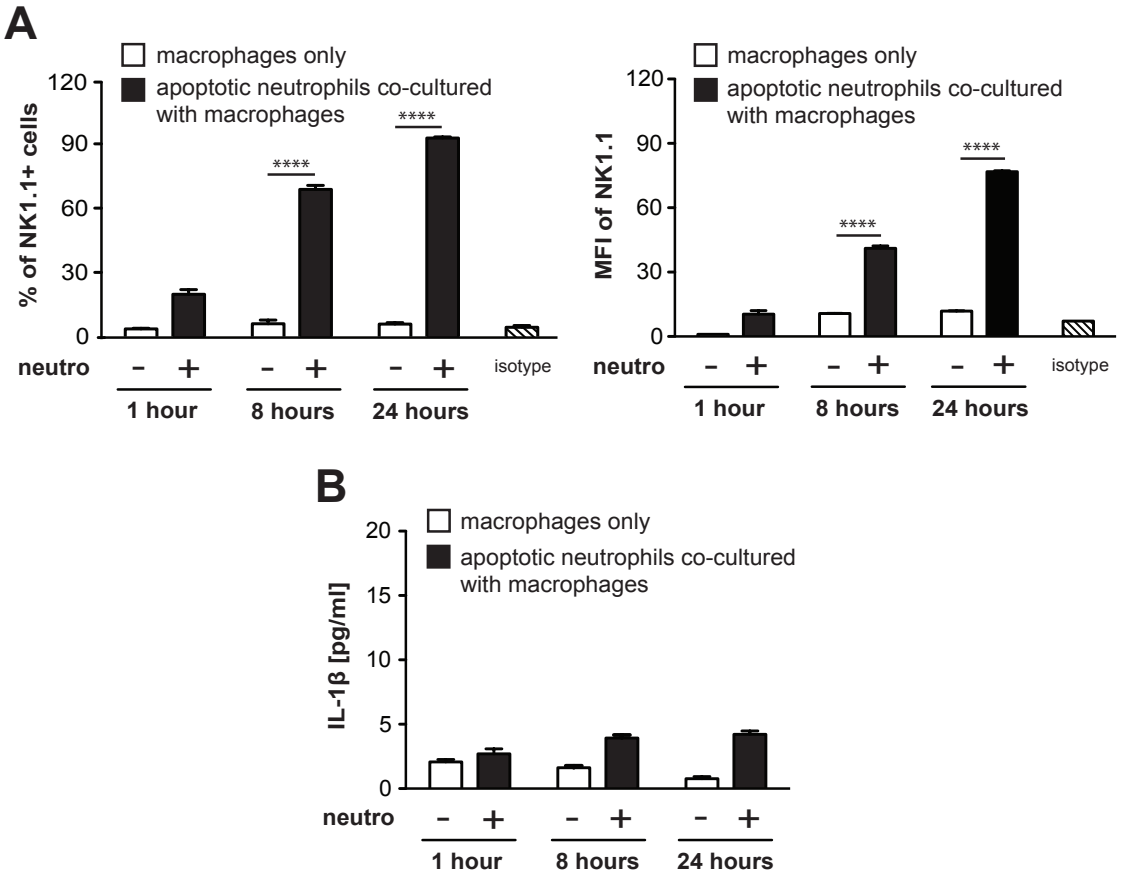

Figure 5.11: Phagocytosis of apoptotic neutrophils induces upregulation of NK1.1 by macrophages. Mice were injected with MSU crystals (3 mg, i.p.). After 18 hours, neutrophils were purified and cultured *ex vivo* overnight to induce apoptosis. Apoptotic neutrophils were co-cultured *in vitro* with naive peritoneal macrophages (cell ratio 5:1) for 1, 8 and 24 hours. **A** The percentage of NK1.1$^+$ cells and the expression of NK1.1 from the single cell populations of macrophages (F4/80$^+$) or the double positive cells (F4/80$^+$ Ly6G$^+$) determined by flow cytometry. **B** Supernatants from the cell culture were analysed for IL-1β by ELISA. Values are the mean -/+ SEM and representative of two independent experiments. **** = $P < 0.0001$ (two-way ANOVA with Bonferroni's post test).

To confirm that phagocytosis of apoptotic neutrophils by macrophages was the primary trigger for NK1.1 upregulation, MSU crystal-recruited neutrophils were purified (section 2.6.5) and cultured *ex vivo* overnight to induce apoptosis as described above. These apoptotic neutrophils were stained with the neutrophil marker Ly6G and then co-cultured *in vitro* with peritoneal macrophages (apoptotic neutrophils:macrophages, cell ratio 5:1) in the presence of the phagocytosis inhibitor CytochalasinD (10 μg/ml). The percentage of macrophages that had phagocytosed apoptotic neutrophils (F4/80$^+$ Ly6G$^+$) significantly decreased with CytochalasinD treatment (red bars) compared to the untreated co-culture of macrophages with apoptotic neutrophils (black bars) (Figure 5.12A).

As demonstrated in Figure 5.12B, blocking phagocytosis with CytochalasinD resulted in a significant decrease in both the percentage of NK1.1$^+$ cells and the levels of NK1.1 expression by macrophages (F4/80$^+$ Ly6G$^+$, red bars). The IL-1β levels from the cell culture supernatants showed that the inhibition of phagocytosis of apoptotic neutrophils by macrophages (red bars) did not alter the production of IL-1β compared to the untreated co-culture of apoptotic neutrophils and macrophages (black bars) (Figure 5.12C). Together, these results confirmed that phagocytosis of apoptotic neutrophils was required to trigger the upregulation of NK1.1 by macrophages.

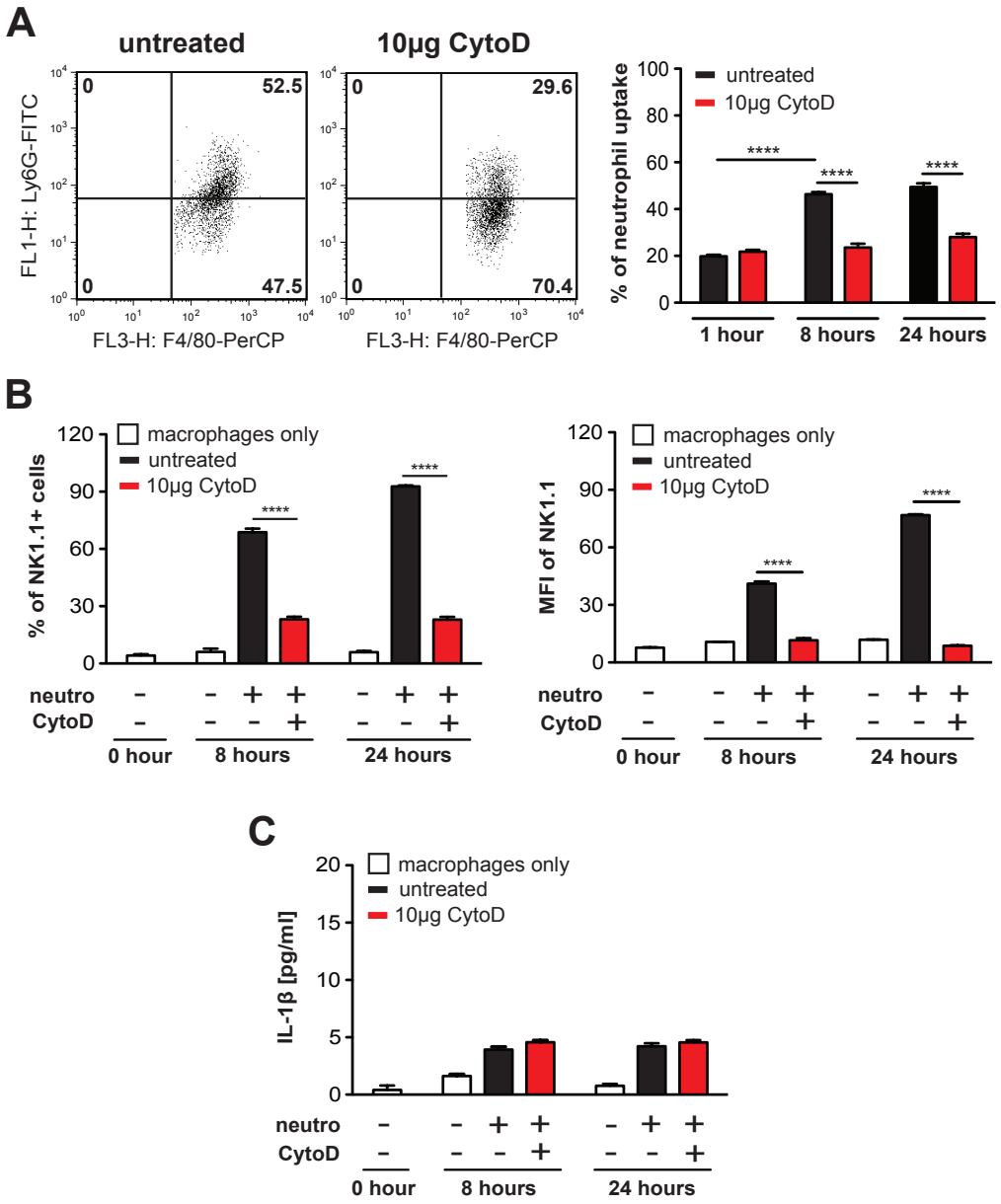

Figure 5.12: Phagocytosis of apoptotic neutrophils is required for NK1.1 expression by macrophages. Mice were injected with MSU crystals (3 mg, i.p.). After 18 hours, neutrophils were purified and cultured *ex vivo* overnight to induce apoptosis. Apoptotic neutrophils were co-cultured *in vitro* with naive peritoneal macrophages (cell ratio 5:1) in the presence of CytochalasinD (10 μg/ml) for 1, 8 and 24 hours. **A** The percentage of macrophages that had phagocytosed apoptotic neutrophils (F4/80$^+$ Ly6G$^+$) determined by flow cytometry. **B** The percentage of NK1.1$^+$ cells and the expression of NK1.1 from the single cell populations of macrophages (F4/80$^+$) or apoptotic neutrophils (Ly6G$^+$) versus the double positive cells (F4/80$^+$ Ly6G$^+$) determined by flow cytometry. **C** Supernatants from the cell culture were analysed for IL-1β by ELISA. Values are the mean -/+ SEM and representative of two independent experiments. **** = $P < 0.0001$ (two-way ANOVA with Bonferroni's post test).

5.3.9 Uptake of fluorescent beads does not induce NK1.1 upregulation by macrophages

The previous section demonstrated that phagocytosis of MSU crystals and apoptotic neutrophils triggers macrophage NK1.1 expression. To determine whether NK1.1 upregulation could be triggered by non-specific phagocytic activity, macrophages were harvested (section 2.6) and incubated with fluorescent beads for 1, 8 and 24 hours (section 2.7.8). After incubation, the phagocytic ability was measured as the percentage of F4/80$^+$ bead$^+$ macrophages by flow cytometry, and the supernatants were collected for IL-1β by ELISA. As shown in Figure 5.13A, approximately 40% of the macrophages (at 1 hour) displayed bead uptake (F4/80$^+$ bead$^+$), which significantly increased (up to 90%) after 24 hours.

Phagocytosis of fluorescent beads by macrophages (F4/80$^+$ bead$^+$, black bars) did not cause a change in the percentage of NK1.1$^+$ macrophages compared to macrophages cultured alone (F4/80$^+$ bead$^-$, white bars) (Figure 13B). While there was no difference in the percentage of NK1.1$^+$ macrophages, the expression of NK1.1 decreased to a low background level in the macrophage population that had phagocytosed fluorescent beads (F4/80$^+$ bead$^+$, black bars) compared to macrophages only (F4/80$^+$, white bars). The uptake of fluorescent beads by macrophages did not induce the production of IL-1β by macrophages, indicating that fluorescent beads were not able to activate the NLRP3 inflammasome to trigger the release of IL-1β (Figure 5.13C). These findings showed that phagocytosis of fluorescent beads by macrophages had no effect on either the expression of NK1.1 or the production of IL-1β. This indicated that the upregulation of NK1.1 did not occur simply as a result of general phagocytosis.

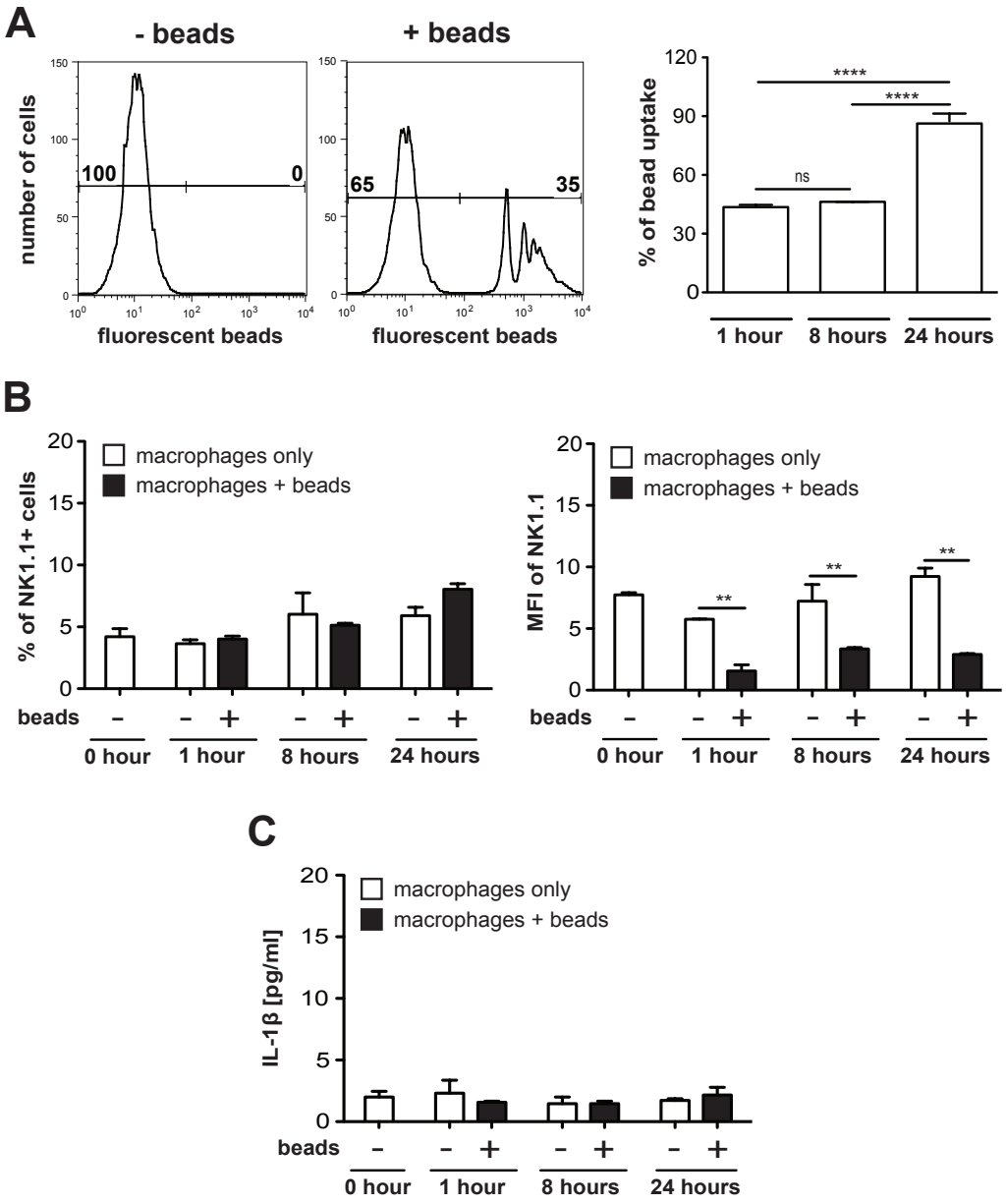

Figure 5.13: Uptake of fluorescent beads has no effect on macrophage NK1.1 expression. Peritoneal lavage fluids were harvested from naive mice and macrophages cultured *in vitro* in the presence of fluorescent beads for 1, 8 and 24 hours. **A** The percentage of macrophages ($F4/80^+$) that had phagocytosed fluorescent beads ($F4/80^+$ $bead^+$) was determined by flow cytometry. **B** The percentage of $NK1.1^+$ cells and the expression of NK1.1 in the single macrophage population ($F4/80^+$) and double positive population ($F4/80^+$ $bead^+$) determined by flow cytometry. **C** Supernatants from the cell culture were analysed for IL-1β by ELISA. Values are the mean -/+ SEM and representative of two independent experiments. ** = $P < 0.01$, **** = $P < 0.0001$ (one-way ANOVA with Tukey's post test and two-way ANOVA with Bonferroni's post test).

5.4 Summary

The data in this chapter showed that the upregulation of the surface marker NK1.1 by macrophages was a phagocytosis-dependent event occurring via two distinct mechanisms (Figure 5.14):

A. In acute gouty inflammation, macrophages play an essential role during the initiation phase, where they become activated through phagocytosis of MSU crystals leading to the production of pro-inflammatory cytokines such as IL-1β and TNFα. The findings here indicated that MSU crystal-activated macrophages produce IL-1β and TNFα, which triggers the upregulation of NK1.1 expression. Therefore, it appears that the upregulation of NK1.1 by macrophages is an activation-driven event occurring via an autocrine cell signalling loop.

B. One characteristic feature of the resolution of MSU crystal-induced inflammation is the clearance of apoptotic neutrophils by macrophages. The results presented in this chapter demonstrated that the second mechanism triggering the upregulation of NK1.1 expression is a consequence of phagocytosis of apoptotic neutrophils by macrophages. This phagocytosis-driven NK1.1 upregulation by macrophages occurs independently of pro-inflammatory cytokine production and therefore represents a non-inflammatory event.

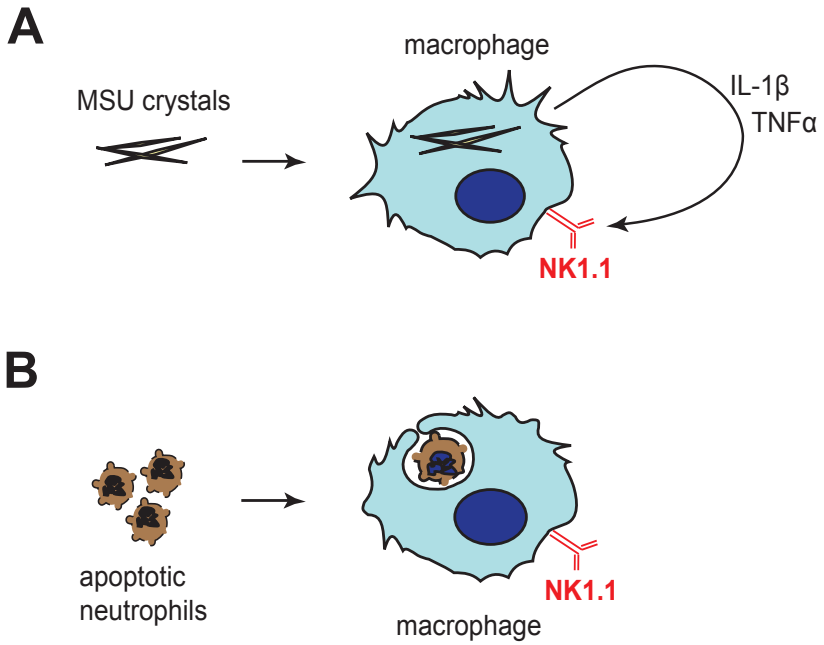

Figure 5.14: NK1.1 expression by macrophages. **A** Macrophage NK1.1 up-regulation that is triggered via a phagocytosis-driven MSU crystal-induced inflammatory response. **B** Apoptotic neutrophils are phagocytosed by macrophages leading to the up-regulation of macrophage NK1.1 expression in a cytokine independent manner. TNFα = tumor necrosis factor alpha; IL-1β = interleukin-1 beta.

Chapter 6

6 General Discussion

6.1 Overview

There have been many studies that have explored the involvement of monocytes, neutrophils and macrophages in acute gouty inflammation. This thesis provides further insights into the mechanisms involved in TGFβ1 production during the spontaneous resolution of MSU crystal-induced inflammation, the effect of TGFβ1 on macrophage differentiation and changes in surface marker expression by MSU crystal-stimulated macrophages.

6.2 Neutrophils driving the resolution of acute gouty inflammation

TGFβ1 has been identified in the synovial fluid of gout patients highlighting a potential role for TGFβ1 in the resolution phase of gout [185; 186]. Consistent with the clinical observation, the data in chapter 3 also showed elevated levels of TGFβ1 during MSU crystal-induced inflammation *in vivo*. The clearance of apoptotic neutrophils by macrophages leading to the generation of TGFβ1 is considered to be a characteristic event in the resolution of inflammation [138; 137; 136], including the shutdown of MSU crystal-induced inflammation [199]. The results of the current work now identify neutrophil phagocytosis of apoptotic neutrophils as a trigger for neutrophil TGFβ1 production. This indicates that as well as being involved in the pro-inflammatory phase of gouty inflammation through the production of ROS and IL-1β [198; 176], neutrophils contribute to the resolution of acute inflammation via TGFβ1 production.

Neutrophils are professional phagocytes and recent literature reports that neutrophils have the capacity to affect non-inflammatory phagocytosis of apoptotic neutrophils *in vitro* and *in vivo* [211; 274]. Interestingly, the literature reports that

neutrophil canibalism is a non-inflammatory event [211]. The data herein provide evidence that TGFβ1 produced by phagocytosing neutrophils suppresses both neutrophil respiratory burst and IL-1β production *ex vivo*. This indicates that rather than being a passive non-inflammatory neutrophil event, neutrophil canibalism actively suppresses neutrophil inflammatory functions via TGFβ1.

Neutrophils are known for their ability to produce ROS upon MSU crystal stimulation [82]. It has been shown that ROS can activate the NLRP3 inflammasome leading to the production of IL-1β in response to MSU crystals indicating a possible link between ROS and IL-1β [275; 276; 243]. In this study, neutrophil TGFβ1 production was shown to suppress both neutrophil ROS and IL-1β production *in vitro* indicative of a link between respiratory burst and IL-1β release. However, *in vivo* studies showed that although TGFβ1 played a part in suppression of ROS production, TGFβ1 was not essential for limiting IL-1β production in MSU crystal-induced inflammation. This indicates that neutrophil TGFβ1 can control neutrophil ROS but may be only one of a number of independent mechanisms involved in regulating the generation of active IL-1β *in vivo*.

Interestingly, the data show that circulating blood neutrophils can also produce TGFβ1 upon phagocytosis of apoptotic cells (Figure 3.11). This indicates that rather than being an inflammatory event, neutrophil clearance and TGFβ1 production is most likely a general function of neutrophils. A recent study has shown that TGFβ1 can be found in detectable concentrations in the human blood of healthy volunteers [277]. As neutrophils are found in high numbers in the blood, neutrophil self-clearance and TGFβ1 production may play a passive role in neutrophil turnover to maintain homeostasis. This mechanism may also play an important role in limiting systemic inflammation where high neutrophil cell death would be present.

Neutrophils are considered to be primarily pro-inflammatory in nature [117; 133; 191]. The data within this thesis show evidence that neutrophils can also exhibit

anti-inflammatory characteristics through regulating neutrophil inflammatory functions. Together, TGFβ1 produced by canibalising neutrophils has the capacity to drive the spontaneous resolution of inflammation in gout, and may also play a role in neutrophil turnover and systemic homeostasis.

Future investigations are needed to unravel the mechanism by which TGFβ1 controls inflammatory functions, such as ROS production by neutrophils. Reports have shown that upon LPS or fMLP stimulation, neutrophils activate the NADPH oxidase, which leads to the generation of ROS [278; 192; 190]. This raises the question: Does TGFβ1 regulate the NADPH oxidase leading to suppression of ROS production by MSU crystal-recruited neutrophils? NADPH oxidase is a multiprotein complex that consists of membrane-bound subunits (such as NOX2, p22phox, p91phox) and cytosolic subunits (such as p47phox, p40phox) that upon activation triggers the production of ROS [243]. Herein, only extracellular ROS production (superoxide) by neutrophils was measured, therefore it would be also of interest to investigate the effect of TGFβ1 on intracellular NADPH oxidase activity. One way to investigate intracellular NADPH oxidase activity by MSU crystal-recruited neutrophils could be to use a p47phox antibody and measure the expression of p47phox by western blot analysis, microscopy or flow cytometry [192]. This may provide insight into the mechanism by which neutrophils self-regulate inflammatory functions via TGFβ1.

6.3 The effect of TGFβ1 on GM-BMMs and M-BMMs

Macrophages have been shown to play an important role in the initiation and progression of MSU crystal inflammation in gouty arthritis. Resident tissue macrophages have been identified to initiate and drive the early inflammatory response [103], whereas MSU crystal-recruited monocyte/macrophage differentiation has been found to play an important role in clearance of apoptosing cells and TGFβ1 production [138], alongside the development of hyper-inflammatory macrophage phenotypes *in*

vivo [149]. The results of this study now provide insight into how TGFβ1 levels may influence these macrophage phenotypes.

TGFβ1 was found to be elevated during both the initiation and resolution phase of the *in vivo* inflammatory response to MSU crystals. As the initiation phase of the inflammatory response is reliant on the resident macrophage phenotype, these findings suggest that TGFβ1 may influence the inflammatory function of resident macrophages. The tissue-resident macrophage phenotype is predominantly under the control of M-CSF [279; 280; 281]. The *in vitro* data in chapter 4 demonstrate that TGFβ1 decreases the *in vitro* production of IL-1β by M-CSF differentiated (M2-like) macrophages in response to MSU crystals. *In vivo* administration of TGFβ1 before or during the early phase of the inflammatory response has been shown to suppress the inflammatory response to MSU crystals and this suppressive effect could be reversed by TGFβ1 neutralisation *in vivo* [161]. Combined with the findings of the current study, early TGFβ1 production may act to suppress MSU crystal-induced activation of the resident macrophage phenotype. Interestingly, the opposite effect was observed when TGFβ1-differentiated M-CSF macrophages were stimulated with LPS indicating that TGFβ1 induces a M-CSF macrophage phenotype tuned for stimulus-specific inflammatory responses.

The presence of TGFβ1 either during or after M-CSF macrophage differentiation showed that M-BMMs were a less differentiated macrophage phenotype as illustrated by the down-regulation of the M-CSF receptor CD115, and F4/80. CD115 receptor expression is important for M-CSF-mediated differentiation and function of M-CSF macrophages [213; 282]. M-CSF signalling through CD115 has been shown to facilitate the activation of signalling pathways including Erk1/2, Akt, and STAT3 that are involved in the production of inflammatory cytokines by BMMs [283; 284] and MSU crystal-stimulated macrophages [155]. Accordingly, it is possible that TGFβ1-mediated down-regulation of CD115 signalling could be associated with the observed hypo-inflammatory responsiveness of MSU crystal-stimulated M-BMMs.

A recent study has reported that MSU crystal-recruited monocytes differentiate into a hyper-inflammatory macrophage phenotype *in vivo* [149]. Combined with this, research within our group has identified that GM-CSF is required for the development of this M1-like macrophage phenotype [unpublished data, manuscript submitted]. There is one report showing that TGFβ1 may prime macrophages to express particulate β1,3-glucan-induced inflammatory gene expression of the platelet-derived growth factor-B (PDGF-B) transcript [285]. The *in vitro* data in chapter 4 now show that TGFβ1 specifically enhances the development of the GM-CSF macrophage inflammatory cytokine response to MSU crystals, including release of active IL-1β, without affecting the response to LPS.

GM-CSF is commonly used in the generation of antigen presenting function in dendritic cells (DCs) [214; 286; 140; 287]. In the presence of TGFβ1, DCs lose their ability to present antigen and drive T cell expansion [226; 288]. Here, GM-CSF macrophages also exhibited APC function that was lost in the presence of TGFβ1. At the same time, the TGFβ1-generated GM-CSF macrophages increased the expression of maturation (F4/80) and activation (CD86) markers consistent with the development of a more mature macrophage phenotype [220; 221; 224]. These data indicate that TGFβ1 switches off APC functions by GM-BMMs and promotes the innate immune response to MSU crystals as demonstrated by increased IL-1β production by MSU crystal-stimulated GM-BMM. Importantly, TGFβ1 needs to be present during the differentiation process for the development of the GM-CSF driven hyper-inflammatory phenotype. This is consistent with the environment present *in vivo*, where the MSU crystal-recruited monocytes differentiate in the presence of GM-CSF and elevated TGFβ1. As such, TGFβ1 may contribute towards the development of the M1-like macrophage phenotype observed *in vivo* allowing these cells to respond with a faster enhanced pro-inflammatory response upon restimulation [149]. This macrophage phenotype may well contribute towards the exacerbated inflammatory responses often seen in recurrent gout attacks [149; 289; 290; 291].

The data show that TGFβ1 increases the expression of CD14 by resting GM-BMMs and M-BMMs. However, upon MSU crystal stimulation, only the M-CSF macrophages significantly increased the expression of CD14. Although CD14 and TLR2/4 have been shown to be involved in MSU crystal-mediated IL-1β production by macrophages [96; 58], the data herein showed that the increased CD14 expression by MSU crystal-stimulated M-BMMs did not correlate with the observed hypo-responsiveness of TGFβ1-differentiated M-BMMs. This indicates that IL-1β signalling by MSU crystal-stimulated BMMs could be regulated via a CD14-independent pathway and that CD14 expression is a poor predictor of inflammatory responses by different macrophage populations to different stimuli.

Recent reports have shown that in response to different stimuli, macrophages and DCs can process IL-1β through two independent signalling pathways: the canonical pathway via caspase 1 and the non-canonical pathway via caspase 8 [245; 292; 246]. The data herein identify for the first time that MSU crystal-stimulated GM-CSF macrophages require both caspase 1 and caspase 8 for the production of IL-1β, as illustrated in Figure 6.1A. Furthermore, the TGFβ1-driven hyper-inflammatory response by GM-BMM in response to MSU crystals also relies on a caspase 1/caspase 8-mediated interaction as well as on an enhanced NLRP3 inflammasome activity. In contrast, although TGFβ1-treated M-CSF macrophages showed increased pro-caspase 1 expression, the cleavage of pro-IL-1β into active IL-1β was blocked consistent with the observed decrease in IL-1β production. It is possible that TGFβ1 blocks caspase 1 cleavage and the interaction between caspase 1/caspase 8, which would negatively affect IL-1β cleavage by TGFβ1-differentiated M-BMMs, as illustrated in Figure 6.1B.

One possible mechanism involved in the differential association of caspase 1 and caspase 8 in TGFβ1-treated macrophages may be the way in which caspase 8 associates with RIP3. Although RIP3 has been linked to the ripoptosome [293; 251; 249; 294] associated with apoptotic cell death [295; 296; 297] and to necrotic cell death

[298; 299; 300], the data herein show that IL-1β production by TGFβ1-differentiated GM-BMMs in response to MSU crystals was not a consequence of RIP3-mediated cell death suggesting a cell death-independent role for RIP3. In this study, TGFβ1 caused the down-regulation of RIP3 by MSU crystal-stimulated GM-BMMs, which could potentially increase the availability of caspase 8 to interact with caspase-1 to drive enhanced inflammasome activation and IL-1β release. In the same way, upregulated RIP3 expression in MSU crystal-stimulated M-BMMs could result in increased RIP3/caspase 8 association, thereby limiting the caspase 1/caspase 8 association and decreasing IL-1β production.

Further investigations are needed to unravel possible interactions that are initiated by TGFβ1, which contribute to the differentiation of the hyper-inflammatory GM-BMM phenotype but shutting down the inflammatory functions of M-CSF macrophages. One way to investigate associations between the inflammasome (such as NLRP3, ASC), caspase 1, caspase 8 and the ripoptosome is to perform immunoprecipitation experiments on TGFβ1-differentiated GM-BMMs and M-BMMs that were stimulated with MSU crystals. This will provide further insight into the mechanisms by which TGFβ1 is regulating cellular signalling events by GM-BMMs and M-BMMs in MSU crystal-induced inflammation.

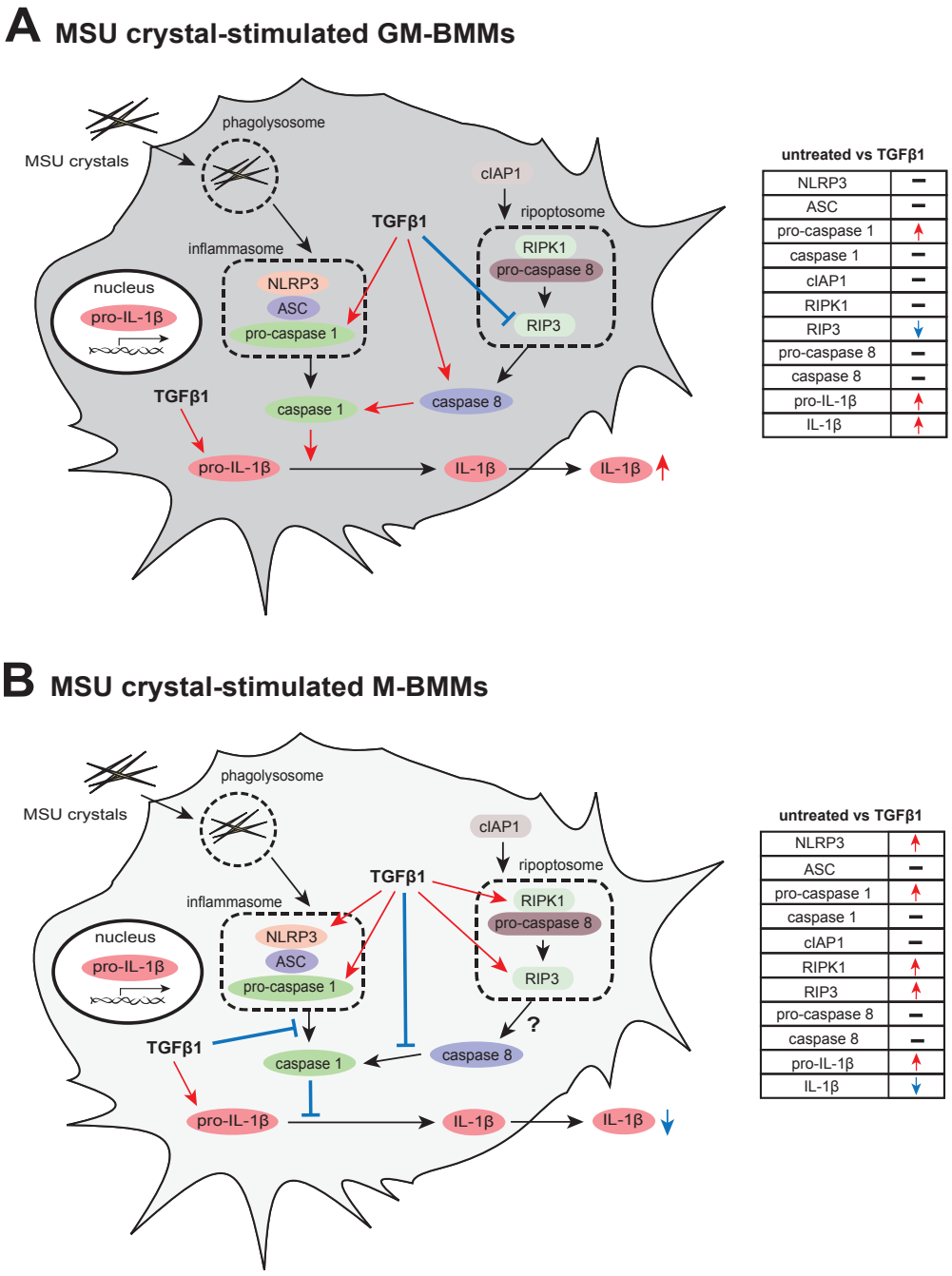

Figure 6.1: Proposed signalling pathway by TGFβ1-differentiated GM-BMMs and M-BMMs in response to MSU crystal stimulation. Red arrows indicate enhanced responses or upregulation, and blue lines represent inhibitory or suppressive functions induced by TGFβ1.

6.4 NK1.1 upregulation by macrophages

NK1.1 is a surface marker primarily used to identify NK cells and NKT cells [253; 254; 255] but has not been previously reported to be expressed on macrophages. The findings in chapter 5 showed that macrophages upregulated the surface marker NK1.1 upon phagocytosis of either MSU crystals or apoptotic neutrophils, an event that did not occur in response to other crystal types or LPS.

The activation of macrophages through phagocytosis of MSU crystals triggers the production of pro-inflammatory cytokines including IL-1β and TNFα [74; 73; 103; 260; 106]. The observed upregulation of NK1.1 by MSU crystal-activated macrophages was partially dependent on IL-1β and TNFα autocrine signalling. Although the inflammatory environment strongly influences macrophage phenotypes [301; 302; 303], the absence of NK1.1 expression by LPS-activated macrophages indicates that pro-inflammatory cytokine production alone is insufficient for triggering NK1.1 upregulation. Phagocytosis of crystals or beads, without pro-inflammatory cytokine production, did not result in NK1.1 upregulation. This indicates that phagocytosis alone is not sufficient for increasing surface marker expression of NK1.1.

Interestingly, NK1.1 upregulation by macrophages also occurred following non-inflammatory phagocytosis of apoptotic neutrophils. In this way, phagocytosis-driven NK1.1 expression by macrophages did not occur simply as a result of general phagocytosis indicating that macrophage NK1.1 expression is more or less a physiological phagocytosis-mediated process.

At this stage, the exact effect of the observed upregulation of NK1.1 on macrophage function is unclear and data on the functional role of NK1.1 are limited. A recent study has shown that signalling through NK1.1 can induce apoptosis by NK cells, while triggering NKT cells to produce IL-4 [256]. In addition, NKDCs have been described to exhibit NK cell-like cytotoxic activities [257; 304]. Furthermore, NK

cells have the ability to kill immune cells, whereby their lytic activity depends on the balance between killer cell activating (KAR) and killer cell inhibitory (KIR) receptors [264; 265]. Interestingly, the results show that *in vitro* cultured macrophages were also able to express KIR but not KAR, and that the expression of KIR by macrophages was independent of their activation status.

There is limited information on whether macrophages can develop NK cell-like functions through the expression of KIR [268]. However, *in vitro* differentiated GM-CSF and M-CSF bone marrow-derived macrophages stimulated with IL-2 have been shown to exhibit NK cell cytotoxicity directed against NK-sensitive target cells [305; 306]. It is therefore possible that the NK1.1-expressing macrophages described here could also display NK cell-like functions, including regulation of cytotoxic function by KIR similar to that observed by NK cells [307; 266; 267]. NK cells are found in the inflamed joints of gout patients and have been linked with the regulation of MSU crystal-induced inflammation [308; 83; 309; 85; 84].

Finally, these data provide further evidence of the variable expression of NK1.1 on different immune cells. In addition to the current study showing that macrophages readily express NK1.1 during inflammation, NKT cells can lose the expression of NK1.1 upon stimulation with IL-2 [310]. Together, these findings highlight the need to take extra care, and use multiple surface markers in combination with NK1.1, to monitor NK or NKT cells in disease settings.

Further research is needed to answer the question of whether NK1.1$^+$ macrophages develop lytic activity against NK-sensitive target cells. One way to investigate this is to co-culture MSU crystal-activated macrophages or macrophages that had phagocytosed apoptotic neutrophils, with CFSE labelled NK-sensitive YAC-1 cells *in vitro*. The levels of NK1.1 macrophage-mediated cytotoxicity/cell death could be determined by flow cytometry using a blue-fluorescent reactive dye. If NK1.1$^+$ macrophages do exhibit cytolytic activity, it would be of interest to investigate

whether NK1.1$^+$ macrophage-mediated killing is dependent on perforin, a cytolytic mediator used by NK cells and cytolytic T lymphocytes (CTLs) to kill target cells [311; 312]. Macrophages from perforin knockout mice could then be used to confirm this killing pathway. This may provide insight into a possible functional role for NK1.1 expression by macrophages.

Future studies could be undertaken to determine whether NK1.1 upregulation by phagocytosing macrophages is associated with TGFβ1 production. The process of phagocytosis of apoptotic neutrophils by macrophages [183; 313] and by neutrophils, as demonstrated in chapter 3, has been linked to the production of TGFβ1. Therefore it is possible that NK1.1 expression by macrophages might be a TGFβ1-mediated phagocytosis-driven event. To investigate this, macrophages could be co-cultured with apoptotic neutrophils in the presence of the anti-TGFβ1 antibody and the expression of NK1.1 by macrophages determined by flow cytometry. This would provide insight of whether NK1.1 upregulation by phagocytosing macrophages occurs via a TGFβ1 autocrine signalling loop.

6.5 Conclusion

The research presented within this thesis focussed on innate immune cells involved in gouty inflammation, which provides new insights into mechanisms contributing to the resolution of inflammation as well as the effect of TGFβ1 on the functional phenotype of monocyte-differentiated macrophages. A proposed model of acute gouty inflammation is illustrated in Figure 6.2.

The deposition of MSU crystals within the joint triggers an acute inflammatory response, which is associated with the generation of cytokines including TGFβ1 and IL-1β primarly produced by tissue resident macrophages referred to as M2-like macrophages. These inflammatory mediators then trigger the upregulation of NK1.1 expression by M2-like macrophages and the infiltration of neutrophils to the

site of inflammation. As neutrophils infiltrate into the joint, their activation by MSU crystals may further augments the inflammatory response through the production of superoxide and IL-1β. In addition, circulating monocytes are also recruited to the joint and over time, these MSU crystal-recruited monocytes differentiate into a hyper-inflammatory macrophage phenotype (M1-like cells) driven by GM-CSF, a cytokine mainly produced by synoviocytes, macrophages, endothelial cells and T cells.

The self-limiting inflammatory response is associated with the phagocytosis of apoptotic neutrophils and the production of TGFβ1 by M1-like macrophages and canibalising neutrophils facilitating resolution of MSU crystal-induced inflammation. Interestingly, phagocytosis-derived TGFβ1 has the ability to suppress neutrophil-inflammatory functions and inflammatory functions of M2-like macrophages in response to MSU crystals. While TGFβ1 contributes to the shutdown of neutrophils and M2-like macrophages, it further primes the hyper-inflammatory GM-CSF macrophage phenotype to respond faster to recurring inflammatory insults.

Taken together, this research highlights the importance of the local inflammatory environment in particular the role of TGFβ1 on the regulation of neutrophil and macrophage functions during the initiation and resolution phase of acute gouty inflammation.

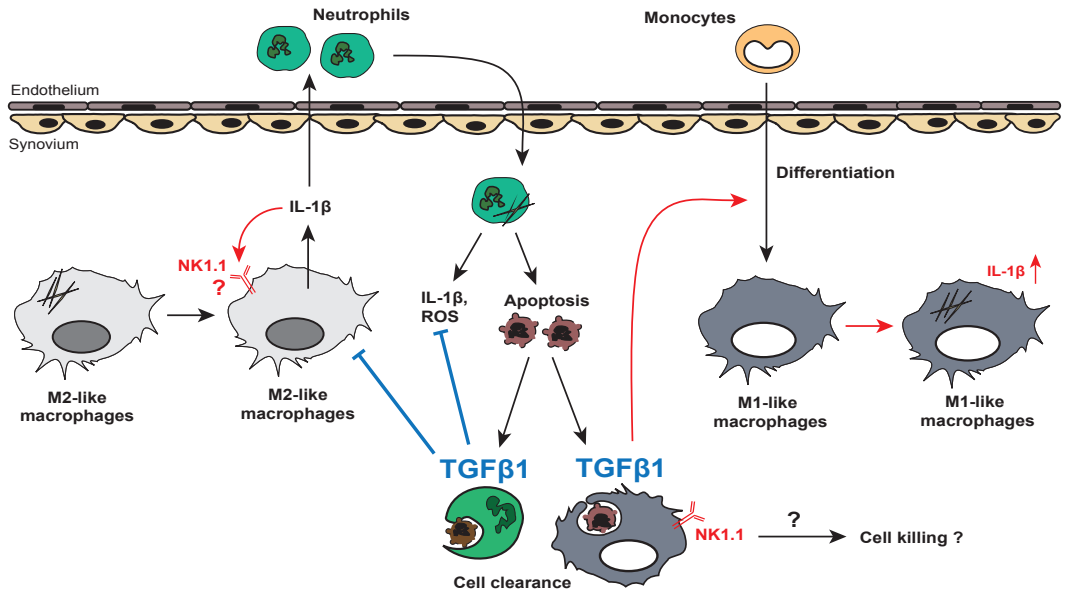

Figure 6.2: Model of acute gouty inflammation. Red arrows indicate enhanced responses or upregulation, and blue lines represent inhibitory or suppressive functions induced by TGFβ1. IL-1β = interleukin-1β; O_2^- = superoxide; TGFβ1 = transforming growth factor β1.

References

[1] **Nuki G and Simkin PA**. A concise history of gout and hyperuricemia and their treatment. *Arthritis Res Ther*, 8 Suppl 1:S1, 2006.

[2] **Wallace KL, Riedel AA, Joseph-Ridge N, and Wortmann R**. Increasing prevalence of gout and hyperuricemia over 10 years among older adults in a managed care population. *J Rheumatol*, 31(8):1582–7, 2004.

[3] **Helmick CG, Felson DT, Lawrence RC, Gabriel S, Hirsch R, Kwoh CK, Liang MH, Kremers HM, Mayes MD, Merkel PA, Pillemer SR, Reveille JD, Stone JH, and Workgroup NAD**. Estimates of the prevalence of arthritis and other rheumatic conditions in the United States. Part I. *Arthritis Rheum*, 58(1):15–25, 2008.

[4] **Lawrence RC, Felson DT, Helmick CG, Arnold LM, Choi H, Deyo RA, Gabriel S, Hirsch R, Hochberg MC, Hunder GG, Jordan JM, Katz JN, Kremers HM, Wolfe F, and Workgroup NAD**. Estimates of the prevalence of arthritis and other rheumatic conditions in the United States. Part II. *Arthritis Rheum*, 58(1):26–35, 2008.

[5] **Zhu Y, Pandya BJ, and Choi HK**. Prevalence of gout and hyperuricemia in the US general population: the National Health and Nutrition Examination Survey 2007-2008. *Arthritis Rheum*, 63(10):3136–41, 2011.

[6] **Harris CM, Lloyd DC, and Lewis J**. The prevalence and prophylaxis of gout in England. *J Clin Epidemiol*, 48(9):1153–8, 1995.

[7] **Karu LT, Bryant L, and Elley CR**. Maori experiences and perceptions of gout and its treatment: a kaupapa Maori qualitative study. *J Prim Health Care*, 5(3):214–22, 2013.

[8] **Klemp P, Stansfield SA, Castle B, and Robertson MC**. Gout is on the increase in New Zealand. *Ann Rheum Dis*, 56(1):22–6, 1997.

[9] **Winnard D, Kake T, Gow P, Barratt-Boyes C, Harris V, Hall DA, Mason H, Merriman T, Dalbeth N, and in Counties Manukau District Health Board MGAG**. Debunking the myths to provide 21st Century management of gout. *N Z Med J*, 121(1274):79–85, 2008.

[10] **Taylor W, Smeets L, Hall J, and McPherson K**. The burden of rheumatic disorders in general practice: consultation rates for rheumatic disease and the relationship to age, ethnicity, and small-area deprivation. *N Z Med J*, 117(1203):U1098, 2004.

[11] **Gibson T, Waterworth R, Hatfield P, Robinson G, and Bremner K**. Hyperuricaemia, gout and kidney function in New Zealand Maori men. *Br J Rheumatol*, 23(4):276–82, 1984.

[12] **Winnard D, Wright C, Taylor WJ, Jackson G, Karu LT, Gow PJ, Arroll B, Thornley S, Gribben B, and Dalbeth N**. National prevalence of gout derived from administrative health data in Aotearoa New Zealand. *Rheumatology (Oxford)*, 51(5):901–9, 2012.

[13] **Lindsay K, Gow P, Vanderpyl J, Logo P, and Dalbeth N**. The experience and impact of living with gout: a study of men with chronic gout using a qualitative grounded theory approach. *J Clin Rheumatol*, 17(1):1–6, 2011.

[14] **Faires J and McCarty D**. Acute arthritis in man and dog after intrasynovial injection of sodium urate crystals. *The Lancet*, 280(7258):682 – 685, 1962.

[15] **Pascual E**. Persistence of monosodium urate crystals and low-grade inflammation in the synovial fluid of patients with untreated gout. *Arthritis Rheum*, 34(2):141–5, 1991.

[16] **Pascual E and Jovaní V**. A quantitative study of the phagocytosis of urate crystals in the synovial fluid of asymptomatic joints of patients with gout. *Br J Rheumatol*, 34(8):724–6, 1995.

[17] **Wallace SL, Robinson H, Masi AT, Decker JL, McCarty DJ, and**

Yü TF. Preliminary criteria for the classification of the acute arthritis of primary gout. *Arthritis Rheum*, 20(3):895–900, 1977.

[18] **Kim KY, Schumacher HR, Hunsche E, Wertheimer AI, and Kong SX**. A literature review of the epidemiology and treatment of acute gout. *Clin Ther*, 25(6):1593–617, 2003.

[19] **Nakayama DA, Barthelemy C, Carrera G, Lightfoot RW, and Wortmann RL**. Tophaceous gout: a clinical and radiographic assessment. *Arthritis Rheum*, 27(4):468–71, 1984.

[20] **Punzi L, Scanu A, Ramonda R, and Oliviero F**. Gout as autoinflammatory disease: new mechanisms for more appropriated treatment targets. *Autoimmun Rev*, 12(1):66–71, 2012.

[21] **So A**. Developments in the scientific and clinical understanding of gout. *Arthritis Res Ther*, 10(5):221, 2008.

[22] **Wu XW, Muzny DM, Lee CC, and Caskey CT**. Two independent mutational events in the loss of urate oxidase during hominoid evolution. *J Mol Evol*, 34(1):78–84, 1992.

[23] **Dincer HE, Dincer AP, and Levinson DJ**. Asymptomatic hyperuricemia: to treat or not to treat. *Cleve Clin J Med*, 69(8):594, 597, 600–2 passim, 2002.

[24] **Campion EW, Glynn RJ, and DeLabry LO**. Asymptomatic hyperuricemia. Risks and consequences in the Normative Aging Study. *Am J Med*, 82(3):421–6, 1987.

[25] **Luk AJ and Simkin PA**. Epidemiology of hyperuricemia and gout. *Am J Manag Care*, 11(15 Suppl):S435–42; quiz S465–8, 2005.

[26] **Jordan KM, Cameron JS, Snaith M, Zhang W, Doherty M, Seckl J, Hingorani A, and et al**. British Society for Rheumatology and British Health Professionals in Rheumatology guideline for the management of gout. *Rheumatol*, 46(8):1372–4, 2007.

[27] **Mikuls TR, Farrar JT, Bilker WB, Fernandes S, Schumacher HR, and Saag KG**. Gout epidemiology: results from the UK General Practice Research Database, 1990-1999. *Annals of the Rheumatic Diseases*, 64(2):267–72, 2005.

[28] **Roubenoff R**. Gout and hyperuricemia. *Rheum Dis Clin North Am*, 16(3):539–50, 1990.

[29] **Hall AP, Barry PE, Dawber TR, and McNamara PM**. Epidemiology of gout and hyperuricemia. A long-term population study. *Am J Med*, 42(1):27–37, 1967.

[30] **Nicholls A, Snaith ML, and Scott JT**. Effect of oestrogen therapy on plasma and urinary levels of uric acid. *Br Med J*, 1(5851):449–51, 1973.

[31] **Hosoyamada M, Takiue Y, Shibasaki T, and Saito H**. The effect of testosterone upon the urate reabsorptive transport system in mouse kidney. *Nucleosides Nucleotides Nucleic Acids*, 29(7):574–9, 2010.

[32] **Basseville A and Bates SE**. Gout, genetics and ABC transporters. *F1000 Biol Rep*, 3:23, 2011.

[33] **Leonardis FD, Govoni M, Colina M, Bruschi M, and Trotta F**. Elderly-onset gout: a review. *Rheumatol Int*, 28(1):1–6, 2007.

[34] **Griebsch A and Zöllner N**. Effect of ribomononucleotides given orally on uric acid production in man. *Adv Exp Med Biol*, 41:443–9, 1974.

[35] **Villegas R, Xiang YB, Elasy T, Xu WH, Cai H, Cai Q, Linton MF, Fazio S, Zheng W, and Shu XO**. Purine-rich foods, protein intake, and the prevalence of hyperuricemia: the Shanghai Men's Health Study. *Nutr Metab Cardiovasc Dis*, 22(5):409–16, 2012.

[36] **Wang Y, Yan S, Li C, Zhao S, Lv J, Wang F, Meng D, Han L, Wang Y, and Miao Z**. Risk factors for gout developed from hyperuricemia

in China: a five-year prospective cohort study. *Rheumatology International*, 33(3):705–10, 2013.

[37] **Choi HK, Atkinson K, Karlson EW, Willett W, and Curhan G**. Alcohol intake and risk of incident gout in men: a prospective study. *Lancet*, 363(9417):1277–81, 2004.

[38] **Choi JWJ, Ford ES, Gao X, and Choi HK**. Sugar-sweetened soft drinks, diet soft drinks, and serum uric acid level: the Third National Health and Nutrition Examination Survey. *Arthritis Rheum*, 59(1):109–16, 2008.

[39] **Choi HK and Curhan G**. Soft drinks, fructose consumption, and the risk of gout in men: prospective cohort study. *BMJ*, 336(7639):309–12, 2008.

[40] **Lee SJ, Terkeltaub RA, and Kavanaugh A**. Recent developments in diet and gout. *Curr Opin Rheumatol*, 18(2):193–8, 2006.

[41] **Dalbeth N, Ames R, Gamble GD, Horne A, Wong S, Kuhn-Sherlock B, MacGibbon A, McQueen FM, Reid IR, and Palmano K**. Effects of skim milk powder enriched with glycomacropeptide and G600 milk fat extract on frequency of gout flares: a proof-of-concept randomised controlled trial. *Annals of the Rheumatic Diseases*, 71(6):929–34, 2012.

[42] **Ichida K, Hosoyamada M, Hisatome I, Enomoto A, Hikita M, Endou H, and Hosoya T**. Clinical and molecular analysis of patients with renal hypouricemia in Japan-influence of URAT1 gene on urinary urate excretion. *J Am Soc Nephrol*, 15(1):164–73, 2004.

[43] **Shima Y, Teruya K, and Ohta H**. Association between intronic SNP in urate-anion exchanger gene, SLC22A12, and serum uric acid levels in Japanese. *Life Sci*, 79(23):2234–7, 2006.

[44] **Enomoto A, Kimura H, Chairoungdua A, Shigeta Y, Jutabha P, Cha SH, Hosoyamada M, Takeda M, Sekine T, Igarashi T, Matsuo H, Kikuchi Y, Oda T, Ichida K, Hosoya T, Shimokata K, Niwa T,**

Kanai Y, and Endou H. Molecular identification of a renal urate anion exchanger that regulates blood urate levels. *Nature*, 417(6887):447–52, 2002.

[45] **Endou H and Anzai N**. Urate transport across the apical membrane of renal proximal tubules. *Nucleosides Nucleotides Nucleic Acids*, 27(6):578–84, 2008.

[46] **Li S, Sanna S, Maschio A, Busonero F, Usala G, Mulas A, Lai S, and et al**. The GLUT9 gene is associated with serum uric acid levels in Sardinia and Chianti cohorts. *PLoS Genet*, 3(11):e194, 2007.

[47] **Stark K, Reinhard W, Neureuther K, Wiedmann S, Sedlacek K, Baessler A, and et al**. Association of common polymorphisms in GLUT9 gene with gout but not with coronary artery disease in a large case-control study. *PLoS ONE*, 3(4):e1948, 2008.

[48] **Graessler J, Graessler A, Unger S, Kopprasch S, Tausche AK, Kuhlisch E, and Schroeder HE**. Association of the human urate transporter 1 with reduced renal uric acid excretion and hyperuricemia in a German Caucasian population. *Arthritis Rheum*, 54(1):292–300, 2006.

[49] **Köttgen A, Albrecht E, Teumer A, Vitart V, Krumsiek J, and Gieger C**. Genome-wide association analyses identify 18 new loci associated with serum urate concentrations. *Nat Genet*, 45(2):145–54, 2013.

[50] **Schumacher HR, Boice JA, Daikh DI, Mukhopadhyay S, Malmstrom K, Ng J, Tate GA, and Molina J**. Randomised double blind trial of etoricoxib and indometacin in treatment of acute gouty arthritis. *BMJ*, 324(7352):1488–92, 2002.

[51] **Rubin BR, Burton R, Navarra S, Antigua J, Londoño J, Pryhuber KG, Lund M, Chen E, Najarian DK, Petruschke RA, Ozturk ZE, and Geba GP**. Efficacy and safety profile of treatment with etoricoxib 120

mg once daily compared with indomethacin 50 mg three times daily in acute gout: a randomized controlled trial. *Arthritis Rheum*, 50(2):598–606, 2004.

[52] **Alloway JA, Moriarty MJ, Hoogland YT, and Nashel DJ**. Comparison of triamcinolone acetonide with indomethacin in the treatment of acute gouty arthritis. *J Rheumatol*, 20(1):111–3, 1993.

[53] **Graham DJ, Campen D, Hui R, Spence M, Cheetham C, Levy G, Shoor S, and Ray WA**. Risk of acute myocardial infarction and sudden cardiac death in patients treated with cyclo-oxygenase 2 selective and non-selective non-steroidal anti-inflammatory drugs: nested case-control study. *Lancet*, 365(9458):475–81, 2005.

[54] **Groff GD, Franck WA, and Raddatz DA**. Systemic steroid therapy for acute gout: a clinical trial and review of the literature. *Semin Arthritis Rheum*, 19(6):329–36, 1990.

[55] **Cattermole GN, Man CY, Cheng CH, Graham CA, and Rainer TH**. Oral prednisolone is more cost-effective than oral indomethacin for treating patients with acute gout-like arthritis. *Eur J Emerg Med*, 16(5):261–6, 2009.

[56] **Man CY, Cheung ITF, Cameron PA, and Rainer TH**. Comparison of oral prednisolone/paracetamol and oral indomethacin/paracetamol combination therapy in the treatment of acute goutlike arthritis: a double-blind, randomized, controlled trial. *Ann Emerg Med*, 49(5):670–7, 2007.

[57] **Janssens HJEM, Janssen M, van de Lisdonk EH, van Riel PLCM, and van Weel C**. Use of oral prednisolone or naproxen for the treatment of gout arthritis: a double-blind, randomised equivalence trial. *Lancet*, 371(9627):1854–60, 2008.

[58] **Scott P, Ma H, Viriyakosol S, Terkeltaub R, and Liu-Bryan R**. Engagement of CD14 mediates the inflammatory potential of monosodium urate crystals. *J Immunol*, 177(9):6370–8, 2006.

[59] **Cronstein BN, Molad Y, Reibman J, Balakhane E, Levin RI, and Weissmann G**. Colchicine alters the quantitative and qualitative display of selectins on endothelial cells and neutrophils. *J Clin Invest*, 96(2):994–1002, 1995.

[60] **Bhat A, Naguwa SM, Cheema GS, and Gershwin ME**. Colchicine revisited. *Ann N Y Acad Sci*, 1173:766–73, 2009.

[61] **Martinon F, Pétrilli V, Mayor A, and Tardivel A**. Gout-associated uric acid crystals activate the NALP3 inflammasome. *Nature*, 2006.

[62] **di Giovine FS, Malawista SE, Nuki G, and Duff GW**. Interleukin 1 (IL 1) as a mediator of crystal arthritis. Stimulation of T cell and synovial fibroblast mitogenesis by urate crystal-induced IL 1. *J Immunol*, 138(10):3213–8, 1987.

[63] **Bonnel RA, Villalba ML, Karwoski CB, and Beitz J**. Deaths associated with inappropriate intravenous colchicine administration. *J Emerg Med*, 22(4):385–7, 2002.

[64] **Sussman JS, Brozena SC, Skop N, Korecka M, and Shaw LM**. Accidental intravenous colchicine poisoning. *Ther Drug Monit*, 26(6):688–92, 2004.

[65] **Terkeltaub RA, Furst DE, Bennett K, Kook KA, Crockett RS, and Davis MW**. High versus low dosing of oral colchicine for early acute gout flare: Twenty-four-hour outcome of the first multicenter, randomized, double-blind, placebo-controlled, parallel-group, dose-comparison colchicine study. *Arthritis Rheum*, 62(4):1060–8, 2010.

[66] **Schlesinger N, Alten RE, Bardin T, Schumacher HR, Bloch M, Gimona A, Krammer G, Murphy V, Richard D, and So AK**. Canakinumab for acute gouty arthritis in patients with limited treatment options: results from two randomised, multicentre, active-controlled, double-

blind trials and their initial extensions. *Ann Rheum Dis*, 71(11):1839–48, 2012.

[67] **So A, Smedt TD, Revaz S, and Tschopp J**. A pilot study of IL-1 inhibition by anakinra in acute gout. *Arthritis Res Ther*, 9(2):R28, 2007.

[68] **So A, Meulemeester MD, Pikhlak A, Yücel AE, Richard D, Murphy V, Arulmani U, and et al**. Canakinumab for the treatment of acute flares in difficult-to-treat gouty arthritis: Results of a multicenter, phase II, dose-ranging study. *Arthritis Rheum*, 62(10):3064–76, 2010.

[69] **Zhang W, Doherty M, Bardin T, Pascual E, Barskova V, Conaghan P, Gerster J, and et al**. EULAR evidence based recommendations for gout. Part II: Management. Report of a task force of the EULAR Standing Committee for International Clinical Studies Including Therapeutics (ESCISIT). *Ann Rheum Dis*, 65(10):1312–24, 2006.

[70] **Becker MA, Schumacher HR, Wortmann RL, MacDonald PA, Eustace D, Palo WA, Streit J, and et al**. Febuxostat compared with allopurinol in patients with hyperuricemia and gout. *N Engl J Med*, 353(23):2450–61, 2005.

[71] **Garay RP, El-Gewely MR, Labaune JP, and Richette P**. Therapeutic perspectives on uricases for gout. *Joint Bone Spine*, 79(3):237–42, 2012.

[72] **Jordan KM**. Up-to-date management of gout. *Curr Opin Rheumatol*, 24(2):145–51, 2012.

[73] **Martinon F**. Mechanisms of uric acid crystal-mediated autoinflammation. *Immunol Rev*, 233(1):218–32, 2010.

[74] **di Giovine FS, Malawista SE, Thornton E, and Duff GW**. Urate crystals stimulate production of tumor necrosis factor alpha from human blood monocytes and synovial cells. Cytokine mRNA and protein kinetics, and cellular distribution. *J Clin Invest*, 87(4):1375–81, 1991.

[75] **Getting SJ, Flower RJ, Parente L, de Medicis R, Lussier A, Woliztky BA, Martins MA, and Perretti M**. Molecular determinants of monosodium urate crystal-induced murine peritonitis: a role for endogenous mast cells and a distinct requirement for endothelial-derived selectins. *J Pharmacol Exp Ther*, 283(1):123–30, 1997.

[76] **Guerne PA, Terkeltaub R, Zuraw B, and Lotz M**. Inflammatory microcrystals stimulate interleukin-6 production and secretion by human monocytes and synoviocytes. *Arthritis Rheum*, 32(11):1443–52, 1989.

[77] **Fields TR, Abramson SB, Weissmann G, Kaplan AP, and Ghebrehiwet B**. Activation of the alternative pathway of complement by monosodium urate crystals. *Clin Immunol Immunopath*, 26(2):249–57, 1983.

[78] **Tramontini N, Huber C, Liu-Bryan R, Terkeltaub RA, and Kilgore KS**. Central role of complement membrane attack complex in monosodium urate crystal-induced neutrophilic rabbit knee synovitis. *Arthritis Rheum*, 50(8):2633–9, 2004.

[79] **Naff GB and Byers PH**. Complement as a mediator of inflammation in acute gouty arthritis. I. Studies on the reaction between human serum complement and sodium urate crystals. *J Lab Clin Med*, 81(5):747–60, 1973.

[80] **Russell IJ, Mansen C, Kolb LM, and Kolb WP**. Activation of the fifth component of human complement (C5) induced by monosodium urate crystals: C5 convertase assembly on the crystal surface. *Clin Immunol Immunopath*, 24(2):239–50, 1982.

[81] **Ryckman C, McColl SR, Vandal K, de Médicis R, Lussier A, Poubelle PE, and Tessier PA**. Role of S100A8 and S100A9 in neutrophil recruitment in response to monosodium urate monohydrate crystals in the air-pouch model of acute gouty arthritis. *Arthritis Rheum*, 48(8):2310–20, 2003.

[82] **Abramson S, Hoffstein ST, and Weissmann G**. Superoxide anion generation by human neutrophils exposed to monosodium urate. *Arthritis Rheum*, 25(2):174–80, 1982.

[83] **Empson VG, McQueen FM, and Dalbeth N**. The natural killer cell: a further innate mediator of gouty inflammation? *Immunol Cell Biol*, 88(1):24–31, 2010.

[84] **Dalbeth N and Callan MFC**. A subset of natural killer cells is greatly expanded within inflamed joints. *Arthritis Rheum*, 46(7):1763–72, 2002.

[85] **Dalbeth N, Gundle R, Davies RJO, Lee YCG, McMichael AJ, and Callan MFC**. CD56bright NK cells are enriched at inflammatory sites and can engage with monocytes in a reciprocal program of activation. *J Immunol*, 173(10):6418–26, 2004.

[86] **Akira S, Takeda K, and Kaisho T**. Toll-like receptors: critical proteins linking innate and acquired immunity. *Nat Immunol*, 2(8):675–80, 2001.

[87] **Matzinger P**. Tolerance, danger, and the extended family. *Ann Rev Immunol*, 12:991–1045, 1994.

[88] **Shi Y, Evans JE, and Rock KL**. Molecular identification of a danger signal that alerts the immune system to dying cells. *Nature*, 425(6957):516–21, 2003.

[89] **Ganesh BB, Bhattacharya P, Gopisetty A, Sheng J, Vasu C, and Prabhakar BS**. IL-1 promotes TGF-1 and IL-2 dependent Foxp3 expression in regulatory T cells. *PLoS ONE*, 6(7):e21949, 2011.

[90] **Sakamaki I, Inai K, Tsutani Y, Ueda T, and Tsutani H**. Binding of monosodium urate crystals with idiotype protein efficiently promote dendritic cells to induce cytotoxic T cells. *Cancer Sci*, 99(11):2268–73, 2008.

[91] **Hu DE, Moore AM, Thomsen LL, and Brindle KM**. Uric acid promotes tumor immune rejection. *Cancer Res*, 64(15):5059–62, 2004.

[92] **Kuhn S, Hyde EJ, Yang J, Rich FJ, Harper JL, Kirman JR, and Ronchese F**. Increased numbers of monocyte-derived dendritic cells during successful tumor immunotherapy with immune-activating agents. *J Immunol*, 191(4):1984–92, 2013.

[93] **PEKIN TJ and ZVAIFLER NJ**. HEMOLYTIC COMPLEMENT IN SYNOVIAL FLUID. *J Clin Invest*, 43:1372–82, 1964.

[94] **Giclas PC, Ginsberg MH, and Cooper NR**. Immunoglobulin G independent activation of the classical complement pathway by monosodium urate crystals. *J Clin Invest*, 63(4):759–64, 1979.

[95] **Hasselbacher P**. Immunoelectrophoretic assay for synovial fluid C3 with correction for synovial fluid globulin. *Arthritis Rheum*, 22(3):243–50, 1979.

[96] **Liu-Bryan R, Scott P, Sydlaske A, Rose DM, and Terkeltaub R**. Innate immunity conferred by Toll-like receptors 2 and 4 and myeloid differentiation factor 88 expression is pivotal to monosodium urate monohydrate crystal-induced inflammation. *Arthritis Rheum*, 52(9):2936–46, 2005.

[97] **Chen CJ, Shi Y, Hearn A, Fitzgerald K, Golenbock D, Reed G, Akira S, and Rock KL**. MyD88-dependent IL-1 receptor signaling is essential for gouty inflammation stimulated by monosodium urate crystals. *J Clin Invest*, 116(8):2262–71, 2006.

[98] **Terkeltaub R, Baird S, Sears P, Santiago R, and Boisvert W**. The murine homolog of the interleukin-8 receptor CXCR-2 is essential for the occurrence of neutrophilic inflammation in the air pouch model of acute urate crystal-induced gouty synovitis. *Arthritis Rheum*, 41(5):900–9, 1998.

[99] **Lee J, Cacalano G, Camerato T, Toy K, Moore MW, and Wood WI**. Chemokine binding and activities mediated by the mouse IL-8 receptor. *J Immunol*, 155(4):2158–64, 1995.

[100] **Hachicha M, Naccache PH, and McColl SR**. Inflammatory microcrystals

differentially regulate the secretion of macrophage inflammatory protein 1 and interleukin 8 by human neutrophils: a possible mechanism of neutrophil recruitment to sites of inflammation in synovitis. *J Exp Med*, 182(6):2019–25, 1995.

[101] **Burt HM and Jackson JK**. The priming action of tumour necrosis factor-alpha (TNF-alpha) and granulocyte-macrophage colony-stimulating factor (GM-CSF) on neutrophils activated by inflammatory microcrystals. *Clin Exp Immunol*, 108(3):432–7, 1997.

[102] **Chapman PT, Yarwood H, Harrison AA, Stocker CJ, Jamar F, Gundel RH, Peters AM, and Haskard DO**. Endothelial activation in monosodium urate monohydrate crystal-induced inflammation: in vitro and in vivo studies on the roles of tumor necrosis factor alpha and interleukin-1. *Arthritis Rheum*, 40(5):955–65, 1997.

[103] **Martin WJ, Walton M, and Harper J**. Resident macrophages initiating and driving inflammation in a monosodium urate monohydrate crystal-induced murine peritoneal model of acute gout. *Arthritis Rheum*, 60(1):281–9, 2009.

[104] **Matsukawa A, Miyazaki S, Maeda T, Tanase S, Feng L, Ohkawara S, Yoshinaga M, and Yoshimura T**. Production and regulation of monocyte chemoattractant protein-1 in lipopolysaccharide- or monosodium urate crystal-induced arthritis in rabbits: roles of tumor necrosis factor alpha, interleukin-1, and interleukin-8. *Lab Invest*, 78(8):973–85, 1998.

[105] **Serbina NV and Pamer EG**. Monocyte emigration from bone marrow during bacterial infection requires signals mediated by chemokine receptor CCR2. *Nat Immunol*, 7(3):311–7, 2006.

[106] **Pétrilli V and Martinon F**. The inflammasome, autoinflammatory diseases, and gout. *Joint Bone Spine*, 74(6):571–6, 2007.

[107] **Martinon F, Burns K, and Tschopp J**. The inflammasome: a molecular platform triggering activation of inflammatory caspases and processing of proIL-beta. *Molecular cell*, 10(2):417–26, 2002.

[108] **Mariathasan S, Newton K, Monack DM, Vucic D, French DM, Lee WP, Roose-Girma M, and et al**. Differential activation of the inflammasome by caspase-1 adaptors ASC and Ipaf. *Nature*, 430(6996):213–8, 2004.

[109] **Uhl J, Newton RC, Giri JG, Sandlin G, and Horuk R**. Identification of IL-1 receptors on human monocytes. *J Immunol*, 142(5):1576–81, 1989.

[110] **Parker KP, Benjamin WR, Kaffka KL, and Kilian PL**. Presence of IL-1 receptors on human and murine neutrophils. Relevance to IL-1-mediated effects in inflammation. *J Immunol*, 142(2):537–42, 1989.

[111] **Mitroulis I, Skendros P, and Ritis K**. Targeting IL-1beta in disease; the expanding role of NLRP3 inflammasome. *Eur J Intern Med*, 21(3):157–63, 2010.

[112] **Masters SL, Simon A, Aksentijevich I, and Kastner DL**. Horror autoinflammaticus: the molecular pathophysiology of autoinflammatory disease (*). *Ann Rev Immunol*, 27:621–68, 2009.

[113] **ATHENS JW, HAAB OP, RAAB SO, MAUER AM, ASHENBRUCKER H, CARTWRIGHT GE, and WINTROBE MM**. Leukokinetic studies. IV. The total blood, circulating and marginal granulocyte pools and the granulocyte turnover rate in normal subjects. *J Clin Invest*, 40:989–95, 1961.

[114] **Dancey JT, Deubelbeiss KA, Harker LA, and Finch CA**. Neutrophil kinetics in man. *J Clin Invest*, 58(3):705–15, 1976.

[115] **Shi J, Gilbert GE, Kokubo Y, and Ohashi T**. Role of the liver in regulating numbers of circulating neutrophils. *Blood*, 98(4):1226–30, 2001.

[116] **Nathan C**. Neutrophils and immunity: challenges and opportunities. *Nat Rev Immunol*, 6(3):173–82, 2006.

[117] **Amulic B, Cazalet C, Hayes GL, Metzler KD, and Zychlinsky A**. Neutrophil function: from mechanisms to disease. *Ann Rev Immunol*, 30:459–89, 2012.

[118] **Cassatella MA**. The production of cytokines by polymorphonuclear neutrophils. *Immunol Today*, 16(1):21–6, 1995.

[119] **Fuchs TA, Abed U, Goosmann C, Hurwitz R, Schulze I, Wahn V, Weinrauch Y, and et al**. Novel cell death program leads to neutrophil extracellular traps. *J Cell Biol*, 176(2):231–41, 2007.

[120] **Brinkmann V, Reichard U, Goosmann C, Fauler B, Uhlemann Y, Weiss DS, Weinrauch Y, and Zychlinsky A**. Neutrophil extracellular traps kill bacteria. *Science*, 303(5663):1532–5, 2004.

[121] **Hornung V, Bauernfeind F, Halle A, Samstad EO, Kono H, Rock KL, Fitzgerald KA, and Latz E**. Silica crystals and aluminum salts activate the NALP3 inflammasome through phagosomal destabilization. *Nat Immunol*, 9(8):847–56, 2008.

[122] **Chapman PT, Jamar F, Harrison AA, Binns RM, Peters AM, and Haskard DO**. Noninvasive imaging of E-selectin expression by activated endothelium in urate crystal-induced arthritis. *Arthritis Rheum*, 37(12):1752–6, 1994.

[123] **Chapman PT, Jamar F, Harrison AA, Schofield JB, Peters AM, Binns RM, and Haskard DO**. Characterization of E-selectin expression, leucocyte traffic and clinical sequelae in urate crystal-induced inflammation: an insight into gout. *Br J Rheumatol*, 35(4):323–34, 1996.

[124] **Barabé F, Gilbert C, Liao N, Bourgoin SG, and Naccache PH**. Crystal-induced neutrophil activation VI. Involvment of FcgammaRIIIB

(CD16) and CD11b in response to inflammatory microcrystals. *FASEB J*, 12(2):209–20, 1998.

[125] **Popa-Nita O, Marois L, Paré G, and Naccache PH**. Crystal-induced neutrophil activation: X. Proinflammatory role of the tyrosine kinase Tec. *Arthritis Rheum*, 58(6):1866–76, 2008.

[126] **Popa-Nita O, Proulx S, Paré G, Rollet-Labelle E, and Naccache PH**. Crystal-induced neutrophil activation: XI. Implication and novel roles of classical protein kinase C. *J Immunol*, 183(3):2104–14, 2009.

[127] **Popa-Nita O, Rollet-Labelle E, Thibault N, Gilbert C, Bourgoin SG, and Naccache PH**. Crystal-induced neutrophil activation. IX. Syk-dependent activation of class Ia phosphatidylinositol 3-kinase. *J Leuk Biol*, 82(3):763–73, 2007.

[128] **Desaulniers P, Fernandes M, Gilbert C, Bourgoin SG, and Naccache PH**. Crystal-induced neutrophil activation. VII. Involvement of Syk in the responses to monosodium urate crystals. *J Leuk Biol*, 70(4):659–68, 2001.

[129] **Weiss SJ**. Tissue destruction by neutrophils. *N Engl J Med*, 320(6):365–76, 1989.

[130] **Mitroulis I, Kambas K, Chrysanthopoulou A, Skendros P, Apostolidou E, Kourtzelis I, Drosos GI, and et al**. Neutrophil extracellular trap formation is associated with IL-1 and autophagy-related signaling in gout. *PLoS ONE*, 6(12):e29318, 2011.

[131] **Schorn C, Janko C, Krenn V, Zhao Y, Munoz LE, Schett G, and Herrmann M**. Bonding the foe - NETting neutrophils immobilize the pro-inflammatory monosodium urate crystals. *Front Immunol*, 3:376, 2012.

[132] **Akgul C, Moulding DA, and Edwards SW**. Molecular control of neutrophil apoptosis. *FEBS Lett*, 487(3):318–22, 2001.

[133] **Shirahama T and Cohen AS**. Ultrastructural evidence for leakage of lyso-

somal contents after phagocytosis of monosodium urate crystals. A mechanism of gouty inflammation. *Am J Pathol*, 76(3):501–20, 1974.

[134] **Gordon S**. The macrophage: past, present and future. *Eur J Immunol*, 37 Suppl 1:S9–17, 2007.

[135] **Geissmann F, Jung S, and Littman DR**. Blood monocytes consist of two principal subsets with distinct migratory properties. *Immunity*, 19(1):71–82, 2003.

[136] **Yagnik DR, Hillyer P, Marshall D, Smythe CD, Krausz T, Haskard DO, and Landis RC**. Noninflammatory phagocytosis of monosodium urate monohydrate crystals by mouse macrophages. Implications for the control of joint inflammation in gout. *Arthritis Rheum*, 43(8):1779–89, 2000.

[137] **Landis RC, Yagnik DR, Florey O, Philippidis P, Emons V, Mason JC, and Haskard DO**. Safe disposal of inflammatory monosodium urate monohydrate crystals by differentiated macrophages. *Arthritis Rheum*, 46(11):3026–33, 2002.

[138] **Yagnik DR, Evans BJ, Florey O, Mason JC, Landis RC, and Haskard DO**. Macrophage release of transforming growth factor beta1 during resolution of monosodium urate monohydrate crystal-induced inflammation. *Arthritis Rheum*, 50(7):2273–80, 2004.

[139] **Warren MK and Vogel SN**. Bone marrow-derived macrophages: development and regulation of differentiation markers by colony-stimulating factor and interferons. *J Immunol*, 134(2):982–9, 1985.

[140] **Verreck FAW, de Boer T, Langenberg DML, Hoeve MA, Kramer M, Vaisberg E, Kastelein R, and et al**. Human IL-23-producing type 1 macrophages promote but IL-10-producing type 2 macrophages subvert immunity to (myco)bacteria. *Proc Natl Acad Sci USA*, 101(13):4560–5, 2004.

[141] **Verreck FAW, de Boer T, Langenberg DML, van der Zanden L,**

and Ottenhoff THM. Phenotypic and functional profiling of human proinflammatory type-1 and anti-inflammatory type-2 macrophages in response to microbial antigens and IFN-gamma- and CD40L-mediated costimulation. *J Leuk Biol*, 79(2):285–93, 2006.

[142] **Smith W, Feldmann M, and Londei M**. Human macrophages induced in vitro by macrophage colony-stimulating factor are deficient in IL-12 production. *Eur J Immunol*, 28(8):2498–507, 1998.

[143] **Zhou LJ and Tedder TF**. CD14+ blood monocytes can differentiate into functionally mature CD83+ dendritic cells. *PNAS*, 93(6):2588–92, 1996.

[144] **Udagawa N, Takahashi N, Akatsu T, Tanaka H, Sasaki T, Nishihara T, Koga T, Martin TJ, and Suda T**. Origin of osteoclasts: mature monocytes and macrophages are capable of differentiating into osteoclasts under a suitable microenvironment prepared by bone marrow-derived stromal cells. *PNAS*, 87(18):7260–4, 1990.

[145] **Mantovani A, Sozzani S, Locati M, Allavena P, and Sica A**. Macrophage polarization: tumor-associated macrophages as a paradigm for polarized M2 mononuclear phagocytes. *Trends Immunol*, 23(11):549–55, 2002.

[146] **Allavena P, Sica A, Vecchi A, Locati M, Sozzani S, and Mantovani A**. The chemokine receptor switch paradigm and dendritic cell migration: its significance in tumor tissues. *Immunol Rev*, 177:141–9, 2000.

[147] **Gordon S and Taylor PR**. Monocyte and macrophage heterogeneity. *Nat Rev Immunol*, 5(12):953–64, 2005.

[148] **Edwards JP, Zhang X, Frauwirth KA, and Mosser DM**. Biochemical and functional characterization of three activated macrophage populations. *J Leuk Biol*, 80(6):1298–307, 2006.

[149] **Martin WJ, Shaw O, Liu X, Steiger S, and Harper JL**. Monosodium urate monohydrate crystal-recruited noninflammatory monocytes differentiate

into M1-like proinflammatory macrophages in a peritoneal murine model of gout. *Arthritis Rheum*, 63(5):1322–32, 2011.

[150] **Leenen PJM and Campbell P**. Heterogeneity of mononuclear phagocytes. *Blood Cell Biochem*, 5:pp 29–85, 1993.

[151] **Sasmono RT, Oceandy D, Pollard JW, Tong W, Pavli P, Wainwright BJ, Ostrowski MC, and et al**. A macrophage colony-stimulating factor receptor-green fluorescent protein transgene is expressed throughout the mononuclear phagocyte system of the mouse. *Blood*, 101(3):1155–63, 2003.

[152] **Hume DA and Gordon S**. Mononuclear phagocyte system of the mouse defined by immunohistochemical localization of antigen F4/80. Identification of resident macrophages in renal medullary and cortical interstitium and the juxtaglomerular complex. *J Exp Med*, 157(5):1704–9, 1983.

[153] **Murakami Y, Akahoshi T, Hayashi I, Endo H, Kawai S, Inoue M, Kondo H, and Kitasato H**. Induction of triggering receptor expressed on myeloid cells 1 in murine resident peritoneal macrophages by monosodium urate monohydrate crystals. *Arthritis Rheum*, 54(2):455–62, 2006.

[154] **Jaramillo M, Naccache PH, and Olivier M**. Monosodium urate crystals synergize with IFN-gamma to generate macrophage nitric oxide: involvement of extracellular signal-regulated kinase 1/2 and NF-kappa B. *J Immunol*, 172(9):5734–42, 2004.

[155] **Jaramillo M, Godbout M, Naccache PH, and Olivier M**. Signaling events involved in macrophage chemokine expression in response to monosodium urate crystals. *J Biol Chem*, 279(50):52797–805, 2004.

[156] **Kozin F, Ginsberg MH, and Skosey JL**. Polymorphonuclear leukocyte responses to monosodium urate crystals: modification by adsorbed serum proteins. *J Rheumatol*, 6(5):519–26, 1979.

[157] **Cherian PV and Schumacher HR**. Immunochemical and ultrastructural

characterization of serum proteins associated with monosodium urate crystals (MSU) in synovial fluid cells from patients with gout. *Ultrastruct Pathol*, 10(3):209–19, 1986.

[158] **Rosen MS, Baker DG, Schumacher HR, and Cherian PV**. Products of polymorphonuclear cell injury inhibit IgG enhancement of monosodium urate-induced superoxide production. *Arthritis Rheum*, 29(12):1473–9, 1986.

[159] **Terkeltaub R, Martin J, Curtiss LK, and Ginsberg MH**. Apolipoprotein B mediates the capacity of low density lipoprotein to suppress neutrophil stimulation by particulates. *J Biol Chem*, 261(33):15662–7, 1986.

[160] **Terkeltaub RA, Dyer CA, Martin J, and Curtiss LK**. Apolipoprotein (apo) E inhibits the capacity of monosodium urate crystals to stimulate neutrophils. Characterization of intraarticular apo E and demonstration of apo E binding to urate crystals in vivo. *J Clin Invest*, 87(1):20–6, 1991.

[161] **Lioté F, Prudhommeaux F, Schiltz C, Champy R, Herbelin A, Ortiz-Bravo E, and Bardin T**. Inhibition and prevention of monosodium urate monohydrate crystal-induced acute inflammation in vivo by transforming growth factor beta1. *Arthritis Rheum*, 39(7):1192–8, 1996.

[162] **Bannenberg GL, Chiang N, Ariel A, Arita M, Tjonahen E, Gotlinger KH, Hong S, and Serhan CN**. Molecular circuits of resolution: formation and actions of resolvins and protectins. *J Immunol*, 174(7):4345–55, 2005.

[163] **Zhang MJ and Spite M**. Resolvins: anti-inflammatory and proresolving mediators derived from omega-3 polyunsaturated fatty acids. *Annu Rev Nutr*, 32:203–27, 2012.

[164] **Fritsche K**. Fatty acids as modulators of the immune response. *Annu Rev Nutr*, 26:45–73, 2006.

[165] **Yan Y, Jiang W, Spinetti T, Tardivel A, Castillo R, Bourquin C, Guarda G, and et al**. Omega-3 fatty acids prevent inflammation and

metabolic disorder through inhibition of NLRP3 inflammasome activation. *Immunity*, 38(6):1154–63, 2013.

[166] **Dubois CM, Ruscetti FW, Palaszynski EW, Falk LA, Oppenheim JJ, and Keller JR**. Transforming growth factor beta is a potent inhibitor of interleukin 1 (IL-1) receptor expression: proposed mechanism of inhibition of IL-1 action. *J Exp Med*, 172(3):737–44, 1990.

[167] **Rédini F, Mauviel A, Pronost S, Loyau G, and Pujol JP**. Transforming growth factor beta exerts opposite effects from interleukin-1 beta on cultured rabbit articular chondrocytes through reduction of interleukin-1 receptor expression. *Arthritis Rheum*, 36(1):44–50, 1993.

[168] **Furst DE**. Anakinra: review of recombinant human interleukin-I receptor antagonist in the treatment of rheumatoid arthritis. *Clin Ther*, 26(12):1960–75, 2004.

[169] **Schiff MH**. Role of interleukin 1 and interleukin 1 receptor antagonist in the mediation of rheumatoid arthritis. *Ann Rheum Dis*, 59 Suppl 1:i103–8, 2000.

[170] **Seckinger P, Klein-Nulend J, Alander C, Thompson RC, Dayer JM, and Raisz LG**. Natural and recombinant human IL-1 receptor antagonists block the effects of IL-1 on bone resorption and prostaglandin production. *J Immunol*, 145(12):4181–4, 1990.

[171] **McColl SR, Paquin R, Ménard C, and Beaulieu AD**. Human neutrophils produce high levels of the interleukin 1 receptor antagonist in response to granulocyte/macrophage colony-stimulating factor and tumor necrosis factor alpha. *J Exp Med*, 176(2):593–8, 1992.

[172] **Ulich TR, Yin SM, Guo KZ, del Castillo J, Eisenberg SP, and Thompson RC**. The intratracheal administration of endotoxin and cytokines. III. The interleukin-1 (IL-1) receptor antagonist inhibits endotoxin- and IL-1-induced acute inflammation. *Am J Pathol*, 138(3):521–4, 1991.

[173] **Chen YH, Hsieh SC, Chen WY, Li KJ, Wu CH, Wu PC, Tsai CY, and et al**. Spontaneous resolution of acute gouty arthritis is associated with rapid induction of the anti-inflammatory factors TGF1, IL-10 and soluble TNF receptors and the intracellular cytokine negative regulators CIS and SOCS3. *Ann Rheum Dis*, 70(9):1655–63, 2011.

[174] **Turner M, Chantry D, Katsikis P, Berger A, Brennan FM, and Feldmann M**. Induction of the interleukin 1 receptor antagonist protein by transforming growth factor-beta. *Eur J Immunol*, 21(7):1635–9, 1991.

[175] **Wahl SM, Costa GL, Corcoran M, Wahl LM, and Berger AE**. Transforming growth factor-beta mediates IL-1-dependent induction of IL-1 receptor antagonist. *J Immunol*, 150(8 Pt 1):3553–60, 1993.

[176] **Roberge CJ, de Médicis R, Dayer JM, Rola-Pleszczynski M, Naccache PH, and Poubelle PE**. Crystal-induced neutrophil activation. V. Differential production of biologically active IL-1 and IL-1 receptor antagonist. *J Immunol*, 152(11):5485–94, 1994.

[177] **Terkeltaub R, Sundy JS, Schumacher HR, Murphy F, Bookbinder S, Biedermann S, Wu R, Mellis S, and Radin A**. The interleukin 1 inhibitor rilonacept in treatment of chronic gouty arthritis: results of a placebo-controlled, monosequence crossover, non-randomised, single-blind pilot study. *Ann Rheum Dis*, 68(10):1613–7, 2009.

[178] **Gratton SB, Scalapino KJ, and Fye KH**. Case of anakinra as a steroid-sparing agent for gout inflammation. *Arthritis Rheum*, 61(9):1268–70, 2009.

[179] **Yoshimura A, Nishinakamura H, Matsumura Y, and Hanada T**. Negative regulation of cytokine signaling and immune responses by SOCS proteins. *Arthritis Res Ther*, 7(3):100–10, 2005.

[180] **Kennedy AD and DeLeo FR**. Neutrophil apoptosis and the resolution of infection. *Immunol Res*, 43(1-3):25–61, 2009.

[181] **Witko-Sarsat V, Pederzoli-Ribeil M, Hirsch E, Hirsh E, Sozzani S, and Cassatella MA**. Regulating neutrophil apoptosis: new players enter the game. *Trends Immunol*, 32(3):117–24, 2011.

[182] **Savill JS, Wyllie AH, Henson JE, Walport MJ, Henson PM, and Haslett C**. Macrophage phagocytosis of aging neutrophils in inflammation. Programmed cell death in the neutrophil leads to its recognition by macrophages. *J Clin Invest*, 83(3):865–75, 1989.

[183] **Fadok VA, Bratton DL, Konowal A, Freed PW, Westcott JY, and Henson PM**. Macrophages that have ingested apoptotic cells in vitro inhibit proinflammatory cytokine production through autocrine/paracrine mechanisms involving TGF-beta, PGE2, and PAF. *J Clin Invest*, 101(4):890–8, 1998.

[184] **Rose DM, Sydlaske AD, Agha-Babakhani A, Johnson K, and Terkeltaub R**. Transglutaminase 2 limits murine peritoneal acute gout-like inflammation by regulating macrophage clearance of apoptotic neutrophils. *Arthritis Rheum*, 54(10):3363–71, 2006.

[185] **Fava R, Olsen N, Keski-Oja J, Moses H, and Pincus T**. Active and latent forms of transforming growth factor beta activity in synovial effusions. *J Exp Med*, 169(1):291–6, 1989.

[186] **Scanu A, Oliviero F, Ramonda R, Frallonardo P, Dayer JM, and Punzi L**. Cytokine levels in human synovial fluid during the different stages of acute gout: role of transforming growth factor 1 in the resolution phase. *Ann Rheum Dis*, 71(4):621–4, 2012.

[187] **Chang SJ, Chen CJ, Tsai FC, Lai HM, Tsai PC, Tsai MH, and Ko YC**. Associations between gout tophus and polymorphisms 869T/C and -509C/T in transforming growth factor beta1 gene. *Rheumatol*, 47(5):617–21, 2008.

[188] **Ren Y and Savill J**. Proinflammatory cytokines potentiate thrombospondin-mediated phagocytosis of neutrophils undergoing apoptosis. *J Immunol*, 154(5):2366–74, 1995.

[189] **Schiltz C, Lioté F, Prudhommeaux F, Meunier A, Champy R, Callebert J, and Bardin T**. Monosodium urate monohydrate crystal-induced inflammation in vivo: quantitative histomorphometric analysis of cellular events. *Arthritis Rheum*, 46(6):1643–50, 2002.

[190] **Tan AS and Berridge MV**. Superoxide produced by activated neutrophils efficiently reduces the tetrazolium salt, WST-1 to produce a soluble formazan: a simple colorimetric assay for measuring respiratory burst activation and for screening anti-inflammatory agents. *J Immunol Meth*, 238(1-2):59–68, 2000.

[191] **Segal AW**. How neutrophils kill microbes. *Ann Rev Immunol*, 23:197–223, 2005.

[192] **Bylund J, Samuelsson M, Collins LV, and Karlsson A**. NADPH-oxidase activation in murine neutrophils via formyl peptide receptors. *Exp Cell Res*, 282(2):70–7, 2003.

[193] **Abraham E**. Neutrophils and acute lung injury. *Crit Care Med*, 31(4 Suppl):S195–9, 2003.

[194] **Chia EW, Grainger R, and Harper JL**. Colchicine suppresses neutrophil superoxide production in a murine model of gouty arthritis: a rationale for use of low-dose colchicine. *Br J Pharmacol*, 153(6):1288–95, 2008.

[195] **Daley JM, Reichner JS, Mahoney EJ, Manfield L, Henry WL, Mastrofrancesco B, and Albina JE**. Modulation of macrophage phenotype by soluble product(s) released from neutrophils. *J Immunol*, 174(4):2265–72, 2005.

[196] **Phelps P and McCarty DJ**. Crystal-induced inflammation in canine joints.

II. Importance of polymorphonuclear leukocytes. *J Exp Med*, 124(1):115–26, 1966.

[197] **Popa-Nita O and Naccache PH**. Crystal-induced neutrophil activation. *Immunol Cell Biol*, 88(1):32–40, 2010.

[198] **Roberge CJ, Grassi J, de Médicis R, Frobert Y, Lussier A, Naccache PH, and Poubelle PE**. Crystal-neutrophil interactions lead to interleukin-1 synthesis. *Agents Actions*, 34(1-2):38–41, 1991.

[199] **Serhan CN and Savill J**. Resolution of inflammation: the beginning programs the end. *Nat Immunol*, 6(12):1191–7, 2005.

[200] **Luo HR and Loison F**. Constitutive neutrophil apoptosis: mechanisms and regulation. *Am J Hematol*, 83(4):288–95, 2008.

[201] **Colotta F, Re F, Polentarutti N, Sozzani S, and Mantovani A**. Modulation of granulocyte survival and programmed cell death by cytokines and bacterial products. *Blood*, 80(8):2012–20, 1992.

[202] **Wardle DJ, Burgon J, Sabroe I, Bingle CD, Whyte MKB, and Renshaw SA**. Effective caspase inhibition blocks neutrophil apoptosis and reveals mcl-1 as both a regulator and a target of neutrophil caspase activation. *PLoS ONE*, 6(1):e15768, 2011.

[203] **Santos-Beneit AM and Mollinedo F**. Expression of genes involved in initiation, regulation, and execution of apoptosis in human neutrophils and during neutrophil differentiation of HL-60 cells. *J Leuk Biol*, 67(5):712–24, 2000.

[204] **Yamashita K, Takahashi A, Kobayashi S, Hirata H, Mesner PW, Kaufmann SH, Yonehara S, and et al**. Caspases mediate tumor necrosis factor-alpha-induced neutrophil apoptosis and downregulation of reactive oxygen production. *Blood*, 93(2):674–85, 1999.

[205] **Schrijvers DM, Martinet W, Meyer GRYD, Andries L, Herman AG,**

and Kockx MM. Flow cytometric evaluation of a model for phagocytosis of cells undergoing apoptosis. *J Immunol Meth*, 287(1-2):101–8, 2004.

[206] **DeFife KM, Jenney CR, Colton E, and Anderson JM**. Disruption of filamentous actin inhibits human macrophage fusion. *FASEB J*, 13(8):823–32, 1999.

[207] **Elliott JA and Winn WC**. Treatment of alveolar macrophages with cytochalasin D inhibits uptake and subsequent growth of Legionella pneumophila. *Infect Immun*, 51(1):31–6, 1986.

[208] **Keller H and Niggli V**. Effects of cytochalasin D on shape and fluid pinocytosis in human neutrophils as related to cytoskeletal changes (actin, alpha-actinin and microtubules). *Eur J Cell Biol*, 66(2):157–64, 1995.

[209] **Jog NR, Rane MJ, Lominadze G, Luerman GC, Ward RA, and McLeish KR**. The actin cytoskeleton regulates exocytosis of all neutrophil granule subsets. *Am J Physiol, Cell Physiol*, 292(5):C1690–700, 2007.

[210] **Ting-Beall HP, Lee AS, and Hochmuth RM**. Effect of cytochalasin D on the mechanical properties and morphology of passive human neutrophils. *Ann Biomed Eng*, 23(5):666–71, 1995.

[211] **Esmann L, Idel C, Sarkar A, Hellberg L, Behnen M, Möller S, van Zandbergen G, and et al**. Phagocytosis of apoptotic cells by neutrophil granulocytes: diminished proinflammatory neutrophil functions in the presence of apoptotic cells. *J Immunol*, 184(1):391–400, 2010.

[212] **Tamassia N, Zimmermann M, and Cassatella MA**. An additional piece in the puzzle of neutrophil-derived IL-1: the NLRP3 inflammasome. *Eur J Immunol*, 42(3):565–8, 2012.

[213] **Fleetwood AJ, Dinh H, Cook AD, Hertzog PJ, and Hamilton JA**. GM-CSF- and M-CSF-dependent macrophage phenotypes display differential dependence on type I interferon signaling. *J Leukoc Biol*, 86(2):411–21, 2009.

[214] **Fleetwood AJ, Lawrence T, Hamilton JA, and Cook AD**. Granulocyte-macrophage colony-stimulating factor (CSF) and macrophage CSF-dependent macrophage phenotypes display differences in cytokine profiles and transcription factor activities: implications for CSF blockade in inflammation. *J Immunol*, 178(8):5245–52, 2007.

[215] **Takasuka N, Tokunaga T, and Akagawa KS**. Preexposure of macrophages to low doses of lipopolysaccharide inhibits the expression of tumor necrosis factor-alpha mRNA but not of IL-1 beta mRNA. *J Immunol*, 146(11):3824–30, 1991.

[216] **Zhang X and Morrison DC**. Lipopolysaccharide structure-function relationship in activation versus reprogramming of mouse peritoneal macrophages. *J Leukoc Biol*, 54(5):444–50, 1993.

[217] **Zhang X and Morrison DC**. Lipopolysaccharide-induced selective priming effects on tumor necrosis factor alpha and nitric oxide production in mouse peritoneal macrophages. *J Exp Med*, 177(2):511–6, 1993.

[218] **Netea MG, Nold-Petry CA, Nold MF, Joosten LAB, Opitz B, van der Meer JHM, van de Veerdonk FL, and et al**. Differential requirement for the activation of the inflammasome for processing and release of IL-1beta in monocytes and macrophages. *Blood*, 113(10):2324–35, 2009.

[219] **Chai LYA, Kullberg BJ, Vonk AG, Warris A, Cambi A, Latgé JP, Joosten LAB, and et al**. Modulation of Toll-like receptor 2 (TLR2) and TLR4 responses by Aspergillus fumigatus. *Infect Immun*, 77(5):2184–92, 2009.

[220] **AJ KSS**. Antigen-presenting Cells. *Encyclopedia of Life Sciences*, pp. 1–8, 2001.

[221] **Steinman RM, Turley S, Mellman I, and Inaba K**. The induction of tolerance by dendritic cells that have captured apoptotic cells. *J Exp Med*, 191(3):411–6, 2000.

[222] **Ferrero I, Michelin O, and Luescher I**. Antigen Recognition by T Lymphocytes. *Encyclopedia of Life Science*, pp. 1–10, 2007.

[223] **Robinson JH and Delvig AA**. Diversity in MHC class II antigen presentation. *Immunology*, 105(3):252–62, 2002.

[224] **Guindi C, Ménard M, Cloutier A, Gaudreau S, Besin G, Larivée P, McDonald PP, and et al**. Differential role of NF-B, ERK1/2 and AP-1 in modulating the immunoregulatory functions of bone marrow-derived dendritic cells from NOD mice. *Cell Immunol*, 272(2):259–68, 2012.

[225] **Lee JK, Kim JK, Lee YR, Kim HS, Im SA, Kim K, and Lee CK**. Exposure to chemokines during maturation modulates antigen presenting cell function of mature macrophages. *Cell Immunol*, 234(1):1–8, 2005.

[226] **Wahl SM, Hunt DA, Wong HL, Dougherty S, McCartney-Francis N, Wahl LM, Ellingsworth L, and et al**. Transforming growth factor-beta is a potent immunosuppressive agent that inhibits IL-1-dependent lymphocyte proliferation. *J Immunol*, 140(9):3026–32, 1988.

[227] **Strobl H and Knapp W**. TGF-beta1 regulation of dendritic cells. *Microbes Infect*, 1(15):1283–90, 1999.

[228] **Yamaguchi Y, Tsumura H, Miwa M, and Inaba K**. Contrasting effects of TGF-beta 1 and TNF-alpha on the development of dendritic cells from progenitors in mouse bone marrow. *Stem Cells*, 15(2):144–53, 1997.

[229] **Hamilton JA and Achuthan A**. Colony stimulating factors and myeloid cell biology in health and disease. *Trends Immunol*, 34(2):81–9, 2013.

[230] **Hume DA and MacDonald KPA**. Therapeutic applications of macrophage colony-stimulating factor-1 (CSF-1) and antagonists of CSF-1 receptor (CSF-1R) signaling. *Blood*, 119(8):1810–20, 2012.

[231] **Dai XM, Ryan GR, Hapel AJ, Dominguez MG, Russell RG, Kapp S, Sylvestre V, and Stanley ER**. Targeted disruption of the mouse colony-

stimulating factor 1 receptor gene results in osteopetrosis, mononuclear phagocyte deficiency, increased primitive progenitor cell frequencies, and reproductive defects. *Blood*, 99(1):111–20, 2002.

[232] **Latz E**. The inflammasomes: mechanisms of activation and function. *Curr Opin Immunol*, 22(1):28–33, 2010.

[233] **Dostert C, Guarda G, Romero JF, Menu P, Gross O, Tardivel A, Suva ML, and et al**. Malarial hemozoin is a Nalp3 inflammasome activating danger signal. *PLoS ONE*, 4(8):e6510, 2009.

[234] **Dostert C, Pétrilli V, Bruggen RV, Steele C, Mossman BT, and Tschopp J**. Innate immune activation through Nalp3 inflammasome sensing of asbestos and silica. *Science*, 320(5876):674–7, 2008.

[235] **Hsing AY, Kadomatsu K, Bonham MJ, and Danielpour D**. Regulation of apoptosis induced by transforming growth factor-beta1 in nontumorigenic rat prostatic epithelial cell lines. *Cancer Res*, 56(22):5146–9, 1996.

[236] **Houde N, Chamoux E, Bisson M, and Roux S**. Transforming growth factor-beta1 (TGF-beta1) induces human osteoclast apoptosis by up-regulating Bim. *J Biol Chem*, 284(35):23397–404, 2009.

[237] **Tu H, Jacobs SC, Borkowski A, and Kyprianou N**. Incidence of apoptosis and cell proliferation in prostate cancer: relationship with TGF-beta1 and bcl-2 expression. *Int J Cancer*, 69(5):357–63, 1996.

[238] **Hogquist KA, Nett MA, Unanue ER, and Chaplin DD**. Interleukin 1 is processed and released during apoptosis. *PNAS*, 88(19):8485–9, 1991.

[239] **Sollberger G, Strittmatter GE, Garstkiewicz M, Sand J, and Beer HD**. Caspase-1: The inflammasome and beyond. *Innate Immun*, 2013.

[240] **Sagulenko V, Thygesen SJ, Sester DP, Idris A, Cridland JA, and et al**. AIM2 and NLRP3 inflammasomes activate both apoptotic and pyroptotic death pathways via ASC. *Cell Death Diff*, 20(9):1149–60, 2013.

[241] **Sordet O, Rébé C, Plenchette S, Zermati Y, Hermine O, Vainchenker W, Garrido C, and et al**. Specific involvement of caspases in the differentiation of monocytes into macrophages. *Blood*, 100(13):4446–53, 2002.

[242] **Droin N, Cathelin S, Jacquel A, Guéry L, Garrido C, Fontenay M, Hermine O, and Solary E**. A role for caspases in the differentiation of erythroid cells and macrophages. *Biochimie*, 90(2):416–22, 2008.

[243] **Martinon F**. Signaling by ROS drives inflammasome activation. *Eur J Immunol*, 40(3):616–9, 2010.

[244] **O'Donnell MA, Perez-Jimenez E, Oberst A, Ng A, Massoumi R, Xavier R, Green DR, and et al**. Caspase 8 inhibits programmed necrosis by processing CYLD. *Nat Cell Biol*, 13(12):1437–42, 2011.

[245] **Gringhuis SI, Kaptein TM, Wevers BA, Theelen B, van der Vlist M, Boekhout T, and Geijtenbeek TBH**. Dectin-1 is an extracellular pathogen sensor for the induction and processing of IL-1 via a noncanonical caspase-8 inflammasome. *Nat Immunol*, 13(3):246–54, 2012.

[246] **Vince JE, Wong WWL, Gentle I, Lawlor KE, Allam R, O'Reilly L, Mason K, and et al**. Inhibitor of apoptosis proteins limit RIP3 kinase-dependent interleukin-1 activation. *Immunity*, 36(2):215–27, 2012.

[247] **Herrera B, Fernández M, Benito M, and Fabregat I**. cIAP-1, but not XIAP, is cleaved by caspases during the apoptosis induced by TGF-beta in fetal rat hepatocytes. *FEBS Lett*, 520(1-3):93–6, 2002.

[248] **Green DR, Oberst A, Dillon CP, Weinlich R, and Salvesen GS**. RIPK-dependent necrosis and its regulation by caspases: a mystery in five acts. *Mol Cell*, 44(1):9–16, 2011.

[249] **He S, Wang L, Miao L, Wang T, Du F, Zhao L, and Wang X**.

Receptor interacting protein kinase-3 determines cellular necrotic response to TNF-alpha. *Cell*, 137(6):1100–11, 2009.

[250] **Darding M and Meier P**. IAPs: guardians of RIPK1. *Cell Death Diff*, 19(1):58–66, 2012.

[251] **Tenev T, Bianchi K, Darding M, Broemer M, Langlais C, Wallberg F, Zachariou A, and et al**. The Ripoptosome, a signaling platform that assembles in response to genotoxic stress and loss of IAPs. *Mol Cell*, 43(3):432–48, 2011.

[252] **Koo GC and Peppard JR**. Establishment of monoclonal anti-Nk-1.1 antibody. *Hybridoma*, 3(3):301–3, 1984.

[253] **Ryan JC, Turck J, Niemi EC, Yokoyama WM, and Seaman WE**. Molecular cloning of the NK1.1 antigen, a member of the NKR-P1 family of natural killer cell activation molecules. *J Immunol*, 149(5):1631–5, 1992.

[254] **Phillips JH and Lanier LL**. Dissection of the lymphokine-activated killer phenomenon. Relative contribution of peripheral blood natural killer cells and T lymphocytes to cytolysis. *J Exp Med*, 164(3):814–25, 1986.

[255] **Wang Y, Wang H, Xia J, Liang T, Wang G, Li X, and Yang YG**. Activated CD8 T cells acquire NK1.1 expression and preferentially locate in the liver in mice after allogeneic hematopoietic cell transplantation. *Immunol Lett*, 150(1-2):75–8, 2013.

[256] **Asea A and Stein-Streilein J**. Signalling through NK1.1 triggers NK cells to die but induces NK T cells to produce interleukin-4. *Immunology*, 93(2):296–305, 1998.

[257] **Plitas G, Chaudhry UI, Kingham TP, Raab JR, and DeMatteo RP**. NK dendritic cells are innate immune responders to Listeria monocytogenes infection. *J Immunol*, 178(7):4411–6, 2007.

[258] **Busso N and Ea HK**. The mechanisms of inflammation in gout and pseudogout (CPP-induced arthritis). *Reumatismo*, 63(4):230–7, 2011.

[259] **Macmullan P and McCarthy G**. Treatment and management of pseudogout: insights for the clinician. *Ther Adv Musculoskelet Dis*, 4(2):121–31, 2012.

[260] **Pope RM and Tschopp J**. The role of interleukin-1 and the inflammasome in gout: implications for therapy. *Arthritis Rheum*, 56(10):3183–8, 2007.

[261] **Dupaul-Chicoine J and Saleh M**. A new path to IL-1 production controlled by caspase-8. *Nat Immunol*, 13(3):211–2, 2012.

[262] **Coles MC, McMahon CW, Takizawa H, and Raulet DH**. Memory CD8 T lymphocytes express inhibitory MHC-specific Ly49 receptors. *Eur J Immunol*, 30(1):236–44, 2000.

[263] **Basu D, Liu Y, Wu A, Yarlagadda S, Gorelik GJ, Kaplan MJ, Hewagama A, and et al**. Stimulatory and inhibitory killer Ig-like receptor molecules are expressed and functional on lupus T cells. *J Immunol*, 183(5):3481–7, 2009.

[264] **Chen Y, Shi Y, Cheng H, An YQ, and Gao GF**. Structural immunology and crystallography help immunologists see the immune system in action: how T and NK cells touch their ligands. *IUBMB Life*, 61(6):579–90, 2009.

[265] **Colonna M**. Natural killer cell receptors specific for MHC class I molecules. *Curr Opin Immunol*, 8(1):101–7, 1996.

[266] **Braud VM, Allan DS, O'Callaghan CA, Söderström K, D'Andrea A, Ogg GS, Lazetic S, and et al**. HLA-E binds to natural killer cell receptors CD94/NKG2A, B and C. *Nature*, 391(6669):795–9, 1998.

[267] **Bakker AB, Phillips JH, Figdor CG, and Lanier LL**. Killer cell inhibitory receptors for MHC class I molecules regulate lysis of melanoma cells

mediated by NK cells, gamma delta T cells, and antigen-specific CTL. *J Immunol*, 160(11):5239–45, 1998.

[268] **Wang J, Whitman MC, Natarajan K, Tormo J, Mariuzza RA, and Margulies DH**. Binding of the natural killer cell inhibitory receptor Ly49A to its major histocompatibility complex class I ligand. Crucial contacts include both H-2Dd AND beta 2-microglobulin. *J Biol Chem*, 277(2):1433–42, 2002.

[269] **Bauer S, Groh V, Wu J, Steinle A, Phillips JH, Lanier LL, and Spies T**. Activation of NK cells and T cells by NKG2D, a receptor for stress-inducible MICA. *Science*, 285(5428):727–9, 1999.

[270] **Mason LH, Anderson SK, Yokoyama WM, Smith HR, Winkler-Pickett R, and Ortaldo JR**. The Ly-49D receptor activates murine natural killer cells. *J Exp Med*, 184(6):2119–28, 1996.

[271] **Gao JX, Liu X, Wen J, Caligiuri MA, Stroynowski I, Zheng P, and Liu Y**. Two-signal requirement for activation and effector function of natural killer cell response to allogeneic tumor cells. *Blood*, 102(13):4456–63, 2003.

[272] **Smith HRC, Heusel JW, Mehta IK, Kim S, Dorner BG, Naidenko OV, Iizuka K, and et al**. Recognition of a virus-encoded ligand by a natural killer cell activation receptor. *PNAS*, 99(13):8826–31, 2002.

[273] **Mandelboim O, Lieberman N, Lev M, Paul L, Arnon TI, Bushkin Y, Davis DM, Strominger JL, Yewdell JW, and Porgador A**. Recognition of haemagglutinins on virus-infected cells by NKp46 activates lysis by human NK cells. *Nature*, 409(6823):1055–60, 2001.

[274] **Rydell-Törmänen K, Uller L, and Erjefält JS**. Neutrophil cannibalism–a back up when the macrophage clearance system is insufficient. *Respir Res*, 7:143, 2006.

[275] **Tschopp J and Schroder K**. NLRP3 inflammasome activation: The conver-

gence of multiple signalling pathways on ROS production? *Nat Rev Immunol*, 10(3):210–5, 2010.

[276] **Mankan AK, Dau T, Jenne D, and Hornung V**. The NLRP3/ASC/Caspase-1 axis regulates IL-1 processing in neutrophils. *Eur J Immunol*, 42(3):710–5, 2012.

[277] **Grainger DJ, Mosedale DE, and Metcalfe JC**. TGF-beta in blood: a complex problem. *Cytokine Growth Factor Rev*, 11(1-2):133–45, 2000.

[278] **Gabelloni ML, Sabbione F, Jancic C, Bass JF, Keitelman I, Iula L, Oleastro M, Geffner JR, and Trevani AS**. NADPH oxidase derived reactive oxygen species are involved in human neutrophil IL-1 secretion but not in inflammasome activation. *Eur J Immunol*, 2013.

[279] **Xu W, Schlagwein N, Roos A, van den Berg TK, Daha MR, and van Kooten C**. Human peritoneal macrophages show functional characteristics of M-CSF-driven anti-inflammatory type 2 macrophages. *Eur J Immunol*, 37(6):1594–9, 2007.

[280] **Xu W, Roos A, Schlagwein N, Woltman AM, Daha MR, and van Kooten C**. IL-10-producing macrophages preferentially clear early apoptotic cells. *Blood*, 107(12):4930–7, 2006.

[281] **Wiktor-Jedrzejczak W, Urbanowska E, Aukerman SL, Pollard JW, Stanley ER, Ralph P, Ansari AA, Sell KW, and Szperl M**. Correction by CSF-1 of defects in the osteopetrotic op/op mouse suggests local, developmental, and humoral requirements for this growth factor. *Exp Hematol*, 19(10):1049–54, 1991.

[282] **Fixe P and Praloran V**. M-CSF: haematopoietic growth factor or inflammatory cytokine? *Cytokine*, 10(1):32–7, 1998.

[283] **Huynh J, Kwa MQ, Cook AD, Hamilton JA, and Scholz GM**. CSF-

1 receptor signalling from endosomes mediates the sustained activation of Erk1/2 and Akt in macrophages. *Cell Signal*, 24(9):1753–61, 2012.

[284] **Hu QH, Zhang X, Pan Y, Li YC, and Kong LD**. Allopurinol, quercetin and rutin ameliorate renal NLRP3 inflammasome activation and lipid accumulation in fructose-fed rats. *Biochem Pharmacol*, 84(1):113–25, 2012.

[285] **Noble PW, Henson PM, Lucas C, Mora-Worms M, Carré PC, and Riches DW**. Transforming growth factor-beta primes macrophages to express inflammatory gene products in response to particulate stimuli by an autocrine/paracrine mechanism. *J Immunol*, 151(2):979–89, 1993.

[286] **Falk LA and Vogel SN**. Comparison of bone marrow progenitors responsive to granulocyte-macrophage colony stimulating factor and macrophage colony stimulating factor-1. *J Leukoc Biol*, 43(2):148–57, 1988.

[287] **Guth AM, Janssen WJ, Bosio CM, Crouch EC, Henson PM, and Dow SW**. Lung environment determines unique phenotype of alveolar macrophages. *Am J Physiol Lung Cell Mol Physiol*, 296(6):L936–46, 2009.

[288] **Kehrl JH, Roberts AB, Wakefield LM, Jakowlew S, Sporn MB, and Fauci AS**. Transforming growth factor beta is an important immunomodulatory protein for human B lymphocytes. *J Immunol*, 137(12):3855–60, 1986.

[289] **Hirsch JD, Terkeltaub R, Khanna D, Singh J, Sarkin A, Shieh M, Kavanaugh A, and Lee SJ**. Gout disease-specific quality of life and the association with gout characteristics. *Patient Relat Outcome Meas*, 2010:1–8, 2010.

[290] **Dubreuil M, Neogi T, Chen CA, Choi HK, Chaisson CE, Hunter DJ, and Zhang Y**. Increased Risk of Recurrent Gout Attacks with Hospitalization. *Am J Med*, 2013.

[291] **Vawter RL and Antonelli MA**. Rational treatment of gout. Stopping an attack and preventing recurrence. *Postgrad Med*, 91(2):115–8, 127, 1992.

[292] **Maelfait J, Vercammen E, Janssens S, Schotte P, Haegman M, Magez S, and Beyaert R**. Stimulation of Toll-like receptor 3 and 4 induces interleukin-1beta maturation by caspase-8. *J Exp Med*, 205(9):1967–73, 2008.

[293] **Cho YS, Challa S, Moquin D, Genga R, Ray TD, Guildford M, and Chan FKM**. Phosphorylation-driven assembly of the RIP1-RIP3 complex regulates programmed necrosis and virus-induced inflammation. *Cell*, 137(6):1112–23, 2009.

[294] **Zhang DW, Shao J, Lin J, Zhang N, Lu BJ, Lin SC, Dong MQ, and Han J**. RIP3, an energy metabolism regulator that switches TNF-induced cell death from apoptosis to necrosis. *Science*, 325(5938):332–6, 2009.

[295] **Depraetere V and Golstein P**. Dismantling in cell death: molecular mechanisms and relationship to caspase activation. *Scand J Immunol*, 47(6):523–31, 1998.

[296] **Thornberry NA**. Caspases: key mediators of apoptosis. *Chem Biol*, 5(5):R97–103, 1998.

[297] **Thornberry NA and Lazebnik Y**. Caspases: enemies within. *Science*, 281(5381):1312–6, 1998.

[298] **Ch'en IL, Tsau JS, Molkentin JD, Komatsu M, and Hedrick SM**. Mechanisms of necroptosis in T cells. *J Exp Med*, 208(4):633–41, 2011.

[299] **Kaiser WJ, Upton JW, Long AB, Livingston-Rosanoff D, Daley-Bauer LP, Hakem R, Caspary T, and et al**. RIP3 mediates the embryonic lethality of caspase-8-deficient mice. *Nature*, 471(7338):368–72, 2011.

[300] **Welz PS, Wullaert A, Vlantis K, Kondylis V, Fernández-Majada V, Ermolaeva M, Kirsch P, and et al**. FADD prevents RIP3-mediated epithelial cell necrosis and chronic intestinal inflammation. *Nature*, 477(7364):330–4, 2011.

[301] **Stout RD and Suttles J**. Functional plasticity of macrophages: reversible adaptation to changing microenvironments. *J Leukoc Biol*, 76(3):509–13, 2004.

[302] **Stout RD and Suttles J**. T cell signaling of macrophage function in inflammatory disease. *Front Biosci*, 2:d197–206, 1997.

[303] **Gordon S, Fraser I, Nath D, Hughes D, and Clarke S**. Macrophages in tissues and in vitro. *Curr Opin Immunol*, 4(1):25–32, 1992.

[304] **Josien R, Heslan M, Soulillou JP, and Cuturi MC**. Rat spleen dendritic cells express natural killer cell receptor protein 1 (NKR-P1) and have cytotoxic activity to select targets via a Ca2+-dependent mechanism. *J Exp Med*, 186(3):467–72, 1997.

[305] **Li H, Pohler U, Strehlow I, Hertig S, Baccarini M, Emmendörffer A, Tschopp J, and Lohmann-Matthes ML**. Macrophage precursor cells produce perforin and perform Yac-1 lytic activity in response to stimulation with interleukin-2. *J Leukoc Biol*, 56(2):117–23, 1994.

[306] **Li H, Schwinzer R, Baccarini M, and Lohmann-Matthes ML**. Cooperative effects of colony-stimulating factor 1 and recombinant interleukin 2 on proliferation and induction of cytotoxicity of macrophage precursors generated from mouse bone marrow cell cultures. *J Exp Med*, 169(3):973–86, 1989.

[307] **Nakamura MC, Niemi EC, Fisher MJ, Shultz LD, Seaman WE, and Ryan JC**. Mouse Ly-49A interrupts early signaling events in natural killer cell cytotoxicity and functionally associates with the SHP-1 tyrosine phosphatase. *J Exp Med*, 185(4):673–84, 1997.

[308] **DeMarco RA, Fink MP, and Lotze MT**. Monocytes promote natural killer cell interferon gamma production in response to the endogenous danger signal HMGB1. *Mol Immunol*, 42(4):433–44, 2005.

[309] **Cooper MA, Fehniger TA, Turner SC, Chen KS, Ghaheri BA, Ghayur T, Carson WE, and Caligiuri MA**. Human natural killer cells:

a unique innate immunoregulatory role for the CD56(bright) subset. *Blood*, 97(10):3146–51, 2001.

[310] **Chen H, Huang H, and Paul WE**. NK1.1+ CD4+ T cells lose NK1.1 expression upon in vitro activation. *J Immunol*, 158(11):5112–9, 1997.

[311] **Podack ER and Konigsberg PJ**. Cytolytic T cell granules. Isolation, structural, biochemical, and functional characterization. *J Exp Med*, 160(3):695–710, 1984.

[312] **Podack ER, Hengartner H, and Lichtenheld MG**. A central role of perforin in cytolysis? *Annu Rev Immunol*, 9:129–57, 1991.

[313] **Huynh MLN, Fadok VA, and Henson PM**. Phosphatidylserine-dependent ingestion of apoptotic cells promotes TGF-beta1 secretion and the resolution of inflammation. *J Clin Invest*, 109(1):41–50, 2002.

Appendix

Appendix

1. Steiger S, Harper JL. Mechanisms of Spontaneous Resolution of Acute Gouty Inflammation. *Curr Rheumatol Rep*, 16:392, 2014.

2. Steiger S, Harper JL. Neutrophil Canibalism Triggers Transforming Growth Factor β1 Production and Self Regulation of Neutrophil Inflammatory Function in Monosodium Urate Monohydrate Crystal-Induced Inflammation in Mice. *Arthritis Rheum*, 2013;65(3):815-23.